Variability of the Automated Perimetric Threshold Response

Caroline Helen Djiallis
Doctor of Philosophy

Cardiff University
January 2005

UMI Number: U584721

UMI

Dissertation Publishing

ProQuest

Caroline Djiallis
Doctor of Philosophy
Cardiff University 2005

Variability of the Automated Perimetric Threshold Response

The thesis investigated aspects of the perimetric threshold estimate with the aim of facilitating the outcome of the visual field examination.

The difference in performance of the three current short-duration commercially available algorithms, SITA Standard, SITA Fast and TOP was investigated, relative to their respective 'gold standards' and to each other, in two separate studies of normal individuals and of patients with open angle glaucoma (OAG). The results for the normal individuals suggested that the TOP algorithm will overestimate the severity of the field loss relative to the Octopus Threshold and SITA Fast algorithms. However, for the patients with OAG, SITA Fast represented a good compromise between performance and examination duration. The inherent differences within- and between-algorithm for TOP suggests that an alternative should be utilised in clinical practice.

The characteristics of the Frequency-of-seeing (FOS) curves for W-W perimetry and for SWAP were investigated for varying eccentricities in normal individuals and in patients with OAG. In the normal individuals, the slope of the FOS curve flattened and the magnitude of the 50th percentile decreased with increase in eccentricity for W-W perimetry and for SWAP. The magnitude of the slope was flatter at any given eccentricity for SWAP than for W-W perimetry. In patients with OAG, the magnitude of the slope was moderately correlated with the severity of field loss for W-W perimetry and for SWAP. The flatter slope of the FOS curve will always yield greater variability for SWAP than for W-W perimetry.

The number of incorrect responses to the False-negative catch trials was investigated in patients with OAG as a function of the fatigue effect. No significant difference was found in the prevalence of incorrect responses with increase in fatigue. The prevalence of incorrect responses was modestly correlated with increasing severity of field loss.

W-W perimetry, SWAP, SITA, TOP, FOS, False-negative catch trials

To Peter and Angela

ACKNOWLEDGEMENTS

LIST OF CONTENTS

LIST OF TABLES

LIST OF FIGURES

CHAPTER 1

Automated Static Perimetry and Perimetric Threshold Algorithms

1.1 Introduction

When the eyes are directed in a fixed, straight ahead, position, it is possible to detect the presence of objects away from the direct line of sight (Anderson and Patella 1999). This region of space in which objects can be detected by a steadily fixating eye, is defined as the visual field. The visual field has been described as "an island of vision in a sea of blindness" (Traquair 1927). The horizontal axis signifies the location within the visual field whilst the vertical axis denotes the sensitivity of the visual system to the stimulus. The summit of the photopic hill of vision, which corresponds to the fovea, has the greatest sensitivity to light, and sensitivity decreases as the hill slopes towards the sea, corresponding to increased retinal eccentricity. The slope of the hill is greater nasally than temporally. The physiological blind spot is located $15°$ temporally and $1.5°$ inferiorly to fixation. It is approximately $5.5°$ wide and $7.5°$ high (Reed and Drance 1972). It is the region in the visual field which corresponds to the retinal location of the optic nerve head, an area of retina devoid of photoreceptors. For a monocularly fixating normal eye, the extent of the visual field is $60°$ nasally and superiorly and $75°$ inferiorly and $100°$ temporally from fixation (Anderson and Patella 1999). This is the relative visual field as the visual field is restricted by the nose and bones of the orbit. Consequently the dimensions of an individual's facial contours may restrict the extent of the measured visual field; for example, deep set eyes, prominent brows or prominent noses (Meyer et al 1993).

The purpose of a visual field (perimetric) examination is to assess the dimensions of the subject's hill of vision and hence the integrity and function of the visual system as a whole (including pre-retinal factors, the retina and the visual pathways extending to the visual cortex). The visual field examination measures the differential light threshold at various locations across the visual field by presenting stimuli with varied luminances and/or sizes: traditionally and most commonly by using a white stimulus superimposed

1

on a white background. The differential light threshold is defined as the minimum stimulus luminance (ΔL) required to elicit a response against a background of constant luminance (L) and is expressed as ΔL/L. Sensitivity is defined as L/ΔL, and is the reciprocal function of that of the differential light threshold. Moving from fixation towards the periphery of the visual field, an increasing reduction in recognition, resolution and colour discrimination occurs such that only brighter or larger stimuli are perceived.

A sinking of the hill of vision into the sea is described as a depression or as diffuse loss and corresponds to a generalised reduction of sensitivity across the entire visual field. A localised area of reduced sensitivity is known as a relative scotoma or a relative focal defect and corresponds to a valley or crater, of varying depth, in the island of vision. Within areas of focal visual field loss larger and/or brighter stimuli are necessary in order to evoke a response. An absolute scotoma is an area of the visual field with no perimetrically recordable perception to light. A constriction or contraction of the field occurs when there is a total loss of sensitivity in the peripheral field.

Damage at distinct locations within the visual pathway produces characteristic visual field loss with distinctly different characteristics. All visual field defects can be classified as prechiasmal, chiasmal or postchiasmal, depending on their anatomical location. Prechisamal lesions include preretinal abnormalities of the ocular media and diseases of the retina and optic nerve, such as glaucoma. Prechiasmal lesions may produce monocular or binocular visual field defects with numerous different characteristics: they may cross the vertical midline (unlike postchiasmal defects) and they often exhibit a distinct horizontal border nasally. Lesions occurring at the optic chiasm or postchiasm (i.e. occipital cortex, optic tract, temporal lobe), respect the horizontal midline and produce a defect in one half of the visual field of the two eyes, (a hemianopia), or a quadrant of the visual field, (a quadrantopia). Lesions affecting the optical chiasm, such as pituitary adenomas, result in a bitemporal hemianopia (Anderson & Patella 1999). Homonymous defects affect the same side of the field, in both eyes whereas heteronymous defects affect opposite sides of the field in each eye. Congruence describes

2

the amount of symmetry of the defect between the two eyes. The central visual field is assumed to be that part within thirty degrees from fixation, further than thirty degrees from fixation is termed the peripheral visual field.

There are two techniques of perimetry, kinetic and static perimetry. Kinetic perimetry involves moving, a stimulus of a constant luminance and size towards the hill of vision from the non-seeing, to the seeing position, until detected by the patient. The eccentricity at which the stimulus is first detected is designated as the threshold. This procedure demarcates the peripheral boundaries of the visual field. The locus of points at threshold is plotted and is termed the isopter, and is analogous to a contour line. Consequently, isopters represent lines which connect locations of equal sensitivity. A number of isopters can be plotted by varying the size and intensity of the stimulus, to provide a detailed topography of the hill of vision. The area within each normal isopter depends upon the size, luminance and colour of the stimulus used to plot it.

However, limitations exist within kinetic perimetry. The velocity of the stimulus presentation, as well as the reaction times of the patient and perimetrist, induce, variability within the results (Lynn 1969; Greve 1973). A moving stimulus will be detected more peripherally than a stationary stimulus because of successive lateral spatial summation (Greve 1973). According to Greve (1973), the optimum stimulus velocity is 2° per second for the central field and 5° per second for the peripheral field. However, the size of a given isopter is reduced at stimulus velocities of 4° per second or greater (Johnson and Keltner 1987). The subject's reaction time is slower in the periphery (Keele 1986).

Due to the limitations of the Goldmann kinetic perimeter, there were several attempts to automate the kinetic perimetric examination. Examples include: the Perikon (Maraffa et al 1989), the Squid (Lewis et al 1986) and the Perimetron (Portney et al 1978; Drance 1981) perimeters. The lack of an intuitive and/or interactive examination mode rendered these perimeters largely unsuccessful.

It is unlikely that fully automated kinetic perimetry will be viable for the investigation of field loss with irregular and unknown borders, but it may be appropriate in instances of well defined profound field loss often resulting from neuro-ophthalmological complaints, or in cases of generalised diffuse reductions in sensitivity (Schiefer et al 2000, 2002).

The principles of manual kinetic perimetry have already been discussed. Manual kinetic perimetry has been virtually obsolete for a number of years, particularly for the investigation of glaucoma, being largely superceded by automated static perimetry. There are several disadvantages of manual kinetic perimetry when compared with automated static perimetry: the results can be perimetrist dependent; there is no digital storage and recall of patient records; there is no auto-calibration of the perimeter; the spatial resolution of the Goldmann instrument is poor within the central visual field (Schiefer 2004). Automated static perimetry, however, is exhausting in cases of advanced visual field loss. Kinetic perimetry can be useful for these patients as it is based on the principles of edge detection and pattern recognition, which is particularly effective in instances where a scotoma has a steep border (e.g. advanced retinal nerve fibre bundle defect, hemianopia and concentric constriction of the visual field).

There has been a resurgence of interest in kinetic perimetry recently due to the new semi-automated kinetic perimetry (SKP) (Schiefer 2004). Semi-automated perimetry was developed in an attempt to combine the benefits of kinetic perimetry whilst minimising the potential detrimental influence of operator procedure and/or skill resulting in standardisation and reproducibility of the kinetic perimetric examination. The cupola of the OCTOPUS 101 perimeter (Haag-Streit, Koeniz, Switzerland) can be used for SKP, if it is installed with the relevant modified software. The modified software enables vector-based SKP that compensates for the RT of the patient and minimises the influence of the perimetrist's role in the examination. The perimetrist still interacts with the patient and has control over the examination, but the procedure is monitored and recorded by the computer. The kinetic targets, size (Goldmann 0 to V are available), luminance (range from 4 to 320 cd/m^2) and angular velocity (up to 25°/s), are chosen by the perimetrist for each of the various vectors. Once selected, the angular velocity is kept constant by the

computer. Using a mouse and the computer's graphical display, the perimetrist determines the location and extent of each vector. Stimulus presentation is possible within an eccentricity ("radius") of up to 84° in each horizontal direction, and up to 60° and 78° within the superior and inferior hemifields, respectively (Schiefer 2004).

The monitor screen and the printout display information which includes: the stimulus characteristics; the vector locations; the patient responses and the isopters and the examination results can be stored in a database. The individual examination details can serve as a patient specific baseline for subsequent follow-up examinations. If required, the precise examination procedure can be retrieved and repeated (Schiefer 2004).

Static perimetry overcomes some of the limitations of manual kinetic perimetry as it is independent of the patient and the perimetrist's reaction time and of stimulus velocity (Greve 1975; Trope and Britton 1987). The stimuli are presented at fixed locations and the luminance is varied using a staircase, or bracketing procedure. The initial stimulus presentation, which can be above or below threshold, is increased or decreased, respectively, in unit steps of brightness depending on the subject's response, until threshold is crossed. The threshold can be crossed again by reversing the direction of the luminance and altering the magnitude of the luminance increment. Any number of crossings with any number of step sizes can be implemented. Static perimetry is also a more sensitive and precise technique than kinetic perimetry because it is able to detect small isolated relative scotomas, which often occur in early glaucoma. (Drance et al 1967; Armaly 1971; Greve and Verduin 1977; Schmied 1980)

Stato-kinetic dissociation (SKD) describes the difference in the measured sensitivity between identical static and kinetic stimuli. SKD manifests as a greater differential light sensitivity for kinetic stimuli in the periphery and greater sensitivity centrally for static perimetry (Fankhauser and Schmidt 1960; Gandolfo 1996). The combination of static and kinetic perimetry has been suggested for the 4% to 11% of patients with glaucoma who demonstrate a normal central field but exhibit a peripheral field defect (Aulhorn and Harms 1967; Greve 1973; Miller et al 1989; Ballon et al 1992). Hudson and Wild (1992)

found using the Humphrey Field Analyzer (HFA) with Goldmann sizes I and II and a kinetic stimulus velocity of 4° per second, that kinetic perimetry overestimated static perimetry by approximately 4 dB, regardless of meridian and eccentricity.

The advent of computerized, automated, static perimetry, enabled the topography of the visual field to be estimated with a reduced examination duration relative to manual static perimetry, and the control of the stimulus presentation, information processing and storage of data (Lynn and Tate 1975). The optimum perimeter, would incorporate efficiency with high sensitivity and specificity. In order to establish the most advantageous examination conditions, many studies have investigated alternative types of stimuli and stimulus parameters, different threshold algorithms, and the influence of extraneous factors on the estimation of threshold.

In the first instance, automated perimetry was undertaken using the Octopus 201 automated perimeter which was initially developed for research (Fankhauser et al 1972; Koch et al 1972; Spahr 1975). The Competer (Heijl and Krakau 1975a, b), the Fieldmaster (Keltner et al 1979), the Peritest (Greve 1980) the HFA (Heijl 1985), the Squid (Lewis et al 1986, Johnson et al 1987) and the Dicon AP2000 (Hart and Gordon 1983; Mills 1984) are all examples of other early automated perimeters.

1.2 Principles of Perimetry
1.2.1 Perimetric Units of Measurement
The decibel (dB), is the unit of differential light sensitivity. The dB scale is a logarithmic scale whereby 1dB represents 0.1 log unit and 10dB represents 1.0 log unit. For example, a 1.0 log unit filter attenuates light to one tenth of its original intensity, a 2.0 log unit filter reduces light intensity by a factor of one hundred. Sensitivity in dB is measured according to the maximum luminance of the perimeter which is represented as 0dB. Consequently, an increase in the dB scale corresponds to an increase in sensitivity (Anderson and Patella 1999).

The differential light threshold is described by the Weber-Fechner Law:

$$\Delta L/L = K$$

where K is a constant.

For a logarithmic scale:

$$\text{Sensitivity (dB)} = k + 10 \log (\Delta L/L)$$

The unit of luminance in perimetry is the candela per square meter (cdm^{-2}), and the apostilb (asb). The cdm^{-2} is proportionally related to Πasb and is an absolute measurement which is used to describe background and stimulus luminances. The dB, however, is a relative measurement used to describe the differential light sensitivity. One asb is equivalent to a 40dB stimulus and is 1/10,000 less intense than the maximum luminance of most perimeters and approximates to the maximum foveal sensitivity in trained young observers (Anderson and Patella 1999).

With the Humphrey Field Analyzer (HFA), L is 10 cdm^{-2} (31.5asb), the maximum stimulus luminance (ΔL) is 3183cdm^{-2} (10,000asb) and the constant, k is 25. Since the decibel scale is a relative measure, calculated from the background illumination and the maximum stimulus intensity, a particular decibel value on one type of perimeter, does not necessarily indicate a similar sensitivity as the same decibel value on another type of perimeter (Anderson and Patella 1999).

1.2.2 Stimulus Parameters
1.2.2.1 Background Illumination and Dynamic Range

The background luminance (L) of the perimeter, performs a critical role in determining retinal sensitivity and it must remain constant within an examination, since it determines the state of retinal adaptation. At low levels of scotopic background illumination, the retina will become dark-adapted and is able to perceive very weak stimuli resulting in a hill of vision with a flat profile and a physiological scotoma at the fovea due to the

absence of rod photoreceptors at this location. The hill of vision becomes steeper, as the background illumination tends towards the mesopic and photopic ranges

The intensity of the background illumination also affects the dynamic range of the perimeter. This is defined as the measurement range over which the neuro-visual system can be tested, using specific equipment with a given set of experimental variables (Fankhauser 1979). Reducing the background luminance or increasing the maximum stimulus luminance or the stimulus size, maximizes the dynamic range (Fankhauser 1979; Heijl 1985; Choplin et al 1990; Zalta 1991). With a background luminance of $1.3cdm^{-2}$ and at an eccentricity of $50°$, a change in the stimulus size from Goldmann I to III increases the dynamic range by 12dB. Increasing the stimulus size and decreasing the background luminance from $12.7cdm^{-2}$ to $1.3cdm^{-2}$ will give a 50 fold (17dB) increase in the dynamic range (Fankhauser 1979). In order to determine the defect depth within the visual field, a large dynamic range is beneficial. Perimeters employing LED stimuli frequently utilise a lower background luminance than perimeters employing projecting stimuli due to the reduced intensity of the LED stimulus. The Medmont M700 and the Easyfield Perimeter are examples of LED perimeters which are currently commercially available.

Reducing the background illumination of a perimeter will increase the dynamic range, but this is at the expense of an increase in the time necessary for the retina to adapt to the lower luminance. The HFA and Octopus 1-2-3 perimeters use a background illumination of $31.5/10cdm^{-2}$. The Octopus 100 and 300 Series employ three options for background illuminations of 31.4asb, 4asb and 314asb. A background luminance of $10cdm^{-2}$ offers a compromise between the requirements of dynamic range and the necessity for minimum adaptation time of the patient from the general room illumination (Heijl 1985). The increase in dynamic range produced by an increase in stimulus luminance can result in light scatter or seepage from the boundaries of the stimulus (Fankhauser and Haeberlin 1980; Dengler-Harles et al 1990).

Under photopic conditions, the relationship between ΔL and L has been assumed to follow the linear Weber-Fechner Law but this only applies at background luminances of greater than $31.8 cdm^{-2}$ (Aulhorn and Harms 1972). However, Weber's law may not apply at the low photopic background illumination levels found in most commonly used clinical perimeters. The Rose de Vries Law ($\Delta L/L^{0.5}$ = constant) demonstrates good approximation at levels of low photopic and mesopic background illumination ($1.3 cdm^{-2}$ - $10 cdm^{-2}$) (Fankhauser 1979; Flanagan et al 1991). A further reduction of the background luminance to less than $0.3 cdm^{-2}$ (1asb), i.e. within the scotopic range, results in a linear relationship dependent on ΔL alone: $\Delta L = K$

1.2.2.2 Generation of Stimuli

Traditionally, the perimetric stimulus can either be presented on a flat screen or on a cupola (hemispherical bowl). Flat screens can only be used to examine the central visual field. The examination of the peripheral field originally required the use of a large hemispherical bowl, requiring a large examination room. The Octopus 1-2-3 and Octopus 300 Series reduced the physical dimensions of the bowl by using a direct projection system in which the stimulus, background illumination and fixation target project onto the retina from optical infinity (Octopus 1-2-3 Operating Instructions 1990; Octopus 301 User's Manual 2001; Octopus Visual Field Digest 2004). The HFA 700 series uses an aspheric bowl, which is considerably smaller than the original hemispherical bowl of the HFA 600 series, without loss of stimulus eccentricity (HFA II User's Guide 1994).

Automated perimeters have employed one of three different methods stimulus generation: light-emitting diodes (LED), fibre-optics, or projection systems. Light-emitting diode (LED) stimuli are relatively inexpensive to manufacture and are mechanically robust which allows for little, if any, maintenance. Because the light intensity of LED stimuli is varied by a high pulse current they can tolerate high luminances. However, each LED must be individually calibrated and the LED light emission is both narrow and variable. The independent control of each LED permits multiple stimulus presentations for the suprathreshold examination of the visual field as implemented in, amongst others, the

Henson series and Dicon range of perimeters. However, LED stimuli are limited to a fixed location and a fixed size in that individual diodes are mounted in apertures at pre-determined locations. Such an approach leads to a fixed given level of spatial resolution. In addition, the wavelength of the given LED stimulus cannot be varied. Early designs of LED perimeters placed the diode slightly recessed from the perimeter surface creating a visible "black-hole". The "black holes" resulted in localised changes in retinal adaptation (Heijl 1985; Britt and Mills 1988) and an increase in threshold variability, particularly in areas of high sensitivity (Desjardins and Anderson 1988). Britt and Mills (1988) concluded that covering the recessed diodes with a diffusing film minimises the "black hole" effect. Such an approach was implemented in the Dicon AP2000 perimeters.

The now obsolete, Fieldmaster and Tubinger 2000 perimeters used the fibre-optic method of stimulus generation. Fibre-optic stimuli employ a single light source from which fiber-optic bundles are directed to pre-determined and fixed locations. The single light source simplified calibration of the stimulus luminance. Coloured stimuli could also be implemented by the use of interference filters that were positioned in front of the light source. However, fibre-optic systems suffer similar limitations to LED systems, namely, the finite number of stimulus positions and the invariability of stimulus size. The high manufacturing costs relative to the other available methods of stimulus generation has limited the utility of the fibre optic presentation technique.

The projection system is the most common form of perimetric stimulus generation. The HFA series and the Octopus 101 use a projection system whereby the stimulus originates from a single light source that is passed through a series of condensing lenses, apertures and filters to project to a stipulated location onto the bowl via a mirror optical system. A rotating neutral density filter is placed in front of the path of the light and is used to vary the stimulus luminance. The size and wavelength of the stimulus is controlled by the aperture and filter wheels. The stimulus location is determined by the orientation of the mirror that is controlled by small stepper motors giving a maximum possible resolution of 0.2° between adjacent stimuli (Fankhauser 1979; Heijl 1985). The fine potential spatial resolution and the flexibility in the direction of the stimulus to a chosen position are

advantages of the projection system. However, the noise that is created by stepper motors can provide audible clues that can lead to an increase in false-positive responses. Incandescent light sources are also prone to ageing; however, photoelectric cells initiate calibration of the light source following power-up of the instrument. The accuracy of the projection system is offset by the expense of the service costs due to its mechanical vulnerability.

The Octopus 1-2-3 and 300 series perimeters utilise a single LED projected onto the retina from optical infinity. The Oculus Centrefield perimeter is a direct projection perimeter. The optics of the direct projection perimeter allows projection of the stimulus from an infinite distance.

1.2.2.3 Spatial Configuration of Stimuli

Visual field loss in glaucoma usually occurs in the central visual field (Werner and Drance 1977; Caprioli and Spaeth 1985). The prevalence of isolated peripheral field defects is low at between 12.0% (Haas & LeBlanc 1994), 0.5% (Ogawa and Suzuki 1979) and 0.8% (Blum et al 1959). The detection of visual field loss in glaucoma, is determined by the the stimulus resolution of the locations examined. In order to maximise the potential for the detection of visual field loss, the ideal configuration would consist of a large number of stimulus locations with a narrow inter-stimulus separation; however, this would generate a protracted examination duration (Fankhauser and Bebié 1979). A theoretical, circular defect of 9° in diameter has a 95% probability of detection when 50 regularly distributed stimulus locations are evenly placed out to 30° eccentricity (Greve 1975). If 452 stimulus locations are used, there is a 100% probability of detecting a visual field defect of 7.5° in diameter, and a 95% probability of detecting a visual field defect of 3° in diameter. Greve (1975) suggested that the optimal arrangement would be 150 locations. However, no significant improvement in the detection rate of clinically significant visual field loss was found when more than 140-150 locations were used (Johnson and Keltner 1981). The relationship between sensitivity and the number of

stimulus locations is logarithmic whilst the specificity is linear (Fankhauser and Bebié 1979; Henson et al 1988).

There are several possible approaches to the selection of the stimulus configuration: systematic sampling by evenly spaced stimuli, higher density sampling in high risk areas of the field, or a combination of the both. (Gutteridge 1984). The arrangement of stimuli usually remains constant during the visual field examination.

The most common approach used for example in the HFA Programs 24-2 and 30-2 and in Octopus Program 32 is a default stimulus separation of 6° with the stimuli located 3° either side of the horizontal and vertical meridian (Fankhauser and Bebié 1979). A focal defect 8.4° in diameter will be detected with 100% probability using a 6° inter-stimulus separation. The probability reduces to 79% for a focal defect of 6° in diameter (Fankhauser and Bebié 1979). However, the detection of the physiological blind spot and small glaucomatous defects can go undetected with a 6° inter-stimulus seperation (Weber and Dobek 1986; King et al 1986; Wild et al 1986). Heijl (1993) suggested that a localised visual field defect is unlikely to incorporate only one stimulus location when using an inter-stimulus separation of 6°. The Octopus G1X and G2 programs use a non-uniform stimulus grid in which the central stimuli are separated by 2° which increases to 8° at an eccentricity of 55° (Flammer et al 1987).

The Spatially Adaptive Program (SAPRO) developed for the Octopus perimeter implemented spatially adaptive techniques whereby the spatial resolution was increased locally in areas which exhibited reduced sensitivity (Haeberlin and Fankhauser 1980). SAPRO adjusted grid resolution in three steps according to the presence or absence of reduced sensitivity (Haeberlin and Fankhauser 1980). The Automatic Diagnostic Test developed for the HFA perimeters which increased spatial resolution locally from a 6° inter-stimulus separation to a 3° separation in areas of the field where the first and second stimulus presentations were 'not seen' at 6dB above threshold. However, Åsman et al (1988) found that this spatial enhancement strategy did not improve sensitivity and specificity compared to that achieved by the 6°default grid. Custom programs can be

developed to specifically investigate regions of interest with a finer spatial resolution, if required.

1.2.2.4 Stimulus Size and Stimulus Duration

Stimulus visibility is affected by both spatial summation and temporal summation. Due to the convergent nature of neural processing within the retina, a ganglion cell may respond equally to a small bright stimulus or a larger dim stimulus. The increase in differential light sensitivity resulting from an increase in stimulus size is described mathematically as:

$$\Delta L \times A^k = Constant$$

where, ΔL is the stimulus luminance, A is the stimulus area and k is the summation coefficient. When k=1, complete spatial summation occurs, in keeping with Ricco's Law. Complete spatial summation breaks down when the stimulus area is increased beyond the size of the critical area and occurs where the relationship between luminance and area is no longer a reciprocal function. Partial spatial summation with a coefficient (k) that lies between 0 and 1, occurs at stimulus sizes larger than the critical area. Pieron's law (k=0.3), Piper's law (k=0.5) and Goldmann's approximation (k=0.8) have all been used to describe partial summation. When k=0, Weber's law applies, therefore an increase in stimulus area has no effect on threshold.

A Goldmann size III stimulus is the default stimulus size for use in automated static perimetry. The size III stimulus has an area of $4mm^2$ and subtends 30.71min of arc (0.471°) on the retina when the eye is placed 30cm from the screen. (There are six Goldmann stimulus sizes: size 0 has an area of $0.0625mm^2$ and subtends 0.05 degrees of arc; size I has an area of $0.25mm^2$ and subtends 0.11 degrees of arc; size II has an area of $1mm^2$ and subtends 0.22 degrees of arc; size IV has an area of $16 mm^2$ and subtends 0.86 degrees of arc and size V has an area of $64 mm^2$ and subtends 1.72 degrees of arc. The size III stimulus is affected less than size I by optical defocus, refractive error, (Heijl

1985) and media opacity (Wood et al. 1987a). For stimulus sizes smaller than size III variability within 30° eccentricity is greater (Gilpin et al 1990; Wall et al 1993) and approximately equal with sizes IV and V (Gilpin et al 1990). However, the use of a Goldmann size I stimulus can enable the detection of a small shallow relative scotoma that would otherwise go undetected when using a Goldmann size III (Zalta and Burchfield 1990). Nevertheless, the dynamic range of a perimeter is reduced by the use of a smaller stimulus, especially in the peripheral visual field. Stimulus sizes larger than size III have been advocated to increase the dynamic range for patients with end-stage glaucoma and in order to monitor defects that are absolute with the size III stimulus (Wilensky et al 1986; Zalta 1991). Weber and Baltes (1995) concluded that the improvement in sensitivity that occurs by increasing the stimulus size from III to V follows a linear function that is independent of eccentricity.

As the stimulus duration increases, stimuli appear brighter. Bloch's Law states that when the duration of the stimulus exceeds the critical duration, the perceived luminance becomes independent of duration.

$$\Delta L \times T^k = \text{Constant}$$

where ΔL is the stimulus luminance, T is the stimulus duration and k is the summation coefficient. Complete temporal summation occurs at stimulus durations of less than the critical time and, therefore, k=1. Partial temporal summation occurs with stimulus durations greater than the critical time and k decreases towards zero. When k=0 and all other stimulus parameters remain constant, an increase in stimulus duration has no further effect on the threshold determination. The critical time in the normal eye is affected by eccentricity and by retinal adaptation. It ranges from 60–100msec (Barlow 1958; Greve 1973; Saunders 1975). Temporal summation is greater for lower background luminances and for smaller stimuli (Barlow 1958; Saunders 1975). Dannheim and Drance (1971) found that at low background luminances equal to or less than $3.2 cdm^{-2}$, the critical time can exceed 100msec. The effects of temporal summation have been shown to be eliminated at stimulus durations between 0.5 and 1 second (Aulhorn and Harms 1972; Greve 1973). The HFA uses a stimulus duration of 200msec which is shorter than the

latency time for voluntary eye movements and long enough for complete temporal summation. The Octopus perimeters use a stimulus duration of 100msec.

1.2.3 Background to Automated Static Perimetry

Automated static perimetry has become the accepted method of visual field examination in glaucoma, over the past 22 (15) years and it is the most precise clinical method for quantifying and evaluating the visual field (Bengtsson et al 1997). It has become an essential component in the detection, monitoring and management of many visual pathway disorders including primary open angle glaucoma (Wild et al 1998).

Automated perimetry was first introduced, almost thirty-seven years ago. Lynn presented an automated perimeter as early as 1968 (Fankhauser et al 1972; Bengtsson et al 1997). Early manually operated static perimeters, usually employed the Method of Limits for threshold determination, (simply altering stimulus intensities from infra- or supra-threshold until the threshold was crossed) (Choplin et al 1973; Heijl & Krakau 1977; Bengsston et al 1997a). The Method of Limits involves either the subject or the perimetrist adjusting the intensity of the stimulus in small steps until the stimulus can just be perceived by the subject. With this technique, the subject's conscious decision for detection and their bias for a particular stimulus can significantly influence the final intensity of the stimulus. There may also be a substantial degree of redundant data as many stimulus presentations are often far from the threshold. Data collected at stimulus levels close to threshold yield more useful information on the threshold value (Taylor 1971). Another technique for threshold estimation used in manual static perimetry, was the Method of Constant Stimuli. This involves the presentation of a large number of stimuli at several predetermined intensities. This procedure requires a large number of possibly less-informative stimulus presentations as the numbers of positive and negative responses are recorded at each stimulus intensity and are subsequently used to plot the psychometric function from which the threshold is then calculated. This technique is both time consuming and open to response bias and criterion effects.

Numerous attempts have been made, since, to improve the sensitivity, specificity and speed of data acquisition for automated perimetry by modifying the perimetric algorithms (Stewart et al 1989; Morales et al 1999; Maeda et al 2000).

1.2.4 Background to Perimetric Algorithms

Several different types of thresholding algorithms have been utilized since the introduction of automated static perimetry. These include: staircase methods; and more computationally complex algorithms devised by psychophysicists, such as PEST (Parameter Estimation by Sequential Testing) (Taylor and Creelman 1967; Pollack 1968; Rose et al 1970), ZEST (Zippy Estimation by Sequential Testing) (Vingrys and Pianta 1999; Turpin et al 2003), QUEST (Quick Estimation by Sequential Testing) (Watson and Pelli 1983; Treutwein 1995; Garcia-Perez 1998; Vingrys and Pianta 1999) and MOBS (modified binary search) (Tyrrell and Owens 1988; Johnson and Shapiro 1989; Turpin et al 2002a,b). These algorithms differ from a staircase algorithm in that a step size or boundary does not limit their intensity levels although obviously, perimeter design will impose certain realistic constraints on the intensities of the stimuli (Bengtsson et al 1997a; Vingrys & Pianta 1999). They also utilize maximum likelihood estimates when determining endpoints. The psychophysical methods to measure thresholds can be divided into two classes: constant stimulus (or fixed psychophysical methods), and adaptive or tritation methods (Rose et al 1970) (discussed previously).

Adaptive methods of stimulus presentation determine the next stimulus intensity according to the subject's response from the previous stimulus. The adaptive methods of threshold estimation require fewer stimulus presentations than the Method of Limits (Cornsweet 1962) and therefore reduce the examination duration. This is because they do not rely on predetermined intensity levels and the stimuli are presented at levels closer to threshold. Staircase algorithms are an example of an adaptive procedure (Wetherill and Levitt 1965).

16

The first generation of perimetric algorithms consisted of staircase procedures (Rose et al 1970; Bebie et al 1976; Heijl 1977) such as the 4-2dB staircase and the 4-2-1dB staircase (these are described in more detail in 1.3.4, 1.3.8.1 and 1.3.8.2). Staircase algorithms have pre-determined rules for stimulus sequences, such as: start intensity, step size, number of reversals, direction of threshold crossing and when to repeat a sequence (Cornsweet 1962; Bengtsson et al 1997a). The threshold algorithms that have been most extensively used in clinical perimetry over the last 20 years have all been of this first generation, staircase, variety. During this time, advances have also been made in psychophysical algorithms and modifications of some of these newer techniques have been incorporated into some of the more recently designed perimetric algorithms (e.g. ZEST for SITA and MOBS for FDP).

Perimetric algorithms have advanced greatly since they were originally introduced. Despite this, advance there is still much scope for improvement before an algorithm with the optimum characteristics is developed. Although many of the newer psychophysical algorithms have reduced examination duration, this has still been to an extent to the detriment of the accuracy of the resultant threshold estimate.

1.2.5 Staircase Algorithms

In threshold static automated perimetry, the threshold at a given location in the visual field is generally determined using a sequential "up-down" staircase procedure that "brackets" the threshold. (Cornsweet 1962; Vingrys and Pianta 1999; Johnson et al 1991). Over successive presentations, the bracket interval (step size) is gradually reduced, as described below, thus converging on the final threshold estimate. This is usually taken to be the 50% point on the psychometric function resulting from the examination. The results obtained with such a bracketing procedure are in close agreement with those obtained by more conventional psychophysical procedures (Miller et al 1983; Tyrrell & Owens 1988). A full staircase procedure provides the most accurate estimation of threshold but is extremely time-consuming when applied to automated

perimetry due to the large number of stimulus locations at which threshold must be estimated.

The truncated Method of Limits, staircase procedure is the most popular method for estimating threshold (Anderson 1992). An initial step size of 4dB is presented at a starting level which is either suprathreshold or infrathreshold. If the starting level is infrathreshold, the stimulus luminance is increased and if the starting level is suprathreshold the stimulus luminance is reduced, in 4dB increments until the threshold is crossed. The subsequent staircase is then reversed in direction and uses 2dB increments (Levitt 1971; Spahr 1975; Fankhauser 1979) until a second crossing of threshold is achieved.

Staircase algorithms may vary in their start levels, seed locations, magnitude of step size, number of staircase procedures per stimulus location, number and direction of crossings of the threshold and their criteria for final endpoint determination of sensitivity. All of these parameters will influence the accuracy of the final threshold estimate. The accuracy of the staircase procedure at any given stimulus location primarily increases: with the use of smaller steps; when the staircase position is close to threshold; with an increase in the number of crossings of threshold; and with an increase in the number of staircases (Johnson et al 1993a; Wild et al 1999a,b).

Staircase strategies are computationally simple and have been studied in detail using both computer simulation and in clinical studies (Heijl et al 1989; Johnson et al 1992a; Spenceley and Henson 1996; Turpin et al 2003). Previous simulations have indicated that modifying the parameters of existing staircase procedures can produce only modest overall improvements in performance (Johnson 1985; Johnson and Shapiro 1989). Consequently, alternative approaches have been investigated in an attempt to improve the level of accuracy and efficiency obtained with staircase procedures.

1.2.6 Modified Binary Search (MOBS)

The binary search is an efficient means of searching an ordered array, which in a manner similar to the bracketing strategy, utilizes information gained with each stimulus presentation to determine the next step of the search.

The modified binary search algorithm (MOBS) has been reported to offer improvements in both accuracy and efficiency for threshold determinations (Tyrrell and Owens 1988). The MOBS algorithm was designed to combine the efficiency of the binary search with the capability of the bracketing procedure to estimate thresholds which may exhibit inherent variability. The sampling range is defined by two boundaries, each boundary comprises a three element stack, with the top element of each stack representing the current boundary value and the lower elements representing previous boundary values. Initially all elements within one stack are set to represent one extreme value of the range, and all of the elements in the other stack are set to represent the other extreme value of the range. With each stimulus presentation, one of the two stacks is updated. The MOBS procedure estimates threshold by bracketing presentations around threshold and continually halving the interval between the stimulus intensity boundaries i.e. the next stimulus presentation in the examination at any given time is the value midway between the top elements of the two stacks (Tyrrell and Owens 1988). These measurements are then used to estimate the threshold at all other remaining stimulus locations in the given program. Johnson and Shapiro (1989) determined whether MOBS could be implemented in automated perimetry comparing its performance to existing staircase algorithms using the KRAKEN computer simulation program. They concluded that MOBS provided an improvement in the accuracy of threshold estimates but at the expense of a reduced efficiency. MOBS, was also found to be more robust to response errors and response variability.

The algorithm RIOTS (Real-time Interactive Optimized Test Sequence) was based upon the MOBS algorithm. RIOTS was a two-phase heuristic algorithm for automated perimetry that used MOBS to obtain thresholds at ordered arrays of twelve threshold seed locations and at two blind spot locations. Johnson & Shapiro (1991), demonstrated a

significant improvement in performance of RIOTS when compared to the staircase procedures typically used for automated perimetry. They found that the examination duration for RIOTS was six to eight minutes for all individuals compared to 12 to 18 minutes for the HFA Full Threshold 4-2dB staircase procedure. Currently, however, RIOTS is not commercially available.

1.2.7 Examination Duration

Threshold strategies that use smaller step sizes and more reversals yield longer staircase sequences and more accurate estimates of threshold (Bengtsson et al 1997a). However, the longer staircase is far from ideal since it leads to a longer perimetric examination, which in turn can often produce erroneous results due to patient fatigue. The fatigue effect, whereby sensitivity decreases during an examination, has been demonstrated for all types of patient groups (Heijl 1977; Johnson et al 1988; Searle et al 1991). This effect is more pronounced in areas adjacent to visual field loss, (Heijl 1977; Holmin & Krakau 1979; Heijl et al 1983; Suzamura et al 1988; Wildberger 1988; Hudson et al 1994). In general, the more time-consuming perimetric tests usually exhibit greater reliability and are more accurate than the shorter ones (Heijl 1977; Johnson 1992; Johnson et al 1992; Sharma et al 2000).

Fixed step sizes yield reduced examination efficiency since the examination duration is dependent upon the relative positioning of the start and endpoints in addition to the actual step size. It has long been recognised that the ideal staircase should use variable step sizes (although most existing perimetric methods do not) and should adopt a fixed step-size when determining an endpoint e.g. 2dB (Watson et al 1983; Weber et al 1995; Garcia-Perez et al 1998; Vingrys et al 1999).

Shorter threshold tests which preserve accuracy, would be highly desirable for improved patient comfort and for the effective management of patients (Bengtsson et al 1998b) and for compatibility with the increasing financial and resource constraints operative within health care provisions (Wild et al 1998).

1.2.8 Variability

The ability of any perimetric algorithm to detect field loss depends directly on the variability of the results in normal individuals, which defines the limits of normality associated with the given algorithm (Bengtsson et al 1999). The threshold estimate is dependent upon the within- and between-examination variability (Heijl et al 1987a). The within-subject, within-examination variability is known as the short-term fluctuation (SF) and the within-subject, between-examination variability is known as the long-term fluctuation (LF).

For visual field examination out to 30° eccentricity in the normal eye, the within-subject within-examination, and the within-subject between-examination, variability of the threshold response increases with increased eccentricity (Katz and Sommer 1986) and with increase in age (Katz and Sommer 1987). The between-subject within-examination normal variability, upon which the confidence limits for normality are related, also increases with increase in eccentricity and with increase in age (Brenton and Phelps 1986; Heijl et al 1987a).

Threshold variability is large in glaucomatous visual fields, regardless of which perimetric algorithm is utilised (Heijl 1977; Holmin & Krakau 1979; Flamer et al 1984; Werner et al 1987; Heijl et al 1989). It is vital that measurement errors are minimized in perimetry to facilitate ease of interpretation of the examination results thereby maximising the effective management of the patient (Bengtsson et al 1997b).

1.2.9 Current Commercially Available Perimetric Threshold Algorithms
1.2.9.1 Full Threshold 4-2dB Staircase Algorithm

The HFA Full Threshold algorithm consists of a staircase strategy with an initial crossing of threshold in 4dB increments and a final crossing in 2dB increments (Johnson et al 1993c; Wild et al 1999a,b). The final crossing occurs in either an ascending or descending direction and threshold is designated as the last-seen stimulus luminance (Haley 1987). For Program 30-2 and 24-2, the Full Threshold algorithm initially determines the threshold twice at each of four primary seed locations situated at 9°, 9°

eccentricity in each quadrant, with a starting luminance of 25dB. Threshold determination at the immediately adjacent locations then starts at an intensity slightly brighter (2dB) than the expected threshold predicted from the threshold of the neighbouring locations from knowledge of the sensitivity at the primary location and of the slope of the normal hill of vision. A second determination of threshold is obtained at locations that deviate from the predicted threshold by greater than 4dB. Additionally, a repeat determination of threshold is obtained at ten pre-selected locations. These ten double determinations are used to calculate the Short-term Fluctuation. The time required to complete the HFA Program 30-2 (i.e. to threshold 76 locations within approximately 27° eccentricity) in glaucoma is generally in the region of 15 to 16 minutes, per eye (Wild et al 1999a).

Perimetric sensitivity derived with the Full Threshold algorithm decreases with increase in examination duration in normal subjects and in ocular hypertensive and glaucoma patients (Heijl 1977; Heijl et al 1983; Johnson et al 1988a,b; Searle et al 1991; Hudson et al 1994; Heijl and Bengtsson 1996; Wild et al 1989c; Wild et al 1999a,b). This effect, which is attributed to fatigue, becomes greater with increasing stimulus eccentricity and with increasing age and is more pronounced in areas of and adjacent to, field loss (Heijl 1977; Heijl and Drance 1983; Johnson et al 1988b). The reduction in sensitivity occurs within and between eyes at a given visit (Searle et al 1991; Hudson et al 1994).

1.2.9.2 4-2-1dB Threshold Staircase Algorithm

The Programs of the Octopus perimeters consist of an equidistant-point matrix with 6° resolution, which straddles over the vertical and horizontal midlines. Program 32 extends 30° out from fixation and the Threshold algorithm can be used, implementing a 4-2-1dB staircase technique to approximate the individual thresholds (Morales et al 2000). This 4-2-1dB staircase can also be employed in the Threshold algorithm of the Octopus perimeter using Programs G1, G1X and G2. The Threshold algorithm of the Octopus perimeters (Octopus Visual Field Digest 2004; Zulauf et al 1994; Flammer et al 1987; Spahr 1975), first evaluates four "anchor" points located near the centre of each quadrant. If the patient fails to respond to the initial stimulus, stimulus luminance is adjusted in

steps of 6dB or 8dB until threshold is exceeded. After the first reversal, 4dB steps are utilised until threshold is exceeded, then after the second reversal, steps of 2dB are utilised until threshold is exceeded again. The threshold is taken to be the average of the last seen and last unseen stimulus, the final 1dB step being achieved by interpolation. The starting level for the surrounding points is determined from the measurement obtained at the nearest anchor location. The staircase procedure, then spreads with further starting levels being calculated from the intermediate values reached in three neighbouring points. Methodological differences exist in the starting point of the staircase procedure between the HFA and the Octopus perimeters.

1.2.9.3 FASTPAC Algorithm

The FASTPAC strategy is an alternative to the 4-2dB Full Threshold strategy of the HFA and attempts to reduce the examination duration without loss of accuracy in the resultant threshold measurement (Flanagan et al 1993a,b). FASTPAC employs a single crossing of threshold with a 3dB step size, and threshold is designated as the last-seen stimulus luminance (Wild et al 1999a,b).

FASTPAC initially determines threshold at the same four primary seed points, as the Full Threshold algorithm. These values are then used to predict threshold, and therefore to determine the initial stimulus intensity presented, for adjacent stimulus locations. The initial starting luminance at each of the secondary locations is presented 1dB brighter than the expected threshold when the expected threshold is an even number and 2dB dimmer than the expected threshold when the expected threshold is an odd number (Flanagan et al 1993a). The final threshold measurement is derived from the last-seen stimulus intensity following a single crossing of the threshold. However, the FASTPAC algorithm re-thresholds any locations for which the measured threshold deviates from the predicted threshold by 4dB in the same way as the Full Threshold algorithm.

The examination duration of the FASTPAC algorithm, is 30% to 43% shorter than that of the Full Threshold algorithm but is at the cost of an approximate 25% increase in the

short-term fluctuation (i.e. the within-test variability) (Flanagan et al 1993a,b; Mills et al 1994; O'Brien et al 1994; Glass et al 1995; Schaumberger et al 1995). It is also apparent that FASTPAC underestimates focal loss in glaucoma compared to the Full Threshold algorithm (Wild et al 1999b). In addition, FASTPAC demonstrates a greater Mean Sensitivity with smaller values of Mean Deviation (MD) and Pattern Standard Deviation (PSD) than the Full Threshold algorithm (Flanagan et al 1993a; O'Brien et al 1994; Schaumberger et al 1995). Most authors have also concluded that FASTPAC is less accurate (O'Brien et al 1994; Glass et al 1995) or exhibits a greater short-term fluctuation than the Full Threshold algorithm (Flanagan et al 1993a; Schaumberger et al 1995; Bengtsson et al 1997a). However, Mills and co-workers (1994), showed that FASTPAC performed as well as the Full Threshold algorithm in normal visual fields and in early glaucomatous field loss (Bengtsson et al 1997a). The increase in measurement error with the FASTPAC strategy becomes more pronounced with increasing age (Flanagan et al 1993b) and severity of defect (Flanagan et al 1993b; Schaumberger et al 1995).

1.2.9.4 Swedish Interactive Threshold Algorithms (SITA)

SITA (Swedish Interactive Threshold Algorithm), is a second generation of threshold algorithm which is available with the Humphrey Field Analyzer 700 Series. There are two SITA algorithms currently available for standard automated perimetry; SITA Standard and SITA Fast. The former is analogous to the Full Threshold algorithm, using a 4-2dB staircase and the latter to the FASTPAC algorithm, using a 4dB staircase (Wild et al 1998). The SITA algorithms are based upon the ZEST (zippy estimating by sequential testing) algorithm (mentioned previously) (Taylor and Creelman 1967; Watson and Pelli 1983; King-Smith et al 1994; Turpin et al 2003).

The SITA algorithms were designed to achieve a more rapid perimetric examination without reducing the accuracy and efficiency of the threshold estimate. They are statistically more sophisticated than any previous algorithms (Wild et al 1999a,b). A reduction in examination duration without a loss in the accuracy of the threshold estimate is obtained, by using two likelihood functions for each stimulus location, one based upon

the threshold estimate of the normal field and one based upon the threshold estimate of the glaucomatous field (Olsson & Rootzen 1994). The two likelihood models (or Baysian posterior probability functions) are derived from the age-corrected normal threshold value at each location, the between-subject variability in the estimation of threshold (Heijl et al 1989a; Heijl et al1987a), the interdependence of threshold values at adjacent visual field locations (Heijl et al 1989a; Olsson and Rootzen 1994; Åsman and Heijl 1992b) and the magnitude, and variation in shape, of the frequency-of-seeing curve between stimulus locations (Olsson et al 1993; Weber and Rau 1992). The threshold estimate at any given stimulus location is governed by the normal frequency-of-seeing curve and the resultant threshold determined by SITA represents the stimulus intensity that has a 50 percent probability of seeing (Bengtsson et al 1998a).

For each stimulus location, the likelihood functions are calculated for the probability of either a normal or a glaucomatous visual field based on the subject's response. At any given moment, the height of the function, describes the most likely threshold value at the given location, and the width describes the accuracy of the threshold estimate (Bengtsson et al 1997b; Wild et al 1999a,b). Both likelihood functions are adjusted following the positive or negative response to each individual stimulus presentation and the shape of the function is modified further, with an increase in the number of responses, as the test progresses. The threshold estimate, at any given stimulus location not only determined by the normal frequency-of-seeing curve but also from the multiple estimated frequency-of-seeing curves for other stimulus locations. All of the patient responses, 'seen' or 'not-seen', contribute to the calculation of the likelihood function, which corresponds to the stimulus intensity that has the greatest potential to be threshold. The thresholding procedure at any given location, may be halted, at a predetermined level of accuracy which is specified by the Error Related Factor (ERF) (Bengtsson et al 1997a; Wild et al1999). The thresholding procedure is halted when the measurement error estimate is smaller at each particular location than the corresponding ERF. The termination of the staircase is not permitted until at least one staircase reversal has been completed (Bengtsson et al 1997a). Once the examination is complete, the sensitivity at each stimulus location, is re-calculated and the frequency of false responses is determined.

The final threshold determination corresponds to the stimulus intensity that has a 50% chance of being seen on the psychometric function (Bengtsson et al 1998a). The efficiency of SITA arises mainly from its ability to present stimuli at or near this 50% frequency-of-seeing level. Therefore, the number of stimuli required to determine the threshold is dramatically reduced.

Other time saving strategies are also incorporated into the SITA algorithm, e.g. a new flexible timing algorithm for stimulus presentation is used. All patient response times are recorded and are used to ensure that subsequent stimuli are presented at a rate that is optimum for the patient (Bengtsson et al 1997b).

The examination duration is reduced further by a unique method of determining false positive responses. In traditional threshold perimetry, the reliability of the patient's response, is assessed by catch trials (Fankhauser et al 1977; Bengtsson et al 1997a). SITA employs a novel method for the estimation of false responses. False-positive responses are measured as part of the threshold estimation procedure (Olsson et al 1997b). This is made possible by utilising periods during the examination when no positive responses are expected. One such period is that between the stimulus onset and the minimum reaction time of the patient measured to be 180-200ms (de Boer et al 1982; Bengtsson et al 1997a). Responses obtained during such periods are considered to be false-positive responses (Bengtsson et al 1997a). This technique enables a more accurate estimation of false responses than is possible using the traditional method (Olsson et al 1997b). The algorithms also use a minimal number of traditional false-negative catch trials. The pattern of responses is analysed at the conclusion of any perimetric examination to determine the frequency of false-positive and false-negative responses (Olsson et al 1988). For the SITA algorithms, the influence of the false-positive responses, is also removed from the derivation of the frequency-of-seeing curve (Olsson et al 1997b).

1.2.9.5 Dynamic Strategy

In 1990, Weber suggested that the step size should be variable throughout the perimetric examination and should be adapted at any given stimulus location to the width of the physiological threshold zone, which is known to be highly dependent on sensitivity (Chauhan et al 1992, 1993; Weber & Rau 1992; Weber et al 1992; Olsson et al 1993 Vingrys et al 1990; Vingrys & Pianta 1999)   The Dynamic strategy of the Octopus perimeter selects the step-size by referring to the width of the frequency-of-seeing curve at a stimulus location of a given sensitivity.   The fixed step sizes employed by the traditional staircase algorithms do not take into account the fact that the width of the frequency-of-seeing curve increases both as a function of eccentricity and of reduced sensitivity (Vingrys et al 1990; Weber & Rau 1992; Chauhan et al 1993). The step size used by the Dynamic Strategy, varies between 2 and 10dB, depending on the sensitivity. Following the first reversal, the step size is half the initial value. The larger step sizes are therefore used when evaluating areas of visual field loss (Takada et al 1998).   The Dynamic Strategy is also available in Germany for the HFA where it is known as the TURBO Strategy, (Weber 1990; Bengtsson et al 1997a). When comparing the Dynamic Strategy to the Threshold algorithm of the Octopus perimeter, Zulauf et al (1994) found that short term fluctuation and long term fluctuation of the Dynamic strategy increased by 15% and 21%, respectively and the examination duration decreased by 43%. Weber and Klimaschka 1995 also found that short term fluctuation increased with the Dynamic Strategy when compared to the Threshold algorithm.   They also concluded that the efficiency of the dynamic strategy was greatest in normal regions of the visual field.

The variability of the Dynamic Strategy was found to be smaller for normal test locations, but higher in relative defects when compared to the Full Threshold algorithm (Weber & Klimischka 1995). In normal and borderline-normal fields, the Dynamic Strategy is superior to traditional strategies as it maintains accuracy whilst significantly reducing examination duration. At locations with reduced sensitivity, however, the reproducibility was reduced (the defect depth often being imprecise) and thus the advantage of the reduced examination duration was of no value (Weber & Klimischka 1994).

1.2.9.6 DELPHI

The software for the Delphi programme could be downloaded from the Internet onto a Humphrey Field Analyzer or an Octopus perimeter. Delphi perimetry allowed estimation of the central visual field using four 'critical points' whose individual sensitivities were each measured three times. The software then compared the values obtained at these critical points with it's database (the database was derived from 382 glaucoma and ocular hypertension patients and 280 normal, age-matched patients). The software estimated the probable sensitivities for all the other locations in the central visual field by comparing the values at the four critical points with the information contained in the database (Gonzalez de la Rosa et al 1990).

The mean examination duration was approximately one minute per eye (Gonzalez de la Rosa et al 1990; Quach et al 1997; Wishart et al 1998). However, results from Delphi perimetry correlated poorly in terms of the number of correctly identified glaucoma patients or in terms of the spatial localisation of the field defect compared to HFA Program 24-2 and the FASTPAC algorithm (Wishart et al 1998).

1.2.9.7 Tendency Oriented Perimetry (TOP)

Tendency Orientated Perimetry (TOP) is a relatively new approach to visual field examination. TOP is a fast thresholding strategy for the Octopus perimeters that relies upon the correlation of the threshold between adjacent stimulus locations. The anatomical and topographical relationship of the pattern of visual field loss, determines proximal interdependence or "tendencies" among the thresholds of neighbouring zones of the visual field. These tendencies are examined and utilized by the software to obtain an estimate of the threshold at each location in the visual field (Gonzalez de la Rosa et al 1996).

TOP assesses the visual field by presenting one stimulus only, per test location. The patient's response is used to calculate the threshold at the specific test location and in the adjacent area by determining the intensity of subsequent stimuli presentations (Gonzalez

de la Rosa et al 1996). The algorithm, divides the stimulus locations within the central field into four matrixes, each consisting of 19 locations that are each separated by 12°. A MOBS procedure is used to begin the estimation of threshold at each location in the first sub-matrix. The initial luminance presented at each of the locations in the first matrix, is half that of the age-corrected normal sensitivity. The initial estimates of threshold for the first sub-matrix are used to update the estimates of thresholds for the remaining sub-matrixes by linear interpolation.

The response from the initial presentation, at each location creates either a positive or a negative (corresponding to a brighter or dimmer stimulus, respectively) adjustment to the first approximation of the threshold estimate at the given stimulus location and also at adjacent locations in the ensuing matrix. The adjustment is equivalent to 4/16 of the expected age-corrected threshold at the given location. The threshold is then determined at the 19 locations of the second matrix and the positive or negative adjustment is repeated for these locations and for the adjacent locations. The adjustment for the second matrix is equal to 3/16 of the age-corrected threshold value. The process is then repeated for the third and fourth matrixes, the adjustments being 2/16 and 1/16 of the age-corrected threshold value, respectively. This procedure enables a rapid perimetric examination. The examination duration is approximately 20% of the time of a Threshold examination for an identical number of stimulus locations, being in the region of 4 minutes per eye for Program 32 (Morales et al 2000; Wadood et al 2002).

TOP underestimates the depth of glaucomatous loss when compared to the Program 32 and the Threshold algorithm of the Octopus (Lachkar et al 1998) and Program 30-2 and the SITA Fast algorithm of the HFA (King et al 2002). . Despite the obvious benefit of the reduced examination duration of TOP, the underestimation of field loss suggests that the algorithm should be used with caution, particularly in the detection of early glaucoma.

1.2.9.8 Frequency Doubling Perimetry (FDP)/ Frequency Doubling Technology (FDT)

Frequency doubling perimetry was designed to provide a rapid, effective and reliable perimetric technique for the early detection of glaucoma. The frequency doubling illusion is the conceptual basis of frequency doubling perimetry and states that a sinusoidal grating of low spatial frequency (0.25 cycles/degree) with a high temporal frequency (>15Hz) will produce a perceived image that is twice its actual spatial frequency (Kelly 1976, 1981; Alward 2000; Burnstein 2000).

The ability to perceive this illusion is thought to be a function of the magnocellular pathway. In glaucoma the magnocellular retinal ganglion cells appear to be damaged early in the disease process (Johnson and Samuels 1997; Quigley 1998; Maddess & Henry 1992). They are considered to be involved in the processing of motion and high-frequency flicker perception (Livingstone & Hubel 1987, 1988). The retinal ganglion cells of the M pathway are sparsely represented and overlapped. They exhibit receptive fields that tend to be particularly responsive to high temporal and low spatial frequency information and to achromatic or luminance information (Kaplan and Shapley 1982). The retinal ganglion cells of the M pathway are sparsely represented and overlapped. The frequency doubling illusion is assumed to be mediated by the M_y ganglion cells, a subset of approximately 15% to 25%, of the M cells (Kaplan and Shapley 1982; Marrocco et al 1982; Maddess & Henry 1992). The M_y ganglion cells may be particularly sensitive to glaucomatous damage.

The apparent tendency of the M cells for early death may represent the true selective loss of these large-diameter nerve fibres or an apparent selection of under-represented fibres for greater relative redundancy. In either case, by testing for early glaucomatous visual field loss, frequency doubling perimetry theoretically should assist in the early detection of glaucoma (Burnstein et al 2000).

The commercially available Frequency Doubling Technology (FDT) perimeter presents stimuli via a 40° horizontal by 40° vertical square display screen. The stimuli which subtend 10° by 10° are presented at random intervals at 17 locations: four in each

quadrant and one centrally of 10° diameter for the C-20 Full Threshold examination and two additional locations above and below the nasal meridian at between 20° and 30° eccentricity for the N-30 Full Threshold examination. Each stimulus comprises a 0.25cycles/degree sinusoidal grating which undergoes counterphase flicker at 25 Hz. In theory, the perceived stimulus is a grating whose spatial frequency appears to have twice the spatial frequency of the presented stimulus. The luminance of the background is 100cdm^{-2} and the fixation target is a small dark (45 min of arc in diameter) central target (Quigley 1998; Sponsel et al 1998; Patel et al 2000; Delgado et al 2002; Wall 2004).

The algorithm used in FDP is the MOBS algorithm (discussed previously). Each stimulus is presented in random order and the target contrast is adjusted during the course of the examination. The range of possible threshold values is between 0dB maximum contrast for the highest threshold, up to 33.1dB for minimum contrast, for the lowest threshold (Adams et al 1999).

1.2.9.9 Fundus Oriented Perimetry and Fine Spatial Resolution Perimetry

Fundus-oriented perimetry (FOP) allows the formation of an individual perimetric grid for each patient, which corresponds to suspicious or manifest changes in the optic nerve head or fundus (Dietrich et al 1999, 2000; Schiefer et al 1996; 2001). The area to which the grid will be applied (the region of interest, ROI) for each eye is determined from stereo-observation of the fundus and is spatially located with the assistance of fundus photographs. In the designated ROI, the spatial resolution of the conventional 6° square stimulus grid out to 30° eccentricity, which consists of 73 stimulus locations, is enhanced by the addition of 64 extra stimulus locations, enabling a maximum of 137 possible stimulus locations. An interactive algorithm ensures that there is a constant inter-stimulus separation for the additional stimulus locations within the ROI. The number of stimulus presentations and the resolution of the stimulus locations are dependent on the dimensions of the ROI. All of the stimulus presentations occur within two sub-examinations. Stimuli from the conventional grid and from the grid corresponding to the ROI are both designated randomly into each sub-examination.

31

Long-term fluctuation can be determined from nine identical reference locations within each grid. One of the nine reference locations is situated at fixation, the remaining eight are situated along the oblique meridians, four at 12.7° eccentricity and four at 29.7° eccentricity respectively (Schiefer et al 1996; 2001).

1.2.9.10 High-Pass Resolution Perimetry

High-pass resolution perimetry (HRP) was first introduced by Frisen (1987a,b). The stimuli consist of rings of 13 different sizes ranging from 10 to 160 minutes of arc, which are generated by filtering a ring stimulus with a high-pass filter. The resultant stimulus is a high spatial frequency ring with dark borders surrounding a lighter core. The dimensions have a consistent ratio, i.e. the width is always 1/5 of the diameter. The core, border, and background luminances are 25, 15 and 20 cd/m², respectively. Each stimulus presentation lasts 165ms.

Unlike conventional perimetry, where sensitivity is determined by varying the luminance of a fixed size stimulus, in HRP, sensitivity is determined by varying the stimulus size independently of luminance. Rings that are too small to be resolved will be invisible, as the core and borders will blend into the background. Within 30° eccentricity, there are 50 stimulus locations. The stimulus locations are divided into 3 groups, each group is thresholded in sequence using a random order within each group. An up-down staircase, of stimulus size, is used to bracket around the threshold using unequal step sizes, and continuously alternating between the stimulus locations. The start size for each stimulus location is based on the threshold information already derived for adjacent locations. As many as ten locations, are re-thresholded to provide an indication of the short-term fluctuation (Frisen 1987a,b)

The threshold for HRP, is directly proportional to local ganglion cell separation. The functional integrity of the visual system at the given stimulus location, can be estimated from the threshold by using resolution thresholds to calculate an index known as the

neural capacity (NC). The NC is calculated as a percentage of the average age-corrected normal value (Frisen 1988, 1989; Wall 1991; Chauhan and House 1991; Kono 1997). Other advantages of HRP are that it exhibits low variability (Martin-Boglind and Wanger 1989; Douglas et al 1989; Drance et al 1989; Chauhan et al 1991; Martin et al 2000) and the examination duration is approximately 5 minutes per eye (Kono et al 1997).

1.2.9.11 High Spatial Resolution Perimetry

Perimetry performed at a higher spatial resolution (HSRP) can obtain more information regarding the luminance sensitivity in selected areas of the visual field (Westcott et al 1997). It has been shown that implementing high resolution perimetry can identify subtle scotomas that were not detected by conventional perimetry (Westcott et al 1997; Orzalesi 1999; Garway-Heath et al 2000). In glaucoma, HSRP has been shown to be one of the methods with the highest sensitivity for detecting visual field loss (Graham et al 1996; Chauhan et al 1999).

A recent development in HSRP is the Nidek MP-1 Micro Perimeter which enables the projection of a fine resolution perimetric grid, of specified dimensions, onto the real image of the fundus on the monitor. This enables the precise retinal location under examination to be precisely mapped (MP-1 Micro Perimeter Operator's Manual, Nidek Technologies Srl., Via Regia, Vigonza, Italy).

1.2.9.12 Suprathreshold Perimetry

Suprathreshold static perimetry presents a stimulus with a luminance at a level that normally should be above the threshold. Suprathreshold tests are also known as screening tests as they offer a rapid method of determining whether the visual field is normal to the given suprathreshold increment (Bebié 1985; Lewis et al 1986; Coffey et al 1993; Katz et al 1993; Dielemans et al 1994; Sponsel et al 1995; Artes et al 2003). The ability of a suprathreshold examination to detect glaucoma is approximately 90% or more (Johnson et al 1978; Keltner and Johnson 1981; Dannheim 1987) Early glaucomatous

visual field loss identified by threshold perimetry, however, can remain undetected with suprathreshold perimetry (Mills et al 1994).

The earlier suprathreshold strategies did not incorporate gradient adapted stimuli i.e. the sensitivity gradient across the visual field was not taken into account in the presentation of the stimulus luminance at different locations. The stimulus luminance during the examination is not at a constant magnitude brighter relative to the actual threshold: if the stimulus is at threshold in the periphery, it will be significantly suprathreshold in the central and paracentral areas. If this is the case, any small relative defects present in the foveal and parafoveal regions, will be missed (Gramer et al 1982). The technique has little application in clinical perimetry due to the limited specificity.

The currently available suprathreshold strategies, are gradient adapted i.e. they utilise a stimulus, the luminance of which increases with increase in eccentricity such that the suprathreshold increment is constant across the visual field. This does improve the sensitivity in detecting focal loss, but does not ensure that shallow defects will not be missed (Keltner et al 1979; Mills et al 1994).

The magnitude of the suprathreshold increment varies between types of perimeter. With these strategies, the visual field can only be graded as either normal or abnormal for the suprathreshold increment in question. The use of an additional stimulus presented at maximum luminance provides the opportunity to grade the field as either, normal, relative or absolute for either of these strategies (Keltner et al 1979).

The suprathreshold increment for gradient-adapted suprathreshold perimetry may be referenced to the age-corrected hill of vision (i.e. age-corrected gradient adapted suprathreshold perimetry) or alternatively, (Stewart et al 1989) referenced to the individual patient's threshold at one or more central locations (threshold-related gradient adapted suprathreshold perimetry). By estimating the threshold at more than one central location the selection of an inappropriate threshold level due to an erroneous response is minimised (Heijl 1985). The threshold-related gradient-adapted strategy may show

considerable intra-individual variation in normal observers of the same age depending on patient reliability and physiological factors (Heijl 1984). The threshold-related gradient adapted technique is still unsatisfactory in detecting a shallow relative scotoma (Stewart et al 1989). As with threshold perimetry, the results from suprathreshold perimetry exhibit a large between examination variability in patients with glaucoma (Spry et al 2000; Artes et al 2003).

Multisampling suprathreshold strategies are those to which probability theory has been applied in order to investigate various suprathreshold pass criteria (i.e. the number of stimuli that have to be seen for a particular stimulus location to be classified as normal). An example of a multisampling suprathreshold strategy is one which requires three 'seen' or three 'not seen' stimuli per stimulus location. Multisampling suprathreshold strategies show a similar sensitivity in the detection of visual field loss to threshold perimetry but are superior to conventional suprathreshold perimetry (Artes et al 2003).

1.3   Presentation of Perimetric Examination Results
1.3.1   Numerical and Greyscale Threshold Printouts
The numerical printout is a representation of the subject's measured sensitivity in decibels at each stimulus location within the visual field. The numerical printout is arranged in terms of the spatial location of the stimulus grid. A location which has undergone a second determination of threshold is generally depicted with the two values of sensitivity, the second determination is often in brackets beneath the initial determination.

The gray scale printout translates the raw data into different depths of gray according to the magnitude of the sensitivity. The grayscale is intended to make the interpretation of the threshold values easier. The grayscale printout interpolates the sensitivity between locations generally based upon the sensitivity of the neighbouring four locations (Fankhauser and Bebié 1979). Linear interpolation gives a smoother outline to the borders of scotoma but mixed interpolation is recommended for research purposes (Weber and Geiger 1989). The depths of gray colour are usually arranged into 5dB

35

intervals. High sensitivity is represented by lighter grays and lower levels of sensitivity are represented by darker grays. Linear calculations parallel to the x and y axes of the grid (Weber and Geiger 1989) or a combination of both may also be performed. Due to the differences in their maximum stimulus luminances and their dynamic ranges, different perimeters have different grayscales. For the HFA, the grayscale is currently optimized for the Full Threshold strategy.

The grayscale printout may be of assistance in swiftly identifying abnormal sensitivities and can be more easily interpreted than the numeric raw data. However, the interpolation between locations gives the impression that there is more data than actually present (Heijl 1984). The grayscale should be interpreted with caution as it is a poor representation of diffuse glaucomatous visual field loss (Flammer 1986); is not corrected either for age or for eccentricity and can mask early visual field loss.

1.3.2 Deviation and Probability Plots

Probability plots show the statistical likelihood of the measured value at any given location lying within the range associated with the age-corrected normal value of sensitivity. The measured value of sensitivity becomes less likely to lie within the normal range, as the probability symbol darkens.

The HFA uses the STATPAC software program that provides probability plots based upon empirical data (Johnson 1989; Heijl et al 1991; Anderson and Patella 1999). The Total Deviation plot numerically displays the deviation between the measured sensitivity and the age-matched normal value, determined for each stimulus location. The Total Deviation probability map displays the associated levels of statistical probability (<5%, <2%, <1% and <0.5%). A value of p<0.5% indicates that the deviation from the age-corrected normal value at that given location would be found in less than 0.5% of the normal population.

The Pattern Deviation values and probability plot, represent the shape of the visual field rather than its height. The Pattern Deviation values are derived from the Total Deviation values by making an adjustment for the 'General Height Index' for the individual's hill of vision. The Pattern Deviation values localise defects by subtracting the effect of a diffuse generalised depression in sensitivity. A diffuse overall depression in sensitivity can result from such factors as uncorrected refractive error, small pupils or cataract.

The adjustment for the General Height Index is made based upon the threshold determined at a representative location in the least depressed region of the visual field and its deviation from the age-corrected normal threshold at that location. For both Programs 30-2 and 24-2, only the locations contained within the 24-2 grid are considered. The three locations situated nearest the blind spot are ignored. Of the remaining 52 stimulus locations, the six locations exhibiting the highest sensitivity relative to the age-corrected normal sensitivity, are not taken into account because it is possible that they may provide a misleading representation of an abnormally high estimate of general sensitivity. Consequently the seventh highest threshold relative to the age-corrected normal threshold is taken to represent the overall General Height Index of the hill of vision. This is the 85th percentile best location. The deviation of this location from its corresponding age-corrected normal value, is subtracted from the deviation from normal, of all examined locations to give the numerical Pattern Deviation plot and is also represented in the Pattern Deviation probability plot (Anderson and Patella 1999). The Pattern Deviation of the seventh best location, therefore becomes zero and the deviations of all other examined locations are adjusted by the same amount. The calculations are made to the nearest 10th of a decibel, but are displayed on the printout rounded to the nearest integer.

Early probability analysis assumes a Gaussian distribution of sensitivity at each location (Schwartz and Nagin 1985). A Gaussian distribution, however, cannot explain the distribution of the deviations from the normal response, particularly with increase in eccentricity (Brenton and Phelps 1986; Heijl et al 1987a). Empirical distributions for the Total Deviation map yield a 10% increase in sensitivity and specificity compared to that

for a Gaussian distribution especially in the peripheral regions of the central field where variability is at its highest (Heijl and Åsman 1989).

The corresponding analyses for the Octopus perimeters, are the Comparison values (equivalent to the Total Deviation values), Corrected Comparison (equivalent to the Pattern Deviation values), Comparison probability plot (equivalent to the Total Deviation probability plot) and Corrected Comparison probability plot (equivalent to the Pattern Deviation probability plot).

1.3.3 Three Dimensional Plots

The hill of vision can be illustrated qualitatively by three-dimensional plots. There is very little standardisation of the display parameters e.g. grid resolution, sensitivity scaling and plot orientation, of such plots (Hart and Hartz 1982; Wild et al 1987). A qualitative representation of the cross-sectional view of the hill of vision can also be provided by profile plots along a particular meridian. However, such representations are of limited clinical value.

1.3.4 Bebié Curve (Cumulative Defect Curve)

The Bebié Curve (also known as the cumulative defect curve), is a graphical display of the cumulative distribution of defect depth at each measured location across the field. It attempts to differentiate normal visual fields from those with early diffuse loss (Bebié et al 1989). The defect depth at each individual stimulus location is ranked in ascending order of severity. The cumulative distribution of the 5th, 95th and 99th percentiles of the age-matched normal data serve as a comparison for the measured distribution (Bebié et al 1989). A normal visual field generates a curve that is situated within the 95th percentile. Visual field loss causes a depression of the curve, below that of the 95th or 99th percentile. The magnitude of the depression of the curve corresponds to the degree of diffuse visual field loss. Diffuse visual field loss exhibits a curve that lies parallel to the shape of the curve for normality, but has a greater overall defect depth. A sharp fall in the curve beyond that of the normal range indicates localised visual field loss. Differentiating

between diffuse and localised loss is often difficult (Funkhouser et al 1992a), because the spatial characteristics of the visual field are lost with the Bebié curve (Åsman and Olsson 1995). For this reason, it is vital that the curve is interpreted in conjunction with spatial displays (Kaufmann and Flammer 1989).

1.3.5 Global Indices

The visual field indices are calculated from the age-corrected normal visual field. They are used to summarise the differences between the subject's measured visual field and the age-corrected normal field. The visual field indices reduce the large amount of numerical data into single summary statistics (Bebié 1985; Flammer 1986; Heijl et al 1987b). The accompanying level of statistical significance delineates whether an index lies outside the normal range. Various visual field indices have been produced for the Octopus (Flammer 1986) and the HFA (Heijl et al 1987b) and subsequent perimeters. The indices for the HFA incorporate a weighting function in order to allow for the physiological variability of sensitivity across the visual field within- and between-subjects. The use of the weighting function in the determination of the indices gives greater influence to the central locations as opposed to the more peripheral locations.

1.3.5.1 Mean Sensitivity

The Mean Sensitivity (MS) represents the mean of the measured sensitivities at all stimulus locations within the visual field. MS does not require any normal values for the calculation and is influenced by diffuse changes, but not greatly by small areas of localised loss (Flammer 1986). The MS is calculated by:

$$MS = \frac{1}{m} \cdot \sum_{i=1}^{m} \overline{x}_i$$

where, $\overline{x}_i = \frac{1}{n} \cdot \sum_{k=1}^{n} x_{ik}$

i, is the test location; x_i is the measured value (the result of the threshold estimation at location I); m, is the number of test locations excluding the blind spot region; and n, is the number of threshold replications (independent measurements within the same examination).

1.3.5.2 Mean Deviation and Mean Defect

The Mean Defect (MDo) is the mean of the difference between the age-matched normal value at each stimulus location and the measured sensitivity and is the index used on the Octopus perimeters. Mean Defect is similar to MS but the comparison to the normal age-matched values allows for easier interpretation as a value of zero indicates normality and a positive value indicates an abnormal visual field (Flammer 1986). The Mean Defect is defined as:

$$MDo = \frac{1}{m} \cdot \sum_{i=1}^{m} (z_i - \bar{x}_i)$$

where, m is the number of stimulus locations excluding the blind spot region; z_i, is the age-corrected normal value at test location; i and x_i, is the measured value. MDo is sensitive to focal loss but is relatively unaffected by diffuse visual field loss.

For the HFA, the Mean Deviation (MD) value is the arithmetic mean of the difference between the measured sensitivity at each stimulus location and the age-corrected normal value. The Mean Deviation summarizes deviations of height (Heijl et al 1987b) and becomes increasingly negative value with increased visual field loss. MD is defined as:

$$MD = \left\{ \frac{1}{n} \cdot \sum_{i=1}^{n} \frac{(\bar{x}_i - N_i)}{s_{1i}^2} \right\} / \left\{ \frac{1}{n} \cdot \sum_{i=1}^{n} \frac{1}{s_{1i}^2} \right\}$$

where, s_{1i}^2 is the variance of normal field measurements at location i.

40

The Mean Deviation is weighted at each location (i) for the variation of threshold concurrent with an increase in eccentricity, s_{1i}^2 (Heijl et al 1992). The weighting of the MD, does not alter the magnitude but improves the accuracy of the index.

Funkhouser and Fankhauser (1991) suggested that weighting the MD for the normal physiological fluctuation in threshold does not account for the additional fluctuation arising in abnormal areas of the field. The unweighted Mean Defect and the weighted Mean Deviation yield similar values in glaucomatous visual fields (Funkhouser and Fankhauser 1991; Flanagan et al 1993c).

1.3.5.3 Pattern Standard Deviation and Loss Variance

The Loss Variance (LV) index for the Octopus perimeter calculates the variance of the localised deviations from the age-corrected normal values and in essence is a summary of the shape of the visual field. LV is expressed in dB^2 and is defined by:

$$LV = \frac{1}{(m-1)} \cdot \sum_{i=1}^{m} (z_i - MD - \bar{x}_i)^2$$

where, MD represents the Mean Defect, z_i represents the age-corrected normal value of sensitivity and x_i is the result of a repeated threshold measurement at location i and m is the number of stimulus locations. The greater the localised defect and/or variability in the subject's response, the greater the value of LV will be.

The analogous index for the HFA is the Pattern Standard Deviation (PSD). The PSD is expressed in dB and is a weighted index which is described by:

$$PSD = \sqrt{\left\{ \frac{1}{n} \cdot \sum_{i=1}^{n} s_{1i}^2 \right\} \cdot \left\{ \frac{1}{n-1} \cdot \sum_{i=1}^{n} \frac{(\bar{x}_i - N_i - MD)^2}{s_{1i}^2} \right\}}$$

where, xi is the measured threshold, Ni is the normal reference threshold at point i, s_{1i2} is the variance of normal field measurements at point i, MD is the Mean Deviation index

and m is the number of stimulus locations excluding the blind spot. Weighting with s_{1i2} optimises the PSD in normal subjects but increases the value of patients with glaucoma (Flanagan et al 1993c).

The magnitudes of LV and PSD are always positive and both increase with increase in the disparity in shape between the measured field and that of the normal reference field. The shape of the measured field closely matches that of the reference field, with or without a uniform reduction in visual field height, as values of LV and PSD tend towards zero.

As the depth of visual field loss increases, the difference between the weighted PSD and unweighted LV becomes more apparent. The characteristics of the normal reference data (Heijl et al 1992) and methodological differences in determining threshold (Fankhauser et al 1988) are thought to account for the difference between the appropriate weighted and unweighted values.

The HFA programs 30-2 and 24-2 produce similar indices and the weighting function slightly elevated Pattern and Corrected Pattern Standard Deviations compared to the non-weighted values of these indices (Flanagan et al 1993c). The weighted versions of hemifield and cluster analyses give a higher level of sensitivity and specificity than the corresponding unweighted analyses (Åsman and Heijl 1992b).

1.3.5.4 Corrected Pattern Standard Deviation and Corrected Loss Variance

The corrected loss variance (CLV) separates the variance associated with visual field loss from the short-term fluctuation (SF). CLV is expressed in dB^2 and is defined by (Flammer 1986):

$$CLV = LV - \frac{1}{n} \cdot (SF)^2$$

42

CLV co-varies with MD in early to moderate glaucomatous field loss defined up to a Mean Defect of approximately 18 dB (Pearson et al 1990). Gollamundi et al (1988) suggested the use of a different index:

$$(CLV)^{-0.5} - MD$$

to differentiate between the severity of glaucomatous visual field loss.

The corrected pattern standard deviation (CPSD) is analogous to the CLV. It is expressed by:

$$CPSD^2 = PSD^2 - k \cdot SF^2$$

where, k is a constant > 1 and is used to compensate for the non-uniform spatial arrangement of the SF. The CLV and CPSD are never assigned a value less than zero because, although the estimates may be less than zero, variances are never negative. Hayashi et al (2001) suggested that the CPSD is the index that most accurately expresses the degree of glaucomatous visual field loss.

1.3.6 Defect Volume

The defect volume (DV) index is defined as the difference between the volume of the measured visual field (VOL_{meas}) and that of the normal age-corrected reference field (VOL_{norm}):

$$DV = VOL_{norm} - VOL_{meas}$$

The DV is an expression of the three-dimensional hill of vision (Langerhorst et al 1985, van den Berg et al 1985). The volume of the visual field has been used to note the learning effect in static perimetry (Wild et al 1987; Wood et al 1987) and in determining the change of the profile of the visual field with age (Jaffe et al 1986).

1.3.7 Diffuse Loss Indices

The relevance of diffuse visual field loss as an indication of the presence of glaucoma is a subject on which there has been much disagreement. Many authors have concluded that the presence of diffuse visual field loss in the absence of focal loss, is an early perimetric indicator of glaucoma (Anctil and Anderson 1984; Glowazki and Flammer 1987; Drance 1991). However, other groups' conclusions were to the contrary (Werner et al 1982; Heijl 1989; Langerhorst et al 1989; Asman and Heijl 1994; Asman et al 1992).

The standard indices used to evaluate diffuse visual field loss are the Mean Deviation and Mean Defect. However, focal loss will strongly influence the value of the Mean Deviation and the Mean Defect, as both indices average the deviations of all measured estimates of sensitivity from the corresponding age-corrected normal values (Asman 2004). Focal loss does not influence the Individual General Sensitivity index, devised by Langerhorst et al (1989).

Another method which attempts to separate diffuse visual field loss from focal loss is the Cumulative Defect Curve (Bebié et al 1989). However, the efficacy of the cumulative defect curves for the detection of pure diffuse loss is limited since the normative limits currently implemented, are based on the results from the mid-peripheral locations (Åsman and Olsson 1995). Threshold variability increases with eccentricity (Parrish et al 1984; Brenton and Phelps 1986; Heijl et al 1987) which suggests that locations exhibiting reduced sensitivity are more likely to exist in the mid-periphery. However, most of the significantly depressed locations in the probability maps of glaucomatous visual fields, are often located more centrally (Anderson 1992; Heijl and Lundquist 1984; Åsman and Olsson 1995). The central locations of a normal visual field usually exhibit less variability than mid-peripheral locations, so even small reductions in sensitivity are significant once location has been taken into consideration by the PD probability map. Cumulative Defect Curves compare the deviation values in central locations with percentiles derived from mid-peripheral locations, so small central reductions in sensitivity will not be identified as abnormal in the Cumulative Defect Curves once the

spatial representation has been removed (Åsman and Olsson 1995). The boundary between diffuse and focal loss in Cumulative Defect Curves is not well defined (Funkhouser et al 1992ab; Åsman and Olsson 1995).

The Diffuse Loss index was devised by Funkhouser (1991) as a refinement to the Cumulative Defect Curve in which the plateau region of the curve was used to calculate an index that specified the mean loss of the plateau and provided an accurate and quick estimation of the general depression (Funkhouser et al 1992b).

The PD probability values are derived from the TD probability values by means of the calculation of the General Height (GH) Index. The GH Index is also applied in the Glaucoma Hemifield Test (GHT) which is discussed later. The GH Index is defined as the 85th percentile (corresponding to the 7th most positive value) of the distribution of the TD values of the 51 locations contained within the Program 24-2 grid (excluding 3 blind spot locations) for both Programs 30-2 and 24-2. Although, the purpose of this index is to extract the effect of diffuse loss, often it may consist of a calculation derived from as many as six locations with normal thresholds (Flanagan et al 1993).

1.3.8 Spatial Correlation and Cluster

The Spatial Correlation (SC) index is the average value obtained by multiplying the Mean Defect at each stimulus location by the defect value at each of the adjacent locations (Bebié 1985). Two or more adjacent abnormal stimulus locations make up a cluster (Chauhan et al 1989). The Spatial Correlation (SC) index is expressed as:

$$SC = \frac{1}{p} \cdot \sum_{(ij)} (z_i - MD - \bar{x}_i) \cdot (z_j - MD - \bar{x}_j)$$

where, p is the number of pairs of stimulus locations (i, j) used in the calculation. The SC describes the extent of the clustering of abnormal stimulus locations exhibiting abnormality. When defects are dispersed throughout the field, the SC is low. When

defects are clustered, the SC is high (Flammer 1986). Cluster analysis has been applied to glaucomatous visual field loss in relation to the spatial arrangement of the RNFL (Åsman et al 1992a; Mandava et al 1993). In glaucoma, clustered locations occur more frequently in the superior hemifield than in the inferior hemifield (Chauhan et al 1988).

Cluster analysis is based upon the assumption that there is a low probability that a normal visual field will display two or more clusters of locations with reduced sensitivities. The Spatial Correlation index describes the degree of adjacency of locations exhibiting abnormality, but cluster analysis specifically describes the clusters themselves. Cluster size (SIZ), cluster depth (CLUS), centroid (mean x-y coordinate), the number of clusters and the total size and depth may be determined (Chauhan et al 1989). PCLUS quantifies the percentage of the MD that is clustered. The sensitivity and specificity of the cluster indices, SIZ, CLUS, and PCLUS, have been compared with the global indices MD, and CLV (Chauhan et al 1990). CLV and PCLUS were more able to differentiate between visual field stability and visual field progression (Chauhan et al 1990). In addition, the cluster indices were more effective in determining progressive loss of sensitivity occurring in the previously normal field than in determining the presence of further deterioration in an already abnormal field (Chauhan et al 1990) particularly in the superior hemifield (Åsman and Heijl 1992a,b).

1.3.9 Third Central Moment and Skewness

The third central moment (M3) is the distribution of deviations from the age-corrected normal reference values. M3 is expressed by,

$$M3 = \frac{1}{m} \cdot \sum_{i=1}^{m} (z_i - MD - \overline{x}_i)^3$$

The M3 index describes those locations that deviate by the greatest degree from their age-matched normal values. M3 is sensitive to deviations at a small number of locations. It has been suggested that M3 may be useful for the detection of very early visual field defects (Flammer 1986) but this claim has not been substantiated.

It has been proposed that Skewness (Q), which is a standardisation of M3 with respect to LV, is a better index to identify locations in which the threshold deviates from the expected value (Brechner and Whalen 1984).

Q is expressed by:

$$Q = \frac{M3}{\sqrt{(LV)^3}}$$

The Q statistic is more effective than M3 in identifying very early defects in those fields exhibiting low variability and less effective in the presence of larger defects, high variability and diffuse loss (Pearson et al 1989).

1.3.10 Glaucoma Hemifield Test (GHT)

Early glaucomatous visual field defects usually occur in isolation in one hemifield (Drance et al 1979; Hart and Becker 1982; Mikelberg and Drance 1984). Hemifield analyses of visual field data have been proposed to identify glaucomatous visual field loss (Duggan et al 1985; Sommer et al 1987; Åsman and Heijl 1992a,b). The advantage of this type of analysis is that the individual field provides its own baseline reference level.

The Glaucoma Hemifield Test (GHT) for the HFA compares the Pattern Deviation probability values in five sectors in the superior hemifield with their mirror images in the inferior field in order to specifically detect localised glaucomatous visual field loss (Åsman and Heijl 1992a,b). The five anatomical sectors each containing between 3 and 6 locations, according to the arrangement of the retinal nerve fibres, are superimposed upon the Program 30-2 stimulus grid. A probability score is calculated for each location within the five sectors based upon the Pattern Deviation probability values (Asman and Heijl 1992a,b). Within each sector, the sum of the transformed probability scores is calculated and the difference compared to the mirror image sector. The visual field is categorised as "outside normal limits" if the difference in any of the five corresponding pairs of sectors

falls outside the 0.5% or 99.5% confidence limits for that pair of sectors. A "borderline" classification is presented when any sector-pair difference exceeds the 3% confidence limit. If the General Height of the field is below the 0.5% limit, the GHT evaluates the field as a "general reduction in sensitivity". A classification of "abnormally high sensitivity" is associated with a high level of false-positive responses. The General Height test is not performed if the visual field has already been classified as "outside normal limits". The GHT is used to detect localised loss which is derived from the pattern deviation plot significance points (Zalta 2000; Åsman and Heijl 1992a).

Katz et al (1995) showed that the repeatability of the GHT between two successive visual field examinations (separated by either 4 or 12 months) is only adequate; different GHT results were found in 17.1% of normal subjects, 20.0% of patients with ocular hypertension and in 9.5% of glaucoma patients with mild to moderate field loss. The sensitivity for glaucomatous abnormality was 80.8% and 81.4% and the specificity was 84.2% and 84.7% at the first examination in patients with ocular hypertension and glaucoma, respectively, for the GHT. At the second examination, sensitivity improved to 69.8% for the patients with ocular hypertension (i.e. these patients were designated as being less likely to exhibit glaucomatous field loss) and 80.0% in the glaucoma patients. The corresponding specificities were 89.5% and 89.9% respectively. However, the GHT should not be exclusively used, or relied upon, to provide information on the presence of visual field loss (Katz et al 1995). Approximately 27% of patients were designated as "within normal limits" by the GHT analysis, but exhibited glaucomatous defects on the Pattern Deviation analysis (Zalta 2000).

1.3.11 Learner's Index (LI)

Perimetric experience is associated with an improvement in reliability, an increase in sensitivity and a reduction in the artefacts associated with the measured sensitivity (Heijl et al 1989c; Marra and Flammer 1991; Olsson et al 1997). Typically, the visual field from a patient inexperienced in perimetry exhibits a depressed mid-peripheral portion of the central visual field and a normal central region of the central visual field. A learning

effect has been demonstrated in normal individuals (Wood et al 1987; Heijl et al 1989c; Searle et al 1991), patients with ocular hypertension (Wild et al 1989; Werner et al 1990) and patients with glaucoma (Werner et al 1988; Marchini et al 1991) and is more pronounced for peripheral rather than central stimulus locations (Wood et al 1987; Heijl et al 1989b; Werner et al 1990; Searle et al 1991; Marchinin et al 1991; Hudson et al 1994). The Learner's Index (LI) was developed to detect regions of apparent low sensitivity which might result from a lack of perimetric experience (Åsman et al 1993; Åsman and Heijl 1994b). Three visual fields were obtained from each of 74 normal individuals, seven of these individuals exhibited a learning effect. The LI was calculated from the first visual field from the "learning" subjects and the third field in all subjects. Each visual field was divided into five concentric zones. The average deviation from the age-corrected normal value was calculated for each zone in the "learning" group. The variances and covariances between the results from the five zones were used to determine a linear discriminant function, the LI. A value of zero indicated an entirely normal visual field, and an average "learner" will exhibit a value of approximately one.

Åsman and Heijl (1994) evaluated the LI in 10 eyes of 10 normal individuals and 20 eyes of 20 glaucoma patients. They found that normal individuals who exhibited abnormal GHT results at the first visual field examination were associated with high LI values, which decreased rapidly towards zero with repeated examination. In the glaucoma group, abnormal GHT results obtained at the first visual field examination were associated with a low LI.

1.3.12 Short-term Fluctuation (SF)

The within-subject, within-examination variability that occurs during a single perimetric examination is known as the Short-term Fluctuation (Bebié et al 1976; Flammer et al 1984a,b) and essentially represents the measurement error. The Short-term Fluctuation is calculated from the differences in repeated measurements of sensitivity at each given location in the field. The Octopus perimeter assumes a constant variance at all locations and expresses the SF with an unweighted index as follows:

$$SF = \sqrt{\frac{1}{m} \cdot \sum_{i=1}^{m} (SD_i)^2}$$

where, m is the number of locations, i is the stimulus location, and SD is the standard deviation of the threshold estimates at location i (Flammer 1986).

It has been shown that, SF varies with eccentricity (Brenton and Phelps 1986). Heijl et al (1987a) found that SF was up to 27% greater at four peripheral locations than at the six most central locations. The variation of SF with eccentricity is taken into account, by the HFA. The HFA obtains double determinations of threshold at each of ten locations in the visual field and calculates a weighted mean of the standard deviation to determine the SF using the equation:

$$SF = \sqrt{\left\{ \frac{1}{10} \cdot \sum_{j=1}^{10} s_{2j^2} \right\} \cdot \left\{ \frac{1}{10} \cdot \sum_{j=1}^{10} \frac{(x_{j1} - x_{j2})^2}{2(s_{2j^2})} \right\}}$$

where, x_{j1}, is the first and, x_{j2}, the second threshold estimate at test location, j. The normal intra-test variance at location, i, is denoted by, s_{2j}^2.

Weighting with $1/s_{2j}^2$ minimises the SF in normal individuals (Heijl et al 1987b) and slightly reduces the SF in patients with glaucoma (Flanagan et al 1993c). The unweighted SF demonstrates a positively-skewed distribution in a normal population (Flammer et al 1984a). The unweighted SF is approximately 0.3 dB greater with the Octopus compared with the unweighted SF of the HFA (Brenton and Argus 1987). The difference in the two SFs may also result, in part, from the difference in determination of threshold between the two perimeters. The standard Threshold algorithm of the Octopus designates the threshold as the arithmetic mean of the last seen and the last unseen stimulus luminances whereas the Full Threshold algorithm the HFA determines threshold as the last seen stimulus.

The short-term fluctuation increases with stimulus sizes less than the Goldmann size III (Gilpin et al 1990). It is independent of background intensities in the low photopic range used in most perimeters (1.3 cdm^{-2} and 10 cdm^{-2}), but increases with mesopic illumination at or less than 0.1 cdm^{-2} (Crosswell et al 1991). Short-term Fluctuation also increases in normal individuals when the visual field is tested using a bright fixation target of 435 cd/m^2 (Safran et al 1992) and when measured along the border of a physiological scotoma such as the blind spot (Haefliger et al 1989). Changes in stimulus duration do not affect the SF (Pennebaker et al 1992). The magnitude of the SF is dependent upon the strategy used to estimate threshold (Bebié et al 1976; Flanagan et al 1993c; Weber and Klimaschka 1995). Individuals who exhibit high rates of fixation losses, false positives and false negatives, also demonstrate a higher SF. The SF cannot be calculated for the SITA algorithms.

1.3.13 Long-term Fluctuation (LF)

The Long-term Fluctuation (LF) is the variability in threshold over a series of examinations when the SF, learning effects and age have been taken into consideration (Bebié et al 1976; Flammer et al 1984b; Blumenthal et al 2000). There are two components of the LF: the Homogenous LF (LF_{HOM}) and the Heterogeneous LF (LF_{HET}). The LF_{HOM} describes the variability which affects all locations equally, and the LF_{HET} varies between locations (Hutchings et al 2000). The LF_{HOM} may be considered as the fluctuation of Mean Sensitivity or Mean Defect/Deviation over time, whereas the LF_{HET} describes variation in localised areas of the field (Zulauf et al 1991). Calculation of the LF for Program 30-2 or 24-2 and the Full Threshold or FASTPAC strategies of the HFA is limited to the 10 double determinations of threshold located within 21° eccentricity. The calculation of LF is limited to sampling the central field and disregards the fluctuation at peripheral locations. The 90% confidence limit for the LF_{HOM} and LF_{HET} is 3.3dB and 3.6dB, respectively (Hutchings et al 2000). The LF can provide the foundation for classifying subsequent visual fields as stable, progressive or fluctuating (Hutchings et al 2000). However, the SF cannot be calculated for the SITA algorithms.

There is a significant positive correlation between the LF and the SF although this relationship is too weak to enable the LF to be predicted for an individual from the SF at a particular examination (Flammer et al 1984b; Boeglin et al 1992) The components of LF are smaller than those of the SF. Flammer et al (1984b) found values for LF_{HOM} of 0.5 dB^2 and for LF_{HET} of 0.2dB^2 for normal individuals. Patients with ocular hypertension and patients with glaucoma demonstrated a significantly higher value of LF_{HOM} than for normal individuals but LF_{HET} was only found to be significantly greater for patients with glaucoma (Flammer et al 1984b). Hutchings et al (1993) found that the magnitude of the LF in patients with glaucoma and in patients with ocular hypertension, are independent of the defect depth and the magnitude of the SF.

Long-term Fluctuation is known to increase with: the age of the subject (Heijl et al 1987a; Katz and Sommer 1987); increasing stimulus eccentricity in normal individuals (Heijl et al 1987a; Rutishauser and Flammer 1988) and for patients with glaucoma (Zulauf et al 1991; Boeglin et al 1992).

The LF has also been expressed in terms of a single component either as the variance (dB^2), the Standard Deviation (dB) or as the range (dB) of repeated thresholds (Boeglin et al 1992) over two or more examinations (Heijl et al 1987a; Katz and Sommer 1987; Blumenthal et al 2000; Boeglin et al 1992). The magnitude of the LF is affected by the duration of time elapsed between the examinations. Visual field examinations over short periods of time may underestimate the magnitude of the LF (Katz and Sommer 1987; Boeglin et al 1992). Werner et al (1989) found a mean total variance of 7.8 dB^2 and a range of 2.0 to 22.1 dB^2 over four examinations in normal subjects and in patients with glaucoma.

Blumenthal et al (2003) investigated the LF for SWAP in normal individuals, in patients with glaucoma and in patients with ocular hypertension. They concluded that the severity of the visual field defect had the greatest influence on the magnitude of the LF.

1.4 Reliability Parameters

Automated static perimetry can often be tiring and challenging for the patient, consequently some individualss are more reliable observers than others. It is vital, therefore, that the reliability of the responses given by the patient is assessed during the perimetric examination. The reliability can be assessed in terms of the rate of fixation losses, the number of false responses to the false-positive catch trials, the number of false responses to the false-negative catch trials and the magnitude of the short-term fluctuation.

1.4.1 Fixation Losses

During perimetry, continuous and consistent fixation of the central fixation target located in the perimeter, must be maintained throughout the examination. If fixation deviates from the fixation target, the resultant visual field will be inaccurate and potentially misleading. There are three methods available to monitor perimetric fixation. A somewhat rudimentary method is for the examiner to subjectively monitor the fixation of the patient with either, a telescope, periscope or video eye monitor that is integral to the fixation target.

The second method of assessing fixation is to determine the location of the physiological blind spot and to present stimuli within the boundaries of the blind spot periodically during the examination. This technique is called the Heijl-Krakau (1977) method. The observer will not respond to the stimulus if optimum fixation is maintained; however, a positive response indicates that an eye movement (i.e. a fixation loss) has occurred. The accuracy of the Heijl-Krakau method is dependent on the correct initial estimation of the blind spot location (Sanabria et al 1991). The precision of the technique used to estimate the position of the blind spot is reduced in instances where there is an enlarged blind spot, which either occurs naturally or results from disease (Fankhauser 1993) or occurs if the blind spot is lying within an area of visual field loss. The Heijl-Krakau technique is also less accurate if there is straylight arising from the ocular media or from the reflection from the blind spot itself (Fankhauser and Haeberlin 1980). The number of stimulus presentations in the blind spot for Program 30-2 of the HFA, may be as many as 10% of

the total number of stimulus presentations during the examination (Katz and Sommer 1988).

Many factors may result in a high rate of fixation losses: poor fixation; a mis-plotted blind spot; or head movements. If the patient appears to be having difficulty maintaining fixation, it can be helpful to straighten the head, reinstruct the subject and/or re-plot the blind spot. The maximum percentage of fixation losses compatible with a reliable examination, is less than or equal to 20%. The most common cause of an unreliable visual field examination in, normal individuals, patients with ocular hypertension and patients with glaucoma, is a fixation loss rate greater than 20% (Katz et al 1991). It has been suggested that ≤20% fixation losses is an unrealistically obtainable number of fixation losses and that the upper limit of normality should be increased from ≤20% to ≤33% (Katz and Sommer 1988; Johnson and Nelson-Quigg 1993; Birt et al 1997).

A gaze tracking system is another method of monitoring perimetric fixation. The HFA 700 Series "gaze tracking" system uses infrared light and image analysis to determine the distance between the centre of the pupil and the first Purkinje image (HFA Primer 2002). The subject's direction of gaze affects this distance, but it is unaffected by head movements less than approximately 2°. Throughout the examination, the gaze tracker monitors the extent of any deviations of the eye from fixation. A graph illustrates the quality of fixation during the examination: an upward deflection of the trace indicates the magnitude of gaze misalignment or fixation stability at the time of stimulus presentation. The extent of the upward deflection is truncated at an amplitude of 10°. A downward deflection represents an inadequate image either due to closure of the lid or to the rupture of the tear film. A continuous downward deviation indicates that the gaze tracker is unable to determine fixation. A significant positive correlation (p < 0.01) has been reported between the number of fixation losses and the number of gaze graph deviations greater than or equal to 3° in magnitude and also greater than or equal to 6° for normal individuals and for patients with glaucoma (Kunimatsu et al 2000). The gaze tracker is a useful tool as it enables fixation to be monitored constantly throughout the examination

rather than merely for the 5% of overall stimulus presentations as is the case with the Heijl-Krakau method.

The Octopus perimeters use an infrared illumination system to produce four Purkinje I reflexes, whose position is tracked in order to monitor fixation (Octopus 301 Visual Field Digest 2004). Any deviations of gaze and the prevalence and duration of a blink, are constantly registered by the perimeter. If any deviation or prolonged closure of the lids occurs, the examination is temporarily paused by the software. The gaze tracking systems of both the HFA and the Octopus perimeters may be adversely affected by excessive lacrimation, dry eye or by reflections from high powered trial lenses.

Kinetic fixation is another method that can be implemented for monitoring fixation. This involves the use of a fixation light that moves between stimulus presentations. The patient is required to follow the moving fixation target which pauses immediately before a stimulus presentation. The principle behind kinetic fixation is to provide a less fatiguing and more interesting task for the subject (Reitner et al 1996). However, kinetic fixation is often associated with an inaccuracy in the determination of the rate of fixation losses which is partly due to an inability to estimate the location of the blind spot (Åsman et al 1999).

1.4.2 False-positive and False-negative Catch Trials

There are two types of catch trials used routinely in perimetry, false-positive and false-negative catch trials. A false-positive catch trial was originally determined by the number of positive responses to an apparent presentation of a stimulus. The apparent presentation was associated with either the mechanical noise and/or the appropriate time delay of a normal stimulus presentation.

A false-negative catch trial is determined by the presentation of a suprathreshold stimulus at a location that was previously found to have a greater sensitivity than the suprathreshold stimulus. The suprathreshold increment is usually 9dB. False-positive

and false-negative responses may be suggestive of an inattentive, anxious, fatigued or malingering patient. The maximum incidence for accepting reliability for a perimetric examination is ≤33% false-positives or ≤33% false-negatives. Above this level of false responses, the sensitivity and specificity of the examination is reduced (Sanabria et al 1991). Other authors have suggested that a criterion of <20% false responses should be used to designate a reliable examination due to the small number of catch trial stimuli that are presented during the examination (Vingrys and Demirel 1998). The reliability of the examination can be improved by explaining and educating the patient only to respond when a stimulus is observed and to expect that it is possible that some stimuli may not be seen. Age, pupil diameter and visual acuity have no affect on the rate of false-positive and of false-negative responses (Katz and Sommer 1988; Bickler-Bluth et al 1989).

Inexperienced perimetric observers often exhibit a high rate of false-positive responses and a high rate of fixation losses (Bickler-Bluth et al 1989; Sanabria et al 1990; Reynolds et al 1990). A high percentage of false-positive responses often co-exists with a higher mean sensitivity and a better mean deviation and mean defect both in normal individuals (Katz and Sommer 1990; Cascairo et al 1991; Demirel and Vingrys 1995) and in patients with glaucoma (Katz and Sommer 1990). A high rate of false-negative responses often occurs in glaucoma and is usually associated with a lower mean sensitivity, and a poorer mean defect and mean deviation (Katz and Sommer 1988; Katz and Sommer 1990; Reynolds et al 1990; Johnson and Nelson-Quigg 1993). Bengtsson and Heijl (2000) suggested that in patients with glaucoma, the increased prevalence of false-negative responses is associated with the increasing extent of visual field loss.

The SITA algorithms employ a different method of false-positive catch trial estimation compared to the more traditional perimetric algorithms (Olsson et al 1997, 1998). False-positive responses are measured as part of the threshold estimation procedure (Olsson et al 1997b; Bengtsson et al 1997). This is made possible by utilising periods during the examination when no positive responses are expected. One such period is that between the stimulus onset and the minimum reaction time of the patient (de Boer et al 1982). Responses obtained during such periods are considered to be false-positive

responses (Bengtsson et al 1997). The algorithms also use a minimal number of traditional false-negative catch trials. The pattern of responses is analysed at the conclusion of any perimetric examination to determine the frequency of false-positive and false-negative responses (Olsson et al 1998)

1.4.3 Short-term Fluctuation

The short-term fluctuation (SF) is the amount of variability, or measurement error, associated with the perimetric sensitivity during a single examination. This is calculated by finding the difference between two determinations of sensitivity at one or more given locations. It has been suggested that a short-term fluctuation above 3dB may constitute an unreliable result in apparently normal individuals. It was originally suggested that this could be a sign of visual dysfunction, poor reliability or visual field damage (Harrington and Drake 1990; Hodapp et al 1993). However, this suggestion has not been confirmed in the subsequent literature. Short-term fluctuation has been discussed further under the section concerning Global Indices.

1.5 Analytical Perimetric Programs
1.5.1 STATPAC 2

The current software program for the HFA is known as STATPAC and enables the statistical analysis of the visual field (Heijl et al 1991). The program contains a seperate age-matched database of normal values of sensitivity for each of the Full Threshold, FASTPAC, SITA Standard and SITA Fast algorithms. The STATPAC analysis may be used with Programs 10-2, 24-2 and 30-2 and can generate four possible formats: Single Field Analysis, Overview, Change Analysis and Glaucoma Change Probability Analysis.

1.5.1.1 Single Field Analysis

The Single Field Analysis simply describes the results of a single threshold examination and consists of: patient data, reliability indices, sensitivity at each location in decibels,

gray scale printout, Total Deviation numeric and probability plots and Pattern Deviation numeric and probability plots.

1.5.1.2 Overview

The results for up to sixteen examinations can be condensed by the Overview analysis and this enables a subjective comparison of the serial fields. The comparison of fields over time is facilitated by the layout of the relevant information; the gray scale and the Total and Pattern Deviation numeric and probability plots are reduced in size and aligned in chronological order. Below each examination result, the global indices, foveal threshold and reliability indices are listed. In order to form a confident judgement concerning the stability of the visual field over time, a minimum of six visual field examinations are usually required (Anderson and Patella 1999).

1.5.1.3 Change Analysis

The Change Analysis program presents data reduction statistics over time for each of up to sixteen examination results. The data reduction statistics include box plots, each of the global indices, MD, SF, PSD and CPSD plotted against time to follow-up, and a linear regression analysis of MD.

The box plot, a modified histogram presents the distribution of pointwise deviations from age-corrected normal values at each stimulus location (Total Deviation values). The box plot is similar to the Cumulative Defect or Bebié Curve, discussed previously. The amount of deviation for each stimulus location is ranked to form upper and lower whiskers of the box plot, which respectively indicate the maximum and minimum deviations. The range of deviations for 70% of the locations, are represented on the vertical rectangle ("box"). The central, bold horizontal line within the box represents the median deviation value of the distribution, the upper centre line of the box represents the eighty-fifth percentile and the lower centre line of the box is the fifteenth percentile of the distribution. The extended lines represent the upper and lower values of the distribution. All results are compared to the normal reference box plot.

The statistical significance of the slope of the MD against time to follow-up can be determined by the linear regression analysis. The unit used to represent the magnitude of the slope is, dB/year in conjunction with the statistical significance (p value) of the slope. When the magnitude of the slope is significantly different from zero, a "significant" message appears. The slope of MD determined by the linear regression analysis separates true changes of the MD with time from variability, sometimes due to the learning effect. Early stages of the progression of visual field loss can be identified by changes in PSD or CPSD over time. Also, an increase in SF could, in theory, signify progressive loss as it includes those locations exhibiting higher variability as the defect becomes manifest. The SF is more frequently used as an indicator of subject reliability rather than visual field progression (Anderson and Patella 1999).

1.5.1.4 Glaucoma Change Probability Analysis

The Glaucoma Change Probability Analysis is used to aid the interpretation of the results of follow-up visual field examinations from patients with suspect or manifest glaucoma. Glaucoma Change Probability Maps (GCPM) utilises a mathematical model which incorporates information such as initial defect depth, stimulus location and the overall level of field loss for an individual field. The follow-up field is compared at each stimulus location with the baseline sensitivities derived from two baseline fields and is designed to separate true change from random variability (Heijl et al 1991). An empirical database of examinations from patients with stable glaucoma is used to calculate the probability of change at each stimulus location. If a location has changed more than could be attributed to change resulting from random variability, that location is considered to be significantly changing (at the p<5% level).

The display features the grayscale, the Total Deviation probability plot, the change in sensitivity from baseline at each location and a plot indicating (designated by a filled triangle) whether the change in Total Deviation from baseline lies outside the between-examination variability known to occur in stable glaucoma. In the presence of

progressive cataract, the evaluation of visual field progression with Total Deviation analysis may be difficult to differentiate. A Change Probability Analysis based on the difference in Pattern Deviation from baseline has been developed to separate changes in the height of the visual field from those changes in shape. The Early Manifest Glaucoma Trial (EMGT) trial used this type of analysis (Heijl 1996). As would be expected with the Pattern Deviation approach, the extent of progressive glaucomatous loss derived by Pattern Deviation Change Analysis, both before and after cataract surgery, is less than with the Total Deviation Change Analysis (Bengtsson et al 1997a).

1.5.2 Octosmart and Program DELTA

Neither the Octosmart nor the DELTA program is currently commercially available. The Octosmart program presented results from the Octopus G1, G1X and G2 Programs by providing the numerical deviations, global indices, rudimentary cluster analysis, a Bebié curve and a summary diagnostic statement (Funkhouser et al 1991). Consistent judgements between the diagnostic statement and experienced observers, was found in cases of obvious field loss (Funkhouser et al 1991; Hirsbrunner et al 1990). However, little was known about the performance of Octosmart in cases of early loss. Program DELTA was an analytical program which permitted the comparison of any two visual fields (Bebié and Fankhauser 1981). A paired t-test between the mean sensitivities of the two given visual field examinations was used to gauge if a deterioration between the two fields existed (Bebié and Fankhauser 1981). The use of the t-test was subsequently shown to be very sensitive to generalised depression of the visual field, but unable to detect small to moderate localised visual field loss (Hills and Johnson 1988).

1.5.3 PeriTrend and PeriData

PeriData and PeriTrend are PC based programs that are capable of transmitting, storing, and processing visual field data from the HFA and Octopus perimeters (Weber and Kriegelstein 1989; Brusini et al 1991). The programs display the conventional indices for the HFA and Octopus perimeters and in addition, the visual field can be analysed

globally, in hemifields, quadrants, sectors, rings, or according to the arrangement of the retinal nerve fibre layer (Peridata 6.3α Users Manual).

1.5.4 Octopus Seven-in-One

The Seven-in-one report for the Octopus is the equivalent to the STATPAC Single Field Analysis for the HFA and combines many of the analyses previously described such as the raw numerical data, greyscale plot, Bebié curve, global indices and Comparison and Corrected Comparison Probability plots.

1.5.5 Progressor

Progressor is a software package that analyses visual field progression using pointwise linear regression slopes of change in sensitivity at each location against time (Noureddin et al 1991; Fitzke et al 1996b). The results are displayed graphically in the form of colour-coded, bar charts at each stimulus location. The length of a bar indicates the depth of a defect (longer bars represent lower sensitivities), and the colour indicates the nature and the statistical significance of the slope. The colour coding is as follows: dark and light bars indicate deterioration ($p<0.05$ and $p<0.01$ respectively), yellow bars non-significant regression slopes, and blue bars outliers. Progressor, linear regression of MD_H and the Glaucoma Change Probability programs of the HFA exhibit good agreement when determining whether a series of visual field examinations are stable or exhibit progression (Birch et al 1995; Fitzke et al 1996b; McNaught et al 1996). Viswanathan and colleagues (1997) found that STATPAC 2 detected glaucomatous visual field progression later than Progressor.

1.6 Factors Potentially Affecting Perimetric Examination Data Collection
1.6.1 Perimetric Artefacts

The measurement of threshold is influenced by a variety of factors which can lead to artefactual contamination of the results from a visual field examination. Visual field artefacts may exacerbate the presence of an existing defect or mimic the presence of a defect. Some artefacts are physical (lens rim scotoma and facial contours), some

physiological (medications, media opacities, refractive defocus and pupil size), some psychological (fatigue and learning effects) and some examiner-related (instructions and reassurance). The various artefacts are discussed below.

1.6.1.1 Age

A linear reduction in sensitivity of between 0.4 and 1.1 dB per decade of age has been found with threshold perimetry out to 30° eccentricity (Brenton and Phelps 1986; Haas et al 1986; Heijl et al 1987a; Zulauf et al 1994). There is a greater age-decline for the peripheral and superior areas of the visual field than the paracentral and inferior areas (Haas et al 1986; Jaffe et al 1986). Consequently, with age, there is a lowering and a steepening in the hill of vision (Haas et al 1986; Jaffe et al 1986; Heijl et al 1987a). There is a shallower decline with age for individuals under the age of fifty years than for individuals over the age of fifty (Johnson and Choy 1987). However, Henson (1994) suggested that the steepening in the slope occured closer to forty rather than fifty years of age.

The age-related decline in differential light sensitivity has been attributed to pupil size (See 1.6.1.3), to ocular media opacity (See 1.6.1.5) and to changes in retinal function. The neural component of the visual pathway is thought to be responsible for the majority of the decline in sensitivity with age (Johnson et al 1989). The photoreceptors, ganglion cells and retinal pigment epithelial cells all reduce in number at a rate of 0.2% to 0.4% per year (Repka and Quigley 1989; Mikelberg et al 1989; Jonas et al 1992c; Panda-Jonas et al 1994). For the photoreceptors, the decline is more pronounced at a retinal eccentricity of 5mm (23°) to 8 mm (37°) than at eccentricities greater than 14mm (65°). The photoreceptor decline occurs at a greater rate for the rods than for the cones (Panda-Jonas et al 1994).

1.6.1.2 Pupil Size

The diameter of the pupil affects the amount of light reaching the retina which in turn, affects the threshold. A change of pupil diameter induces a change in retinal illumination, under photopic conditions, but would not be expected to alter the threshold due to Weber's law. Weber's law does not apply, however, under mesopic and low photopic conditions; hence, a brighter stimulus luminance is needed when the size of the pupil decreases (Lindenmuth et al 1989). The following equation represents the amount of retinal illumination (D), in Trolands assuming the distance of the nodal point from the retina is 16.7 mm:

$$D = 0.36 \bullet \tau_\lambda \bullet s \bullet B$$

where τ_λ is the transmission factor of the ocular media, s is the area of the pupil in cm^2 and B is the luminance of the light source. The transmission factor, τ_λ is dependent upon the wavelength of light and varies from 0.1 for violet light to 0.7 in the red region of the spectrum. For white light, τ_λ is approximately 0.5 (Davson 1990).

Lindenmuth et al (1989) found that pupillary miosis induced by 2% pilocarpine lead to a worsening of the MD by an average of 0.67dB. The foveal threshold and SF were unaffected. In patients with glaucoma, the MD worsened by 1.5dB when miosis was induced (Webster et al 1993).

Pupillary dilation induced with 1% tropicamide leads to a worsening in MD by, on average, 0.8dB but has little affect on foveal threshold, SF and PSD, although CPSD worsened by 0.60dB (Lindenmuth et al 1990). However, Wood et al (1988) concluded that induced pupillary dilation resulted in an increase in perimetric sensitivity which was of greater magnitude for the more peripheral stimulus locations.

1.6.1.3 Refractive Defocus

Uncorrected refractive error gives rise to optical defocus, which, in turn, results in reduced visual acuity and contrast sensitivity at high spatial frequencies (Campbell and

Green 1965). Similarly, optical defocus increases the area of the stimulus on the retina, whilst reducing the luminance of the centre of the image. This change in the luminance gradient at the edge of the target will alter the effectiveness of the perimetric stimulus hence depressing sensitivity.

There is no statistically significant change in group mean Mean Sensitivity, within the range of ±2.00DS of defocus using the default stimulus size for automated perimetry of Goldmann III. However, there is, rapid reduction in sensitivity in the central visual field compared to the peripheral field with defocus greater than +3.00DS (Benedeto and Cyrlin 1985). When using the size III stimulus, it has been suggested that each diopter of refractive blur will depress the hill of vision by approximately 1dB (Anderson and Patella 1999). It is vital, therefore, that all refractive errors greater than 1.00D should be corrected. For presbyopic individuals, the correction should be adjusted for the appropriate viewing distance of the perimeter. The HFA is programmed to calculate the appropriate trial lens based upon the subject's distance prescription, age and the viewing distance of the perimeter.

Stimulus sizes smaller than Goldmann size III, are more affected by refractive defocus than are larger stimuli (Atchison 1987; Anderson and Patella 1999). It has been suggested that the Goldmann size V stimulus is less affected by optical defocus, as it contains a greater proportion of low spatial frequencies (Adams et al 1987a).

A small pupil will increase the depth of focus and therefore the change in sensitivity per dioptre of defocus will be greater for subjects with larger pupils. Prismatic effects can occur for high myopes and aphakic subjects due to the necessary strength of the correcting lens combined with the vertex distance, consequently, using contact lenses for such subjects, can be beneficial (Zalta 1989).

1.6.1.4 Media Opacities

Opacities within the cornea, crystalline lens or vitreous may affect the light entering the eye in two ways: by absorption which filters the amount and wavelength of light reaching the retina or by scattering the light (the dispersion of a point source of light as it passes through the media) , thereby reducing the contrast of the stimulus.

With ageing, a discolouration of the layers within the lens occurs and leads to both such an increase in light absorption and an increase in light scatter. This increased absorption of light by the crystalline lens, preferentially attenuates the shorter wavelengths (Sample et al 1988; Moss et al 1995). For conditions where Weber's Law applies, the threshold estimate is unaffected but for conventional white-on-white perimetry, the stimulus and background are both affected.

Light scatter is the main cause of visual loss in cataract (Greve 1980; Bettelheim and Ali 1985) and can be subdivided into forward light scatter (straylight reaching the retina), (Philipson 1969; Bettleheim and Chylack 1985; Wood et al 1989; Dengler-Harles et al 1990), and backward light scatter (light reflected away from the crystalline lens). The extent of light scatter is virtually independent of the wavelength of the incident light (Whitaker et al 1993). The dispersion of a point source as it passes through the ocular media, can be described mathematically as the Point Spread Function (PSF) (van den Berg 1987). The overall reduction in perimetric sensitivity, increases as the magnitude of light scatter increases, in patients with cataract (Dengler-Harles et al 1990; Moss and Wild 1994; Moss et al 1995). Normal and abnormal areas of the visual field have been found to depress equally (Budenz et al 1993), especially when the age-matched normal values are corrected for light scatter (Dengler-Harles et al 1990).

The size and position of the opacity within the ocular media will govern the resultant magnitude of the image degradation. Opacities close to the nodal point of the eye, such as a posterior subcapsular cataract, will elicit a greater attenuation than opacities at other positions within the crystalline lens (Baraldi et al 1987). Many studies have concluded that, in general, cataract causes a diffuse loss of sensitivity (Guthauser and Flammer

1988; Lam et al 1991; Budenz et al 1993; Stewart et al 1995). Increasing cataract with age complicates the detection of progressive glaucomatous visual field loss (Stewart et al 1995; Bengtsson et al 1997a). It is therefore important to differentiate apparent visual field progression caused by media opacities from true glaucomatous progression.

The investigation of the effect of surgical extraction of nuclear cataract on perimetric data found that it has minimal effect on the MD, PSD or the total decibel attenuation within the GHT sectors (Stewart et al 1995). Stewart et al (1995) hypothesized that light scatter might evoke a response from a larger area of the retina, which would result in an apparently higher measured sensitivity. Therefore, in the pseudophakic eye, the absence of light scatter would mean that stimuli are incident upon a smaller area of retina and would require a brighter stimulus to elicit a response.

1.6.1.5 General Health and Medical Therapy

A number of systemic factors are known to potentially influence the visual field. In individuals who suffer from migraine, the peripheral visual field may be affected for several days (Drummond and Anderson 1992). Physical exercise can result in an improvement of the MD (Koskela et al 1990). Reduced patient reliability (Zulauf et al 1986) and a deterioration in the visual field indices, MD, PSD and CPSD (Wild et al 1990), correlate with a low level of systemic blood alcohol (Zulauf et al 1986).

Systemic pharmacological agents may influence the measurement of the visual field. Central nervous system medications, such as diazepam, can reduce the MS (Haas and Flammer 1985). More recently, the anti-convulsant drug, vigabatrin, has been shown to constrict the visual field (Eke et al 1997; Wild et al 1999c; Harding et al 2000; Midelfart et al 2000). The SF increases with the use of anti-histamines, but the other visual field indices and reliability parameters remain unaffected (Wild et al 1989a). Treatment with chloroquine and hydroxychloroquine which are known to cause retinal toxicity does not cause a reduction in visual function, over 8 months (Mann et al 1988). Rynes (1983) concluded that long-term hydroxychloroquine therapy can result in visual field loss but

usually only in those individuals receiving daily doses far higher than were routinely prescribed. Patients with autosomal dominant retinitis pigmentosa and/or glaucoma who are treated with acetazolamide, exhibit an apparent improvement in sensitivity (Flammer and Drance 1983); glaucoma patients with severe visual field loss demonstrate the greatest improvement (Flammer and Drance 1983).

1.6.1.6 Learning Effect

Previous perimetric experience influences the outcome of a visual field examination, in normal individuals, (Wood et al 1987b; Heijl et al 1989b; Wild et al 1989c; Autzen and Work 1990; Searle et al 1991), in patients with ocular hypertension (Wild et al 1989c, 1991; Werner et al 1990) and in patients with glaucoma (Kulze et al 1990; Heijl and Bengtsson 1996). An improvement of approximately 1-2dB in the MS and in the MD has been reported between the first and second examinations, in addition to a reduction in SF (Werner et al 1990, 1988).

The improvement in sensitivity can occur during the examination of a given eye (Flammer et al 1984a) can occur between eyes at the same visit (Wilensky and Joondeph 1984) or between visits for the same eye (Heijl et al 1989; Wild et al 1989).

The learning effect is often greater in the superior field and increases with eccentricity (Wood et al 1987a; Heijl et al 1989). The improvement in the sensitivity for the superior hemifield, may be caused by patients learning to raise their upper eyelid during the examination (Wood et al 1987a).

The learning effect is greatest for intermediate levels of defect depth (Wild et al 1989c; Heijl et al 1989b; Heijl and Bengtsson 1996). However, the extent of the learning effect is independent of age (Heijl et al 1989b; Kulze et al 1990)

The initial examination results of a patient previously naïve to perimetry must, therefore, be interpreted with caution. A baseline of two fields is considered by most clinicians to be the minimum required for the interpretation of the visual field. It has been suggested that if the fields from the first two visits demonstrate a difference in the MD of less than

2dB, then the presence of a learning effect is unlikely (Hodapp et al 1993). However, the learning effect can remain over the first five examinations (Wood et al 1987b) and can be minimised by prior training in the visual field examination (Heijl et al 1989b; Werner et al1988, 1990). The learner's index (LI), which was discussed earlier, was devised to identify defect patterns that may be caused by perimetric inexperience (Olsson et al 1997a).

1.6.1.7 Fatigue Effect

The visual field is also influenced by the fatigue effect whereby sensitivity declines with an increase in the examination duration (Heijl and Drance 1983; Hudson et al 1994). The fatigue effect is present in normal individuals (Searle et al 1991; Hudson et al 1994), in patients with ocular hypertension, (Wild et al 1991; Hudson et al 1994), in patients with glaucoma (Heijl and Drance 1983; Johnson et al 1988a) and in neuro-ophthalmological disorders (Keltner and Johnson 1995). In the normal eye, the fatigue effect within an examination leads to a general reduction in sensitivity of between 1dB (Johnson et al 1988a) and 2.5dB (Hudson et al 1994). This reduction in sensitivity becomes more pronounced with examination durations of greater than 5 minutes (Marra and Flammer 1991). The overall reduction in sensitivity, due to fatigue, within an examination for patients with ocular hypertension is on average, 2.2dB (Hudson et al 1994) and approximately 3dB in glaucoma (Johnson et al 1988a). With increased examination duration, the loss variance also increases and this increase is greater for normal subjects than for patients with ocular hypertension (Hudson et al 1994).

In normal individuals (Searle et al 1991) and in patients with ocular hypertension (Hudson et al 1994), the fatigue effect is greater for the second eye examined. Therefore, the order in which the eyes are examined should be taken into account when the results of a visual field examination are interpreted (Searle et al 1991).

The fatigue effect is greatest in areas of the visual field adjacent to or within a focal defect (Heijl and Drance 1983). It also increases with increase in eccentricity (Johnson et

68

al 1988a; Hudson et al 1994), particularly in glaucoma patients (Johnson et al 1988a). In addition, the immediate central stimulus locations may show normal or near normal sensitivity as these locations are thresholded in the earlier stages of the visual field examination, but the more peripheral locations which are thresholded at a later stage in the examination can exhibit depressed sensitivity producing a distinctive cloverleaf pattern in the grayscale printout (Anderson and Patella 1999). Global short-term fluctuation (SF) remains relatively unchanged over the duration of a single examination, in both, normal and OHT subjects (Hudson et al 1994).

Introducing rest periods within an examination can minimise the fatigue at a given visit (Johnson et al 1988a) as can the shorter thresholding algorithms, such as the SITA algorithms, that do not exhibit any loss in accuracy compared to the longer Full Threshold algorithm (Bengtsson et al 1997b; Wild et al 1999b). At follow-up visits, the fatigue effect can still occur, even though the learning effect is no longer present (Wild et al 1991).

1.6.1.8 Examiner Instructions

The successful outcome of the visual field examination relies on the optimum interaction between the examiner and patient. Perimetric results can be markedly affected by the instructions given by the examiner. An increase in the MS of 6.6dB for older (mean age 67.5 years, range 62 to 71 years) subjects arises from an extensive instruction compared to that arising from a brief instruction (Kutzko et al 2000). Encouragement and reassurance from the examiner, reduces patient anxiety and increases examination reliability (Anderson and Patella 1999). Patient errors must also be rectified early on in the examination to avoid poor quality results. In order to allow optimum subject concentration the examination environment should be quiet and free from distractions.

The outcome of the quality of the perimetric examination has been shown to improve if supervision is provided throughout the examination (Van Coevorden et al 1999) This is especially the case for those subjects with a low level of formal education, of advanced

age, and/or a with a prior history of unreliable visual field examinations. For those subjects who lack obvious risk factors for poor performance, Van Coevorden et al (1999) suggested that supervision could be withdrawn.

Johnson et al (1992), evaluated the effect of intermittent versus continuous monitoring of the patient by the perimetrist during automated static perimetry on the reliability indices. The mean fixation losses, false-positive and false-negative errors were not significantly different between the continuously and intermittently monitored patient groups. It has been demonstrated that showing a prospective subject a training video explaining the perimetric examination prior to their own first perimetric examination, can improve the reliability criteria (i.e. the number of subjects exhibiting less than 20% rate of fixation losses, less than 33% false-positive response rate and less than 33% false-negative response rate) of their subsequent visual field (Sherafat et al 2003).

1.7 The Grading and Progression of Visual Field Loss

Some of the methods available to monitor visual field progression have already been discussed previously.

1.7.1. Hodapp Visual Field Loss Classification

The Hodapp classification (1993) classifies visual field loss into three categories: early, moderate and severe defects based upon Program 24-2 and the Full Threshold algorithm. An early visual field defect comprised an MD upto -6dB together with fewer than 25% of the locations on the Pattern Deviation plot depressed below the 5% level, fewer than 10 locations depressed below the 1% level and no location within 5° of fixation exhibiting a sensitivity of less than 15dB. A moderate defect comprised an MD up to -12 dB, together with fewer than 50% of the locations depressed below the 5% level on the Pattern Deviation plot, fewer than 20 locations depressed below the 1% level, no location within 5° of fixation exhibiting a sensitivity of 0dB, and only one hemifield containing a location with a sensitivity of <15dB within 5° of fixation. A severe defect comprised either an MD worse than -12dB; or more than 50% of the locations depressed below the

70

5% level on the Pattern Deviation plot or more than 20 locations depressed below the 1% level; or a location within 5° of fixation exhibiting a sensitivity of 0dB; or locations in both hemifields with a sensitivity of <15dB within 5° of fixation.

1.7.2 Litwak Visual Field Loss Classification

The Litwak (2001) glaucomatous visual field loss classification is discussed in Chapter 4.

1.7.3 Ocular Hypertension Treatment Study (OHTS)

The Ocular Hypertensive Treatment Study was established in order to evaluate the safety and efficacy of topical hypotensive pharmaceutical therapy in preventing and/or delaying the onset of open-angle glaucoma in individuals with ocular hypertension and no evidence of glaucomatous damage (Gordon & Kass 1999: Gordon et al 2002; Johnson et al 2002).

The perimetric inclusion criteria for the study, were that two out of a possible three HFA 30-2 Full Threshold examinations for any potential participant must be considered both "reliable" and "normal". Normality was defined according to the HFA STATPAC 2 criteria for age-matched normal visual field indexes for MD, PSD, SF, CPSD and GHT and by clinical review by two senior readers at the OHTS Visual Field Reading Centre (VFRC). A visual field was only deemed normal if both STATPAC 2 and the VFRC readers concluded it was normal. A visual field was considered to be reliable if a less than a rate of 33% of incorrect responses to each of the false-positive, false-negative and fixation loss catch trials occurred (Johnson et al 2002).

1.7.4 Collaborative Initial Glaucoma Treatment Study (CIGTS)

The Collaborative Initial Glaucoma Treatment Study (CIGTS) was a longitudinal study, established to determine whether patients with newly diagnosed open-angle glaucoma were better treated initially by medicine or by immediate filtration surgery (Janz et al 2001).

The CIGTS study classified visual field loss according to a point score system based upon the probability levels of the Total Deviation analysis. A stimulus location which had a Total Deviation exhibiting a probability value of 5% or less was classed as a deviating location. The scoring system was based on three contiguous locations (the deviating location and the two most depressed neighbouring locations). Each of the 52 stimulus locations for Program 24-2 could exhibit a possible score from 0 to 4 depending upon the probability level associated with the given location. The total score was transformed to a scale ranging from 0 (no defect) to 20 (end stage visual field loss). Visual field progression was defined as an increase of 3 or more points on the scale in three consecutive follow-up fields (Musch et al 1999; Vesti et al 2003).

1.7.5 Advanced Glaucoma Intervention Study (AGIS)

The Advanced Glaucoma Intervention Study (AGIS) was a randomized longitudinal study of progressive visual field loss in glaucoma (Katz 1999; Katz et al 1999; Wilson et al 2002; Vesti et al 1993; AGIS 1994; AGIS 1998; Nouri-Mahdavi et al 2004). The AGIS scoring system divided the stimulus locations of Program 24-2 into three segments: the nasal area and the remaining superior and inferior hemifield regions. A location was classed as abnormal when the defect depth was equal to or worse than between 5 and 9 dB depending upon the location. A nasal defect was considered to be a group of three or more contiguous depressed locations that may cross the horizontal midline. Visual field loss was scored between 0 and 20. The magnitude of the score depended upon the type, depth and area of defect. Progression was defined as an increase in 4 or more points on the scale in three consecutive follow-up fields (AGIS 1994; AGIS 1998; Vesti et al 2003).

1.7.6 Early Manifest Glaucoma Trial (EMGT)

The Early Manifest Glaucoma Trial (EMGT) consisted of patients with open-angle glaucoma, patients with normal tension glaucoma and patients with exfoliation glaucoma divided into treated and a non-treated subgroups (Heijl et al 2002, 2003).

The EMGT visual field progression criteria were designed to have high sensitivity and specificity and were based on glaucoma change probability maps based upon the Pattern Deviation analysis (Heijl et al 1991, 2003). Glaucoma change probability maps (GCPM) employ a mathematical model of random threshold variability in the fields of patients with glaucomatous visual field loss. The model takes into account, defect depth, stimulus location and the overall severity of field loss. The threshold value in any follow-up field is compared to an average of the threshold values from the same stimulus location at two baseline visual fields. Locations are considered to be significantly changing (p<5% level) if they have changed more than would be expected due to random variability. The EMGT study defined definite visual field progression as three or more locations in any area of the visual field (not necessarily contiguous), which exhibited deterioration in sensitivity from baseline at the p<5% level over each of three consecutive examinations. Tentative visual field progression was considered to be three or more locations exhibiting deterioration at each of two consecutive examinations (Heijl et al 1991, 2003; Bengtsson et al 1997). Heijl et al (2003) concluded that the average amount of visual field deterioration to be considered as progression was a worsening in MD of -2dB and an increase of five or more of locations exhibiting an abnormal probability level.

Katz et al (1999) analysed the visual fields of 67 eyes of 56 patients with glaucoma using the EMGT, CIGTS and AGIS progression analysis methods. The EMGT and CIGTS methods produced rates of apparent progression that were twice those of the AGIS method. Although the EMGT and CIGTS scoring systems exhibited similar rates of progression, they identified different patients as having exhibited progression.

Vesti et al (2003) used a computer simulation to generate, from the fields of 76 patients with glaucoma, interim semi-annual visual fields under conditions of low, moderate and high variability and applied the progression analysis methods of AGIS, CIGTS, the Glaucoma Change Probability analysis (GCP) and Point-wise Linear Regression Analysis (PLRA). They concluded that the AGIS and CIGTS methods had high specificity but resulted in fewer cases of progression than the other methods. The GCP method

identified progression earliest, but generally had a lower specificity. The longest time to the determination of progression was with the PLRA method.

CHAPTER 2

Rationale

2.1 Introduction to Perimetry and its Use in Open Angle Glaucoma

Open angle glaucoma is a chronic condition that can cause permanent visual field loss and affects a large number of people worldwide (Quigley 1996; Fraser et al 1999; Musch et al 1999; Gasch et al 2000). According to the Beaver Dam Eye Study, 2.1% of the population over the age of 40 have glaucoma (Klein et al 1992). It is thought to be the second most common cause of blindness in the world, affecting approximately 67 million people (Quigley 1996; Wilson 1996; Flanagan 1998) with 6.7 million of those with glaucoma being bilaterally blind (Quigley 1996). Epidemiological studies in developed countries have shown that approximately 50% of glaucoma sufferers remain undiagnosed (Sommer et al 1991; Tielsch et al 1991; Quigley 1996).

Glaucoma can be defined as a progressive optic neuropathy associated with characteristic optic nerve head and retinal nerve fiber layer changes and visual field loss (Garway-Heath et al 2000; Burk and Rendon 2001). One third to one half of patients with glaucoma exhibit normal intraocular pressure (IOP) at the initial examination (Sommer et al 1991). It follows, therefore, that detailed observation of the optic nerve head and accurate visual field examination is very important for the detection of glaucoma, to prevent functional visual loss and to identify progressive damage and to facilitate the consequent therapeutic management of the disease. The early detection of glaucoma is vital. Therefore, diagnostic glaucoma case finding tests are required, which are accurate, reliable, rapid, easily administered, and cost effective (Trible et al 2000).

Interest in static automated perimetry for the diagnosis and follow up of glaucoma is based primarily on two major objectives (Flammer et al 1985; de Natale et al 1984; Hills et al 1988; Maeda et al 2000): to detect glaucoma in its early stages and to reduce the duration of the perimetric examination. The increase in accuracy of a threshold estimate is usually at the expense of an increase in examination time. The quest for a perimetric

technique that is sensitive to detecting early glaucoma has resulted in the formulation of newer tests, which examine different aspects of visual function compared to conventional perimetry. Examples include: Short Wavelength Automated Perimetry (SWAP), high-pass resolution perimetry, flicker perimetry and frequency doubling perimetry (Johnson et al 1993; Frisen 1988; Schenone et al 1997; Johnson et al 1997; Maddess 2000; Maeda et al 2000).

2.2 Previous Work

This thesis was a continuation of work previously undertaken, within the School of Optometry and Vision Sciences, Cardiff University, Cardiff and, previously, in the Department of Vision Sciences, Aston University, Birmingham. The studies described in this thesis are a development of the previous research concerning perimetric algorithms and perimetric variability conducted by the Group with W-W perimetry and with SWAP.

The Group has previously investigated the FASTPAC algorithm of the HFA in normal individuals (Flanagan et al 1993a) and in glaucoma (Flanagan et al 1993b) and the SITA algorithms in normal individuals and in glaucoma (Wild et al 1999a,b). The latest study of perimetric algorithms described in Chapters 3 and 4, examines the variability of perimetric sensitivity in the normal and glaucomatous eye, respectively, as a function of five algorithms, namely, the HFA Full Threshold, SITA Standard, SITA Fast, Octopus Threshold and TOP algorithms.

Various aspects of variability in perimetry are addressed in Chapters 3, 4, 5 and 6 of this thesis and are a continuation of these, amongst many other, previous publications, by the Group, on the subject: time-related variation in normal automated static perimetry (Searle et al 1991); the long-term fluctuation of the visual field in stable glaucoma (Hutchings et al 2000); the variability associated with the threshold response in normal individuals (Wild et al 1999a) and in patients with glaucoma (Wild et al 1999b) and the variability of the threshold response in the normal eye as a function of stimulus size in the central and peripheral visual field (in preparation).

76

The study described in Chapter 5 investigates the shape of the frequency-of-seeing (FOS) curve in normal individuals and in patients with glaucoma for W-W perimetry and for SWAP. There are no publications describing the characteristics of the FOS curve in SWAP. With the advent of SITA SWAP which uses information from the FOS curve to derive threshold, it is important that variability in the FOS curve for SWAP is elucidated. Previous studies of SWAP, by the Group, have included: the optimisation of stimulus parameters (Hudson et al 1993); the effects of light scatter and of ocular media and macular pigment absorption (Moss and Wild 1994; Moss et al 1995; Wild and Hudson 1995); the learning effect in normal subjects (Wild and Moss 1996); the variability of threshold estimation (Wild et al 1998); stimulus size and the variability of the threshold response in SWAP (Wild et al 2001) and the effect of previous perimetric experience on SWAP (in submission).

The study described in Chapter 6 investigates the influence of fatigue on the prevalence of the false-negative response in perimetry. The study developed from previous work concerning visual fatigue in normal individuals and in patients with ocular hypertension (Hudson et al 1992) and the time-dependent performance of the reliability indices in glaucoma and ocular hypertension.

2.3 Perimetric Sensitivity in the Normal and Glaucomatous Eye as a Function of the Full Threshold, SITA Standard, SITA Fast, Octopus Threshold and Octopus TOP Algorithms.

As described in detail in Chapters 3 and 4, the conventional staircase algorithm used in perimetry, crosses the threshold initially using a step size of 4dB followed by a second crossing of threshold with a step size of 2dB. In the case of the HFA, sensitivity is designated as the last 'seen' stimulus. For the Octopus perimeters, the final sensitivity is taken to be the average of the last seen and last unseen stimuli, the final 1dB step being achieved by interpolation. Using Program 30-2 of the HFA and the Full Threshold algorithm, the average examination duration is approximately 15 minutes per eye. Such an examination duration is fundamentally unacceptable given the financial constraints

operative in the current healthcare environment, and it is tedious and tiring for both the patient and perimetrist. Consequently, new threshold strategies have been developed in an attempt to reduce the examination duration, without any loss of accuracy.

The FASTPAC strategy for the HFA uses a single crossing of threshold with a step size of 3dB (Wild et al 1999a,b). The Group concluded that FASTPAC provided a 40% reduction in examination duration when compared to the HFA Full Threshold algorithm, but at the expense of an increased variability in threshold determination- the short-term fluctuation increased by 24% (Flanagan et al 1993a,b).

The Dynamic Strategy was designed to use variable step sizes depending on the sensitivity, in an attempt to reduce the examination duration (Weber and Klimaschka 1995). The Dynamic Strategy exhibits a reduction in the duration of a perimetric examination, by on average, 46% (Weber and Klimaschka 1995). Although the Dynamic Strategy was shown to reduce the measurement variability at normal levels of sensitivity, it exhibited an increase in the within-examination variability, at reduced sensitivities, when compared to the Octopus standard strategy (Weber and Klimaschka 1995; Zulauf et al 1994). Consequently, the benefit of the reduced examination duration is negligible once the accompanying increased short-term fluctuation has been taken into account (Zulauf et al 1994).

The SITA algorithms are a further development in the search for an efficient and accurate perimetric strategy (Bengtsson and Heijl 1997; Bengtsson et al 1998a,b; Bengtsson and Heijl 1999; Wild et al 1999; Artes et al 2002; Budenz et al 2002). The two algorithms, SITA Standard and SITA Fast, implement a more interactive thresholding strategy, than the conventional staircase algorithms, reliant on sophisticated computations during the test procedure by: adapting detailed prior models of the normal and of the glaucomatous visual field; combining and applying the information acquired from the interdependency of adjacent locations in the visual field, and using the proportions of the frequency-of-seeing curve. For the SITA Standard and SITA Fast algorithms using Program 30-2, the average examination duration for a normal individual, is approximately 8 minutes and 5

minutes, respectively which in the case of SITA Standard is approximately half the examination duration of the 4-2dB staircase algorithm (Bengtsson et al 1997b, 1998).

Another relatively new, commercially available, fast thresholding perimetric algorithm, is Tendency-Oriented-Perimetry (TOP) which is available on the Octopus perimeters. The examination duration is approximately 4 minutes per eye for the TOP strategy using Program 32 (Morales et al 2000) and this short examination time is achieved by only presenting a single stimulus at each test location. The TOP strategy relies on the interdependency of the threshold between adjacent stimulus locations, however, unlike SITA, TOP divides all visual field locations of the available Octopus Programs into 4 matrixes. The examination starts with stimulus exposures at half the intensity of the age-corrected normal threshold values in the first matrix. Then brighter or dimmer stimuli, determined as fractions of the age-corrected normal values, are presented in the three remaining matrixes.

The threshold estimate of any perimetric algorithm is influenced greatly by the Short-term fluctuation (SF) (the within-subject, within-examination variability), and the Long-term fluctuation (LF) (the within-subject, between-examination variability) (Heijl et al 1987a; Flammer et al 1984a,c). The outcome of the visual field examination is difficult to interpret due to these fluctuations in sensitivity (Heijl et al 1987a; Flammer et al 1984a,c; Katz and Sommer 1984; Chauhan et al 1995). Consequently, it is extremely difficult, firstly, to differentiate between physiological variability in the threshold and the presence of early visual field loss and secondly to differentiate the increased threshold variability that accompanies visual field loss from the actual progression of the visual field loss. It is paramount that an accurate knowledge of the normal hill of vision and its normal variation is acquired in order to enable the effective interpretation of the results from a visual field examination (Heijl et al 1987a). In order to conclude that visual field progression has occurred, the difference between two visual field examinations must be greater than the associated concomitant physiological fluctuation (Werner et al 1989).

In the normal eye, variability increases with eccentricity (Greve 1973; Parrish 1984; Lewis et al 1986; Heijl et al 1987) and with an increase in age (Katz and Sommer 1987). This applies to variability within-subject within-examination, within-subject between-examination and variability between individuals (Heijl et al 1987a). The between-subject within-examination normal variability, upon which the confidence limits for normality are determined, increases, with increasing eccentricity and increasing age (Brenton and Phelps 1986; Heijl et al 1987a). The magnitude of the within- and between- examination variability is greater in patients with glaucoma than in normal individuals (Flammer et al 1984; Heijl et al 1989a,b; Boeglin et al 1992; Smith et al 1996). The within-subject, within-examination variability in the abnormal eye for W-W perimetry increases with increased defect depth up to approximately 12dB after which the variability reduces as the sensitivity tends towards 0dB (Heijl et al 1989a).

A cross-sectional prospective observational study was undertaken to determine how the recent, commonly applied, commercially available algorithms (HFA Full Threshold; HFA SITA Standard; HFA SITA Fast; Octopus Threshold and Octopus TOP) compare in terms of examination duration, and variability, for normal individuals and patients with glaucoma. The study was intended, in particular, to provide further information about the validity of the TOP algorithm in the estimation of normal sensitivity and its feasibility as a screening, diagnostic and management tool for glaucoma. More specifically, the intention was to determine the within-visit between-algorithm differences, and the between-visit within-algorithm differences for the five algorithms.

There is a notable void in the literature, since the effects of these five algorithms have not previously been investigated simultaneously either in normal individuals or in patients with glaucoma.

2.4 Derivation of the Frequency-of-seeing Curve for SWAP and for W-W Perimetry in Normal Individuals and in Patients with Glaucoma.

In perimetry, threshold is defined as the stimulus intensity at which the frequency of perception is 50%. Around the threshold, there is a transition zone in which the

frequency of perception ranges from 0% to 100%. The frequency of perception can be plotted against stimulus intensity, measured on a logarithmic scale, and the resultant curve, which has a characteristic, cumulative frequency or sigmoid/S-shaped appearance with a linear section in the middle (Weber & Rau 1992), is designated as the frequency-of-seeing (FOS) curve. Since the frequency-of-seeing curve is a psychometric function, it never actually reaches either 100% or 0%. In W-W perimetry, the between-subject and between-location variability, is highly correlated with the threshold level and influences the slope of the frequency-of-seeing curve which can vary between normals, glaucoma suspects and patients with glaucoma (Weber and Rau 1992; Chauhan et al 1993; Olsson et al 1993; Wall et al 1996). A frequency-of-seeing curve with a steep slope is considered more likely to occur with a high sensitivity and/or low level of variability and a frequency-of-seeing curve with a flat slope is considered more likely to occur with a low sensitivity and/or high level of variability. There is very little literature on the subject of frequency-of-seeing curves, associated with perimetry, with the exception of the studies cited above, despite the fact that the SITA perimetric algorithms use the frequency-of-seeing curve to assist in threshold estimation. Consequently, all of the theories relating to the characteristics of the FOS curve, require either confirmatory or further investigation.

Short Wavelength Automated Perimetry (SWAP) is available on the HFA and some of the Octopus perimeters, whereby a 440 nm narrow band blue Goldmann size V stimulus is presented against a 100 cdm^{-2} broadband (500-700nm) yellow background (Sample et al 1996). The high luminance, broadband yellow background suppresses the rods and the medium (green)- and long (red)- wavelength sensitive cones. The blue stimulus preferentially stimulates the short-wavelength sensitive (blue) pathway (Adams et al 1991). SWAP uses a Goldmann size V, (1.75° diameter) stimulus and a 200 msec stimulus duration on the HFA and a 100 msec duration on the Octopus perimeters, to maximize spatial and temporal summation, short-wavelength isolation and dynamic range.

It has been shown that SWAP apparently differentiates between normal and glaucomatous eyes; shows deficits in many suspect eyes when W-W fields remain normal (Sample et al 1986, 1988, 1990, 1992; Heron et al 1988; 1993; de Jong et al 1990; Hart et al 1990; Adams et al 1991; Sample and Weinreb 1992; Casson et al 1993; Johnson et al 1993ab,1995; Wild et al 1995); indicates more extensive damage than evidenced by W-W fields; and shows progressive loss sooner than W-W fields in patients with glaucoma (Sample et al 1993; Johnson et al 1993a,b). The incidence of progressive loss in glaucoma is similar to that in W-W perimetry (Caprioli 2001).

Research within the Group (Wild et al 1995; Wild and Moss 1996; Hutchings et al 2001) and from other investigators (Kwon et al 1998) has reported that SWAP demonstrates greater between-subject variability than standard W-W perimetry. Also, the short-term fluctuation (SF) and long-term fluctuation (LF) are greater for normal subjects in SWAP than in W-W perimetry (Wild and Moss 1996; Kwon et al 1998). SWAP is currently time consuming and difficult for the patient to perform. As a consequence, the response exhibits unacceptably high within- and between-examination variability compared to W-W perimetry. The large between-subject normal variability renders the statistical analytic package for SWAP (SWAPPAC) of little value when compared to that for W-W perimetry (STATPAC). The visual field recorded by SWAP can be difficult to interpret due to the difficulty in differentiating test-retest variability from actual and progressing visual field loss. This difficulty obviously has consequences for the effective and efficient management of patients undergoing SWAP. It is clear, therefore, that methods to minimise the inherent variability associated with SWAP must be developed before SWAP can become a viable clinical test.

Due to the inherent greater variability in any given SWAP examination, it can be hypothesised that any frequency-of-seeing curve at any given location for any given individual should exhibit a shallower slope for SWAP than for W-W perimetry. There are no publications concerning the frequency-of-seeing curve in SWAP for normal individuals and patients with glaucoma. There has been a resurgence of interest in SWAP with the advent of the SITA SWAP algorithm, which incorporates, amongst other

methods, the frequency-of-seeing curve to aid threshold estimation (Bengtsson 2003; Bengtsson and Heijl 2003).

As a consequence, a study was designed to determine the format of the FOS curve in SWAP as a function of: stimulus eccentricity; sensitivity and defect depth; in normal individuals and in patients with glaucoma. The corresponding information was also derived for W-W perimetry. The results of the study will provide further information for the design and interpretation of new perimetric algorithms for SWAP which are essential if the technique is to exhibit lower variability and a decreased examination time.

2.5 The Influence of Fatigue on the Prevalence of False-negative Responses in Perimetry.

The False-negative catch trial comprises the presentation of a stimulus 9dB above the threshold recorded earlier in the examination. Failure to respond to the stimulus may be due to increased variability greater than the 9dB increment or due to the inattention in a subject with normal variability or variability of less than 9dB (Fankhauser et al 1977; Anderson and Patella 1992; Bengtsson and Heijl 2000). Thus, the index cannot differentiate between the two possible contributing factors. A high percentage of false-negative responses is associated with a lower mean sensitivity, higher mean defect and lower mean deviation and often occurs in glaucoma (Katz and Sommer 1988, 1990; Reynolds et al 1990; Johnson and Nelson-Quigg 1993). Bengtsson (2000) and Bengtsson and Heijl (2000) found that as the area and severity of visual field loss increases, it is more probable that the number of false-negative responses will also increase.

The fatigue effect is the term given to the decline in sensitivity and increase in variability, with increasing examination duration (Heijl and Drance 1983; Hudson et al 1994) The fatigue effect has been noted in normal subjects (Searle et al 1991, Hudson et al 1994), in patients with ocular hypertension (Wild et al 1991; Hudson et al 1994) and in patients with glaucoma (Heijl 1977; Heijl and Drance 1983, Johnson et al 1988b).

In the normal eye, the fatigue effect within an examination may cause a general reduction in sensitivity of between 1dB (Johnson et al 1988a) and 2.5 dB (Hudson et al 1994). The reduction in sensitivity increases as a function of the examination duration (Heijl 1977b; Heijl and Drance 1983; Johnson et al 1988b; Searle et al 1991; Hudson et al 1994; Marra and Flammer 1991); is greater for the second eye tested (Searle et al 1991; Hudson et al 1994); is more pronounced in more eccentric locations (Johnson et al 1988a; Hudson et al 1994), particularly for glaucoma patients (Johnson et al 1988a); and is greater in areas adjacent to and within regions of focal loss (Holmin 1979; Suzamura 1988; Heijl and Drance 1983). The fatigue effect is discussed in depth in Chapter 6.

In patients with glaucoma, perimetric threshold variability (Flammer et al 1984, Heijl 1989; Werner 1989; Boeglin 1992; Bengtsson and Heijl 2000) and visual fatigue (Heijl 1977; Heijl and Drance 1983; Katz and Sommer 1988), are greater than for normal individuals. The larger fluctuations in sensitivity and/or the increased visual fatigue in glaucoma which can result in increased variability, can independently, or jointly, explain the greater number of false-negative responses in patients with glaucomatous field loss (Katz and Sommer 1988; Bengtsson and Heijl 2000).

A prospective cross-sectional exploratory observational study was designed to investigate whether the prevalence of false-negative responses increased with an increase in visual fatigue in patients with glaucoma. The findings of this study will provide useful information concerning the relevance of rest breaks during perimetry and their effect on the reliability and/or variability of the threshold estimate.

2.6 Logistics

The research was undertaken at the Cardiff School of Optometry and Vision Sciences, Cardiff University Cardiff, and at the Cardiff Eye Unit, University Hospital of Wales. Where appropriate, Ethical Committee approval for the research was obtained from the Bro Taf Local Research Ethics Committee, Cardiff. Ethical approval for the perimetric algorithm study described in Chapters 3 and 4, was granted in the first instance without

the need for revision. The ethical submission for the FOS study discussed in Chapter 5, required resubmission following some minor amendments, before ethical approval was granted which delayed the commencement of the study by an additional two months. Further delays in the collection of data, arose prior to beginning the perimetric algorithm study, due to a faulty perimeter. The Octopus 301 was providing erroneous results and initially, the appointments for 9 patients had to be cancelled and rebooked at a later date. During subsequent perimetric examinations, the Octopus perimeter began pausing randomly which was frustrating for both the perimetrist (the author) and the subject. Strangely, the random pauses did not occur for all subjects consequently, there were several instances when the perimeter appeared to have returned to its normal function, only to relapse soon after, with another subject. It took some time to establish that, the newly delivered Octopus perimeter contained out of date and faulty software. It took additional time for the problem to be rectified.

Normal individuals were recruited from the Eye Clinic and Staff of Cardiff University and from old-age pensioner associations. Numerous letters were written to local employers and societies, requesting volunteers from the workforce/society members to participate in the study. Informed consent and a signed consent form were obtained from each study participant after explanation of the procedures and possible consequences of the studies had been provided. A full ophthalmic examination was undertaken for each normal individual.

Glaucoma patients were recruited from the University Hospital of Wales, Cardiff. The diagnosis of glaucoma was provided by Mr James Morgan, Reader and Honorary Consultant Ophthalmologist, University Hospital of Wales. The recruitment of glaucoma patients was time consuming as copious amounts of patient notes had to be read (approximately 1500 patient notes in total) in order to establish which patients met the inclusion criteria. The majority of the notes did not meet the strict inclusion criteria, as glaucoma has a greater prevalence with age as do so many other ocular and systemic conditions, which were excluded from the study. On many occasions it would be necessary to spend a day, reading numerous patient notes, waiting for a particular patient

to arrive to request their participation in the study, only for the request to be declined. In order to minimise the time lost on this task, on occasion, numerous letters were sent out to patients requesting participation in the study. The ratio of volunteers coming forward relative to the vast number of letters sent was poor. Several other local researchers were recruiting volunteers from the same cluster of patients at that time, so care had to be taken to ensure that no patient was participating in more than one study at any one time and that no patients were being inundated with requests to assist with research projects.

The recruitment of normal subjects and patients with glaucoma posed a further problem due to the number, and length, of the visits required for each study (4 visits for the perimetric algorithm study, 5 visits for the FOS study and 2 visits for the false-negative study). It was frequently found that normal individuals who complied with the inclusion criteria were unable or unwilling to participate in any of the studies due to work commitments or due to difficulties in travelling. The recruitment of suitable patients with glaucoma was also difficult due to the rigid inclusion criteria, despite the fact that some were keen to assist. Participation in the studies required several visits for perimetry and therefore a great amount of commitment from the potential volunteer.

Neither the normal individuals nor the patients with glaucoma formed truly random samples, due to the method of selection and the difficulty in acquiring volunteers. Some of the volunteers had participated in previous perimetric and/or non-perimetric studies within the School and inevitably the patients with glaucoma had more previous perimetric experience overall than the normal individuals.

In order to provide an incentive to encourage study participation by those who met the inclusion criteria for both the normal individuals and patients with glaucoma, all volunteers were paid for their time (£30 was given to each participant on completion of all the visits for both algorithm studies and the FOS study and £10 was given to each patient for the FN study). All volunteers also had their travel expenses reimbursed. In some instances, individuals would volunteer to take part and then fail to complete the necessary number of visits required to complete the study so the acquired data had to be

discarded. In total 5 subjects dropped out for the FOS study and 3 subjects dropped out of the algorithm studies.

In total, 97 volunteers provided 1335 visual fields, 156 ocular media absorption examinations for a total of 378 visits, consisting of approximately 600 hours of perimetric and ocular examination time, for the analysis in the thesis. The vast quantity of perimetric data had to be inputted manually into the computer before any analysis could be carried out. For each perimetric examination (1335 in total), a minimum of 216 numbers and 8 separate indicators of subject data had to be inputted. This inevitably was extremely time-consuming.

Although, several difficulties were encountered during the recruitment and implementation of the studies described in this thesis, many of the subjects who volunteered to participate in the study/studies were very kind and generous with their time and a pleasure to meet and therefore made the overall experience an enjoyable one.

CHAPTER 3

Perimetric Sensitivity in the Normal Eye as a Function of the Full Threshold, SITA Standard, SITA Fast, Octopus Threshold and TOP Algorithms.

3.1 INTRODUCTION

Static automated perimetry is used routinely in clinical ophthalmological practice to assess the functional integrity of the visual field. In order to improve patient comfort and to reduce visual fatigue, thresholding strategies have been developed which are significantly faster at estimating the sensitivity across the visual field, than the conventional staircase techniques (Bengtsson et al 1997a; Vingrys et al 1999; Turpin et al 2002).

Several different perimetric algorithms are available. The currently accepted gold standard algorithms are the Full Threshold algorithm of the HFA and the Threshold algorithm of the Octopus perimeters. Recently, three new, more rapid, algorithms have become commercially available: SITA Standard and SITA Fast for the HFA, and TOP for the Octopus perimeters. The SITA and TOP algorithms are based upon fundamentally different methods of computation which have already been discussed in detail in Chapter 1.

3.1.1 HFA Full Threshold and Octopus Threshold Algorithms

The 'gold standard' HFA Full Threshold and Octopus Threshold algorithms use a repetitive bracketing strategy to estimate the threshold at each test location. As was pointed out in Chapter 1, the Full Threshold algorithm of the HFA uses a 4-2dB double staircase strategy. Threshold is designated as the 'last seen' stimulus (Haley 1987). The Octopus Threshold algorithm employs a 4-2-1dB strategy. Threshold is taken as the average of the last "seen" and last "not seen" stimuli. The final 1dB step is achieved by interpolation. Due to the differences in calculation of the threshold between the two algorithms, the HFA will record a value of sensitivity that is apparently 1dB lower than

that recorded by the Octopus, were all the stimulus parameters identical between the two systems (Zeyen et al 1993).

In patients with glaucomatous visual field loss, the examination duration of the Full Threshold or the Threshold algorithms, can frequently approach 16-17 minutes per eye for the 76 stimulus locations contained within Program 30-2 or Program 32. At this examination duration, patient compliance may be reduced and the fatigue effect becomes exaggerated (Heijl 1977b; Heijl and Drance 1983; Johnson et al 1988b; Marra and Flammer 1991; Searle et al 1991; Wild et al 1991; Hudson et al 1994; Wild et al 1999).

As was also discussed in Chapter 1, the fatigue effect becomes greater with increasing stimulus eccentricity and with increasing age and is more pronounced in areas of, and adjacent to, visual field loss (Heijl 1977; Heijl and Drance 1983; Heijl et al 1989; Johnson et al 1988b; Flanagan et al 1993). The reduction in sensitivity occurs within- and between-eyes at a given visit (Searle et al 1991; Hudson et al 1994). The fatigue effect can give rise to an apparent increase in both the depth and area of the measured visual field defect. In addition, a protracted examination duration is incompatible with the financial constraints associated with modern health care.

3.1.2 Swedish Interactive Threshold Algorithm, (SITA) Standard and (SITA) Fast
The HFA 700 Series offers the SITA Standard and SITA Fast algorithms. These algorithms were discussed in detail, in Chapter 1 and are, respectively, analogous to the Full Threshold and FASTPAC algorithms. However, the characteristics of both SITA algorithms are considerably more sophisticated than previous generations of algorithm (Wild et al 1999).

SITA reduces the examination duration without loss of accuracy in the threshold estimate by using two likelihood models for each stimulus location, one for normal responses and one for glaucomatous responses (Olsson and Rootzen 1994; Wild et al 1999a,b). The two likelihood models are derived from the age-corrected normal threshold value at each

location, the between-subject variability in the estimation of threshold (Heijl et al 1987a), the interdependence of threshold values at adjacent visual field locations (Heijl et al 1989a; Åsman and Heijl 1992b; Olsson and Rootzen 1994) and the magnitude, and variation in shape, of the frequency-of-seeing curve between stimulus locations (Weber and Rau 1992; Olsson et al 1993). The threshold estimate at any given stimulus location is determined by SITA represents the stimulus intensity that has a 50 percent probability of seeing (Bengtsson et al 1998a,b).

As a consequence, the SITA algorithms utilize considerably fewer stimulus presentations than the Full Threshold algorithm (Bengtsson et al 1997; Bengtsson and Heijl 1998ab; Szatmary et al 2002). In a normal individual, Program 30-2 of the HFA, using the Full Threshold algorithm, takes approximately 15 minutes and requires between 500 and 600 stimulus presentations per eye (Sekhar et al 1998). The number of stimuli presented by the SITA Standard algorithm is reduced by an average of approximately 29% in normal fields and 26% in glaucomatous fields compared to the Full Threshold algorithm (Bengtsson et al 1997; Bengtsson and Heijl 1998ab; Sekhar et al 1998; Wild et al 1999; Budenz et al 2000; Schimiti et al 2001; Szatmary et al 2002). For glaucoma patients, the examination duration for the SITA Standard algorithm is approximately 50%, and for the SITA Fast algorithm approximately 70%, of that of the Full Threshold algorithm (Bengtsson and Heijl 1998ab; Wild et al 1999; Sekhar et al 2000; Sharma et al 2000; Wall et al 2001; Budenz et al 2002). As the severity of the glaucoma increases, the reduction in examination duration for both SITA algorithms is reduced when compared to the Full Threshold algorithm (Bengtsson and Heijl 1998; Wild et al 1999b; Sekhar et al 2000; Budenz et al 2002).

The SITA Fast algorithm exhibits increased test-retest variability compared to the SITA Standard algorithm for defect depths of more than approximately 10dB (Artes et al 2002). SITA Fast slightly underestimates the true extent of visual field loss in glaucoma when compared to the SITA Standard algorithm (Bengtsson and Heijl 1998c; Bengtsson and Heijl 1999; Wild et al 1999b; Sharma et al 2000). The reliability of the perimetric examination, as indicated by the number of responses to catch trials, is lower with the

90

SITA Standard algorithm compared to the Full Threshold algorithm probably as a result of the reduced examination duration and the consequent reduction in fatigue (Sharma et al 2000).

Due to the superior efficiency of the SITA algorithms, it has been suggested that eventually the SITA algorithms will replace the Full Threshold algorithm as the accepted gold standard for the HFA (Bengtsson and Heijl 1998a; Budenz et al 2002).

3.1.3 Tendency Oriented Perimetry (TOP) Algorithm

Tendency Oriented Perimetry (TOP), (OCTOPUS Tendency Oriented Perimetry (1997), Interzeag AG, Switzerland), has been discussed in detail in Chapter 1 and is a fast thresholding strategy for the Octopus perimeters that relies upon the inter-dependency of the threshold between adjacent stimulus locations. TOP divides the 76 stimulus locations of the standard Program 32 into four sub-matrixes of 19 locations that are each separated by 12° (Gonzalez de la Rosa et al 1997). A MOBS procedure is used to begin the estimation of the threshold at each location in the first sub-matrix. The initial estimates of threshold for the first sub-matrix are used to update the estimate of threshold at each location in the remaining sub-matrices by linear interpolation. Each test location is examined with a single stimulus only. This procedure has also been discussed in detail in Chapter 1.

TOP enables a rapid visual field examination. The examination duration is approximately 2.5 minutes per eye (Morales et al 2001; Wadood et al 2002; Anderson 2003). However, the reduced examination duration of TOP is at the expense of an inaccurate calculation of the depth of glaucomatous loss when compared to the Threshold algorithm with Program 32 of the Octopus (Gonzalez de la Rosa 1997, 2001; Lachkar et al 1998) and to the SITA Fast algorithm with Program 30-2 of the HFA (King et al 2002).

Gonzalez de la Rosa et al (1996), found an excellent correlation between the global Mean MD ($r=0.96$), the MD of each quadrant ($r=0.92$ to $r=0.96$), the Loss Variance ($r=0.91$)

and individual thresholds (r=0.84) when comparing TOP to the Threshold algorithm of the Octopus using Program 32. In a similar study, Takada et al (1998), found a correlation of 0.95 for MD and 0.89 for LV between the Threshold and TOP algorithms of the Octopus perimeter using Program 32. On average, the MS is 1.0-1.5dB higher, and the MD 1.0-1.5dB better, than the Threshold strategy. The difference in the indices between the two algorithms may be attributable to the fact that the fatigue effect is probably negligible, or absent entirely, during the examination with TOP (Gonzalez de la Rosa et al 1996). However, some studies have found that TOP gives significantly reduced values for LV compared to the Threshold strategy (Lachkar et al 1998; Maeda et al 2000; Anderson 2003). It is possible that this reduction in LV with TOP could also be attributed to the absence, or reduction, of the fatigue effect.

However, short perimetric algorithms may be more sensitive to the learning effect than longer algorithms. The general rule that the first perimetric examination should not be accepted as the true representation of the field, especially if the field is abnormal, also applies to short perimetric strategies (Morales et al 2000). Any abnormal visual field detected at the first examination should be repeated, regardless of the algorithm, before it can be utilized to dictate patient management.

Inaccuracies may occur in the appearance of the borders of severe defects measured with TOP. For example, the borders of hemianopsia (and focal defects in general) (Gonzalez de la Rosa 1997, 2000; Morales et al 2000) often become blurred, receding slightly over the midline. This is likely to arise as a result of the spatial averaging inherent in the TOP thresholding procedure. Whilst some researchers have concluded that spatial averaging reduces the examination variability (Fitzke et al 1995) and consequently improves the ability to monitor progression of visual field loss (Crabb et al 1997), others have found that spatial averaging masks the ability to detect the progression of small visual field defects (Spry et al 2002; Anderson 2003).

The TOP algorithm usually overestimates sensitivity, and underestimates the LV, for small defects comprising one or two locations, compared with the Threshold algorithm of

the Octopus perimeter using Program 32. With relatively large defects of nine contiguous points or more, both the defect depth and the LV are predicted with reasonable accuracy by TOP, although normal locations surrounding such a defect exhibit a reduced sensitivity, consistent with the 'blurring' of the borders of defects reported clinically (Anderson 2003). Local absolute defects are missed by TOP (Takada et al 1998). TOP has a number of unusual spatial characteristics that prevent it from accurately estimating the spatial extent and absolute sensitivity of visual field loss (Morales et al 2000; Anderson 2003).

A false-response by the subject in the earliest stages of the TOP thresholding procedure, when the lower numbered sub-matrices are being examined will have the greatest impact as the information from the false response will indirectly effect all of the remaining sub-matrices (Anderson 2003). The TOP algorithm is less sensitive to isolated errors in the patient's response and is very sensitive to clustered defects compared to the Threshold algorithm. Thus, if focal loss is detected, it is unlikely that it will be the result of inaccurate data obtained from a normal visual field (Gonzalez de la Rosa 1996).

TOP is capable of detecting moderate to advanced glaucomatous visual field loss (Lachkar et al 1998; Takada et al 1998; Anderson 2003). TOP has not yet been subjected to sufficient detailed independent research. However, the format of the threshold estimating procedure and the research completed to date (Maeda et al 2000; King et al 2002; Anderson 2003) suggests that TOP will underestimate early visual field loss in glaucoma.

The reduction in examination duration of TOP when compared to the other commercially available perimetric algorithms, makes it an extremely appealing algorithm to implement in the current financially-stretched climate of health care provision. However, if as already suggested in the literature thus far, TOP fails to detect glaucomatous field loss in its earliest stages, and/or underestimates the extent and depth of such loss, its application as a screening and diagnostic test is rendered inappropriate. The prognosis for any patient with glaucoma is improved considerably with the early diagnosis of the disease.

The failure to detect functional visual loss by the employment of an inadequate visual field examination, could potentially have major ramifications on the diagnosis and subsequent management of a patient with glaucoma. It is vital that further research is conducted into the performance of the TOP algorithm in normal individuals and in patients with glaucoma, before conclusions about its merit as a perimetric algorithm can be made.

3.2 AIMS

A cross-sectional prospective observational study was undertaken to determine the performance, in normal individuals, of the SITA Standard, SITA Fast and TOP algorithms. The Full Threshold and Threshold algorithms were included in the study as reference algorithms for the SITA and TOP algorithms, respectively. There is a notable void in the literature, in that these five algorithms have not previously been investigated simultaneously on either normal individuals or patients with glaucoma. The study was intended, in particular, to provide further information concerning the viability of the use of the TOP algorithm in the accurate estimation of normal sensitivity.

More specifically, the purpose of the study was twofold: firstly to determine the within-visit, between-algorithm differences in the measured sensitivity for the five algorithms; and, secondly, the between-visit, within-algorithm differences in the measured sensitivity for the five algorithms.

3.3 METHODS
3.3.1 Cohort

The cohort comprised 24 consecutively presenting normal individuals (9 males and 15 females) who volunteered to take part in the study and who met the inclusion criteria. The subjects were recruited from the Eye Clinic at the School of Optometry and Vision Sciences of Cardiff University and from local old-age pensioner associations. The mean age for the Group was 65.5 years (SD 12.31) and the age range was 34-82 years. The age distribution is shown in Table 3.1 overleaf. The individuals were deliberately recruited to

bias the age of the distribution to that representative of the population normally undergoing perimetry.

Age (years)	Number of Normal Individuals
30-39	2
40-49	0
50-59	3
60-69	10
70-79	7
80+	2

Table 3.1 The age distribution within the Group.

The individuals attended for 4 visits. At the first visit, all individuals underwent a routine eye examination to determine whether they met the inclusion criteria for entry into the study. The inclusion criteria, comprised, a distance visual acuity of 6/9 or better in either eye, distance refractive error of less than or equal to 5 dioptres mean sphere and less than 2.5 dioptres cylinder, lenticular changes not greater than NCIII, NOIII, CI or PI by LOCS III (Chylack et al 1993), intraocular pressure of less than 22mmHg, a normal optic nerve head appearance, open anterior chamber angles, no medication known to affect the visual field, no previous ocular surgery or trauma, no history of diabetes mellitus and no family history of glaucoma.

3.3.2 Examination Protocol

The study comprised a two period cross-over design with order randomization between visits. All volunteers attended for three visual field visits; each visit consisted of two sessions. Perimetry was undertaken on one randomly selected eye of each individual, using the HFA 740 and the Octopus 301 perimeters. The order of algorithm within each session and the order of the sessions within a visit was randomized for each subject but

held constant between sessions over each of the three visits. Each session lasted approximately 25-30 minutes and was separated by a rest period of 30 minutes. At one session, the designated eye was examined with the Octopus TOP algorithm using Program 32, the Octopus Threshold algorithm using Program 32 and the HFA SITA Fast algorithm using Program 30-2. At the remaining session, the designated eye underwent examination with the HFA SITA Standard and the HFA Full Threshold algorithms, using Program 30-2.

In order to minimize the fatigue effect, rest periods of approximately one minute were given at 4 minute intervals during those examinations whose duration extended to 4 minutes or more. The examination with each algorithm was separated by a rest period of 2 minutes. The protocol at the second and third visits was identical to that of the first visual field visit for each subject i.e. the combinations of program and algorithm were held constant between-sessions at each visit and between-visits. The three visual field visits were carried out at weekly intervals. The first visual field visit was considered as a familiarisation session and the results were discarded prior to data analysis in order to minimise the influence of the learning effect.

The appropriate refractive correction for the viewing distance of the bowl of each perimeter was used for the designated eye of each patient and the non-tested eye was occluded with an opaque patch. Fixation was monitored continuously using the video monitor of each perimeter, the gaze tracker and the standard Heijl-Krakau technique of the HFA and the eye fixation control system of the Octopus perimeter (discussed in Chapter 1).

Ethical Committee approval had been obtained for the study on 21st November 2001 from The Bro Taf Health Authority.

3.3.3 Analysis

For simplicity, the third and fourth study visits will be referred to from hereon in as Visit 1 and Visit 2, respectively.

The results for the left eyes were converted into right eye format. The stimulus locations immediately above and below the physiological blind spot were excluded from the analyses. At locations exhibiting double threshold determinations, the mean of the two determinations was used as the threshold value. The MD values for each Octopus examination were converted to HFA format prior to the analysis, i.e. all positive values for the MD of the Octopus examinations were converted to negative values and vice versa. Similarly, the LV values of the Octopus were made compatible with the HFA PSD by taking the square root of the LV. The examination durations for all visual field examinations were converted from the minutes and seconds format of the HFA and Octopus perimeters into minutes in decimal format prior to data analysis. The Full Threshold algorithm of the HFA is the only algorithm of the five implemented in this study that provides a measure of short-term fluctuation, consequently comparative analysis of the SF was not possible.

The results were analysed in three separate ways. Firstly, the differences in each of the visual field indices: MS; the two types of MD; the two types of indices describing focal loss ($PSD/LV^{0.5}$); and in the examination duration between the five algorithms within each of Visits 1 and 2 and the differences within-algorithm between-visits were analysed using separate repeated measures Analysis of Variances (ANOVA). The type of algorithm, the order of the two sessions, and the order of presentation of the algorithm within a session were considered as separate within-subject factors. Patient age was considered as a between-subject factor.

For the second analysis, the difference in sensitivity at each stimulus location for all individuals between each pair of algorithms at the second visit (i.e. the within-visit between-algorithm variability) was calculated and expressed as a function of the sensitivity at the given stimulus location recorded at the same visit with the comparison

algorithm of the given pair. Similarly, the difference in sensitivity at each stimulus location for all patients for a given algorithm between Visit 1 and Visit 2 (i.e. the within-algorithm between-visit variability) was calculated and expressed as a function of the sensitivity recorded at the second visit at the given stimulus location with the given algorithm.

For the third analysis, the within-algorithm, between-visit differences in the shape analysis probability values across each stimulus location for all 24 individuals at visit 2 was expressed as a 5 x 5 contingency table for each pair of algorithms. The difference between the number of probability values lying above the diagonal in each contingency table and the number of probability values lying below the diagonal was tested for statistical significance based upon the binomial distribution. However, the probability values within each cell are not independent of those in other cells and the format of the contingency table can be influenced by one or more anomalous or outlying visual fields from one or more individuals. As a consequence, an arbitrary correction factor was applied namely, the division by two of the frequency within each cell. Such an approach considered, for example, the contribution of 10 probability levels from one individual to the given contingency table to be equivalent to the contribution of one probability level from each of five people

An identical analysis was undertaken for the between-algorithm within-visit differences in the Pattern Deviation probability values.

3.4   RESULTS

All visual field examinations met the inclusion criteria for reliability, namely, less than 20% fixation losses and less than 33% false-responses to the false-positive and false-negative catch trials.

98

3.4.1 General Characteristics
3.4.1.1 Group Mean MS
The Group Mean MS and one SD for Visit 1 and for Visit 2 for each of the algorithms is shown in Table 3.2a. The corresponding ANOVA summary table is shown in Table 3.2b.

Algorithm	HFA Full Threshold	HFA SITA Standard	HFA SITA Fast	Octopus Threshold	Octopus TOP
Visit 1	28.12 (2.69)	28.77 (2.98)	29.13 (2.30)	24.99 (2.80)	26.48 (7.92)
Visit 2	28.04 (2.56)	28.50 (2.71)	29.44 (2.21)	27.15 (8.17)	24.66 (3.40)

Table 3.2a The Summary Table for the Group Mean MS, expressed in dB, and one SD of the Mean at Visits 1 and 2 for each of the five algorithms.

Source	Df	Sums of Squares	Mean Square	F value	P
Algorithm	4	501.28	125.32	10.00	<0.0001
Session	1	16.79	16.79	1.34	0.249
Visit	1	0.22	0.22	0.02	0.896
Algorithm x Session	3	83.68	27.89	2.27	0.082

Table 3.2b The ANOVA Summary Table for the Group Mean MS at Visits 1 and 2.

The Group Mean MS varied between algorithms (p<0.0001) across each of the two visits (p=0.896). The Group Mean MS was highest with the SITA Fast algorithm at both Visits 1 and 2. The Octopus Threshold algorithm exhibited the lowest Group Mean MS at Visit 1 and the TOP algorithm the lowest Group mean MS at Visit 2.

3.4.1.2 Group Mean MD
The Group Mean MD and one SD of the mean for Visit 1 and Visit 2 for each of the algorithms is shown in Table 3.3a. The corresponding ANOVA summary table is shown in Table 3.3b.

Algorithm	HFA Full Threshold	HFA SITA Standard	HFA SITA Fast	Octopus Threshold	Octopus TOP
Visit 1	0.60 (1.94)	0.22 (2.29)	1.55 (4.84)	-1.09 (2.33)	-0.80 (2.40)
Visit 2	0.57 (1.78)	0.05 (2.03)	0.87 (1.55)	-0.48 (2.15)	-1.03 (2.90)

Table 3.3a The Summary Table for the Group Mean MD, expressed in dB, and one SD of the mean at Visits 1 and 2 for each of the five algorithms.

Source	Df	Sums of Squares	Mean Square	F value	P
Algorithm	4	104.77	26.19	26.87	<0.0001
Session	1	12.58	12.58	12.90	0.0004
Visit	1	0.71	0.71	0.94	0.395
Algorithm x Session	3	13.06	4.35	4.70	0.0034

Table 3.3b The ANOVA Summary Table for the Group Mean MD index at Visits 1 and 2.

The Group Mean MD varied between algorithms (p<0.0001) across each of the two visits (p=0.395). The Group Mean MD was most negative (i.e. lowest/worst) with the Octopus algorithms at both Visits 1 and 2. The Octopus Threshold algorithm exhibited the most negative Group Mean MD at Visit 1 and the TOP algorithm the most negative Group Mean MD at Visit 2. The most positive Group Mean MD was that of the SITA FAST algorithm at both Visit 1 and Visit 2.

The Group Mean MD was better (i.e. more positive) at the second session compared to the first session (p=0.0004) of the given visit and this between-session difference in the MD was more pronounced at the second visit (p=0.0034).

3.4.1.3 Group Mean PSD/LV$^{0.5}$

The Group Mean Pattern Standard Deviation (PSD) and one SD of the mean for each of the algorithms at Visit 1 and Visit 2 is shown in Table 3.4a. The corresponding ANOVA Summary Table is shown in Table 3.4b. The Group Mean PSD/LV$^{0.5}$ was highest for the Octopus Threshold algorithm at both visits. It was lowest for the SITA Standard algorithm at Visit 1 and for the SITA Fast algorithm for Visit 2. However, these differences did not reach statistical significance.

Algorithm	HFA Full Threshold	HFA SITA Standard	HFA SITA Fast	Octopus Threshold	Octopus TOP
Visit 1	1.97 (0.51)	1.91 (0.75)	2.30 (3.38)	2.63 (1.12)	1.97 (0.84)
Visit 2	2.09 (0.63)	1.99 (0.69)	1.56 (0.51)	2.43 (0.80)	2.20 (0.96)

Table 3.4a The Group Mean PSD/LV$^{0.5}$, expressed in dB, and one SD of the mean at Visits 1 and 2 for each of the five algorithms.

Source	Df	Sums of Squares	Mean Square	F value	P
Algorithm	4	11.45	2.86	2.33	0.057
Session	1	0.19	0.19	0.15	0.698
Visit	1	0.57	0.57	0.46	0.469
Algorithm x Session	3	13.06	4.35	4.70	0.084

Table 3.4b The ANOVA Summary Table for the Group Mean PSD/LV$^{0.5}$ index at Visits 1 and 2.

The potential difference in the Group Mean PSD/LV$^{0.5}$ between the five algorithms failed to reach statistical significance.

3.4.1.4 Group Mean Examination Duration

The Group Mean examination duration for each algorithm at Visit 1 and Visit 2 is shown in Table 3.5a. The corresponding ANOVA Summary Table is shown in Table 3.5b. The Group Mean examination duration, was significantly different as would be expected, between algorithms (p<0.0001) across each of the two visits (p=0.504). The shortest algorithm at both visits was the Octopus TOP algorithm. The longest algorithm at both visits was the HFA Full Threshold algorithm.

Algorithm	HFA Full Threshold	HFA SITA Standard	HFA SITA Fast	Octopus Threshold	Octopus TOP
Visit 1	13.79 (1.30)	6.95 (1.18)	4.15 (0.79)	13.20 (1.46)	2.51 (0.21)
Visit 2	14.15 (1.23)	6.92 (1.12)	3.90 (0.62)	12.75 (0.88)	2.54 (0.28)

Table 3.5a The Group Mean examination duration, expressed in minutes, and one SD of the mean at Visits 1 and 2 for each of the five algorithms.

Source	Df	Sums of Squares	Mean Square	F value	P
Algorithm	4	5153.72	1288.43	2180.27	<0.0001
Session	1	2.63	2.63	4.45	0.036
Visit	1	0.264	0.264	0.45	0.504
Algorithm x Session	3	1.61	0.54	0.91	0.438

Table 3.5b The ANOVA Summary Table for the Group Mean examination duration at Visits 1 and 2.

3.4.1.5 Within-visit (Visit 2), Between-algorithm Difference in the MD

The within-visit (Visit 2) between-algorithm differences in the MD for the 24 individuals (i.e. the between-subject difference), is shown in Figures 3.1a and 3.1b. The range for the 95% confidence intervals of the difference in the MD ranged from 2.85dB to 2.94dB for all comparisons between the HFA Full Threshold, SITA Standard and SITA Fast algorithms. The corresponding range between the two Octopus algorithms was 5.71dB and that between the TOP algorithm and SITA Standard and SITA Fast was 7.79dB and 8.5dB, respectively.
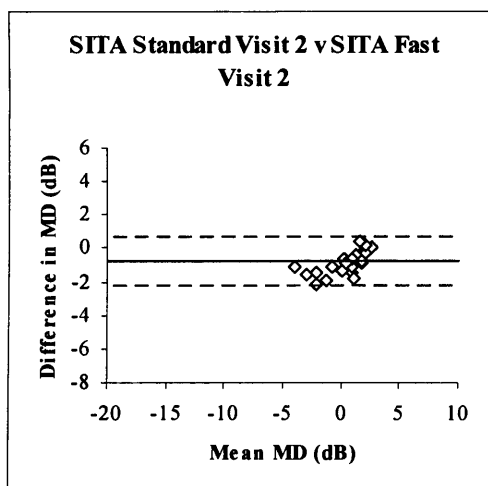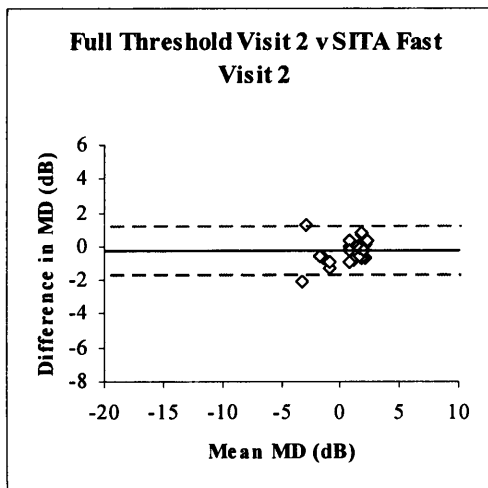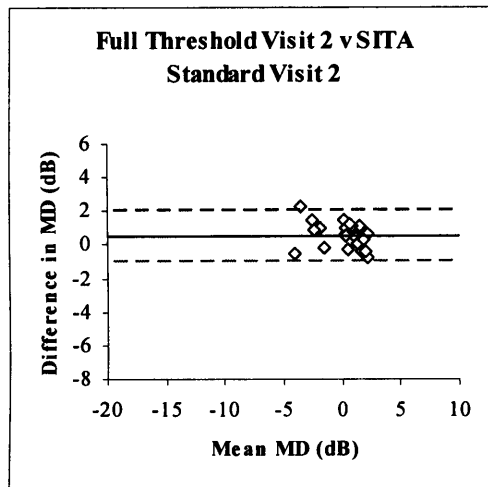
Figure 3.1a The within-visit (Visit 2), between-algorithm difference in the MD, for each of the 24 subjects, against the mean of the two MDs. Top: HFA Full Threshold v SITA Standard algorithms. Middle: HFA Full Threshold v SITA Fast algorithms. Bottom: SITA Standard v SITA Fast. The solid line indicates the mean of the differences and the dotted line the 95% confidence intervals.
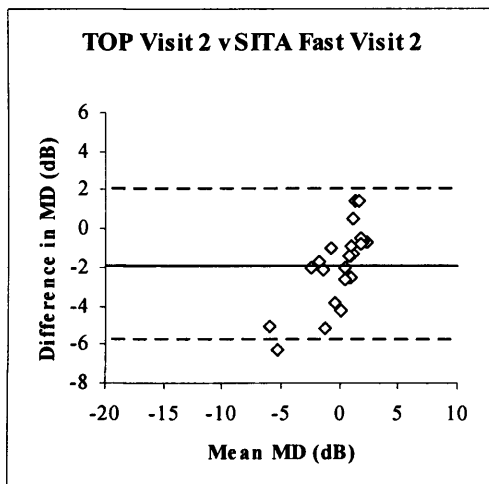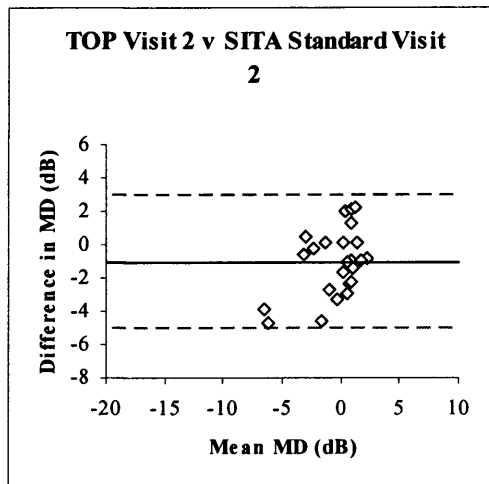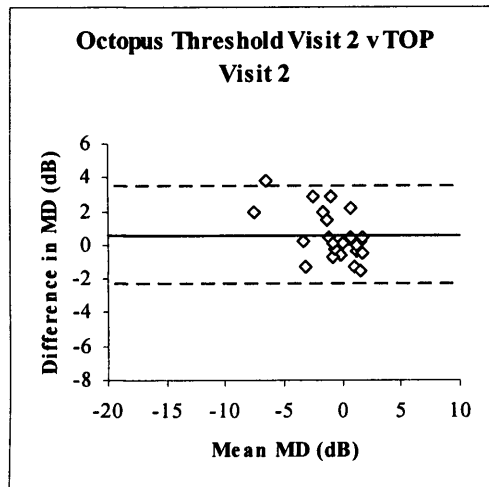
Figure 3.1b The within-visit (Visit 2), between-algorithm difference in the MD, for each of the 24 subjects, against the mean of the two MDs. Top: Octopus Threshold v TOP algorithms. Middle: TOP v SITA Standard algorithms. Bottom: TOP v SITA Fast algorithms. The solid line indicates the mean of the differences and the dotted line the 95% confidence intervals.

105

3.4.1.6 Between-visit Within-algorithm Differences in MD

The between-visit, within-algorithm differences in the MD for each of the 24 individuals (i.e. the between-subject difference) is shown in Figures 3.2a and 3.2b. The range for the 95% confidence intervals of the difference in the MD was smallest for the HFA Full Threshold (2.06dB) and SITA Fast (2.54dB) algorithms. It was greatest for the Octopus TOP (5.95dB) and this was closely followed by the Octopus Threshold algorithm (4.57dB) and the SITA Standard (5.27dB) algorithm.
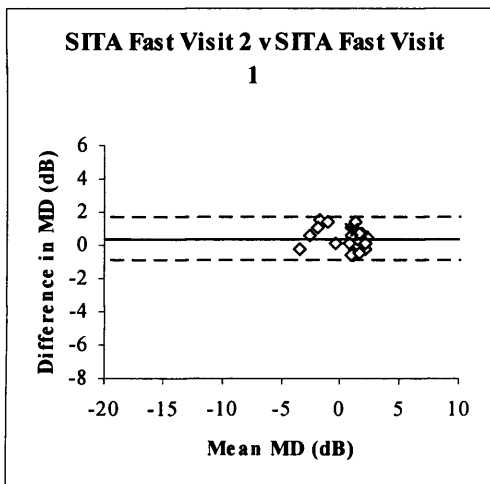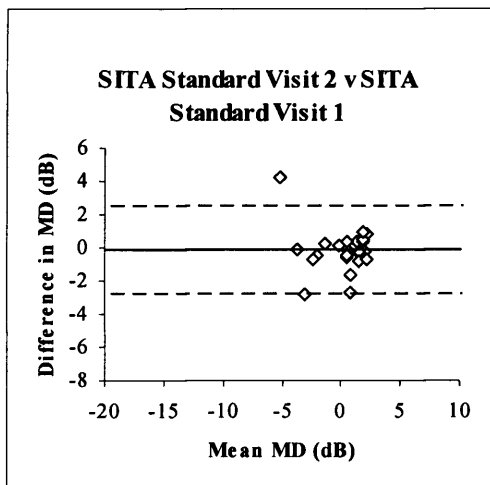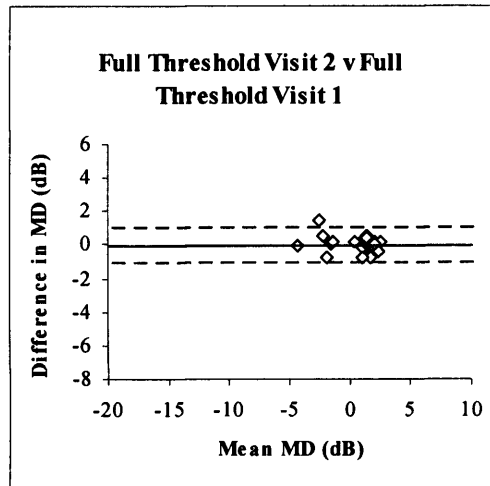
Figure 3.2a The between-visit, within-algorithm difference in the MD against the mean of the MDs at each visit. Top: HFA Full Threshold algorithm. Middle: SITA Standard algorithm. Bottom: SITA Fast algorithm. The solid line indicates the mean of the differences and the dotted line the 95% confidence intervals.

107
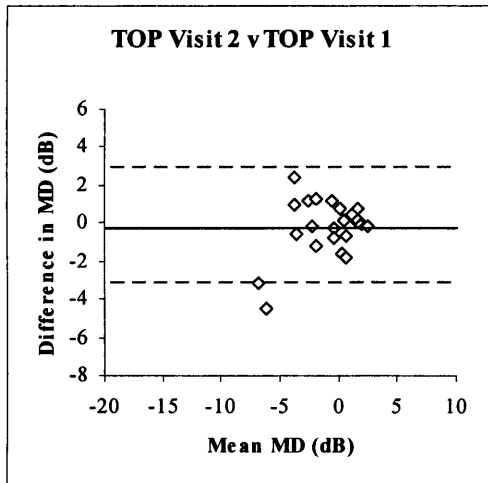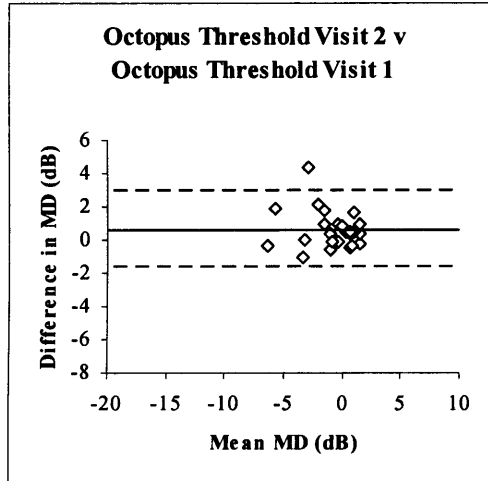
Figure 3.2b The between-visit, within-algorithm group difference in the MD against the mean of the MDs at each visit. Top: Octopus Threshold algorithm. Bottom: TOP algorithm. The solid line indicates the mean of the differences and the dotted line the 95% confidence intervals.

108

3.4.1.7 Within-visit (Visit 2) Between-algorithm Difference in Pointwise Sensitivity

The 10th, 50th and 90th percentiles of the distribution of the within-visit between-algorithm difference in sensitivity at each sensitivity level between each of the five algorithms at Visit Two are illustrated in Figures 3.3a and 3.3b. The 50th percentile of the difference in sensitivity between the HFA Full Threshold and the SITA Standard algorithms (Figure 3.3a, top) approximated to zero regardless of the level of sensitivity. However, the corresponding percentile between the HFA Full Threshold and SITA Fast algorithms (Figure 3.3a, middle) became more negative as sensitivity derived with the Full Threshold algorithm declined. This indicates that the SITA Fast algorithm overestimated sensitivity relative to the HFA Full Threshold algorithm and that the magnitude of the overestimation increased as sensitivity with the Full Threshold algorithm declined. A similar finding was present for the SITA Fast algorithm compared to the SITA Standard algorithm (Figure 3.3a, bottom).

The 50th percentile of the difference in sensitivity between the Octopus Threshold and TOP algorithms (Figure 3.3b, top) and between the TOP and SITA Fast algorithms (Figure 3.3b, bottom) approximated to zero regardless of the level of sensitivity. However, the SITA Standard algorithm overestimated sensitivity relative to the TOP algorithm and that the magnitude of the overestimation increased as sensitivity with the TOP algorithm declined.
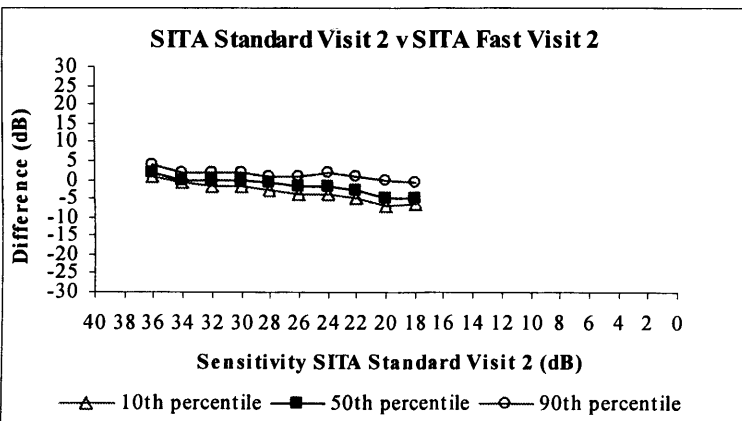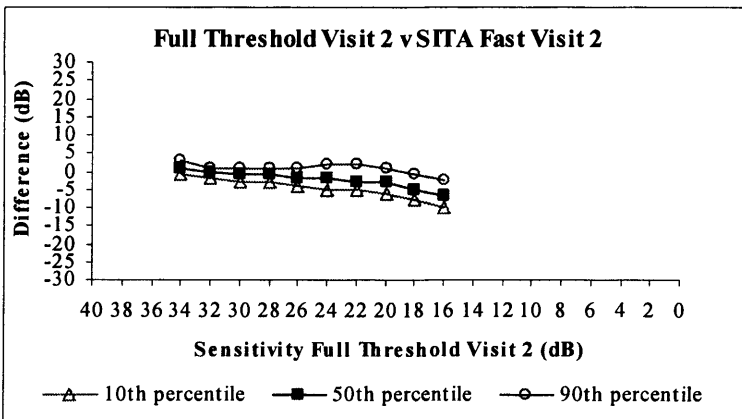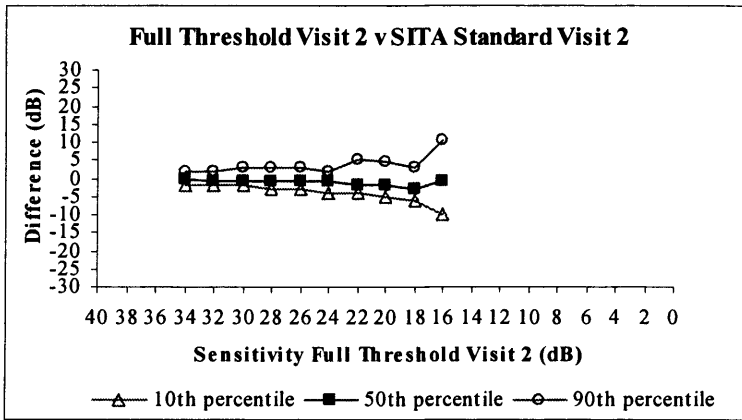
Figure 3.3a The 90th, 50th and 10th percentiles of the distribution of the differences in sensitivity across all stimulus locations at Visit 2. Top: HFA Full Threshold v SITA Standard algorithms. Middle: HFA Full Threshold v SITA Fast algorithms. Bottom: SITA Standard v SITA Fast algorithms.
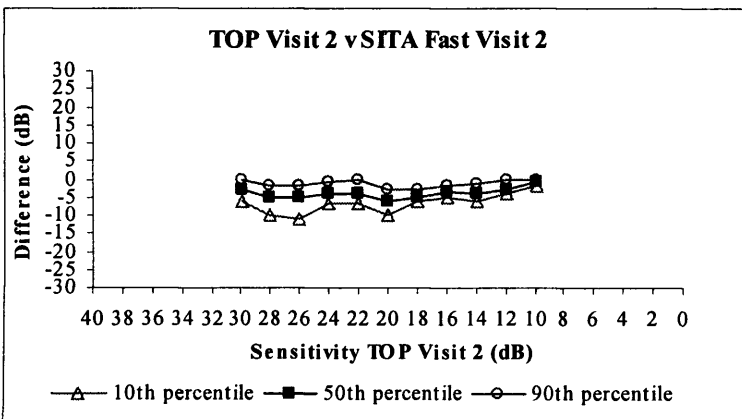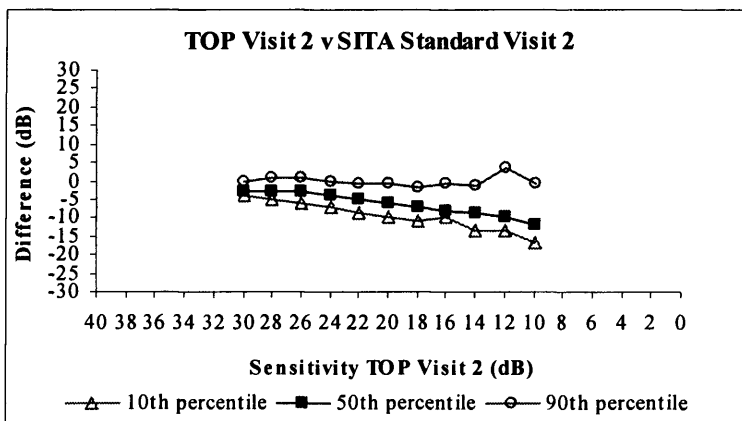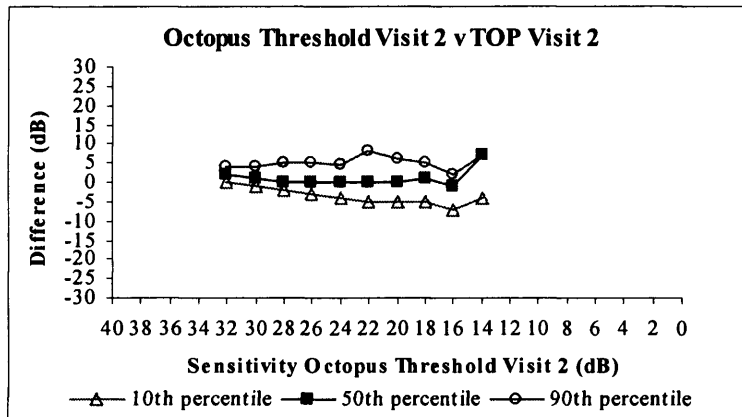
Figure 3.3b The 90th, 50th and 10th percentiles of the distribution of the differences in sensitivity across all stimulus locations at Visit 2. Top: Octopus Threshold v TOP algorithms. Middle: Octopus TOP v SITA Standard algorithms. Bottom: TOP v HFA SITA Fast algorithms.

111

3.4.1.8 Between-visit Within-algorithm Difference in Pointwise Sensitivity

The 10th, 50th and 90th percentiles of the distribution of the between-visit within-algorithm difference in sensitivity at each sensitivity level for each of the five algorithms at Visit 2 are illustrated in Figures 3.4a and 3.4b. The 50th percentile of the difference in sensitivity for the HFA Full Threshold, SITA Standard, SITA Fast (Figure 3.4a, top, middle, bottom) and Octopus Threshold algorithms (Figure 3.4b, top), as would be expected in the absence of a learning effect, approximated to zero regardless of the level of sensitivity at Visit 2. However, the corresponding distribution for the TOP algorithm indicated a higher sensitivity at Visit 1 compared to Visit 2 for locations exhibiting sensitivity up to approximately 16dB. In addition, the magnitude of this difference increased as sensitivity at Visit 2 declined.
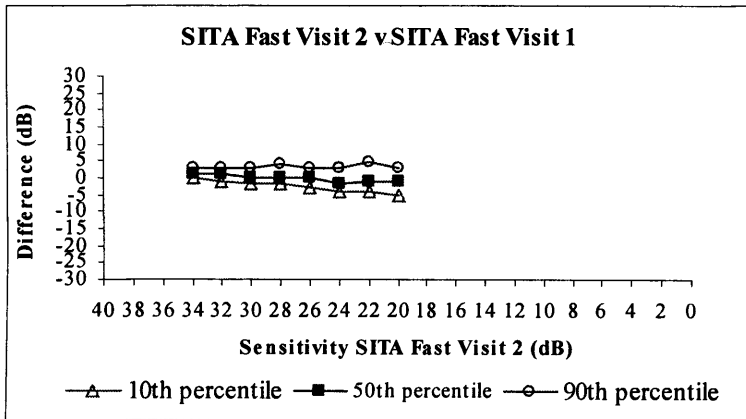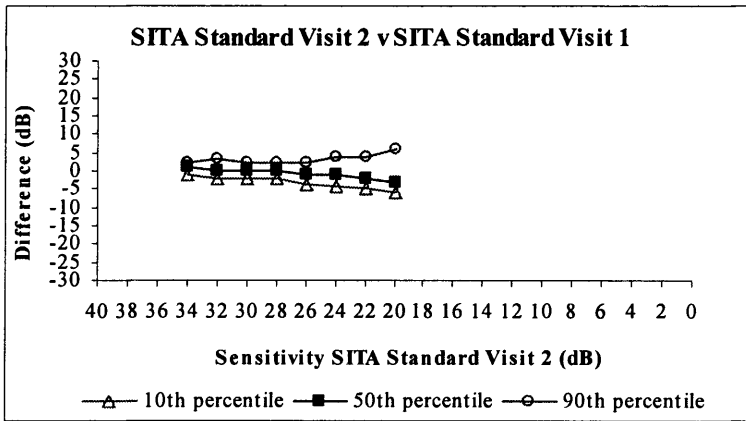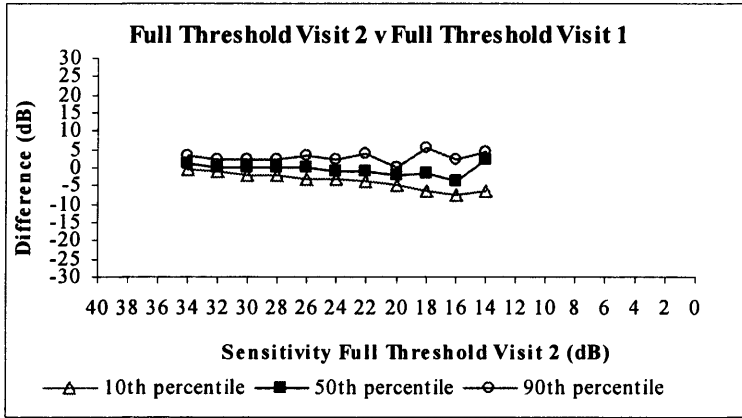
Figure 3.4a The 90th, 50th and 10th percentiles of the distribution of the differences in sensitivity across all locations between Visits 2 and 1. Top: HFA Full Threshold algorithm. Middle: SITA Standard algorithm. Bottom: SITA Fast algorithm.

Octopus Threshold Visit 2 v Octopus Threshold Visit 1

TOP Visit 2 v TOP Visit 1
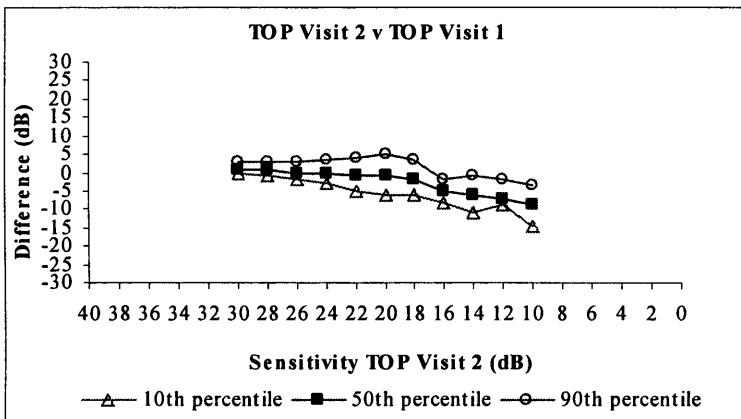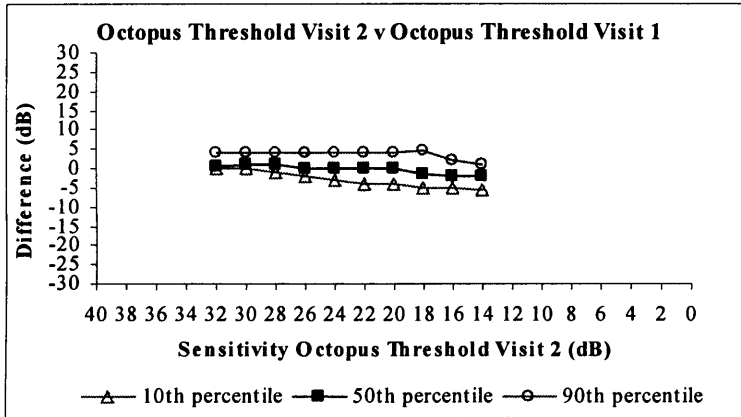
Figure 3.4b The 90th, 50th and 10th percentiles of the distribution of the differences in sensitivity across all locations between Visits 2 and 1. Top: Octopus Threshold algorithm. Bottom: TOP algorithm.

3.4.1.9 Within-visit (Visit 2) Between-algorithm Differences in the Pattern Deviation Probability level.

The difference in the magnitude of the Pattern Deviation probability levels at Visit 2 between the Full Threshold and the SITA Standard and SITA Fast algorithms, respectively is given in Table 3.6a, top and Table 3.6a, middle. The SITA algorithms generated a greater number of locations exhibiting apparent abnormality by Pattern Deviation probability analysis. Similarly, the SITA Standard algorithm generated a greater number of locations exhibiting apparent abnormality by Pattern Deviation probability analysis than the SITA Fast algorithm (Table 3.6a, bottom) and the TOP algorithm more locations than the Octopus Threshold (Table 3.6b, top) and SITA Fast algorithms (Table 3.6b, middle and bottom).

SITA Standard Visit 2						
		NS	< 5%	< 2%	<1%	<0.5%
Full Threshold Visit 2	NS	1597	72	32	12	5
	< 5%	21	4	5	3	3
	< 2%	8	1	1	2	0
	<1%	1	1	1	1	1
	<0.5%	0	2	0	0	3

p=<0.0001; Corrected p<0.0001

SITA Fast Visit 2						
		NS	< 5%	< 2%	<1%	<0.5%
Full Threshold Visit 2	NS	1639	52	14	10	3
	< 5%	26	5	4	1	0
	< 2%	10	1	0	1	0
	<1%	5	0	0	0	0
	<0.5%	3	0	1	1	0

p=<0.0001; Corrected p<0.0001

SITA Fast Visit 2						
		NS	< 5%	< 2%	<1%	<0.5%
SITA Standard Visit 2	NS	1558	43	14	9	3
	< 5%	69	4	5	2	0
	< 2%	34	5	0	0	0
	<1%	13	4	0	1	0
	<0.5%	9	2	0	1	0

p=<0.0001; Corrected p=0.007

Tables 3.6a The difference in the magnitude of the Pattern Deviation Probability Level between-algorithm at Visit 2. Top: Full Threshold v SITA Standard algorithms. Middle: Full Threshold v SITA Fast algorithms. Bottom: SITA Standard v SITA Fast algorithms.

116

TOP Visit 2						
		NS	< 5%	< 2%	<1%	<0.5%
Octopus Threshold Visit 2	NS	1589	43	22	3	20
	< 5%	28	10	6	1	3
	< 2%	15	1	2	1	0
	<1%	6	3	1	0	2
	<0.5%	7	4	1	1	7

p=0.003; Corrected p=0.040

TOP Visit 2						
		NS	< 5%	< 2%	<1%	<0.5%
SITA Standard Visit 2	NS	1607	37	15	11	13
	< 5%	46	8	1	1	2
	< 2%	12	3	2	0	2
	<1%	9	0	1	0	3
	<0.5%	3	0	0	0	0

p=0.58; Corrected p=0.66

TOP Visit 2						
		NS	< 5%	<2%	<1%	<0.5%
SITA Fast Visit 2	NS	1580	56	22	4	21
	< 5%	45	3	7	1	2
	< 2%	11	2	2	0	4
	<1%	6	0	1	1	5
	<0.5%	3	0	0	0	0

p=0.0001; Corrected p=0.016

Tables 3.6b The difference in the magnitude of the Pattern Deviation Probability Level between-algorithm at Visit 2. Top: Octopus Threshold v TOP algorithms. Middle: SITA Standard v TOP algorithms. Bottom: SITA Fast v TOP algorithms.

3.4.1.10 Between-visit Within-algorithm Difference in the Pattern Deviation Probability Level.

The difference in the magnitude of the Pattern Deviation probability levels between Visit 2 and Visit 1 for the Full Threshold and the SITA Standard and SITA Fast algorithms, respectively is given in Table 3.7a. and for the Octopus Threshold and TOP algorithms, in Table 3.7b. As would again be expected in the absence of a learning effect, these differences did not reach statistical significance. However, the Octopus Threshold algorithm (Table 3.7b, top) generated a greater number of locations exhibiting apparent abnormality by Pattern Deviation probability analysis at Visit 1 compared to Visit 2.

Full Threshold Visit 1						
		NS	< 5%	< 2%	<1%	<0.5%
	NS	1703	33	4	2	0
Full Threshold Visit 2	< 5%	28	5	1	1	1
	< 2%	8	2	1	1	0
	<1%	3	1	1	0	0
	<0.5%	3	0	1	1	0

p=0.84; Corrected p=0.88

SITA Standard Visit 1						
		NS	< 5%	< 2%	<1%	<0.5%
	NS	1557	50	15	20	9
SITA Standard Visit 2	< 5%	59	11	3	2	5
	< 2%	32	4	2	0	1
	<1%	11	1	1	4	1
	<0.5%	7	1	0	1	3

p=0.90; Corrected p=0.86

SITA Fast Visit 1						
		NS	< 5%	< 2%	<1%	<0.5%
	NS	1637	49	12	6	3
SITA Fast Visit 2	< 5%	40	11	3	2	2
	< 2%	12	3	1	1	2
	<1%	8	1	2	1	1
	<0.5%	3	0	0	0	0

p=0.18; Corrected p=0.36

Tables 3.7a The difference in the magnitude of the Pattern Deviation Probability Level within-visit (Visit 2) between-algorithm. Top: HFA Full Threshold algorithm. Middle: SITA Standard algorithm. Bottom: SITA Fast algorithm.

Octopus Threshold Visit 1					
		NS	< 5%	< 2%	<1%	<0.5%
	NS	1599	53	19	11	19
Octopus Threshold Visit 2	< 5%	27	7	4	2	8
	< 2%	11	2	4	2	0
	<1%	5	6	1	0	0
	<0.5%	9	3	0	1	7

p<0.0001; Corrected p<0.0001

Octopus TOP Visit 1					
		NS	< 5%	< 2%	<1%	<0.5%
	NS	1588	36	19	8	18
Octopus TOP Visit 2	< 5%	52	6	2	0	1
	< 2%	21	6	3	1	1
	<1%	5	0	0	0	1
	<0.5%	22	3	1	3	3

p=0.186; Corrected p=0.32

Tables 3.7b The difference in the magnitude of the Pattern Deviation Probability Level within-visit (Visit 2) between-algorithm. Top: Octopus Threshold algorithm. Bottom: Octopus TOP algorithms.

3.5 DISCUSSION
3.5.1 Global Indices
The Group Mean MS was highest for SITA Fast at both Visit 1 and Visit 2. Compared to the Full Threshold Algorithm, the Group Mean MS was 1.01dB higher for Visit 1 and 1.40dB higher for Visit 2. The Group Mean MS for SITA Standard was 0.65dB and 0.46dB higher than that for the Full Threshold algorithm at Visits 1 and 2 respectively. These results are compatible with previous studies (Bengtsson and Heijl 1999; Shirato et al 1999; Wild et al 1999a). Bengtsson and Heijl (1999) found, for normal individuals, that SITA Fast exhibited a Group Mean MS which was 1.6dB higher than that of the Full Threshold algorithm and that SITA Standard exhibited a Group Mean MS which was 1.2dB higher than the Full Threshold algorithm. Wild et al (1999a) found that SITA Fast and SITA Standard yielded Group Mean MSs which were 1.5dB higher and 0.8dB higher, respectively, than the Full Threshold algorithm. They also noted that these between-algorithm differences did not alter with age. Shirato et al (1999) found that the Group Mean MS was approximately 1.0dB higher for SITA Standard compared to Full Threshold both in normal individuals and in patients with glaucoma.

The Octopus algorithms exhibited the lowest Group Mean MS; the Octopus Threshold algorithm was the lowest for Visit 1 and the TOP algorithm was the lowest for Visit 2. The Group Mean MS was 1.49dB higher for the TOP algorithm compared to the Octopus Threshold algorithm for Visit 1 and 2.49dB lower for the TOP algorithm compared to the Octopus Threshold algorithm for Visit 2. The reason for the lower value for MS recorded with the Octopus perimeter is unknown.

Each of the five algorithms is compared to the specific age-corrected normative data base for the given algorithm. As such, a comparison of the MD index between algorithms should theoretically be referenced to normative databases derived from the same individuals. Alternatively, the use of a given normative database is an intrinsic part of the given algorithm. If the given databases are representative of the normal population, the use of different individuals between the various databases should exert little impact on the MD index. The Octopus algorithms exhibited the most negative Group Mean MD. The HFA SITA Fast algorithm produced the most positive Group Mean MD at both

Visits. The Group Mean MDs were closest in magnitude between the Full Threshold and SITA Standard algorithms (the HFA Full Threshold was 0.38dB and 0.52dB higher for Visit 1 and Visit 2, respectively). The reason for the apparent underestimation of sensitivity with the Octopus algorithms relative to the Full Threshold, SITA Standard and SITA Fast algorithms is unknown. Although the MSs for the Octopus algorithms were the lowest, it would have been expected that the MD between the five algorithms would have exhibited near equivalent values. It is possible that the apparent underestimation of sensitivity with the Octopus Threshold and TOP algorithms, as designated by the MD, arises from the fact that the algorithms for the HFA use a weighting function whereby the values of sensitivity derived from the central locations contribute more to the MD index than the peripheral locations. The weighting function is used to account for the increase in variability of the threshold estimate with increase in eccentricity. The calculation of the weighting function is proprietary to the manufacturer; however, the impact of the weighting function is considered to be minimal and is unlikely to have accounted for the differences between the various HFA and Octopus algorithms. Flanagan et al (1993) calculated the unweighted MD for a cohort of patients with glaucoma using Program 30-2 of the HFA and found that this differed by 0.10dB when compared to the corresponding weighted MD. The individual MDs for the HFA Full Threshold, SITA Standard and SITA Fast algorithms could have been recalculated to remove the effect of the weighting function. However, the modification of the given MD index in this manner mitigates against the comparisons of the various indices as recorded on the print-out and as experienced in the clinical situation.

The ANOVA did not reveal any significant differences in the $PSD/LV^{0.5}$ index between algorithms. This outcome is not unduly surprising given that the cohort was composed of normal individuals. However, it should be noted that the MD index is incorporated in the calculation of the $PSD/LV^{0.5}$ index. It is possible that a difference in the $PSD/LV^{0.5}$ index might have become apparent if the weighting function had been removed from the PSD index. However, the impact of the weighting function on the PSD index has been calculated to produce PSD values of 0.5dB higher than the unweighted equivalent. (Flanagan et al 1993).

3.5.2 The Between-algorithm Within-visit and the Within-algorithm Between-visit, Difference in the MD against the Mean of the MDs

The within-visit between-algorithm difference in the MD against the mean MD (Figures 3.1a to 3.1b) documents the between-subject contribution to the potential difference between any pair of algorithms. The corresponding between-visit within-algorithm graphs (Figures 3.2a to 3.2b) show the between-subject contribution to the test-retest variability within the given algorithm.

The confidence intervals for the between-algorithm within-visit evaluation were similar between the Full Threshold and SITA Standard; the Full Threshold and SITA Fast; and the SITA Standard and SITA Fast comparisons. The largest confidence intervals existed between the comparisons for TOP and both of the SITA algorithms.

The within-algorithm between-visit analysis suggested that the TOP algorithm was the least repeatable of the algorithms and was closely followed by SITA Standard and then by the Octopus Threshold algorithm. The confidence limits were narrowest for the Full Threshold algorithm. Bengtsson et al (1998) found that the test-retest variability for both SITA Standard and SITA Fast was comparable to that for the Full Threshold algorithm and that these were all considerably lower than that for the Fastpac algorithm. Wild et al (1999a) concluded that the between-subject variability was smaller for both the SITA algorithms compared to Fastpac and the Full Threshold algorithm.

3.5.3 The Within-visit Between-algorithm and the Between-visit Within-algorithm Difference in Pointwise Sensitivity

The MD is not the optimum indicator of performance between-algorithms or within an algorithm since it is the summary measure, across all locations, of the difference between the measured sensitivity and the age-corrected normal sensitivity at each location. Clearly identical MDs between any given two fields can be obtained from different locations exhibiting different defect depths. The purpose of the within-visit between-algorithm and the between-visit within-algorithm pointwise analyses was to determine the distribution of the differences in the absolute value of sensitivity at each stimulus location

The within-visit between-algorithm pointwise analysis showed that the TOP and SITA Standard comparison yielded the greatest disparity, closely followed by the TOP and SITA Fast comparison. As sensitivity declined, the SITA Standard algorithm yielded relatively higher estimates of threshold than the TOP algorithm. As sensitivity increased, the SITA Fast yielded relatively higher measures of sensitivity compared to the TOP algorithm. For the Full Threshold and SITA Fast comparison, as sensitivity declined, the difference became greater suggesting that SITA Fast yields higher sensitivities than the Full Threshold algorithm, especially in areas of reduced sensitivity. Pacey (1998) also found on pointwise analysis that the SITA algorithms exhibited a higher sensitivity which became more apparent as sensitivity declined when compared to the Full Threshold algorithm. Similarly, the SITA algorithms have been shown to exhibit greater between-individual variability at the more peripheral areas of the central visual field (Wild et al 1999a).

The between-visit within-algorithm pointwise analysis revealed that all of the algorithms yielded similar differences across the two visits. The TOP algorithm was the most variable on test-retest.

The within-visit between-algorithm and the between-visit within-algorithm pointwise analyses could have been undertaken in terms of the difference in pointwise deviations from each respective normal database. The pointwise analysis in absolute sensitivity does not take into account the between-individual differences in sensitivity due to age and the within- and between-individual differences at any given stimulus location due to the partial co-variance of sensitivity with increase in eccentricity. The age of the sample ranged from 34-82 years and the mean age was 65.5 years (SD 12.31) with all but two individuals lying between the ages of 50 and 82. The age-decline in sensitivity in normal individuals, varies with eccentricity but is approximately 0.7dB per decade irrespective of algorithm (Heijl et al 1987; Wild et al 1999a). Consequently, the maximum possible between-individual discrepancy at any given eccentricity with age would in general be approximately 2.3dB i.e normally within one interval of the scale of the abscissa in Figures 3.3a, 3.3b, 3.4a and 3.4b.

3.5.4 The Within-visit Between-algorithm and the Between-visit Within-algorithm Differences in the Pattern Deviation/Corrected Comparison Probability Level.

The within-visit between-algorithm analysis of the PD/CC probability levels showed that the SITA Standard and SITA Fast algorithms both exhibited an overestimation of apparent abnormality, and therefore narrower confidence limits, compared to the Full Threshold algorithm. A similar finding was present for the SITA Standard algorithm compared to the SITA Fast algorithm (Tables 3.6a bottom) indicating narrower confidence limits for the SITA Standard algorithm; for the TOP algorithm compared to the Octopus Threshold algorithm (Tables 3.6b top) indicating narrower confidence limits for the TOP algorithm; and for the TOP algorithm relative to the SITA Fast algorithm (Tables 3.6b bottom). The comparison of the probability levels between the TOP and SITA Standard algorithms indicated equivalent results between the two algorithms. Schimiti et al (2002) found that for normal individuals, there were more statistically significant probability values on the PD/CC probability plots for SITA Standard than for the Full Threshold algorithm. Wild et al (1999a) concluded that the between-individual normal variability was less for the SITA algorithms than for the Full Threshold algorithm within the central 21° of the visual field and the SITA algorithms consequently exhibit narrower confidence limits for normality. The findings of Bengtsson and Heijl (1999) are compatible with those of Wild et al (1999a).

The comparison of the between-visit within-algorithm PD/CC probability levels, as would be expected, were similar within 4 of the five algorithms. However, and surprisingly, the Octopus Threshold algorithm exhibited a greater number of probability levels reaching statistical significance at Visit 1 compared to Visit 2. The reason for this is unknown.

3.5.5 General Comments

The SITA algorithms were not compared to the Octopus Threshold algorithm and the TOP and Octopus Threshold algorithms were not compared to the HFA Full Threshold

algorithm. It was felt that such potential comparisons went beyond the scope of clinical utility.

The study did not evaluate the performance of the Fastpac algorithm of the HFA or the Dynamic strategy of the Octopus perimeter. These algorithms have been discussed in Chapter 1. They exhibit examination durations in the region of 6-8 minutes per eye for 76 locations but have been largely superseded by the SITA and TOP algorithms, respectively. In addition, the incorporation of these algorithms into the study would have increased the duration of each session by approximately 6-8 minutes. An additional 12-16 minutes of perimetry was considered to be unacceptable.

3.6 CONCLUSION

The results concerning the comparisons for the Full Threshold and the SITA algorithms, are consistent with previous studies. These findings confirm the representative nature of the cohort and, therefore, the results in relation to the comparative performance of the TOP and Octopus Threshold algorithms can be interpreted with confidence. The performance of TOP in normal individuals both within- and between- algorithms was of particular interest as TOP has not been extensively researched and all five algorithms have never been simultaneously compared for a given cohort.

In terms of the examination duration and the associated financial implications, TOP would seem to be ideal to implement in a clinical setting. However, the results reveal that the time-saving benefits are at the expense of reduced performance. TOP has exhibited decreased performance at almost every stage of the analysis compared to the remaining algorithms. The TOP algorithm manifested the second lowest MS of the five algorithms for both visits; the MD was the second most negative (i.e. most severe) at Visit 1 and the most negative at Visit 2. The within-algorithm between-visit mean of the MDs against the differences in MD showed the largest confidence interval of the five algorithms. The pointwise analysis for sensitivity also revealed that the TOP algorithm was the least repeatable of the five algorithms. The comparison of the PD/CC probability

levels suggested that the TOP algorithm overestimated abnormality compared to the Octopus Threshold and compared to the SITA Fast algorithm. The latter findings can be explained by the reduced between-individual variability of the TOP algorithm resulting in narrower confidence limits for normality.

The apparent poor performance for the TOP algorithm can be attributed to the fact that each stimulus location is only examined once and that the responses to the first matrix are used to govern the luminance of the presentations within the remaining matrixes and so on. If errors are made by the subject in the initial stages of the examination, there is little scope for these errors to be rectified and any such errors will potentially have an impact on the remaining stimulus presentations. In the early stages of any perimetric examination, it is possible that the patient is learning the requirements of the task. It is likely that the fatigue effect may be reduced or, indeed, absent from the TOP examination. Therefore, the TOP algorithm is likely to be extremely vulnerable to the learning effect especially on the first perimetric examination for a given individual.

Given the disappointing performance of the TOP algorithm relative to the SITA algorithms in the current study, it was essential to investigate the performance in patients with glaucoma. It is difficult, from the results in normals, to predict the performance of the TOP algorithm in the measurement of the visual field in OAG. The results suggest that the TOP algorithm will overestimate the severity of the field loss relative at least to the Octopus Threshold and SITA Fast algorithms. However, the impact of patient induced error on the matrix-based evaluation of threshold cannot be predicted.

CHAPTER 4

Perimetric Sensitivity in the Glaucomatous Eye as a Function of the Full Threshold, SITA Standard, SITA Fast, Octopus Threshold and TOP Algorithms.

4.1 INTRODUCTION

The findings from Chapter 3 indicated that the SITA Standard and SITA Fast algorithms generated a MS which was less negative, in terms of the Group Mean, compared to the HFA Full Threshold algorithm by approximately 0.55dB and 1.25dB, respectively. However, in terms of the MD, the HFA Full Threshold yielded an MD which was 0.45dB more positive than SITA Standard whereas the SITA FAST algorithm yielded an MD that was approximately 0.40dB more positive than the Full Threshold algorithm. It is again clear from the literature that there are no studies evaluating the comparative performance of the five algorithms in the examination of the glaucomatous visual field.

4.2 AIMS

A cross sectional prospective observational study was undertaken to determine how the five, commonly applied, commercially available algorithms (HFA Full Threshold; HFA SITA Standard; HFA SITA Fast; Octopus Threshold and Octopus TOP) compared in terms of the difference in the threshold estimate for patients with glaucoma. The study was intended, in particular, to provide further information about the validity of the TOP algorithm in the estimation of glaucomatous sensitivity and its feasibility as a screening, diagnostic and monitoring tool for glaucoma.

The specific aims were, firstly, to determine the extent of any differences in the estimation of both global and pointwise sensitivity between the Full Threshold, SITA Standard, SITA Fast, Octopus Threshold and TOP algorithms. More specifically, the intention was to determine the within-visit, between-algorithm and within-algorithm differences in the threshold estimate.

4.3 METHODS
4.3.1 Cohort
The cohort comprised 29 (13 males and 16 females) consecutively presenting patients with open angle glaucoma recruited from the Glaucoma Clinic at the Cardiff Eye Unit, University Hospital of Wales, Cardiff, who were willing to participate in the study and who were within the specified age requirements for the study. The mean age of the patients was 65.03 years (SD 8.59) and the range was 49-83 years (Table 4.1 below). The patients were such that the age profile matched as closely as possible that of the normal group described in Chapter 3.

Age (years)	Number of Patients
30-39	0
40-49	1
50-59	9
60-69	11
70-79	6
80+	2

Table 4.1 The age distribution within the Group.

The diagnosis of glaucoma was made by Mr James Morgan, Reader and Honorary Consultant Ophthalmologist, University Hospital of Wales, Cardiff. The inclusion criteria for the patients with OAG was similar to that of the normal individuals described in Chapter Three and comprised a distance visual acuity of 6/9 or better in either eye; distance refractive error of less than or equal to 5 dioptres mean sphere and less than 2.5 dioptres cylinder; lenticular changes not greater than NCIII, NOIII, CI or PI by LOCS III (Chylack et al 1993); no medication known to affect the visual field; no previous ocular surgery, except for surgery for OAG; no history of diabetes mellitus; a pre-therapy IOP consistently above 21mmHg; and an optic nerve head characteristic of OAG including increase in cup size, increase in cup/disc ratio, disc asymmetry, changes in the lamina cribrosa, loss of neuroretinal rim, pallor, evidence of peripapillary atrophy, vessel changes or disc margin haemorrhage.

The classification for the severity of visual field loss was determined relative to the examination with the HFA Full Threshold and Program 30-2 which was carried out at the initial visual field visit at the School of Optometry and Vision Sciences, Cardiff University. The visual field loss was classified using a modification to that of Litwak (2001). The classification was modified slightly by extending the linear classification to form an additional group designated as Very Early loss.

Very early visual field loss comprised a MD of greater than -3dB for the HFA, and <5 locations below the 1% level on the Pattern Deviation Plot for the HFA and no location within 5° eccentricity exhibiting a sensitivity of <20dB.

Early visual field loss comprised an MD of -3dB to -6dB for the HFA, and 9-18 locations below the 5% level and 5-10 locations below the 1% level on the Pattern Deviation Plot (PD) for the HFA and no location within 5° eccentricity exhibiting a sensitivity of <20dB.

Moderate visual field loss comprised an MD of -6dB to -12dB for the HFA, and 10-20 locations below the 1% level on the PD Plot for the HFA or central locations exhibiting a sensitivity of 10dB-20dB in one hemifield.

Severe visual field loss comprised an MD of worse than -12dB for the HFA, or >36 locations below the 5% level and >20 locations below the 1% level on the PD Plot for the HFA or locations with sensitivity < 20 dB in both hemifields in central 5 degrees.

The cohort consisted of 11 patients with very early visual field loss; 10 patients with early field loss; 5 patients with moderate field loss and 3 patients with severe visual field loss. Four of the patients had undergone previous bilateral trabeculectomies, one patient had undergone a previous trabeculectomy in the eye examined in the study and two patients had undergone trabeculectomies in the eye not used for the study. Twenty-three patients were undergoing therapy for IOP reduction during their participation in the study. Ten patients were receiving the single topical agent Latanoprost (prostaglandin analogue), one patient a single agent Carteolol hydrochloride (Teoptic) (beta-blocker),

one patient combination therapy of Dorzolamide hydrochloride (Trusopt) (carbonic anhydrase inhibitor) and Timolol maleate combined (Cosopt), six patients combination therapy of Latanoprost and Timolol maleate, two patients Latanoprost and Carteolol hydrochloride and two patients Latanoprost and Dorzolamide hydrochloride. No patients were on systemic carbonic anhydrase inhibitors. All patients had been on the therapy a minimum of six weeks prior to entry into the study and remained on the same therapy during the course of the study.

4.3.2 Examination Protocol

All patients each attended the School of Optometry and Vision Sciences, Cardiff University for three visits consisting of visual field examinations. The protocol was identical to that previously described in Chapter 3 for the normal Group.

4.3.3 Analysis

As in Chapter 3, the first visual field examination visit was considered as a familiarisation visit and the results were discarded prior to analysis. As also in Chapter 3, the second and third visits will also be referred to, from hereon in, as Visit 1 and Visit 2, respectively.

The results for left eyes were converted into right eye format. The stimulus locations immediately above and below the physiological blind spot were excluded from the analyses. At locations exhibiting double threshold determinations, the mean of the two determinations was taken as the threshold value. The MD values for each Octopus examination were converted into HFA format prior to the analysis, i.e. all positive values of MD derived from examinations with the Octopus were converted to negative values and vice versa. Similarly, the Loss Variance (LV) values of the Octopus were also converted into HFA format by taking the square root. The examination durations for all visual field examinations were converted, prior to data analysis, from the minutes and

seconds format contained in the print-outs for the HFA and Octopus perimeters into minutes, in decimal format.

The results were analysed in three separate ways. Firstly, the general characteristics of each algorithm were evaluated. The differences in the examination duration and in each of the visual field indices Mean Sensitivity (MS), Mean Deviation/Defect (MD) and Pattern Standard Deviation/Loss Variance$^{0.5}$ (PSD/LV$^{0.5}$) between the five algorithms within each of Visits 1 and 2 and the differences within-algorithm between-visits was analysed using separate repeated measures Analysis of Variances (ANOVA). The age of the patient and the severity of the visual field loss were considered as separate between-subject factors. The type of algorithm, the order of the two sessions, and the order of presentation of the algorithm within a session were considered as separate within-subject factors.

For the second analysis, the difference in sensitivity at each stimulus location for all patients between each pair of algorithms at the second visit (i.e., the within-visit between-algorithm variability) was calculated and expressed as a function of the sensitivity at the given stimulus location recorded at the same visit with the comparison algorithm of the given pair. Similarly, the difference in sensitivity at each stimulus location for all patients for a given algorithm between Visit 1 and Visit 2 (i.e. the within-algorithm between-visit variability) was calculated and expressed as a function of the sensitivity recorded at the second visit at the given stimulus location with the given algorithm.

For the third analysis the between-algorithm differences in the Pattern Deviation/ Corrected Comparison (CC) probability levels at each stimulus location at Visit 2, was expressed as a 5 x 5 contingency table for each pair of algorithms across all 29 patients and also for each level of field loss: very early, early, and moderate/severe. An identical analysis was undertaken for the within-algorithm between-visit differences in the Pattern Deviation/Corrected Comparison probability levels. The three types of analysis were identical to those undertaken on the data derived from the normal group (See Chapter 3).

4.4 RESULTS

All visual field examinations met the inclusion criteria for reliability, namely, less than 20% fixation losses, and less than 33% for each of the false-positive and false-negative response catch trials.

4.4.1 General Characteristics
4.4.1.1 Group Mean MS

The Group Mean MS and one SD of the mean for Visit 1 and Visit 2 for each of the algorithms is shown in Table 4.2a. The corresponding ANOVA summary table is shown in Table 4.2b.

Algorithm	HFA Full Threshold	HFA SITA Standard	HFA SITA Fast	Octopus Threshold	Octopus TOP
Visit 1	23.85 (4.65)	24.63 (4.66)	25.94 (3.42)	20.75 (4.77)	20.98 (5.33)
Visit 2	24.10 (4.48)	24.71 (4.76)	25.98 (3.39)	21.04 (4.58)	21.45 (4.89)

Table 4.2a The Summary Table for the MS, expressed in dB, and one SD of the mean at Visits 1 and 2 for each of the five algorithms.

Source	Df	Sums of Squares	Mean Square	F value	P
Algorithm	4	1103.49	275.87	102.68	<0.0001
Session	1	7.27	7.27	2.71	0.101
Visit	1	3.54	3.54	1.32	0.252
Severity	2	2179.12	1089.56	405.55	<0.0001
Algorithm x Session	3	5.21	1.74	0.69	0.559
Algorithm x Severity	8	66.78	8.35	3.32	0.001
Session x Severity	2	3.28	1.64	0.65	0.522

Table 4.2b The ANOVA Summary Table for the Group Mean MS at Visits 1 and 2.

As would be expected the MS declined with increase in severity of the field loss (p<0.0001). The Group mean MS varied between algorithms (p<0.0001) across each of the two visits (p=0.252). The Group mean MS was highest with the SITA Fast algorithm at both Visits 1 and 2. The Octopus Threshold algorithm exhibited the lowest Group mean MS at both Visits. The difference between the algorithms became more apparent as the severity of the field loss increased (p=0.0001).

4.4.1.2 Group Mean MD

The group mean MD and one SD of the mean for Visit 1 and Visit 2 for each of the algorithms is shown in Table 4.3a. The corresponding ANOVA summary table is shown in Table 4.3b. As would also be expected, the MD declined (i.e. became more negative) with increase in severity of the field loss (p<0.0001). The Group Mean MD varied between algorithms (p<0.0001) across each of the two visits (p=0.334). The Group mean MD was highest (i.e. least negative) with the SITA Fast algorithm at both Visits 1 and 2. The Octopus Threshold algorithm exhibited the most severe Group Mean MD at both Visits. The difference between the algorithms became more apparent as the severity of the field loss increased (p=0.0015).

Algorithm	HFA Full Threshold	HFA SITA Standard	HFA SITA Fast	Octopus Threshold	Octopus TOP
Mean MD Visit 1	-3.49 (4.50)	-3.75 (4.50)	-2.62 (3.35)	-5.45 (4.68)	-4.70 (4.66)
Mean MD Visit 2	-3.36 (4.33)	-3.56 (4.63)	-2.58 (3.24)	-5.26 (4.53)	-4.36 (4.59)

Table 4.3a The Group Mean MD, expressed in dB, and one SD of the mean at Visits 1 and 2 for each of the five algorithms.

134

Source	Df	Sums of Squares	Mean Square	F value	P
Algorithm	4	265.67	66.42	27.58	<0.0001
Session	1	6.33	6.33	2.63	0.106
Visit	1	2.26	2.26	0.94	0.334
Severity	2	2256.42	1128.21	12.37	0.0002
Algorithm x Session	3	4.59	1.53	0.68	0.567
Algorithm x Severity	8	58.79	7.35	3.25	0.0015
Session x Severity	2	4.04	2.02	0.89	0.410

Table 4.3b The ANOVA Summary Table for the Group Mean MD at Visits 1 and 2.

4.4.1.3 Group Mean PSD/LV$^{0.5}$

The Group Mean PSD, and one SD of the mean, for Visit 1 and Visit 2 for each of the algorithms is shown in Table 4.4a. The corresponding ANOVA Summary Table is shown in Table 4.4b. As would also be expected, the PSD/LV$^{0.5}$ increased with increase in severity of the field loss (p=0.0002). The Group mean PSD/LV$^{0.5}$ varied between algorithms (p<0.0001) across each of the two visits (p=0.192). It was highest for the HFA Full Threshold algorithm at both Visits 1 and 2 and lowest for the TOP algorithm at both Visits 1 and 2. The difference between the algorithms became more apparent as the severity of the field loss increased (p=0.0002).

The Group Mean PSD/LV$^{0.5}$ was greater at the second session (p=0.008) and this difference between sessions was more pronounced as the severity of the field loss increased (p= 0.002).

Algorithm	HFA Full Threshold	HFA SITA Standard	HFA SITA Fast	Octopus Threshold	Octopus TOP
Visit 1	5.39 (2.81)	5.30 (3.35)	4.98 (2.76)	5.22 (1.81)	3.95 (1.66)
Visit 2	6.05 (3.03)	5.96 (3.17)	4.99 (2.75)	5.39 (1.88)	4.15 (1.47)

Table 4.4a The Group Mean PSD/LV$^{0.5}$, expressed in dB, and one SD of the mean at Visits 1 and 2 for each of the five algorithms.

Source	Df	Sums of Squares	Mean Square	F value	P
Algorithm	4	78.98	19.75	10.85	<0.0001
Session	1	12.95	12.95	7.12	0.008
Visit	1	3.12	3.12	1.71	0.192
Severity	2	2256.42	1128.21	12.37	0.0002
Algorithm x Session	3	0.218	0.073	0.04	0.988
Algorithm x Severity	8	30.25	3.78	2.30	0.021
Session x Severity	2	21.80	10.90	6.64	0.002

Table 4.4b The ANOVA Summary Table for the Group Mean PSD/LV$^{0.5}$ at Visits 1 and 2.

4.4.1.4 Group Mean Examination Duration

The Group Mean examination duration for each algorithm at Visits 1 and 2 is shown in Table 4.5a. The corresponding ANOVA Summary Table is shown in Table 4.5b.

Algorithm	HFA Full Threshold	HFA SITA Standard	HFA SITA Fast	Octopus Threshold	Octopus TOP
Visit 1	16.21 (1.99)	8.32 (1.35)	4.73 (0.86)	14.19 (1.62)	2.67 (0.30)
Visit 2	16.19 (1.77)	8.24 (1.21)	4.70 (0.91)	14.58 (2.20)	2.68 (0.42)

Table 4.5a Glaucoma Group Mean examination duration, expressed in minutes and one SD of the mean at Visits 1 and 2 for all five algorithms using Program 30-2.

Source	Df	Sums of Squares	Mean Square	F value	P
Algorithm	4	7529.57	1882.39	1623.78	<0.0001
Session	1	0.701	0.701	0.60	0.4375
Visit	1	0.194	0.194	0.17	0.683
Severity	2	75.20	37.60	32.44	<0.0001
Algorithm x Session	3	2.29	0.76	0.68	0.567
Algorithm x Severity	8	18.72	2.34	2.07	0.039
Session x Severity	2	0.847	0.434	0.38	0.687

Table 4.5b The ANOVA Summary Table for the Glaucoma Group Mean examination duration at Visits 1 and 2.

As would be expected, the Group Mean examination duration varied between algorithms (p<0.0001) across each of the two visits (p=0.683). The Group mean examination duration was longest with the HFA Full Threshold algorithm at both Visits 1 and 2 and shortest for the TOP algorithm at each of the two visits. The difference in the examination duration between the algorithms became more apparent as the severity of the field loss increased (p=0.039).

4.4.1.5 Within-visit (Visit 2), Between-algorithm Difference in the MD.

The within-visit (Visit 2) between-algorithm differences in the MD for the 29 individuals is shown in Figures 4.1a and 4.1b. The range for the 95% confidence intervals of the difference in the MD ranged from 6.17 to 7.83dB for the comparisons of the HFA Full Threshold, SITA Standard and SITA Fast Algorithms and of the two Octopus algorithms. The corresponding range between the TOP algorithm and each of the SITA algorithms was between 10.69 dB and 11.83dB.
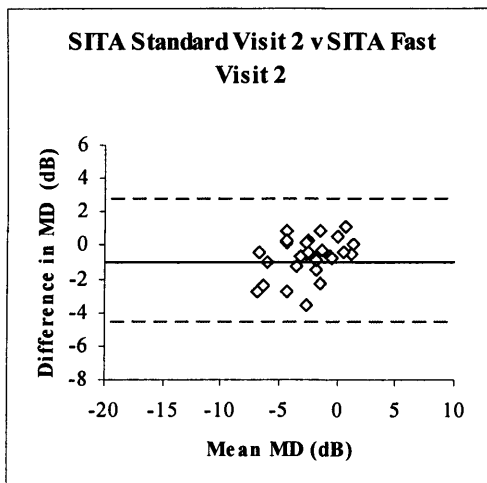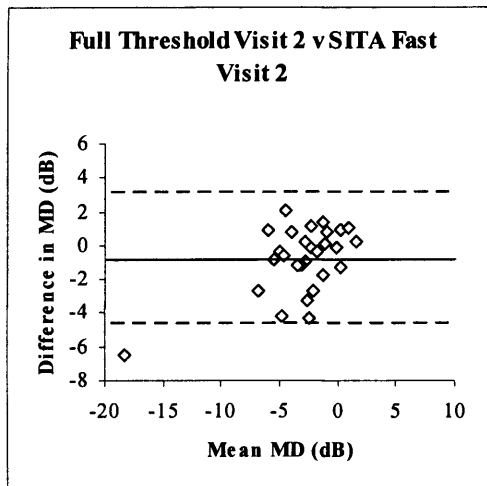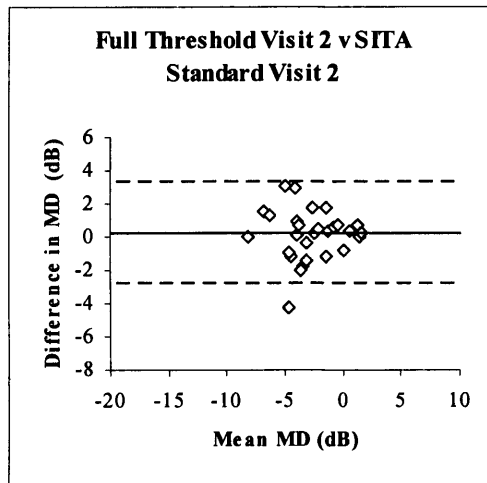
Figure 4.1a. The within-visit (Visit 2), between-algorithm difference in the MD, for each of the 29 subjects, against the mean of the two MDs. Top: HFA Full Threshold v SITA Standard algorithms. Middle: HFA Full Threshold v SITA Fast algorithms. Bottom: SITA Standard v SITA Fast. The solid line indicates the mean of the differences and the dotted line the 95% confidence intervals.
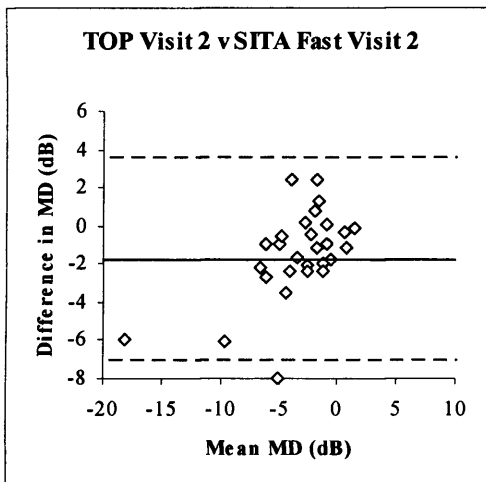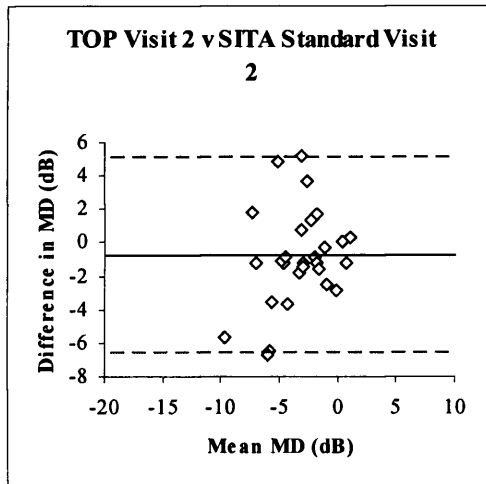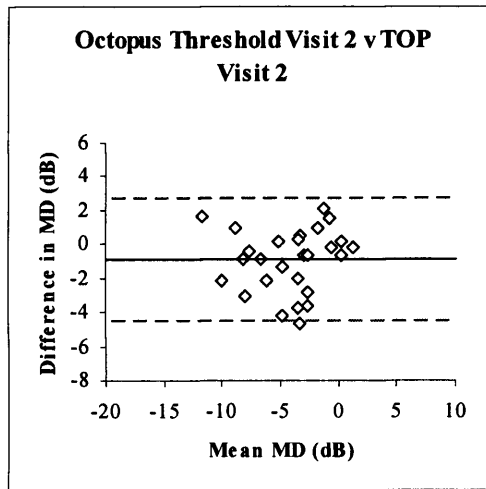
Figure 4.1b The within-visit (Visit 2), between-algorithm difference in the MD, for each of the 29 subjects, against the mean of the two MDs. Top: Octopus Threshold v TOP algorithms. Middle: TOP v SITA Standard algorithms. Bottom: TOP v SITA Fast algorithms. The solid line indicates the mean of the differences and the dotted line the 95% confidence intervals.

139

4.4.1.6 Within-visit (Visit 2), Between-algorithm Difference in the PSD/LV$^{0.5}$

The within-visit (Visit 2) between-algorithm differences in the PSD/LV$^{0.5}$ for the 29 individuals is shown in Figures 4.2a and 4.2b. The range for the 95% confidence intervals of the difference in the PSD ranged from 5.18dB to 8.08dB for the comparisons of the HFA Full Threshold, SITA Standard and SITA Fast Algorithms and of the two Octopus algorithms. The corresponding range between the TOP algorithm and each of the SITA algorithms was between 10.15 dB and 11.97dB.
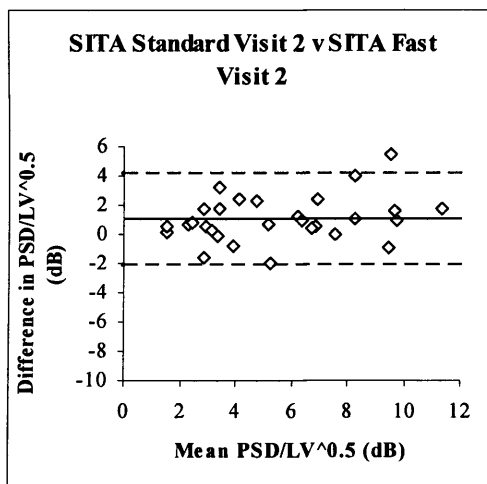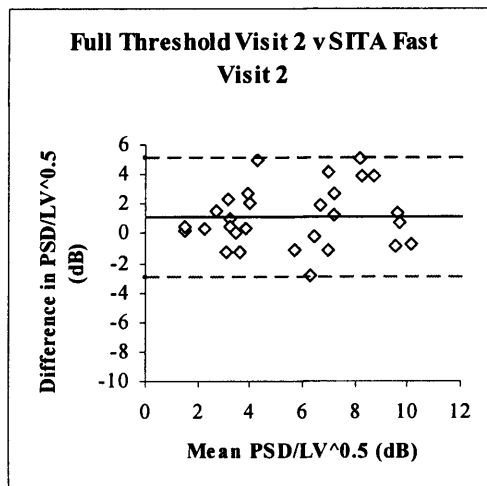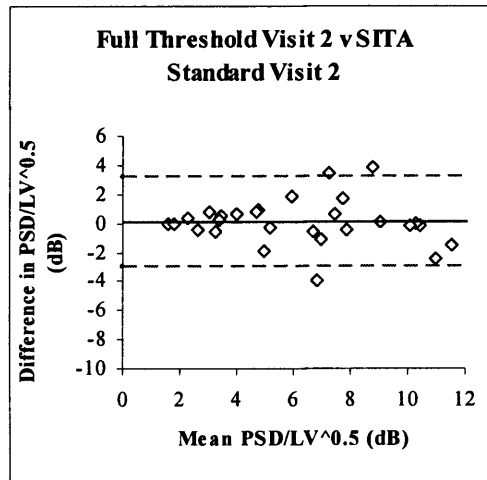
Figure 4.2a The within-visit (Visit 2), between-algorithm difference in the PSD/LV$^{0.5}$, for each of the 29 subjects, against the mean of the two PSDs. Top: HFA Full Threshold v SITA Standard algorithms. Middle: HFA Full Threshold v SITA Fast algorithms. Bottom: SITA Standard v SITA Fast. The solid line indicates the mean of the differences and the dotted line the 95% confidence intervals.
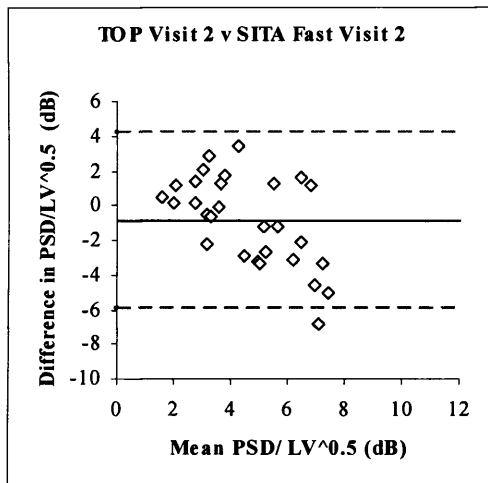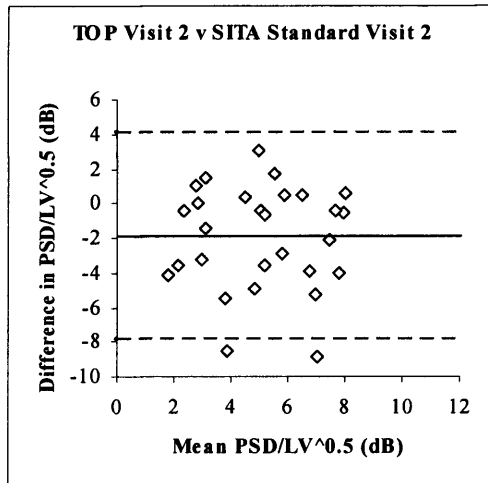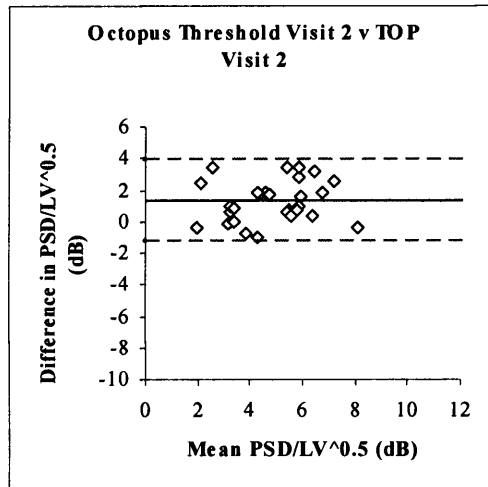
Figure 4.2b The within-visit (Visit 2), between-algorithm difference in the $PSD/LV^{0.5}$, for each of the 29 subjects, against the mean of the two PSDs. Top: Octopus Threshold v TOP algorithms. Middle: TOP v SITA Standard algorithms. Bottom: TOP v SITA Fast algorithms. The solid line indicates the mean of the differences and the dotted line the 95% confidence intervals.

4.4.1.7 Between-visit Within-algorithm Differences in MD

The between-visit, within-algorithm differences in the MD for each of the 29 individuals is shown in Figures 4.3a and 4.3b. The range for the 95% confidence intervals of the difference in the MD was clinically similar for all five algorithms: HFA Full Threshold (7.21dB), SITA Standard (6.88dB), SITA Fast (4.78dB), Octopus Threshold (5.27dB) and TOP (5.62dB) algorithms.
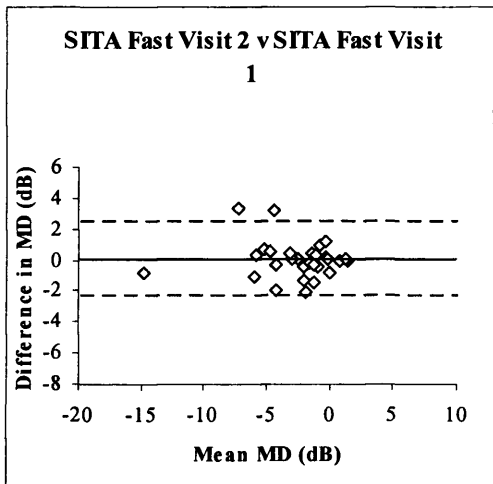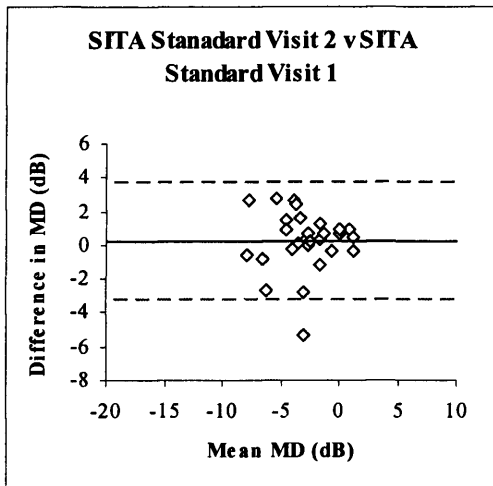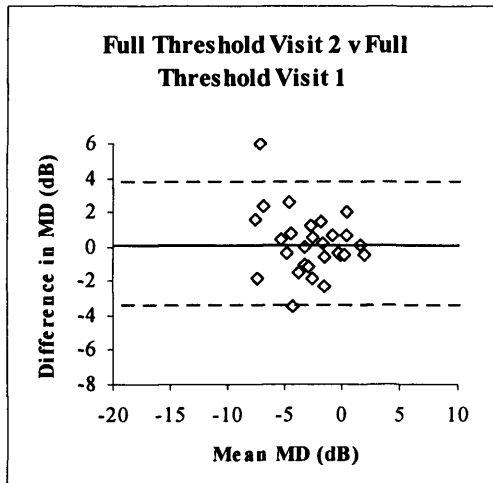
Figure 4.3a The between-visit, within-algorithm difference in the MD against the mean of the MDs at each visit. Top: HFA Full Threshold algorithm. Middle: SITA Standard algorithm. Bottom: SITA Fast algorithm. The solid line indicates the mean of the differences and the dotted line the 95% confidence intervals.

144
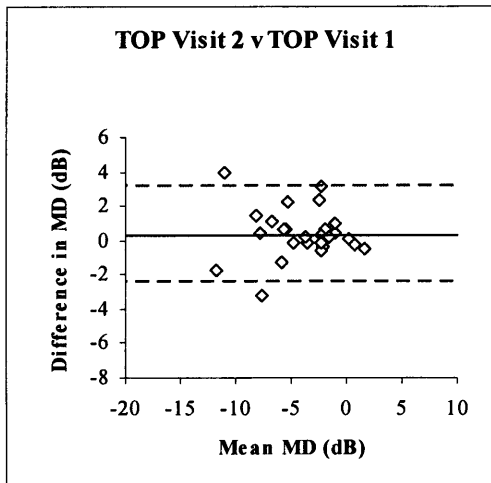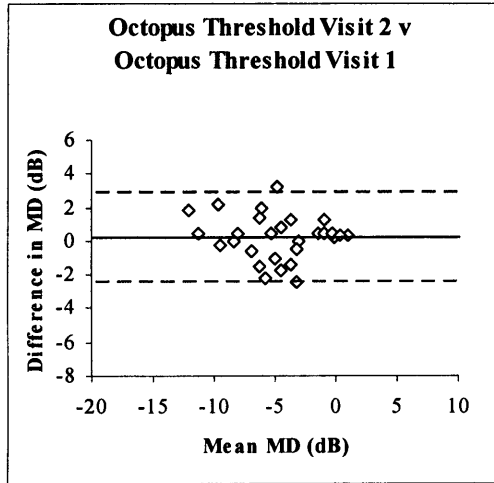
Figure 4.3b The between-visit, within-algorithm group difference in the MD against the mean of the MDs at each visit. Top: Octopus Threshold algorithm. Bottom: TOP algorithm. The solid line indicates the mean of the differences and the dotted line the 95% confidence intervals.

4.4.1.8 Between-visit Within-algorithm Differences in PSD/LV$^{0.5}$

The between-visit, within-algorithm differences in the PSD for each of the 29 individuals (i.e. the between-subject difference) is shown in Figures 4.4a and 4.4b. The range for the 95% confidence intervals of the difference in the PSD/LV$^{0.5}$ was clinically similar between the algorithms within each perimeter: HFA Full Threshold (6.63dB), SITA Standard (6.22dB), SITA Fast (4.43dB), Octopus Threshold (3.60dB) and TOP (2.27dB) algorithms.
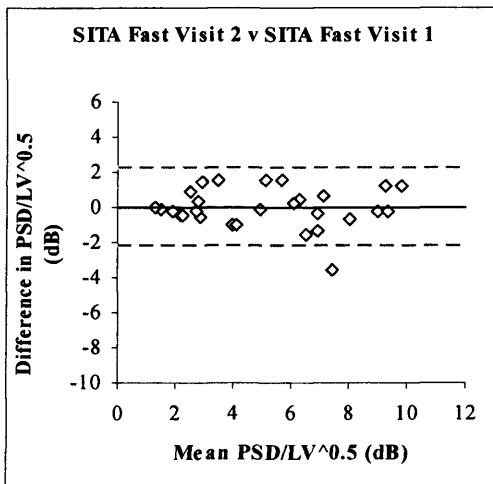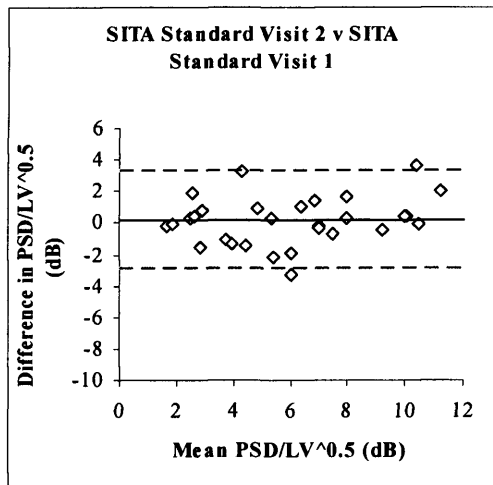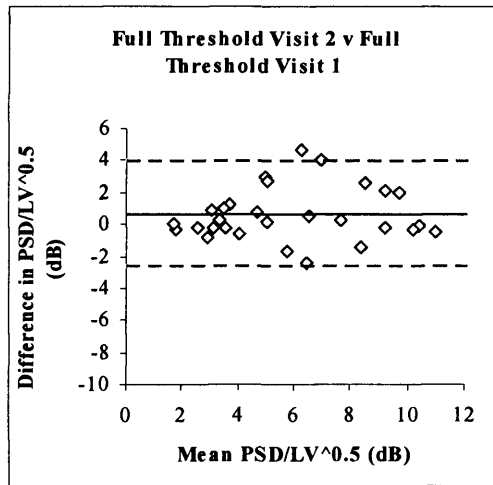
Figure 4.4a The between-visit, within-algorithm difference in the $PSD/LV^{0.5}$ against the mean of the $PSD/LV^{0.5}$s at each visit. Top: HFA Full Threshold algorithm. Middle: SITA Standard algorithm. Bottom: SITA Fast algorithm. The solid line indicates the mean of the differences and the dotted line the 95% confidence intervals.

147
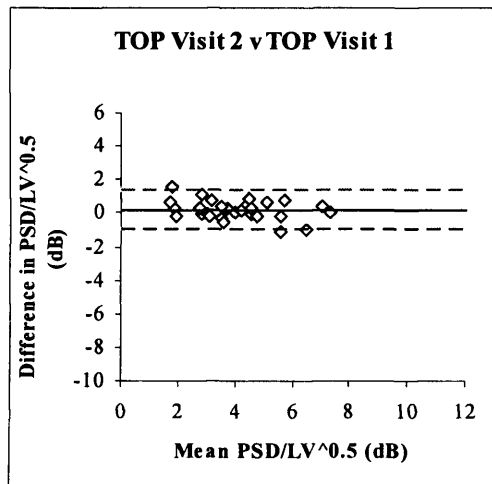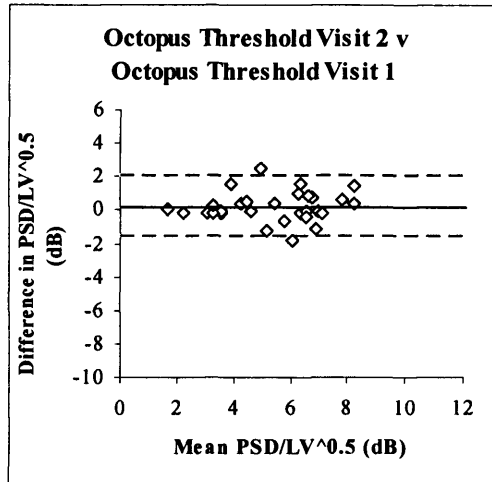
Figure 4.4b The between-visit, within-algorithm group difference in the PSD/LV$^{0.5}$against the mean of the PSD/LV$^{0.5}$s at each visit. Top: Octopus Threshold algorithm. Bottom: TOP algorithm. The solid line indicates the mean of the differences and the dotted line the 95% confidence intervals.

4.4.1.9 Within-visit (Visit 2) Between-Algorithm Difference in Pointwise Sensitivity

The 10th, 50th and 90th percentiles of the distribution of the within-visit between-algorithm difference in sensitivity at each sensitivity level between each of the five algorithms at the second visit are illustrated in Figures 4.5a and 4.5b.

The 50th percentile of the difference in sensitivity between the HFA Full Threshold and the SITA Standard algorithms (Figure 4.5a, top) approximated to zero regardless of the level of sensitivity. However, the corresponding percentile between the HFA Full Threshold and SITA Fast algorithms (Figure 4.5a, middle) became more negative as sensitivity derived with the Full Threshold algorithm declined. This indicates that the SITA Fast algorithm overestimated sensitivity relative to the HFA Full Threshold algorithm and that the magnitude of the overestimation increased as sensitivity with the Full Threshold algorithm declined. A similar finding was present for the SITA Fast algorithm compared to the SITA Standard algorithm (Figure 4.5a, bottom).
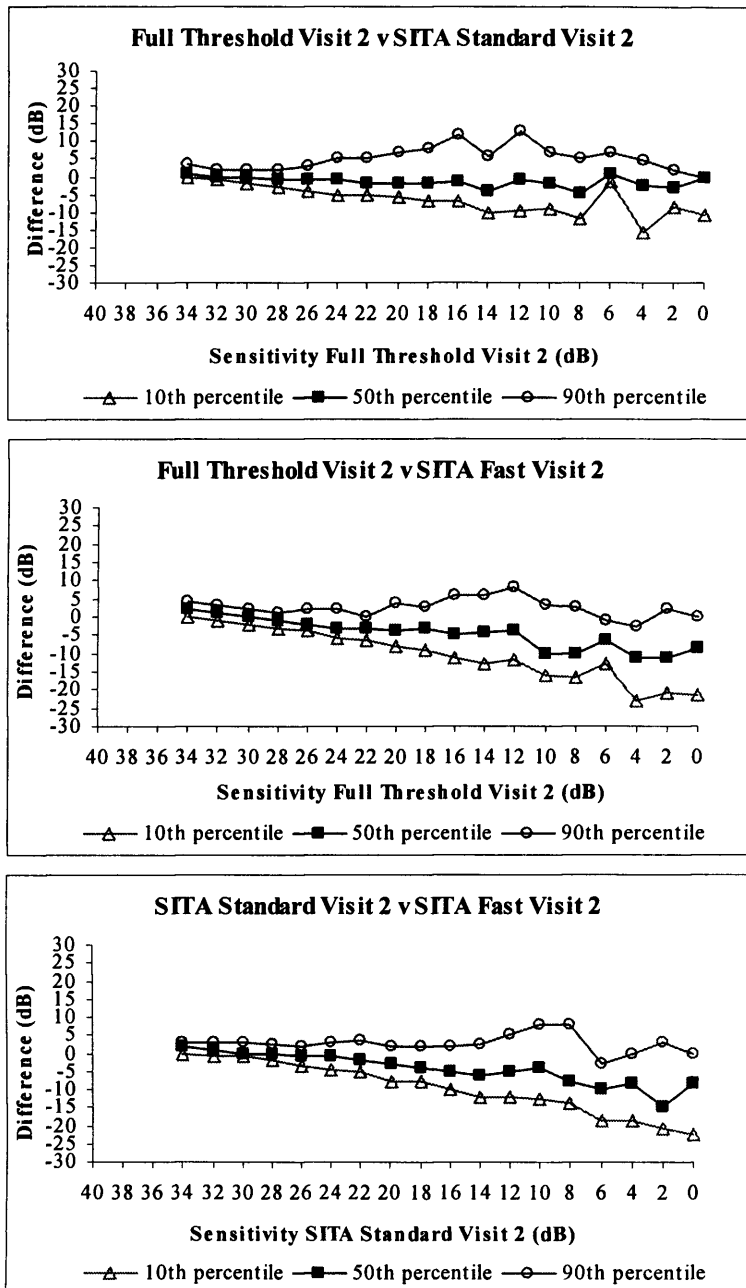
Figure 4.5a The 90th, 50th and 10th percentiles of the distribution of the differences in sensitivity across all stimulus locations at Visit 2. Top: HFA Full Threshold v SITA Standard algorithms. Middle: HFA Full Threshold v SITA Fast algorithms. Bottom: SITA Standard v SITA Fast algorithms.
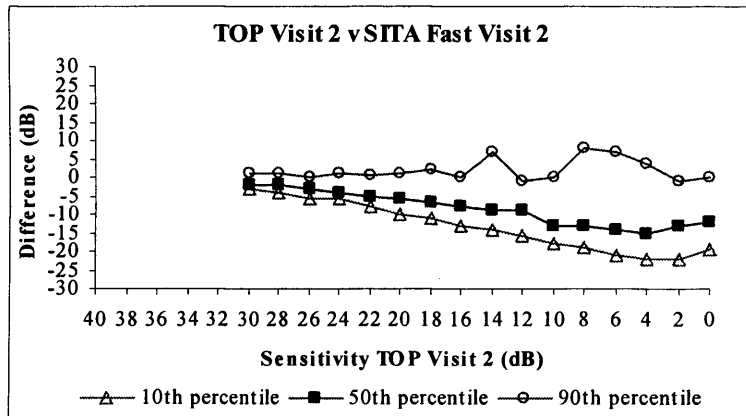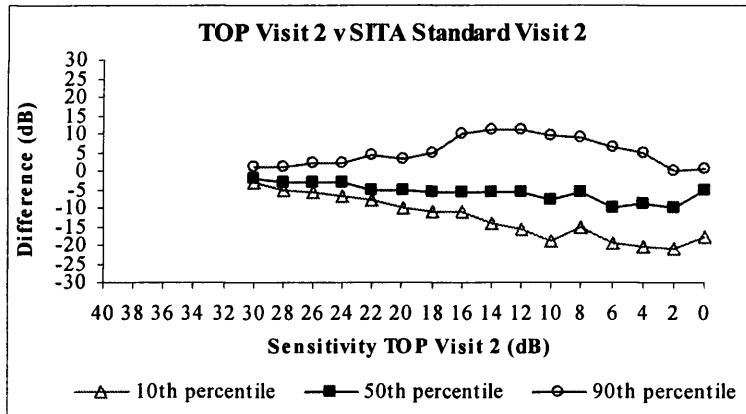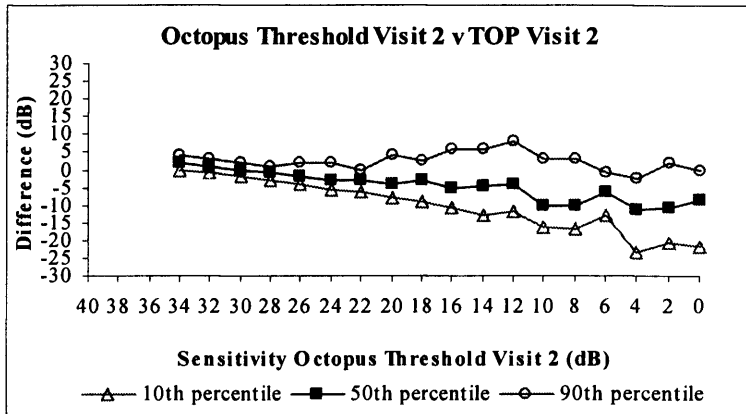
Figure 4.5b The 90th, 50th and 10th percentiles of the distribution of the differences in sensitivity across all stimulus locations at Visit 2. Top: Octopus Threshold v TOP. Middle: Octopus TOP v HFA SITA Standard. Bottom: Octopus TOP v HFA SITA Fast algorithms.

151

4.4.1.10 Between-visit Within-algorithm Difference in Pointwise Sensitivity

The 10th, 50th and 90th percentiles of the distribution of the between-visit within-algorithm difference in sensitivity at each sensitivity level between each of the five algorithms at the second visit are illustrated in Figures 4.6a to 4.6b inclusive.
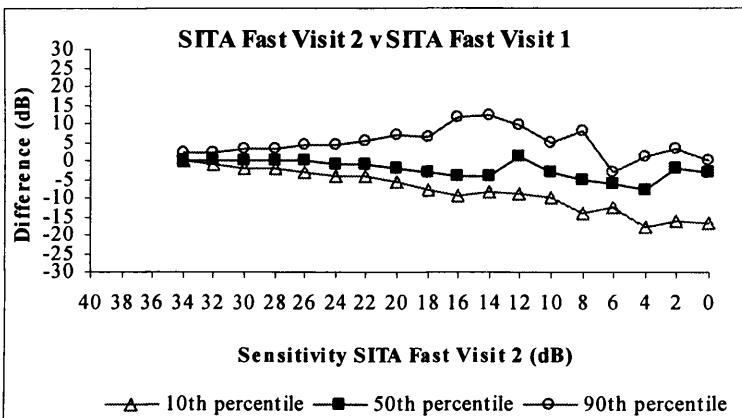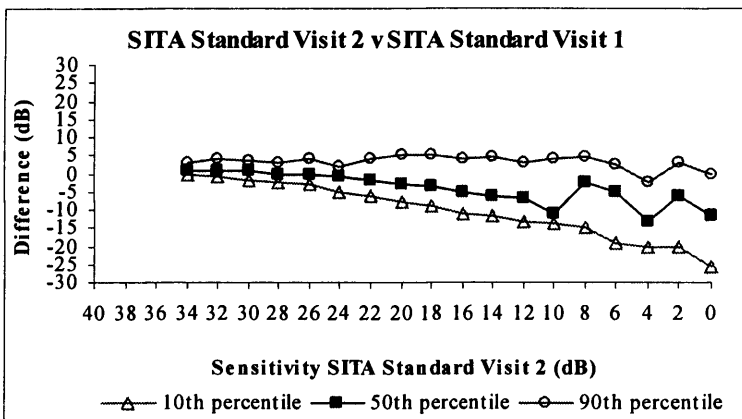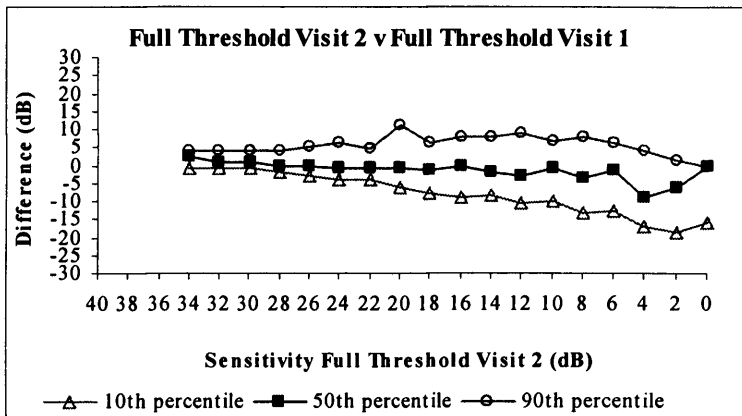
Figure 4.6a The 90th, 50th and 10th percentiles of the distribution of the differences in sensitivity across all locations between Visits 2 and 1. Top: HFA Full Threshold algorithm. Middle: SITA Standard algorithm. Bottom: SITA Fast algorithm.
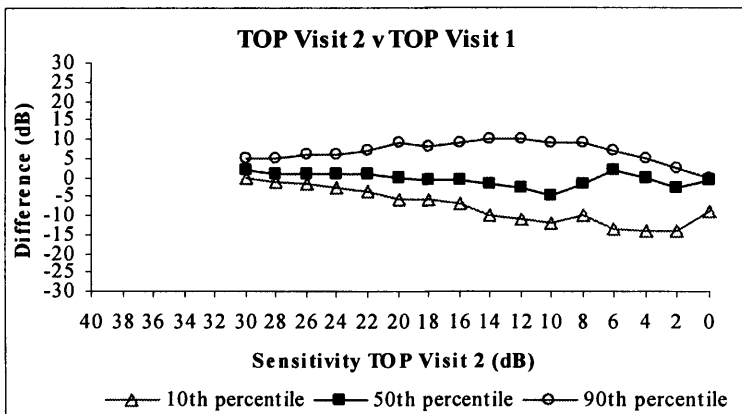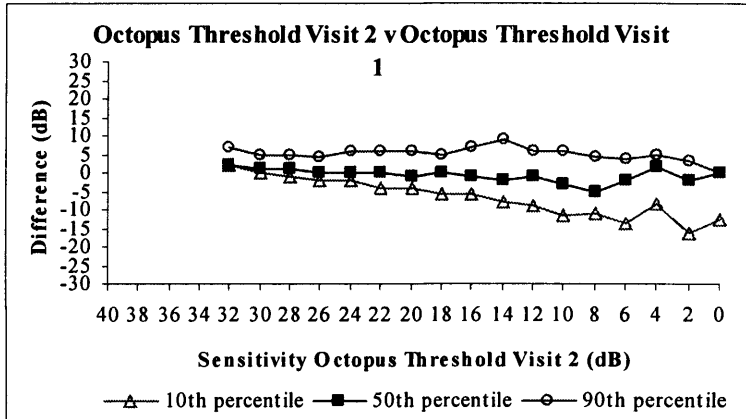
Figure 4.6b The 90th, 50th and 10th percentiles of the distribution of the differences in sensitivity across all locations between Visits 2 and 1. Top: Octopus Threshold algorithm. Bottom: TOP algorithm.

4.4.1.11 Within-visit (Visit 2) Between-algorithm Differences in the Pattern Deviation/Corrected Comparison Probability Level

The difference in the magnitude of the Pattern Deviation/Corrected Comparison probability levels at Visit 2 across the 29 patients with glaucoma, between the Full Threshold and the SITA Standard and SITA Fast algorithms, respectively is given in Table 4.6a, top and Table 4.6a, middle. The SITA Fast algorithm generated a greater number of locations exhibiting apparent abnormality by Pattern Deviation/Corrected Comparison probability analysis compared to the Full Threshold algorithm. Similarly, the SITA Standard algorithm generated a greater number of locations exhibiting apparent abnormality by Pattern Deviation/Corrected Comparison probability analysis than the SITA Fast algorithm (Table 4.6a, bottom) and the Octopus Threshold algorithm more locations than the TOP algorithm (Table 4.6b, top) and SITA Fast algorithms (Table 4.6b, bottom).

The difference in the magnitude of the Pattern Deviation/Corrected Comparison probability levels at Visit 2 for the patients with Very Early, Early and Moderate and Severe field loss, between the Full Threshold and the SITA Standard and SITA Fast algorithms, respectively is given in Table 4.7a, top and Table 4.7a, middle; Table 4.8a, top and 4.8a middle and 4.9a, top and 4.9a middle. The corresponding Deviation/Corrected Comparison comparisons for each Group in order of severity for the Octopus and TOP algorithms are shown in Table 4.7b, Table 4.8b and Table 4.9b, respectively.

The SITA Standard and the SITA Fast algorithms generated a greater number of locations exhibiting apparent abnormality by PD/CC analysis than the Full Threshold algorithm for the patients with Very Early field loss.

The patients with Early field loss generated a greater number of locations exhibiting apparent abnormality by PD/CC analysis for the SITA Standard algorithm compared to the Full Threshold algorithm and compared to the SITA Fast algorithm. When

155

compared to the TOP algorithm, both the Octopus Threshold and the SITA Standard algorithms exhibited more locations by PD/CC analysis with apparent abnormality.

For the patients with Moderate and Severe field loss, the SITA Standard and SITA Fast algorithms exhibited greater loss by PD/CC analysis compared to the HFA Full Threshold algorithm. The TOP algorithm exhibited greater loss than the two SITA algorithms.

SITA Standard Visit 2					
		NS	< 5%	< 2%	<1%	<0.5%
Full Threshold Visit 2	NS	1407	107	81	45	62
	< 5%	51	18	13	18	23
	< 2%	23	15	12	10	26
	<1%	17	7	6	10	23
	<0.5%	12	7	9	17	127

p<0.0001; Corrected p<0.0001

SITA Fast Visit 2					
		NS	< 5%	< 2%	<1%	<0.5%
Full Threshold Visit 2	NS	1494	97	38	36	37
	< 5%	62	22	10	15	14
	< 2%	48	11	7	8	12
	<1%	22	11	4	8	18
	<0.5%	37	13	6	14	102

p<0.0001; Corrected p=0.007

SITA Fast Visit 2					
		NS	< 5%	< 2%	<1%	<0.5%
SITA Standard Visit 2	NS	1361	72	21	29	27
	< 5%	105	23	10	11	5
	< 2%	78	19	7	5	12
	<1%	46	19	10	8	17
	<0.5%	73	21	17	28	122

p<0.0001; Corrected p<0.0001

Tables 4.6a The difference in the magnitude of the Pattern Deviation/Corrected Comparison Probability level between-algorithm at Visit 2 for the 29 patients with glaucoma. Top: Full Threshold v SITA Standard algorithms. Middle: Full Threshold v SITA Fast algorithms. Bottom: SITA Standard v SITA Fast algorithms.

TOP Visit 2						
		NS	< 5%	< 2%	<1%	<0.5%
	NS	1272	87	42	24	47
Octopus Threshold Visit 2	< 5%	75	19	12	7	20
	< 2%	75	11	2	6	16
	<1%	29	8	4	4	21
	<0.5%	121	25	33	25	161

p=<0.0001; Corrected p=0.004

TOP Visit 2						
		NS	< 5%	< 2%	<1%	<0.5%
	NS	1266	79	47	38	80
SITA Standard Visit 2	< 5%	97	24	8	5	20
	< 2%	66	14	12	5	24
	<1%	49	8	9	6	28
	<0.5%	94	25	17	12	113

p=0.46; Corrected p=0.64

TOP Visit 2						
		NS	< 5%	<2%	<1%	<0.5%
	NS	1357	101	61	38	106
SITA Fast Visit 2	< 5%	96	21	9	5	23
	< 2%	36	7	7	5	10
	<1%	39	7	5	6	24
	<0.5%	44	14	11	12	102

p<0.0001; Corrected p<0.0001

Tables 4.6b The difference in the magnitude of the Pattern Deviation/Corrected Comparison Probability Level between-algorithm at Visit 2 for the 29 patients with glaucoma. Top: Octopus Threshold v TOP algorithms. Middle: SITA Standard v TOP algorithms. Bottom: SITA Fast v TOP algorithms.

SITA Standard Visit 2						
		NS	< 5%	< 2%	<1%	<0.5%
Full Threshold Visit 2	NS	627	46	21	17	15
	< 5%	12	6	3	6	6
	< 2%	4	4	1	2	5
	<1%	5	2	1	3	5
	<0.5%	1	2	3	4	13

p<0.0001; Corrected p<0.0001

SITA Fast Visit 2						
		NS	< 5%	< 2%	<1%	<0.5%
Full Threshold Visit 2	NS	647	36	17	19	7
	< 5%	17	8	4	2	2
	< 2%	8	3	2	1	2
	<1%	5	3	1	2	5
	<0.5%	6	0	1	2	14

p<0.0001; Corrected p=0.0003

SITA Fast Visit 2						
		NS	< 5%	< 2%	<1%	<0.5%
SITA Standard Visit 2	NS	591	32	10	12	4
	< 5%	46	5	2	4	3
	< 2%	18	3	3	1	4
	<1%	12	8	6	2	4
	<0.5%	16	2	4	7	15

p=0.02; Corrected p=0.10

Tables 4.7a The difference in the magnitude of the Pattern Deviation/Corrected Comparison Probability Level between-algorithm at Visit 2 for the 11 patients with Very Early field loss. Top: Full Threshold v SITA Standard algorithms. Middle: Full Threshold v SITA Fast algorithms. Bottom: SITA Standard v SITA Fast algorithms.

TOP Visit 2						
		NS	< 5%	< 2%	<1%	<0.5%
Octopus Threshold Visit 2	NS	608	42	17	11	20
	< 5%	21	8	2	3	4
	< 2%	12	2	2	1	3
	<1%	9	3	1	1	1
	<0.5%	18	4	4	5	12

p=0.20; Corrected p=0.08

TOP Visit 2						
		NS	< 5%	< 2%	<1%	<0.5%
SITA Standard Visit 2	NS	562	41	16	12	18
	< 5%	44	10	2	1	3
	< 2%	20	3	3	2	1
	<1%	22	2	3	3	2
	<0.5%	20	3	2	3	16

p=0.48; Corrected p=0.64

TOP Visit 2						
		NS	< 5%	<2%	<1%	<0.5%
SITA Fast Visit 2	NS	592	39	18	13	21
	< 5%	33	8	3	2	4
	< 2%	17	4	2	1	1
	<1%	17	5	1	1	2
	<0.5%	9	3	2	4	12

p=0.22; Corrected p=0.38

Table 4.7b The difference in the magnitude of the Pattern Deviation/Corrected Comparison Probability Level between-algorithm at Visit 2 for the 11 patients with Very Early field loss. Top: Octopus Threshold v TOP algorithms. Middle: SITA Standard v TOP algorithms. Bottom: SITA Fast v TOP algorithms.

160

SITA Standard Visit 2					
		NS	< 5%	< 2%	<1%	<0.5%
Full Threshold Visit 2	NS	494	36	29	9	23
	< 5%	15	6	5	6	8
	< 2%	8	5	6	2	12
	<1%	2	4	2	1	5
	<0.5%	5	2	3	8	44

p<0.0001; Corrected p<0.0001

SITA Fast Visit 2					
		NS	< 5%	< 2%	<1%	<0.5%
Full Threshold Visit 2	NS	538	25	6	7	15
	< 5%	23	6	3	5	3
	< 2%	20	4	2	4	3
	<1%	9	3	0	0	2
	<0.5%	16	11	3	2	30

p=0.32; Corrected p=0.44

SITA Fast Visit 2					
		NS	< 5%	< 2%	<1%	<0.5%
SITA Standard Visit 2	NS	491	18	4	6	5
	< 5%	42	8	1	2	0
	< 2%	28	8	2	2	5
	<1%	16	3	0	2	5
	<0.5%	29	12	7	6	38

p<0.0001; Corrected p<0.0001

Tables 4.8a The difference in the magnitude of the Pattern Deviation/Corrected Comparison Probability Level between-algorithm at Visit 2 for the 10 patients with Early field loss. Top: Full Threshold v SITA Standard algorithms. Middle: Full Threshold v SITA Fast algorithms. Bottom: SITA Standard v SITA Fast algorithms.

TOP Visit 2					
		NS	< 5%	< 2%	<1%	<0.5%
Octopus Threshold Visit 2	NS	468	20	12	2	8
	< 5%	42	2	1	3	2
	< 2%	37	2	0	2	2
	<1%	14	2	0	1	6
	<0.5%	53	10	10	3	38

p<0.0001; Corrected p<0.0001

TOP Visit 2					
		NS	< 5%	< 2%	<1%	<0.5%
SITA Standard Visit 2	NS	479	13	11	6	15
	< 5%	36	6	4	2	5
	< 2%	29	4	2	0	10
	<1%	17	0	3	1	5
	<0.5%	53	13	3	2	21

p<0.0001; Corrected p<0.0001

TOP Visit 2					
		NS	< 5%	<2%	<1%	<0.5%
SITA Fast Visit 2	NS	535	22	18	6	25
	< 5%	37	6	1	2	3
	< 2%	13	0	1	0	0
	<1%	11	1	1	1	4
	<0.5%	18	7	2	2	24

p=0.66; Corrected p=0.74

Tables 4.8b The difference in the magnitude of the Pattern Deviation/Corrected Comparison Probability Level between-algorithm at Visit 2 for the 10 patients with Early field loss. Top: Octopus Threshold v TOP algorithms. Middle: SITA Standard v TOP algorithms. Bottom: SITA Fast v TOP algorithms.

SITA Standard Visit 2		NS	< 5%	< 2%	<1%	<0.5%
Full Threshold Visit 2	NS	286	25	31	19	24
	< 5%	24	6	5	6	9
	< 2%	11	6	5	6	9
	<1%	10	1	3	6	13
	<0.5%	6	3	3	5	70

p<0.0001; Corrected p<0.0001

SITA Fast Visit 2		NS	< 5%	< 2%	<1%	<0.5%
Full Threshold Visit 2	NS	309	36	15	10	15
	< 5%	22	8	3	8	9
	< 2%	20	4	3	3	7
	<1%	8	5	3	6	11
	<0.5%	15	2	2	10	58

p=0.003; Corrected p=0.038

SITA Fast Visit 2		NS	< 5%	< 2%	<1%	<0.5%
SITA Standard Visit 2	NS	279	22	7	11	18
	< 5%	17	10	7	5	2
	< 2%	32	8	2	2	3
	<1%	18	8	4	4	8
	<0.5%	28	7	6	15	69

p=0.004; Corrected p=0.035

Tables 4.9a The difference in the magnitude of the Pattern Deviation/Corrected Comparison Probability Level between-algorithm at Visit 2 for the 8 patients with Moderate or Severe field loss. Top: Full Threshold v SITA Standard algorithms. Middle: Full Threshold v SITA Fast algorithms. Bottom: SITA Standard v SITA Fast algorithms.

TOP Visit 2						
		NS	< 5%	< 2%	<1%	<0.5%
Octopus Threshold Visit 2	NS	196	25	13	11	19
	< 5%	12	9	9	1	14
	< 2%	26	7	0	3	11
	<1%	6	3	3	2	14
	<0.5%	50	11	19	17	111

p=0.082; Corrected p=0.24

TOP Visit 2						
		NS	< 5%	< 2%	<1%	<0.5%
SITA Standard Visit 2	NS	225	25	20	20	47
	< 5%	17	8	2	2	12
	< 2%	17	7	7	3	13
	<1%	10	6	3	2	21
	<0.5%	21	9	12	7	76

p<0.0001; Corrected p=0.002

TOP Visit 2						
		NS	< 5%	<2%	<1%	<0.5%
SITA Fast Visit 2	NS	230	40	25	19	60
	< 5%	26	7	5	1	16
	< 2%	6	3	4	4	9
	<1%	11	1	3	4	18
	<0.5%	17	4	7	6	66

p<0.0001; Corrected p<0.0001

Tables 4.9b The difference in the magnitude of the Pattern Deviation/Corrected Comparison Probability Level between-algorithm at Visit 2 for the 8 patients with Moderate or Severe field loss. Top: Octopus Threshold v TOP algorithms. Middle: SITA Standard v TOP algorithms. Bottom: SITA Fast v TOP algorithms.

4.4.1.12 Between-visit Within-algorithm Difference in the Pattern Deviation/Corrected Comparison Probability Level

The difference in the magnitude of the Pattern Deviation/Corrected Comparison probability levels between Visit 2 and Visit 1 across the 29 patients with glaucoma for the Full Threshold and the SITA Standard and SITA Fast algorithms, respectively, is given in Table 4.10a and for the Octopus Threshold and TOP algorithms, in Table 4.10b. As would again be expected in the absence of a learning effect, these differences did not reach statistical significance. The same algorithm comparisons are shown for the patients with Very Early, Early and Moderate and Severe field loss in Table 4.11a and Table 4.11b; Table 4.12a and 4.12b and Table 4.13a and 4.13b, respectively.

The Octopus Threshold algorithm was the only algorithm to exhibit a within-algorithm between-examination difference in the number of locations exhibiting apparent abnormality by PD/CC analysis for the cohort with Very Early loss. A similar difference was also present for the Octopus Threshold algorithm and the TOP algorithm for the patients with Early field loss. The Full Threshold and SITA Standard algorithms exhibited a within-algorithm between-examination difference for the patients with Moderate and Severe field loss.

Full Threshold Visit 1						
		NS	< 5%	< 2%	<1%	<0.5%
Full Threshold Visit 2	NS	1453	113	67	32	66
	< 5%	92	11	7	5	8
	< 2%	54	8	9	7	8
	<1%	35	6	5	9	8
	<0.5%	88	12	3	7	62

p=0.063; Corrected p=0.19.

SITA Standard Visit 1						
		NS	< 5%	< 2%	<1%	<0.5%
SITA Standard Visit 2	NS	1240	75	56	59	109
	< 5%	106	17	9	7	15
	< 2%	68	16	12	13	12
	<1%	49	7	9	7	28
	<0.5%	101	14	23	17	106

p=0.88; Corrected p=0.76

SITA Fast Visit 1						
		NS	< 5%	< 2%	<1%	<0.5%
SITA Fast Visit 2	NS	1391	103	67	46	85
	< 5%	109	19	6	7	13
	< 2%	41	9	3	3	9
	<1%	47	12	6	4	12
	<0.5%	79	11	5	14	74

p=0.22; Corrected p=0.40

Tables 4.10a The difference in the magnitude of the Pattern Deviation/Corrected Comparison Probability Level within-algorithm between-visit for all 29 patients. Top: Full Threshold v SITA Standard algorithms. Middle: Full Threshold v SITA Fast algorithms. Bottom: SITA Standard v SITA Fast algorithms.

Octopus Threshold Visit 1					
		NS	< 5%	< 2%	<1%	<0.5%
	NS	1178	84	71	22	146
Octopus Threshold Visit 2	< 5%	85	16	13	4	15
	< 2%	61	16	15	4	14
	<1%	36	7	5	3	15
	<0.5%	148	22	23	13	159

p=0.76; Corrected p=0.80

Octopus TOP Visit 1					
		NS	< 5%	< 2%	<1%	<0.5%
	NS	1285	101	57	34	124
Octopus TOP Visit 2	< 5%	108	20	9	5	8
	< 2%	58	6	3	5	21
	<1%	38	7	4	5	12
	<0.5%	119	21	15	10	100

p=0.80; Corrected p=0.84

Tables 4.10b The difference in the magnitude of the Pattern Deviation/Corrected Comparison Probability Level within-algorithm between-visit for all 29 patients. Top: Octopus Threshold v TOP algorithms. Middle: SITA Standard v TOP algorithms. Bottom: SITA Fast v TOP algorithms.

Full Threshold Visit 1					
		NS	< 5%	< 2%	<1%	<0.5%
Full Threshold Visit 2	NS	706	21	8	2	0
	< 5%	20	8	3	0	2
	< 2%	5	7	1	1	2
	<1%	10	4	0	2	0
	<0.5%	12	2	1	2	6

p=0.10; Corrected p=0.22

SITA Standard Visit 1					
		NS	< 5%	< 2%	<1%	<0.5%
SITA Standard Visit 2	NS	599	25	16	13	7
	< 5%	38	10	4	4	4
	< 2%	20	2	3	1	3
	<1%	13	2	7	5	5
	<0.5%	15	5	4	4	16

p=0.44; Corrected p=0.62

SITA Fast Visit 1					
		NS	< 5%	< 2%	<1%	<0.5%
SITA Fast Visit 2	NS	631	33	19	5	6
	< 5%	39	4	2	3	2
	< 2%	14	5	2	1	3
	<1%	14	5	2	1	4
	<0.5%	8	3	2	4	13

p=0.42; Corrected p=0.60.

Tables 4.11a The difference in the magnitude of the Pattern Deviation/Corrected Comparison Probability Level within-algorithm between-visit for the 11 patients with Very Early field loss. Top: Full Threshold algorithm. Middle: SITA Standard algorithm. Bottom: SITA Fast algorithm.

Octopus Threshold Visit 1					
		NS	< 5%	< 2%	<1%	<0.5%
Octopus Threshold Visit 2	NS	614	29	28	8	30
	< 5%	26	4	2	0	6
	< 2%	9	2	4	1	4
	<1%	8	2	1	0	4
	<0.5%	6	7	9	0	21

p=0.0002; Corrected p=0.007.

Octopus TOP Visit 1					
		NS	< 5%	< 2%	<1%	<0.5%
Octopus TOP Visit 2	NS	603	32	13	7	24
	< 5%	44	10	0	1	4
	< 2%	12	3	4	3	4
	<1%	9	1	3	3	5
	<0.5%	15	4	5	1	15

p=0.44; Corrected p=0.62.

Table 4.11b The difference in the magnitude of the Pattern Deviation/Corrected Comparison Probability Level within-algorithm between-visit for the 11 patients with Very Early field loss. Top: Octopus Threshold algorithm. Bottom: TOP algorithm.

Full Threshold Visit 1					
		NS	< 5%	< 2%	<1%	<0.5%
Full Threshold Visit 2	NS	542	40	9	3	7
	< 5%	28	4	4	1	3
	< 2%	14	1	9	6	3
	<1%	5	2	3	2	2
	<0.5%	16	4	4	7	31

p=0.20; Corrected p=0.34.

SITA Standard Visit 1					
		NS	< 5%	< 2%	<1%	<0.5%
SITA Standard Visit 2	NS	484	19	7	9	15
	< 5%	37	5	3	4	4
	< 2%	25	5	4	8	3
	<1%	6	5	2	5	8
	<0.5%	21	6	7	7	51

p=0.14; Corrected p=0.34

SITA Fast Visit 1					
		NS	< 5%	< 2%	<1%	<0.5%
SITA Fast Visit 2	NS	540	31	23	13	9
	< 5%	30	7	6	2	4
	< 2%	9	4	0	0	1
	<1%	7	3	1	3	4
	<0.5%	12	4	1	7	29

p=0.10; Corrected p=0.44

Tables 4.12a The difference in the magnitude of the Pattern Deviation/Corrected Comparison Probability Level within-algorithm between-visit for the 10 patients with Early field loss. Top: Full Threshold algorithm. Middle: SITA Standard algorithm. Bottom: SITA Fast algorithm.

Octopus Threshold Visit 1						
		NS	< 5%	< 2%	<1%	<0.5%
	NS	467	20	14	5	14
Octopus Threshold Visit 2	< 5%	36	6	2	1	5
	< 2%	23	4	6	1	9
	<1%	10	4	2	2	5
	<0.5%	34	13	13	3	51

p=0.001; Corrected p=0.026

Octopus TOP Visit 1						
		NS	< 5%	< 2%	<1%	<0.5%
	NS	467	20	14	5	14
Octopus TOP Visit 2	< 5%	36	6	2	1	5
	< 2%	23	4	6	1	9
	<1%	10	4	2	2	5
	<0.5%	34	13	13	3	51

p=0.001; Corrected p=0.026

Tables 4.12b The difference in the magnitude of the Pattern Deviation/Corrected Comparison Probability Level within-algorithm between-visit for the 10 patients with Early field loss. Top: Octopus Threshold algorithm. Bottom: TOP algorithm.

Full Threshold Visit 1					
		NS	< 5%	< 2%	<1%	<0.5%
Full Threshold Visit 2	NS	303	33	26	11	20
	< 5%	27	7	7	3	6
	< 2%	11	5	9	6	6
	<1%	9	5	4	8	7
	<0.5%	3	7	3	6	57

p<0.0001; Corrected p<0.0001

SITA Standard Visit 1					
		NS	< 5%	< 2%	<1%	<0.5%
SITA Standard Visit 2	NS	264	23	20	10	28
	< 5%	15	5	8	5	8
	< 2%	14	8	10	8	7
	<1%	7	6	4	6	19
	<0.5%	6	3	10	14	92

p<0.0001; Corrected p<0.0001

SITA Fast Visit 1					
		NS	< 5%	< 2%	<1%	<0.5%
SITA Fast Visit 2	NS	299	25	19	14	25
	< 5%	29	12	2	4	8
	< 2%	11	7	1	2	5
	<1%	14	6	4	4	9
	<0.5%	10	5	3	11	71

p=0.108; Corrected p=0.26

Tables 4.13a The difference in the magnitude of the Pattern Deviation/Corrected Comparison Probability Level within-algorithm between-visit for the 8 patients with Moderate or Severe field loss. Top: Full Threshold algorithm. Middle: SITA Standard algorithm. Bottom: SITA Fast algorithm.

172

Octopus Threshold Visit 1						
		NS	< 5%	< 2%	<1%	<0.5%
Octopus Threshold Visit 2	NS	209	19	15	5	24
	< 5%	15	10	5	4	11
	< 2%	17	6	10	3	11
	<1%	6	4	4	3	11
	<0.5%	28	15	12	10	143

p=0.26; Corrected p=0.38

Octopus TOP Visit 1						
		NS	< 5%	< 2%	<1%	<0.5%
Octopus TOP Visit 2	NS	216	26	13	9	34
	< 5%	28	14	6	3	4
	< 2%	16	5	2	4	17
	<1%	15	2	4	4	9
	<0.5%	39	15	11	9	95

p=0.36; Corrected p=0.40

Tables 4.13b The difference in the magnitude of the Pattern Deviation/Corrected Comparison Probability Level within-algorithm between-visit for the 8 patients with Moderate or Severe field loss. Top: Octopus Threshold algorithm. Bottom: TOP algorithm.

4.5 DISCUSSION
4.5.1 Global Indices
As for the normal individual cohort (Chapter 3), the Group Mean MS was highest for the SITA Fast algorithm for both Visit 1 and Visit 2; it was lowest for the Octopus Threshold algorithm for both Visit 1 and Visit 2.

The Group Mean MS in the current study, across the two visits, was 0.70dB greater for the SITA Standard algorithm compared to the Full Threshold algorithm, 1.98dB greater for SITA Fast compared to the Full Threshold algorithm. Bengtsson and Heijl (1998) found that, in a cohort of patients with OAG, the MS was 2.18dB higher for the SITA Standard algorithm and 1.66dB higher for the Fastpac algorithm compared to the Full Threshold algorithm. Similarly, Wild et al (1999b) reported a Group mean MS which was 1.0dB greater for SITA Standard than for the Full Threshold algorithm and 0.9dB greater for the SITA Fast than for the SITA Standard algorithm. The SITA Standard algorithm has been compared to the Full Threshold algorithm in patients with optic neuropathies and hemianopsia (Wall et al 2001); the Group Mean MS was found to be approximately 1.0dB greater for SITA Standard than for the Full Threshold algorithm.

The Group Mean MSs were 20.90dB and 21.22dB across the two visits for the Octopus Threshold and TOP algorithms, respectively. Morales and colleagues found, in a cohort comprising normal individuals, patients with early glaucoma, patients with advanced glaucoma, patients with neuro-ophthamic disease and patients with retinal disease exhibiting field loss, that the Group Mean MS was 1dB greater (i.e.more positive) for the TOP algorithm compared to the Octopus Threshold algorithm (Morales et al 2000).

As with the cohort of normal individuals, the Group Mean MD was least negative for the SITA Fast algorithm for both Visit 1 and Visit 2. The Octopus Threshold algorithm was most negative at both Visit 1 and Visit 2. The Group Mean MD for the SITA Standard algorithm, across the two visits, was 0.46dB more negative than that of the HFA Full Threshold algorithm. The Group Mean MD for the SITA Fast algorithm, across the two visits, was 0.83dB less negative than that of the HFA Full Threshold algorithm. These differences compare favourably with those of Wild et al (1999b). In a similar

174

experimental design involving patients with OAG, they found that the Group Mean MD of the SITA Standard algorithm, across the two visits was 0.23dB more negative than that of the HFA Full Threshold algorithm (based upon a Group Mean value for the Full Threshold algorithm of -4.96dB) and 0.13dB less negative for the SITA Fast algorithm. However, Budenz et al (2002) found that the Group Mean MD in their cohort of patients with OAG was less negative for SITA Standard (-9.6 ± 7.1dB) and for SITA Fast (-9.1 ± 6.7dB) compared to the Full Threshold algorithm (-10.3 ± 7.1dB). The explanation for the disparity between the results of Budenz and colleagues and those of the current study is most likely to be explained by the difference in the severity of the field loss between the two cohorts.

The Octopus Threshold algorithm produced a Group Mean MD over the two visits of -5.36dB and the TOP algorithm -4.53dB. The underestimate by 0.83dB in the magnitude of the MD for the TOP algorithm relative to the Octopus Threshold algorithm can be compared with that in the study by Morales et al (2000), and described previously, overleaf. They found that the Group Mean MD was 1dB lower (i.e less severe) for the TOP algorithm compared to the Octopus Threshold algorithm (Morales et al 2000). Gonzalez de la Rosa et al (1996) compared the Octopus Threshold and TOP algorithms in normal individuals, patients with glaucoma and patients with optic neuropathy, and found that the Group Mean MD was 1.65dB more positive for the TOP algorithm.

The results of the current study suggests that both SITA algorithms underestimate the MD relative to the TOP algorithm by a difference in the Group Mean MD of 0.87dB and 1.93dB for SITA Standard and SITA Fast, respectively.

In the cohort of normal individuals, the Group Mean $PSD/LV^{0.5}$ was not significantly different between the various algorithms (Chapter 3). In the current study, the Group Mean $PSD/LV^{0.5}$ varied between the algorithms. It was largest for the Full Threshold algorithm and smallest for the TOP algorithm at both Visit 1 and Visit 2. The Group Mean $PSD/LV^{0.5}$ for the SITA Standard algorithm, across the two visits, was almost identical (0.07dB more negative) to that of the HFA Full Threshold algorithm. These

differences again compare favourably with those of Wild et al (1999b). In a similar experimental design involving patients with OAG, they found that the Group Mean MD of the SITA Standard algorithm, across the two visits was 0.23dB more positive than that of the HFA Full Threshold algorithm (based upon a Group Mean value for the Full Threshold algorithm of 5.72dB) and 0.75dB less positive for the SITA Fast algorithm. The SITA Standard Group Mean PSD was approximately 0.2dB higher than the Full Threshold PSD and the SITA Fast PSD was 0.51dB less positive. Budenz et al (2002) found that the PSD was greater for the SITA Standard algorithm compared to the SITA Fast algorithm but that the difference between the algorithms was not significant.

In agreement with the findings of this study, King et al (2002), in a cohort of normal individuals and patients with glaucoma, found that TOP underestimated the severity of MD relative to SITA Fast by 1.02dB (relative to a Group Mean MD for SITA Fast of -6.48dB) compared to 2.15dB in the current study. The TOP algorithm underestimated focal loss (ie had the smallest PSD/LV$^{0.5}$) relative to the SITA Fast algorithm by 1.52dB (relative to a Group Mean PSD/LV$^{0.5}$ for SITA Fast of 7.29dB) compared to 0.95dB in the current study. King and colleagues also found that the respective differences in MD and in PSD/LV$^{0.5}$, between the two algorithms increased with increase in severity of field loss. Several studies have also found that the TOP algorithm underestimates LV compared to the Octopus Threshold algorithm (Gonzales de la Rosa et al 1998; Lachkar et al 1998; Maeda et al 2000; Anderson 2003). Maeda and colleagues found that in a cohort of patients with glaucoma that the LV was significantly smaller (although the values are not provided) for the TOP algorithm compared to the Octopus Threshold and the Dynamic Strategy (2000).

In the current study, the Group Mean PSD/LV$^{0.5}$ was smallest for the two fastest algorithms over each of the two visits. This finding may be attributable to the reduction, or even absence, of the fatigue effect associated with the Full Threshold and Threshold algorithms in particular. Indeed, the magnitude of the Group Mean PSD/LV$^{0.5}$ increased with the ranked order of the examination duration across the five algorithms. However, the MD for the TOP algorithm was more negative than each of the MDs for the HFA

176

algorithms thus ruling out the explanation based upon the presence of a fatigue effect. The 0.93dB underestimation of the PSD/LV$^{0.5}$ by the TOP algorithm relative to the SITA Fast algorithm is suggestive of a difference attributable to the difference in the method for estimating threshold between the two algorithms. The difference between the examination duration of the five algorithms became more apparent as the severity of the field loss changed.

4.5.2 The Between-algorithm Within-visit (Visit 2) and the Within-algorithm Between-visit Difference in the MD against the Mean of the MDs

The confidence limits associated with the between-algorithm, within-visit difference in the MDs against the mean MD were widest for TOP compared to each of the SITA algorithms. The within-algorithm between-visit graphs produced similar ranges for the confidence limits across the five algorithms. These findings suggest that in terms of the MD, TOP is reasonably repeatable from one examination to another but shows poor correspondence when compared to the SITA algorithms. Sekhar et al (2000) reported, in a cohort of patients with glaucoma, correlation coefficients for the MD between test and retest examinations of 0.92 for the Full Threshold algorithm, 0.92 for the SITA Standard algorithm and 0.70 for the SITA Fast algorithm. Correlational analysis is an inappropriate analytical method for this type of data; such high correlations would be expected.

4.5.3 The Between-algorithm Within-visit (Visit 2) and the Within-algorithm Between-visit Difference in the PSD/LV$^{0.5}$ against the Mean of the PSD/LV$^{0.5}$

The confidence limits associated with the between-algorithm, within-visit difference in the PSD/LV$^{0.5}$ against the mean PSD/LV$^{0.5}$ suggests that the HFA Full Threshold algorithm yielded broadly similar results to the SITA Standard algorithm. Although, both the HFA Full Threshold and the SITA Standard algorithms yielded a PSD/LV$^{0.5}$ which was higher than that of the SITA Fast, the difference was independent of the severity of field loss. The TOP algorithm, overall, substantially underestimated the PSD/LV$^{0.5}$ compared to the SITA Fast algorithm. However, the difference changed markedly as a

177

function of defect depth: for values of $PSD/LV^{0.5}$ up to approximately 4dB, the SITA Fast algorithm generated a higher $PSD/LV^{0.5}$ whilst above this value, the TOP algorithm generated the higher $PSD/LV^{0.5}$. The difference between the $PSD/LV^{0.5}$ for the TOP algorithm compared to the SITA Standard algorithm was independent of severity of field loss; however, the wide confidence limits indicate the general lack of agreement between the two algorithms.

The confidence limits for the within-algorithm between-visit comparison were narrowest for the TOP and Octopus Threshold algorithms followed in increasing order of magnitude by the SITA Fast and the SITA Standard and HFA Full Threshold algorithms The correlation coefficients for the PSD reported by Sekhar and colleagues between the test and retest examinations of the Full Threshold, SITA Standard and SITA Fast algorithms were 0.95, 0.91 and 0.78 respectively.

4.5.4 The Within-visit (Visit 2) Between-algorithm and the Between-visit Within-algorithm Difference in Pointwise Sensitivity

The within-visit between-algorithm pointwise analysis, was clinically similar across all comparisons.

The between-visit within-algorithm pointwise analysis revealed that all of the algorithms yielded broadly similar results. However, the SITA Standard algorithm was possibly more variable as sensitivity declined. Sharma et al (2000) concluded that the average pointwise sensitivity was 1.31dB greater for SITA Standard than for the Full Threshold algorithm but that this difference was greater in areas of reduced sensitivity in glaucomatous eyes. Artes et al (2002) found that for sensitivities above 25dB, SITA Fast and SITA Standard exhibited lower test-retest differences than the Full Threshold algorithm; for sensitivities below 25dB, SITA Fast exhibited greater test-retest differences, and SITA Standard slightly less, relative to that for the Full Threshold algorithm.

4.5.5 The Within-visit (Visit 2) Between-algorithm and the Between-visit Within-algorithm Differences in the Pattern Deviation/Corrected Comparison Probability Level.

The Pattern Deviation/Corrected Comparison Probability analysis was undertaken for the Group as a whole and for each of the levels of severity of field loss. The within-visit between-algorithm analysis for the Group as a whole revealed that both SITA algorithms manifested greater loss than the HFA Full Threshold algorithm. The SITA Standard algorithm manifested greater loss than the SITA Fast algorithm. These results were also compatible with the findings described in Chapter 3 for the normal individuals. The findings can be explained by the narrower confidence limits for each of the SITA algorithms (Bengtsson et al 1998a; Wild et al 1999a; Sekhar et al 2000; Wall et al 2001; Schimiti et al 2002) compared to the Full Threshold algorithm and by the narrower confidence limits for SITA Standard compared to SITA Fast (Nordmann et al 1998; Bengtsson and Heijl 1999; Wild et al 1999b). These findings are in agreement with those of Wild et al (1999b) who found a statistically greater defect on PD probability analysis in patients with OAG, together with a slightly higher sensitivity, for SITA Standard and for SITA Fast compared to the Full Threshold algorithm. Similarly, Sekhar et al (2000) found that defects significant at p<0.5% in the PD probability plots were more common for each of the SITA algorithms than for the Full Threshold algorithm.

For the cohort of 29 patients with glaucoma, the Octopus Threshold algorithm exhibited greater loss than the TOP algorithm but the TOP algorithm manifested greater loss than the SITA Fast algorithm, suggesting narrower confidence limits for the TOP algorithm than for SITA Fast. This latter finding was also present for the normal individuals described in Chapter 3. There was no difference in the Pattern Deviation/Corrected Comparison probability levels between the SITA Standard and the TOP algorithm; a similar finding was also present for the normal individuals described in Chapter 3.

For the patients with Very Early field loss both SITA algorithms again exhibited a statistically significantly greater number of abnormal PD probability values compared to the HFA Full Threshold algorithm. However, there was no difference for the TOP algorithm compared to the Octopus Threshold and compared to each of the SITA

algorithms. Such a finding mitigates against the argument of narrower confidence limits for the TOP algorithm compared to the SITA Fast algorithm and was contrary to that found for the Group as a whole and for the normal individuals.

For the patients with Early field loss the SITA Standard algorithm again exhibited a statistically significantly greater number of abnormal PD probability values compared to the HFA Full Threshold algorithm and compared to SITA Fast. However, there was no difference between the SITA Fast and Full Threshold algorithms. The Octopus Threshold and SITA Standard algorithms both demonstrated greater loss than the TOP algorithm. There was no difference between the TOP and SITA Fast algorithms.

For the patients with Moderate and Severe field loss, both SITA algorithms again exhibited a statistically significantly greater number of abnormal PD probability values compared to the HFA Full Threshold algorithm. The SITA Standard algorithm exhibited greater loss than the SITA Fast. However, the latter two findings were only at marginal significance. Surprisingly, the TOP algorithm generated greater loss than either of the SITA algorithms. It could also be a product of the thresholding technique that TOP employs. The TOP algorithm only presents one stimulus at each location, and once the first matrix has been examined, the presentations of the subsequent matrixes are adjusted accordingly. In a glaucomatous eye with more advanced visual field loss, more stimulus locations in the visual field will exhibit reduced sensitivity than in the eye of a normal individual. Consequently, if the initial matrix consists of few responses from the patient as a result of poor sensitivity, or even inexperience at the start of a perimetric examination, the following stimulus presentations for the subsequent matrix will also be at low luminance levels.

As would be expected, the within-algorithm between-visit difference in the Pattern Deviation/Corrected Comparison probability levels, for the Group as a whole, did not reach statistical significance for any of the five algorithms. However, the same analysis as a function of category of severity of field loss revealed some interesting findings. The Octopus Threshold algorithm exhibited greater loss at Visit 1 than Visit 2 for the Very

Early category of field loss. However, both the Octopus algorithms exhibited greater loss at Visit 2 for the patients with Early field loss. Conversely, the Full Threshold and SITA Standard algorithms exhibited greater loss at Visit 1 than at Visit 2 for the patients with Moderate or Severe field loss.

The results for the within-algorithm between-visit differences and the within-visit between-algorithm differences as a function of severity of field loss must be interpreted with caution due the small numbers of patients within each cohort.

4.5.6 General Comments

As discussed in Chapter 3, the TOP algorithm was again not evaluated with regard to the HFA Full Threshold algorithm, the SITA algorithms were not evaluated with regard to the Octopus Threshold algorithm and the HFA Full Threshold was not evaluated with regard to the Octopus Threshold algorithms. It was again felt that such comparisons were outside the scope of clinical interest. Similarly, it was felt that the inclusion of the HFA Fastpac and the Octopus Dynamic strategy in the study would have resulted in two unacceptably long sessions for the patient.

As also discussed in Chapter 3, the pointwise comparison of the difference in sensitivity did not consider the between-individual differences in sensitivity due to age and the within- and between-individual differences at any given stimulus location due to the parial covariance of sensitivity with increase in eccentricity and with defect depth. The age of the cohort ranged from 49 to 83 years with a mean of 65 years. Thus, the maximum between-individual discrepancy at any given stimulus location due to age would be in the region of 2.1dB i.e. generally within one interval of the scale on the abscissa of Figures 4.5a, 4.5b, 4.6a and 4.6b. The magnitude of the normal variation in sensitivity across the field derived by Program 30-2 varies with region, has an upper limit of approximately 9dB (Heijl et al 1987) and governs the maximum within- and between-individual discrepancy between a normal peripheral value and an abnormal central value. The effect of age could have been removed by considering the between-algorithm

difference in sensitivity at the given stimulus location in terms of the deviation of the measured sensitivity of the reference algorithm from the age-corrected normal value. This latter approach was adopted by Heijl and colleagues but still does not distinguish normal reductions in sensitivity due to eccentricity from identical reductions in sensitivity due to disease. The analysis of the pointwise Total and Pattern Deviation probability values overcomes any limitations in the comparison of the absolute values of sensitivity since the respective confidence limits are corrected for both age and eccentricity.

4.6 CONCLUSIONS

This is the first study that has examined the comparative performance of five current perimetric algorithms in patients with OAG. It is also the first study to evaluate the performance of the Octopus TOP and Threshold algorithms in terms of the pointwise difference in sensitivity between the two algorithms and in terms of a comparison of the Corrected Comparison probability levels.

The results confirm the notion that SITA Standard and SITA Fast have narrower confidence limits than the HFA Full Threshold algorithm. The narrower confidence limits could, theoretically, result in increased sensitivity and reduced specificity for the detection of field loss, relative to the HFA Full Threshold algorithm. The TOP algorithm appeared to have similar confidence limits to the SITA Standard algorithm but narrower confidence limits than the SITA Fast algorithm. The latter finding suggests that the TOP algorithm will exhibit an increased sensitivity and reduced specificity for the detection of field loss, relative to the SITA Standard algorithm. However, it would seem, relative to the Octopus Threshold algorithm, at least, that the TOP algorithm exhibits a tendency to underestimate the depth of focal field loss.

CHAPTER 5

Frequency-of-seeing Curves for SWAP and W-W Perimetry in Normal Individuals and in Patients with Open Angle Glaucoma

5.1 INTRODUCTION

5.1.1 Magnocellular, Parvocelluluar and Koniocellular Pathways

The retinal ganglion cells are damaged in glaucoma. As a consequence, the Magnocellular (M) Parvocellular (P) and Koniocellular parallel pathways are of particular interest in glaucoma. The differentiation of the parallel pathways arises from the structural characteristics of the retinal ganglion cells and from the anatomical arrangement of the neural synapses in the lateral geniculate nucleus (LGN). Ninety percent of the optic nerve fibers, emerging from retinal ganglion cells, terminate in the LGN (Yücel et al 2000, 2001). The LGN is composed of six distinct lamellae, four dorsal P layers and two ventral M layers.

The M and P pathways have distinct functional properties that tend to code for separate aspects of vision within the system. The M pathway is comprised of the parasol ganglion cells that have relatively large receptive fields, are more sensitive to low spatial frequency and high temporal frequency and generally give a similar type of response to all wavelengths. The M-cells synapse in the M layers and approximate to 10% of the total number of ganglion cells (Shapley and Perry 1986). The P pathway consists of the midget retinal ganglion cells. These cells have small receptive fields that are responsive to chromatic information, are more sensitive to high spatial frequency and are less sensitive to high temporal frequency stimuli (Lennie 1980; Merigan and Maunsell 1993; Callaway 1998). The P-cells synapse in the P layers and represent approximately 80% of the total number of retinal ganglion cells (Shapley and Perry 1986). The koniocellular (K) pathway consists of the small bi-stratified ganglion cells which probably account for the remaining 10% of the ganglion cells. The pathway projects to various layers within the LGN, including the thin layers between the P and M layers. Eventually, the K pathway

projects to sections of the visual cortex that are involved in colour vision, object recognition and visual resolution (Casagrande 1994; Hendry and Reid 2000). The K pathway may also have a modulatory effect on activity in the M-cell and P-cell pathways and may also play a part in the suppression of vision during saccadic eye movements (Casagrande 1994; Callaway 1998). The presence of the K pathway suggests a re-interpretation of the various types of visual processing (Hendry and Reid 2000).

The M and P pathways are not restricted to specific visual functions. The M- and P-cells show similar responses to stimuli of similar spatial frequency (Crook et al 1988). Also, there is an overlap for the range of luminances over which each system operates (Pupura et al 1990) and it is unlikely that the processing of visual stimuli remains separated as the two pathways reach the temporal and parietal regions of the primary visual cortex (Merigan and Maunsell 1993). It has been suggested that the M- and P-cell pathways have specialized, but overlapping, detectors and functions (Merigan and Maunsell 1993).

Chromatic responses are predominantly mediated by the P pathway (Merigan and Maunsell 1993; Felius et al 1995) and by the K pathway. There are three types of cone photoreceptors which combine into a color-opponent system that is based upon two channels. The LWS and MWS cones form the red-green channel and the blue-yellow channel receives input from the SWS cones and is antagonistic to input from a combination of the LWS and MWS cones (DeValois et al 1978). Ganglion cells mediating the SWS pathway have a larger diameter than the ganglion cells mediating the medium-wavelength sensitive (MWS) and long-wavelength sensitive (LWS) cells (de Monasterio 1978; Dacey 1993) but a smaller diameter than the ganglion cells mediating the M pathway.

The characteristics of the SWS cones are very different from the LWS and MWS cones. The SWS cones do not contribute to the achromatic (luminance) pathway (Eisner and MacLeod 1980) and are less plentiful than the LWS cones and MWS cones, making up

only 5-10% of the total number of cones (de Monasterio et al 1985; Curcio et al 1991; Calkins 2001). The SWS pathway consists of the S cones, the S-cone bipolar cells and the small bi-stratified ganglion cells (de Monasterio et al 1981; Dacey and Lee 1994; Dacey 2000). The SWS cones have more permeable membranes (de Monasterio et al 1981) and exhibit higher metabolic requirements which could make them more vulnerable to damage from hypoxia and ischemia (Greenstein et al 1989; Yamamoto et al 1996) than the MWS and LWS cones. Similar to the rod photoreceptors, the SWS cones are absent from the centre of the fovea and are diffusely spread throughout the perimacular region thereby undersampling the retinal image (Livingstone and Hubel 1988). The distribution of the SWS cones peaks at approximately 1.5° retinal eccentricity and declines until approximately 7°–8° retinal eccentricity (Volbrecht et al 2000). In addition, the functional organisation of the synaptic network of the SWS cone pathway is considered to be quite different from that of the MWS or LWS cone pathways (deMonasterio and Hubel 1978). Preferential damage and vulnerability of the SWS cones may be expected because of the differing response functions of the three cone types. The SWS cones exhibit a narrower luminance response range which would suggest that, in retinal disease, the SWS cones could saturate while the MWS and LWS cones maintain some sensitivity (Dacey 2000; Cho et al 2000). However, Wygnanski and associates (1995) demonstrated that the SWS cones were unaffected in glaucoma.

5.1.2 Retinal Ganglion Cell Damage in Glaucoma

Histological studies suggest that as many as 40% to 50% of the retinal nerve fibres are lost before a glaucomatous visual field defect becomes manifest with W-W perimetry (Quigley et al 1982; 1989; Harwerth 2002). Once glaucomatous field loss is detected by W-W perimetry, a good correlation is present between ganglion cell loss and perimetric sensitivity (Quigley et al 1989; Garway-Heath et al 2004). It has been shown that in perimetric locations exhibiting a 5dB attenuation in sensitivity, 20% of the normal number of cells are absent and in locations exhibiting a 10dB decrease, 40% of the normal number of cells are absent (Quigley et al 1989).

It has been suggested that the larger optic nerve fibres are preferentially lost in glaucoma (Quigley et al 1988). The larger retinal ganglion cells are positioned in the weakest areas of the optic nerve head which may render them vulnerable to selective damage due to mechanical deformation and/or physiological insult such as elevated IOP (Quigley 1987; 1998; Radius 1987; Nork et al 2000). However, the assertion of preferential loss of the larger retinal ganglion cells is refuted by Morgan (1994) and is not substantiated by the psychophysical evidence in glaucoma which indicates functional damage to the P-pathway as well as to the M-pathway. An alternative hypothesis has been suggested to explain the psychophysical evidence. Ganglion cell types which are more sparsely populated relative to other types exhibit undersampling, or minimal overlap, of the their receptive fields: glaucoma damages all ganglion cell types equally but functional defects are detected earlier due to the proportionately greater loss of the sparsely populated types. This hypothesis is known as the 'reduced redundancy' hypothesis and implies that the pathway with the least amount of redundancy will be most susceptible to damage (Johnson 1994; Lynch et al 1997).

The 'reduced redundancy' hypothesis can be applied to the SWS ganglion cells. These cells are fewer in number than the other ganglion cell types. Damage to the pathways from glaucoma reduces the numbers of each of the SWS, MWS and LWS ganglion cells equally. However, the SWS ganglion cells are the most sparsely populated; therefore, a psychophysical test designed to isolate the SWS mechanism would seem to detect a selective loss in function rather than a selective loss of ganglion cell type (i.e 'sick' cells rather than 'dead' cells) for this pathway (Lynch et al 1997; Johnson 2001).

5.1.3 Short-wavelength Automated Perimetry (SWAP)

Stiles (1939) designed a two-colour increment threshold that isolated the SWS mechanisms using specific stimulus conditions. The peak wavelength for the blue stimulus approximates to the peak response of the SWS cones and is presented on a high luminance yellow background. The high luminance yellow background helps to reduce the response of the MWS and LWS cones and to simultaneously suppress rod activity

186

thereby isolating SWS cone activity. The technique has been applied clinically as SWAP for the detection of visual field loss in glaucoma, ocular hypertension and suspect glaucoma.

5.1.3.1 Optimum Stimulus Parameters for SWAP

The stimulus and background characteristics in SWAP govern the magnitude of SWS isolation. The parameters selected for the commercially available SWAP are a compromise between maximising the dynamic range and maximising the isolation of the SWS channel.

Sample and colleagues (Sample and Weinreb 1992; Sample et al 1993) employed a narrowband blue stimulus that ensured SWS pathway isolation and was less susceptible to shifts in the peak retinal wavelength caused by ocular media absorption (OMA) (Sample et al 1996). As the peak wavelength of the stimulus filter decreases, SWS isolation increases at the cost of an increase in OMA and a reduction in the dynamic range of the perimeter (Moss et al 1995; Hudson et al 1993). A stimulus filter with a broader spectral transmission increases the dynamic range of the perimeter (Johnson et al 1988b; Adams et al 1991; Hudson et al 1993; Johnson et al 1993b,c; Moss and Wild 1994, Johnson et al 1995; Moss et al 1995; Wild and Hudson 1995) but results in some stimulation of the MWS pathway and hence incomplete isolation of the SWS pathway (Sample and Weinreb 1990; Sample et al 1993). A cataract affects the peak retinal wavelength of a narrowband stimulus less than the peak retinal wavelength of a broadband stimulus. The stimulus for the commercially available SWAP is a narrowband 440 nm (27 nm half-peak width) filter (Sample et al 1996) with the HFA and a 440 nm (15 nm bandwidth) filter with the Octopus perimeter.

The maximum stimulus brightness for SWAP with the HFA is 65asb ($20.6cdm^{-2}$) compared to 10,0000asb ($3183cdm^{-2}$) for W-W perimetry. In cases of moderate to advanced glaucoma, the benefit of SWAP may be reduced in defective areas of the visual

field because of the reduced dynamic range of SWAP compared to W-W perimetry and also because the stimulus may be detected by the MWS and LWS channels due to a reduction in the SWS isolation. SWAP is therefore more suited for the investigation of any extension in the area of existing field loss and for the examination of patients with ocular hypertension and patients with early visual field loss by W-W perimetry. The detection of SWS stimuli in more extensive areas of visual field damage (Harwerth et al 1993) is mediated by the achromatic luminance channel (the mediating detection for W-W perimetry rather than the SWS channel; thus no advantage is gained from using SWAP in moderate to advanced visual field loss (Demirel and Johnson 2000). There is some evidence that early glaucomatous damage is not restricted to the SWS channel. All chromatic pathways may be affected in patients with ocular hypertension or with early glaucoma (Felius et al 1995; Greenstein et al 1996; Harwerth et al 1999a,b).

Early studies with SWAP used a range of background luminances from 80.9cdm^{-2} (Sample and Weinreb 1990) to 330cdm^{-2} (Hudson et al 1993; Moss et al 1995; Wild et al 1995; Wild and Moss 1996). A background luminance of 300cdm^{-2} has been advocated for the adequate saturation of the rod pathway (Yeh et al 1989). However, it has been suggested that a background luminance greater than 80.9cdm^{-2} merely increases the SWS threshold rather than increasing the magnitude of isolation (Sample and Weinreb 1990). The background luminance used for the commercially available SWAP with both the HFA and Octopus perimeters is a 100cdm^{-2} with a broadband (500-700nm) yellow background.

A 2° diameter stimulus provides maximal SWS pathway isolation (King-Smith and Carden 1976). Temporal summation is maximal for the SWS pathway at a stimulus duration of 200msec (King-Smith and Carden 1976). The default stimulus for SWAP therefore comprises a Goldmann size V (1.74° diameter) blue stimulus and 200msec stimulus duration to maximise spatial and temporal summation.

The SWS stimulus is preferentially absorbed by the ocular media (Johnson et al 1988b; Sample and Weinreb 1990; 1992; Johnson et al 1995; Wild and Hudson 1995; Wild et al 1998). In the normal eye, and particularly for older age groups, ocular media absorption (OMA) exhibits large between-individual variability (Johnson et al 1988b; Sample et al 1988; Siik et al 1991; Savage et al 1993). OMA leads to a reduction in the height of the hill of vision resulting from the reduced transmission of the SWS stimulus and confounds the measurement and interpretation of the visual field derived by SWAP (Wild 2001) in that analysis of abnormality solely in terms of Total Deviation or Comparison probability analysis (i.e. abnormalities of height) cannot be relied upon. Cataract causes a predominantly general reduction in sensitivity in both W-W perimetry and SWAP and the reduction of SWAP has been shown to be far greater than that of W-W perimetry (Kim et al 2001).

The estimation of OMA by means of a scotopic threshold technique, has been extensively used (Sample et al 1989; Johnson et al 1989; Lutze and Bresnick 1991; Johnson and Marshall 1995; Wild et al 1995; Polo et al 1998) but is not clinically feasible due to the time necessary to acquire the measurement. The between-subject normal variability of the threshold estimate is reduced following correction for absorption measured by the scotopic threshold technique (Wild et al 1998) or by autofluorescence (Teesalu et al 1996).

Forward intraocular light scatter arising from cataract also leads to the reduction in the height of the hill of vision (Moss and Wild 1994). Posterior subcapsular cataracts have a greater effect on the SWAP hill of vision than other types of cataract due to the increased forward light scatter and concomitant reduction in pupil size resulting from the increased background luminance of SWAP (Moss et al 1995).

5.1.3.2 The Use of SWAP in Glaucoma

SWAP is seemingly able to detect glaucomatous visual field loss prior to conventional W-W perimetry (Heron et al 1988; Sample et al 1988; de Jong et al 1990; Hart et al 1990;

Adams et al 1991; Sample and Weinreb 1992; Casson et al 1993; Johnson et al 1993a,b; Sample et al 1993; Johnson et al 1995; Wild et al 1995). Patients with glaucoma demonstrate a significant loss of SWS function throughout the central visual field (Heron et al 1988) and show wider and/or deeper defects with SWAP than with W-W perimetry (de Jong et al 1990; Hart et al 1990; Sample and Weinreb 1990; Adams et al 1991; Sample and Weinreb 1992; Johnson et al 1993b; Casson et al 1993; Wild et al 1995). The extent of visual field deficit is similar between SWAP and W-W perimetry for more advanced visual field defects (Hart et al 1990; Wild et al 1995). Several longitudinal studies involving patients considered to be suspect for developing glaucoma, have demonstrated the presence of visual field loss with SWAP prior to its occurrence with W-W perimetry (Sample et al 1993; Johnson et al. 1993a,b) by at least three to five years (Johnson et al 1993a,b). SWAP seemingly also detects progressive visual field loss in patients with glaucoma earlier than W-W perimetry (Sample and Weinreb 1992; Sample et al 1993; Johnson et al 1993a,b). However, the various studies do not clearly define the criteria for visual field progression with SWAP and also employed small cohorts of patients (Wild 2001).

However, the analysis of abnormality has largely been based upon deviations in the height of the visual field from the age-corrected normal value rather than on deviations in shape (Johnson et al. 1993a,b; Sample et al 1993). In addition, many studies which have suggested earlier visual field loss with SWAP, have utilized small cohorts of elite perimetric observers (Johnson et al 1993a,b; Sample et al 1993). Gray scale artifacts also occur with SWAP because the gray scales are neither age-corrected nor eccentrically compensated (Wild 2001). The combination of the lower sensitivity of the superior field and the greater age-decline in sensitivity for SWAP results in a darker appearance of the gray scale in the superior field. Excessive cases of OMA and reduced dynamic range, particularly using a narrowband filter also result in a uniformly darker appearance of the gray scale (Wild 2001) which can be mistaken for field loss.

190

5.1.3.3 Normal Hill of Vision for SWAP

The sensitivity gradient for SWAP is flatter than that for W-W perimetry in the normal eye (de Jong et al 1990). The greater rate of decline increases with increase in eccentricity particularly in the superior nasal field (Johnson et al 1988b; Sample et al 1997). Slopes of 1.5dB to 2.2dB per decade for the SWAP hill of vision have been reported for broadband stimuli (Johnson et al 1988; Johnson and Marshall 1995) and of 1.5 to 2.2dB per decade for the narrowband stimulus used in the commercially available SWAP (Wild et al 1998).The hill of vision for W-W perimetry exhibits an average decline of 0.58dB per decade (Haas et al 1986).

The normal age-related decline in sensitivity is also greater for the SWS channel, than for the MWS and LWS channels by approximately 0.3dB per decade (Johnson et al 1988b). There are several possible explanations for the greater age-decline in the SWAP sensitivity gradient. The foveal cone photopigment (Van Norren and Van Meel 1985; Kilbride et al 1986), photoreceptor density (Gartner and Henkind 1981; Farber et al 1985), ganglion cell density and morphology (Dolman et al 1980; Balaszi et al 1984) and the number and morphology of cortical cells (Scheibel et al 1975; Devaney and Johnson 1980) all decrease with advancing age and may therefore, separately or collectively, account for the greater age-decline in the SWAP sensitivity gradient.

5.1.3.4 Variability of the Threshold Response

The threshold estimate is dependent upon the within- and between-examination variability (Heijl et al 1987a). The within-subject, within-examination variability of the threshold response is known as the short-term fluctuation (SF) and the within-subject, between-examination variability as the long-term fluctuation (LF) (See Chapter 1). For central field examination out to 30° eccentricity in the normal eye, the SF and the LF, increases with increase in eccentricity (Katz and Sommer 1986) and with increase in age (Katz and Sommer 1987). The within-examination between-subject normal variability, upon which the confidence limits for normality are based, also increases with increase in eccentricity and with increase in age (Brenton and Phelps 1986; Heijl et al 1987a).

5.1.3.5 Short-term and Long-term Fluctuation in SWAP

The SF derived in normal individuals by SWAP is larger than for W-W perimetry by between 17% (Wild et al 1998) and 55% (Kwon et al 1998). Patients with glaucoma demonstrate an increased SF for W-W perimetry (Flammer et al 1984a,b) and for SWAP (Sample and Weinreb 1993; Wild et al 1995) compared to patients with ocular hypertension although the two techniques exhibit similar magnitudes (Sample and Weinreb 1993; Wild et al 1995). The LF is greater for SWAP compared to W-W perimetry in normal individuals and in patients with glaucoma. Hutchings and colleagues (2001) found the two components of the classically defined LF to be larger for SWAP compared to W-W perimetry by 79% and 43%, respectively, in glaucoma suspects and by 25% and 34% in patients with glaucoma. A surrogate measure of the LF for SWAP (which included the influence of the SF) across the central field in normal subjects was found to be larger than for W-W perimetry by 107% and 41% using the HFA and the Octopus perimeters, respectively, (Kwon et al 1998). The LF at each stimulus location using a similar surrogate measure in patients with stable glaucoma was 23% greater than that for W-W perimetry (Blumenthal et al 2000). The greater SF and LF for SWAP compared to that of W-W perimetry indicates that the identification of progressive visual field loss for SWAP will be more difficult than that for W-W perimetry (Hutchings et al 2001).

5.1.3.6 Between-individual Normal Variability for SWAP

The between-individual variation in the normal threshold at each stimulus location using the commercially available SWAP is, on average, 2.7 times greater for SWAP than for W-W perimetry and 1.9 times greater after correction for OMA (Wild et al 1998). The between-individual normal variability for SWAP is similar for both the 4-2dB double crossing of threshold employed in the Full Threshold algorithm of the HFA and the 3dB single crossing of threshold employed in the FASTPAC algorithm (Wild et al 1998). As a result of the increased variability, the reduction in sensitivity required to indicate abnormality for SWAP is proportionately greater than for W-W perimetry .

5.1.4 Frequency-of-Seeing Curve

The perimetric stimulus parameters such as intensity, size, duration and wavelength, together with the background luminance can be adjusted to promote, or prevent, detection of the stimulus. The stimulus intensity is the parameter that is usually varied in automated static perimetry. As the intensity of the stimulus increases, the likelihood of a positive response increases until it approaches 100%. The frequency-of-seeing curve, or psychometric function, is generated when the logarithm of stimulus intensity is plotted against the probability of a positive response. The curve has a characteristic, cumulative frequency or sigmoid appearance with a linear part in the middle (Weber & Rau 1992). In perimetry, threshold is defined as the stimulus intensity at which the subject gives a positive response on 50% of the occasions.

The frequency-of-seeing curve never actually reaches 100% or 0% due to the presence of false-negative and false-positive responses, respectively. The between-subject and between-location variation, which is highly correlated with the threshold level, influences the slope of the frequency-of-seeing curve (Chauhan et al 1993; Olsson et al 1993; Weber and Rau 1992) which, itself, varies between normals, glaucoma suspects and patients with glaucoma. Glaucoma patients can produce elevated thresholds with steep, precise curves and "noisy", flatter curves with near normal thresholds (Chauhan et al 1993). The statistical nature of the frequency-of-seeing curve is of paramount importance in visual field assessment.

The between-subject normal variability is greater at each stimulus location for SWAP compared to W-W perimetry (Wild et al 1997, 1995). This greater variability for SWAP is more noticeable at increased eccentricities and with increased age (Wild et al 1997, 1995) and is likely to result from a flatter FOS curve for SWAP (Olsson et al 1998). The increased variability for SWAP compared to W-W perimetry can also be attributed to the increased within- and between-subject intraocular light scatter of the blue stimulus (Moss and Wild 1994), the between-subject variation in the density of macular pigment (Wild and Hudson 1995) and the within- and between-subject variations in OMA (Moss et al 1995).

5.2 AIMS

Despite the increased variability for SWAP compared to W-W perimetry, the shape of the FOS curve in SWAP has never been formally documented either in the normal eye or in glaucoma. The purpose of the study therefore was twofold. Firstly to determine, in the normal eye, the slope of the FOS curve as a function of eccentricity for both W-W perimetry and SWAP. Secondly, to determine, for both W-W perimetry and SWAP, the relationship between the magnitude of the slope and the magnitude of sensitivity in glaucomatous field loss.

5.3 METHODS
5.3.1 Cohort of Normal Individuals

The sample comprised 17 normal individuals (9 males and 8 females) recruited from the Eye Clinic of the Cardiff School of Optometry and Vision Sciences, Cardiff University and from local old-age pensioner associations. The mean age for the normal group was 64.3 years (SD 11.5) and the range was 44-81 years.

At the first visit, all of the normal individuals underwent a routine eye examination to determine whether they met the inclusion criteria for entry into the study. The inclusion criteria were the same as that described in Chapter 3 for the normal individuals and comprised in either eye, a visual acuity of 6/9 or better, distance refractive error of less than or equal to 5 dioptres mean sphere and less than 2.5 dioptres cylinder, lenticular changes not greater than NCIII, NOIII, CI or PI by LOCS III (Chylack et al 1993), IOP's of less than 22mmHg, normal optic nerve head appearances, open anterior chamber angles, no medication known to affect the visual field, no previous ocular surgery or trauma, no history of diabetes mellitus and no family history of glaucoma.

One eye was chosen for each volunteer for inclusion in the study. The designated eye of a given individual was selected as the more normal of the two eyes based upon the study inclusion criteria described above.

5.3.2 Examination Protocol

The subjects then each attended for a further four visits at the Cardiff School of Optometry and Vision Science, Cardiff University. Each visit consisted of two sessions. Each session lasted approximately 30 minutes and was separated by a rest period of 30 minutes. At the second visit, volunteers underwent W-W perimetry using the SITA Standard algorithm with stimulus size III and Program 24-2 of the Humphrey Field Analyzer (HFA) in the designated eye, at one session and, at the second session, two examinations of the same eye, with SWAP using the FASTPAC algorithm with stimulus size V and Program 24-2 of the HFA 750. The data collected from this familiarization session was used to determine the FOS locations chosen for the glaucoma patients. The order of sessions was randomized between-individuals but remained constant between-visits for each individual.

At the second and third visits, FOS curves were derived for W-W perimetry and for SWAP using the HFA. At one session at each of these visits, FOS curves for W-W perimetry were obtained at each of 4 locations using 5 stimulus presentations at each of 8 luminance levels (this was achieved by using two separate repetitions of each of the 2 FOS custom programs, each comprising 4 luminances). At the second session at each of the two visits, the SWAP FOS curves were obtained at the same 4 locations using the same procedure. The order of the custom programs within each session and the order of the sessions within a visit were randomized for each subject but held constant within a subject between sessions over the second and third visits.

The stimulus presentations necessary for the derivation of the 4 FOS curves were contained within custom programs on the HFA. The custom programs were proprietary software to Carl Zeiss Meditec (Dublin Ca.). Each of two custom programs derived the threshold at each of three stimulus locations (two FOS locations and a distractor location). The locations (FOS and distractor) were constant for all individuals and were chosen to correspond to the nerve fibre bundle distribution of the retina. For all normal subjects, the 4 FOS stimulus locations (specified in terms of the right eye) were: (3°, 9°);

195

(3°, -15°); (-9°, -3°); (-21°, 3°). All FOS locations described in this Chapter are expressed as cartesian co-ordinates in degrees. The eight different stimulus luminances were at +1dB, -1dB, +2dB, -2dB, +3dB, -3dB, +5dB and -5dB increments relative to the threshold measured using the conventional 4-2dB staircase algorithm for each stimulus location.

Each of the two custom programs took approximately 7 minutes. In total, therefore, there was approximately one hour of perimetry for both W-W perimetry and SWAP at each of visits two and three. Each session was separated by a rest period of 30 minutes. Individuals were given regular breaks within- and between-examinations within a session to facilitate optimum vigilance and to ensure the best opportunity for quality data.

At the fourth visit, volunteers underwent measurement of ocular media absorption (OMA) in the designated eye. OMA was determined using a modified HFA 640 and the procedure has been described in detail below. The command structure software of the HFA was modified to extinguish the background illumination and to alter the duration of the stimulus presentation from 200 to 100 msec. An infra-red illumination system was used to facilitate the monitoring of patient fixation. Subjects were dark adapted for 30 minutes. A size V target was presented at an eccentricity of 15° in the superior, inferior and temporal retina. Thresholds were obtained for 410nm and 560nm stimuli. These stimuli were selected since the 410nm stimulus causes the least attenuation in the dynamic range of the perimeter. The eccentricity was chosen to eliminate the effects of absorption of the short-wavelength stimulus by the macular pigment and also to ensure maximal contribution from the rods. The threshold was obtained three times at each stimulus location for each stimulus wavelength. The difference in the thresholds between the two wavelengths can be assumed to be a measure of ocular media absorption. This threshold procedure took approximately 15 minutes.

The results for SWAP were corrected using the procedure of Van Norren and Vos (1974) which was adapted and implemented more recently by Sample et al (1988, 1989). The

technique is based upon the CIE (Commission Internationale Eclairage) absorption spectrum of rhodopsin. A pair of narrowband stimuli consisting of a short-wavelength and a medium-wavelength stimulus are selected which are equally absorbed by rhodopsin (390nm and 568nm, 400nm and 565nm, or 410nm and 561nm). The difference in scotopic thresholds to these stimuli may be attributed to absorption of the short-wavelength stimulus by the ocular media.

This technique for measurement of OMA was that used by the Group and other investigators, previously (Johnson et al 1988, 1995; Sample et al 1989, 1993; Moss et al, 1995; Lutze and Bresnick 1991; Wild and Hudson 1995; Polo et al. 1998; Wild et al 1998). Blocking material had been applied to the surround of the perimeter bowl to prevent light leakage from the stimulus projection system onto the bowl surface. A six log unit neutral density gelatin filter had been applied over the perimeter monitor to further reduce extraneous light entering the perimeter cupola. The command structure software of the HFA had been modified to extinguish the background illumination and to alter the duration of the target exposure from 200 to 100msec. A red Cinelux 406 filter (Strand Lighting Ltd, Middlesex, UK) had been positioned over the fixation target in order to preserve dark adaptation.

Fixation was monitored with the aid of an infra-red source, consisting of an M92 20 W 12 V tungsten halogen lamp (Osram Ltd, Middlesex, UK) mounted behind a Schott RG830 "black light" filter transmitting wavelengths beyond 750nm. The infrared assembly had been encased within a steel tube and fixed to the frame of the HFA such that the infra-red radiation was reflected off the bowl surface and onto the subject.

The dB printout from these measurements does not take into account the attenuation caused by the introduction of each narrowband stimulus filter. The true threshold was therefore calculated for the 410nm and 560nm stimuli before the measure of ocular media absorption was calculated. OMA at 410nm was scaled to the 440nm stimulus wavelength

employed in SWAP using the equations of Van Norren and Vos (1974). Knowledge of the maximum stimulus luminance of the 410nm and 560nm stimuli was required to perform these calculations. These measurements had been carried out using an LMT 3001 spot photometer (LMT Lichtmesstechnik GMBH, Berlin, Germany). OMA was expressed as the mean of the four eccentricities tested.

The four visits were carried out at weekly intervals. Refractive correction, in the form of full aperture trial lenses, appropriate for the viewing distance of the perimeter bowl, was used for the designated eye of each patient. The contralateral eye was occluded with an opaque patch. Fixation was monitored continuously using the video monitor and the gaze tracker and the standard Heijl-Krakau technique.

5.3.3 Analysis
The sensitivity at each location derived by SWAP was corrected for OMA (as described previously).

The sensitivity values averaged across Visits 2 and Visit 3 for W-W perimetry and for SWAP were separately fitted for each individual at each of the four stimulus locations using the neural activation function:

$$y = 1/(1 + e^{k(x-z_0)})$$

where y is the frequency of seeing, expressed as a percentage; k is the slope, x is the sensitivity, and z_0 is the sensitivity corresponding to the 50th percentile (50% frequency of seeing). The preliminary modelling of the data indicated that the function was the most suitable. The parameters of the best fitting curve were found by successive approximation using proprietary software written in Matlab (*.mat file). The successive approximation was achieved by using two different loops to test all possible combinations of z_0 and of k.

The successive approximation was divided into three successive stages. In the first stage, values of z_0 from from the minimum to the maximum at the given eccentricity for the given patient, in increments of 1.0dB, were substituted into the activation function. Each z_0 value was combined with a slope which ranged from 0.0001 to 8 in increments of 1.0. The root mean square error between the derived curve and the measured data was calculated for each combination of z_0 and k. The first approximation for z_0 was the combination which yielded the smallest root mean square error. The second stage of the successive approximation used a range of potential z_0 values extending ± 1.0dB either side of the first approximation of z_0, in increments of 0.1dB. The range for the slope was 0.0001 to 8 in increments of 0.5. The third stage of the successive approximation used a range of potential z_0 values extending ± 0.1dB either side of the second approximation of z_0, in increments of 0.01dB. The range for the slope was 0.0001 to 8 in increments of 0.01. The third and final approximation derived the values considered to represent z_0 and k.

The same procedure was undertaken to derive the values for z_0 and k at each eccentricity based upon the Group Mean value, and upon the Group Median, for each of the eight different stimulus luminances at the given eccentricity.

Separate repeated measures ANOVAs were undertaken for z_0, k and the root mean square error. Eccentricity and the type of perimetry (i.e. W-W perimetry or SWAP) were considered as within subject factors. The ANOVA for the slope was undertaken using a logarithm transform of the data to ensure a normal distribution.
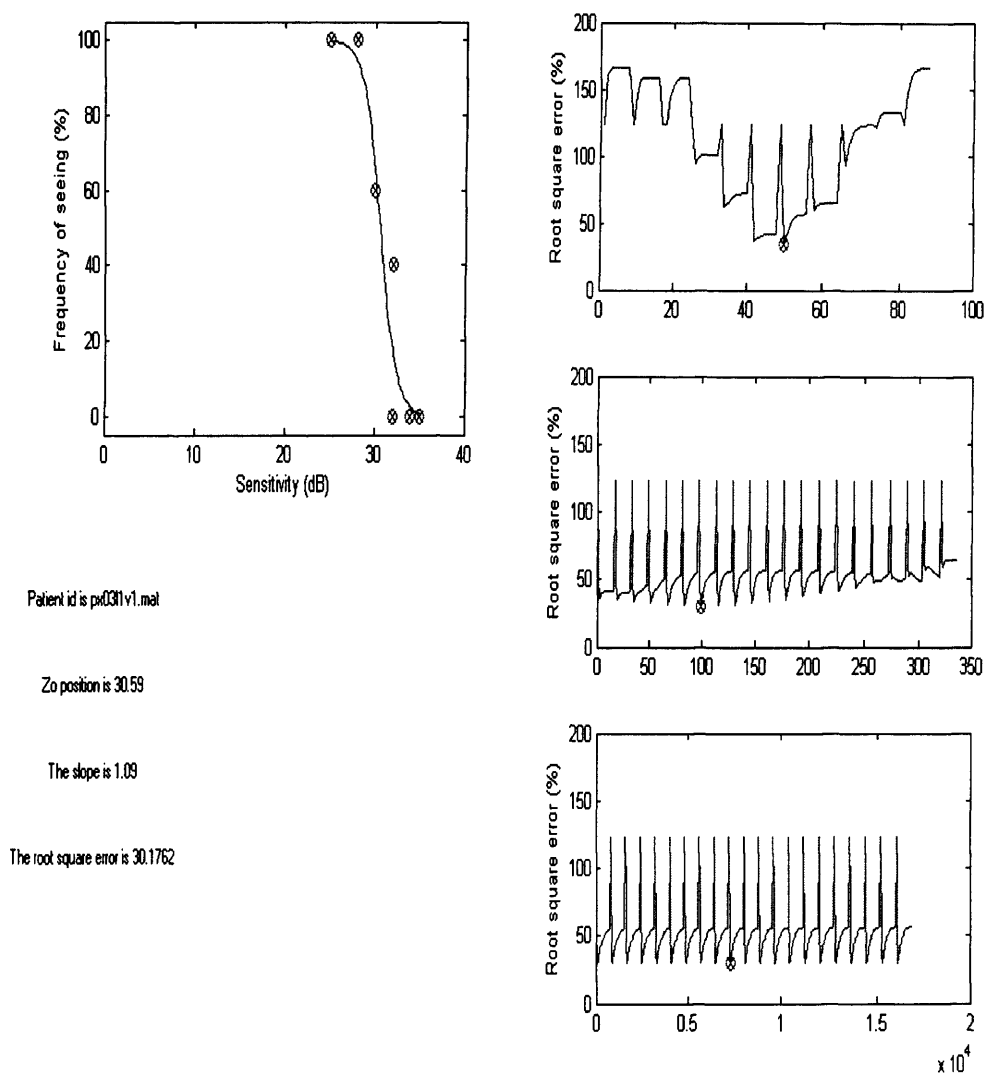
Figure 5.1 Illustrating the printout from the proprietary software used to derive the parameters of the FOS curve. The figure shows the steps involved in the application of the neural activation function to the data for an individual at a particular eccentricity (3,-15) for W-W perimetry: the root mean square error against the number of possible models (top right); the second (middle left) and third (bottom left) approximations and the resultant FOS curve (top left). The corresponding values for z_0, the slope and the error are listed below the FOS curve.

200

5.4 RESULTS

The Group Mean and one SD for OMA was 7.28 dB and 3.98, respectively. OMA as a function of age for the 17 individuals is given in Figure 5.1. With the exception of one obvious outlier, OMA increased linearly with increase in age.

The magnitude of the slope for each normal individual for both FOS visits combined, for W-W perimetry and SWAP is shown in Figures 5.3a and 5.3b, respectively. The correlation matrices for z_0, k, and the root mean square error derived at the third approximation between eccentricities for W-W perimetry and for SWAP and based upon the individual results from the 17 individuals are given in Tables 5.1a, 5.1b and 5.1c, respectively. A reasonable correlation was present for z_0 which decreased with increasing separation between stimulus locations for both W-W perimetry and SWAP. Surprisingly, the correlations for z_0 were higher for SWAP than for W-W perimetry. Minimal correlation was present between eccentricities in the slope for both W-W perimetry and SWAP. A slightly higher, but non-significant correlation was present between eccentricities in the root mean square error.
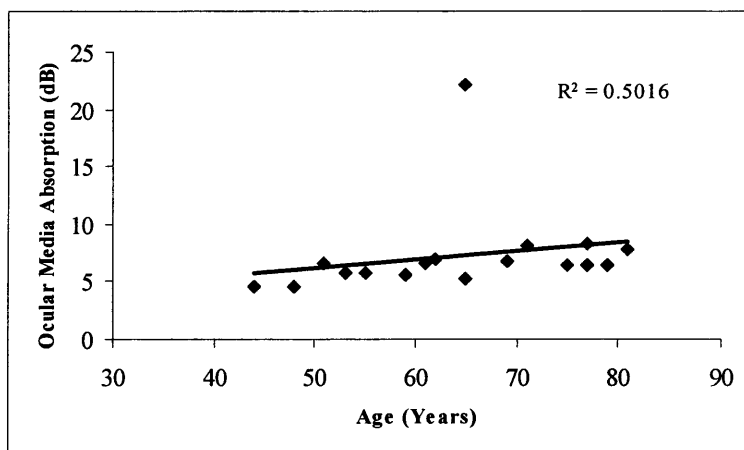
Figure 5.2 OMA against age. There is one obvious outlying data point. This data point was removed prior to the calculation of R^2 and the equation of the trendline, (y=0.066x+2.10).
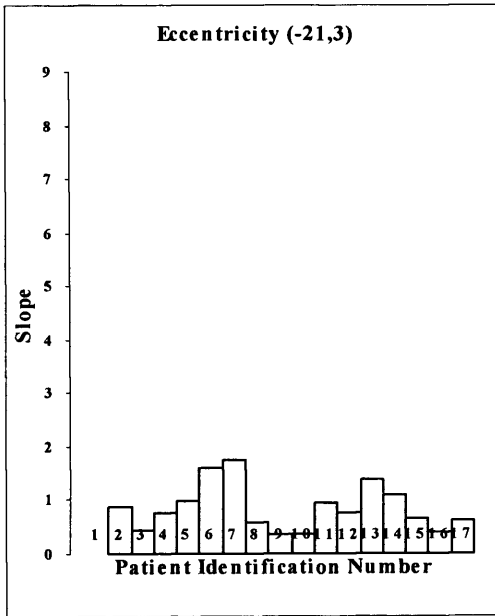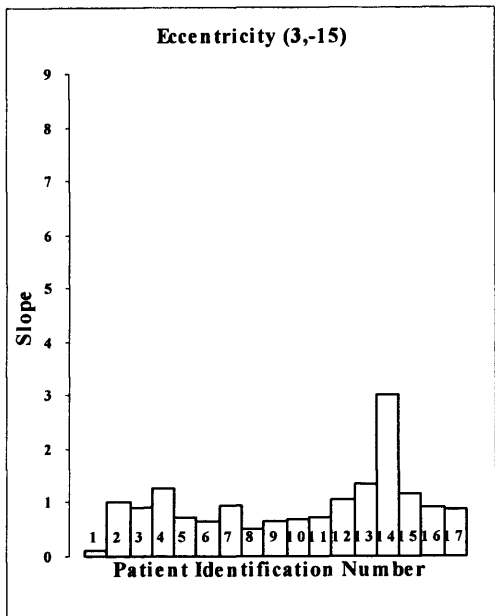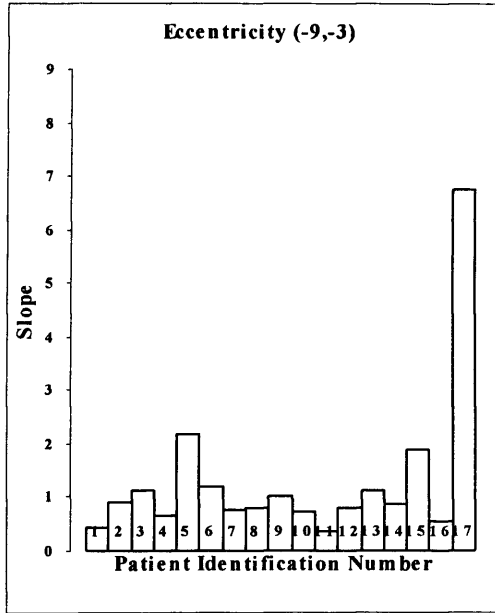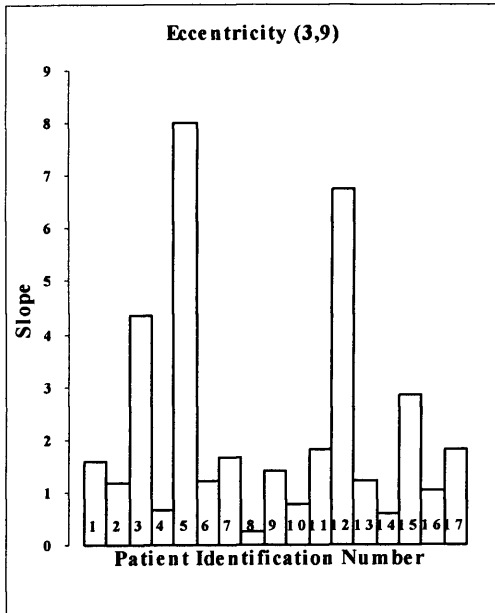
Figure 5.3a The range of the magnitude of the slopes for the FOS curves for W-W perimetry for both FOS visits combined for each normal individual at each of the four FOS eccentricities.
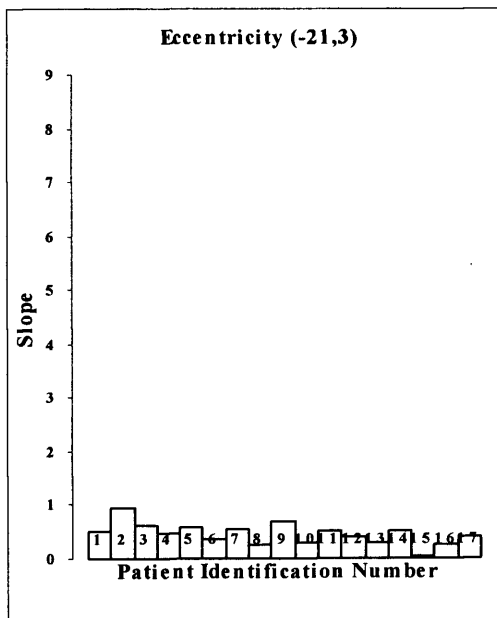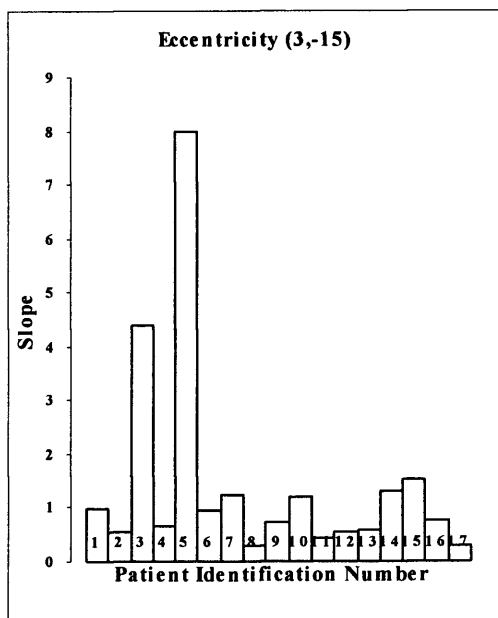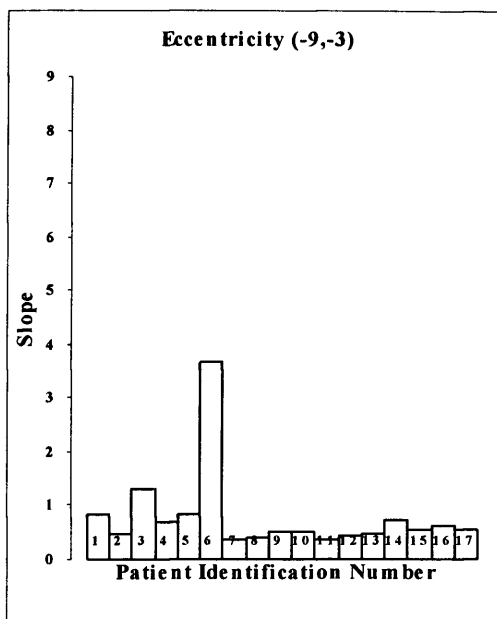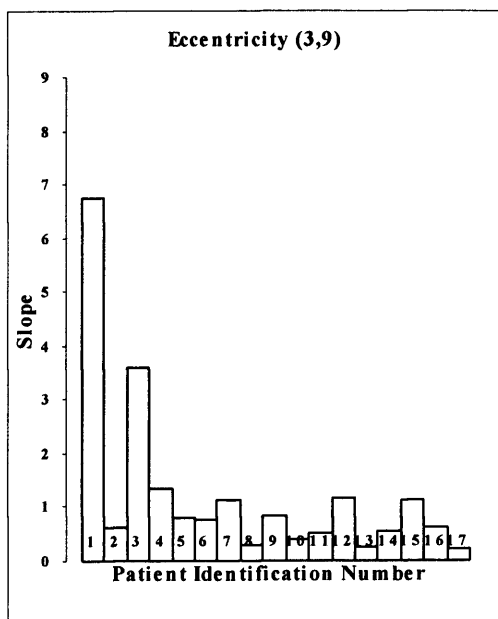
Figure 5.3b The range of the magnitude of the slopes for the FOS curves for SWAP, for both FOS visits combined for each normal individual at each of the four FOS eccentricities.

	W-W perimetry				SWAP			
	(x=3, y=9)	(x=9, y=-3)	(x=3, y=-15)	(x=-21, y=3)	(x=3, y=9)	(x=9, y=-3)	(x=3, y=-15)	(x=-21, y=3)
W-W (x=3, y=9)		**0.78** p=0.0003	**0.33** p=0.19	**0.39** p=0.13	0.71 p=0.001	0.41 p=0.10	0.57 p=0.017	0.61 p=0.009
(x=9, y=-3)			**0.21** p=0.427	**0.49** p=0.05	0.61 p=0.010	0.63 p=0.007	0.53 p=0.029	0.51 p=0.036
(x=3, y=-15)				**-0.24** p=0.347	0.52 p=0.031	0.32 p=0.203	0.57 p=0.016	0.29 p=0.257
(x=-21, y=3)					**0.19** p=0.46	**0.25** p=0.324	**0.14** p=0.60	**0.33** p=0.192
SWAP (x=3, y=9)						**0.63** p=0.006	**0.80** p=0.0001	**0.57** p=0.017
(x=9, y=-3)							**0.85** p<0.0001	**0.68** p=0.003
(x=3, y=-15)								**0.72** p=0.001
(x=-21, y=3)								

Table 5.1a The correlation matrix for z_0 at each eccentricity for W-W perimetry and for SWAP.

		W-W perimetry				SWAP			
		(x=3, y=9)	(x=9, y=-3)	(x=3, y=-15)	(x=-21, y=3)	(x=3, y=9)	(x=9, y=-3)	(x=3, y=-15)	(x=-21, y=3)
W-W	(x=3, y=9)		**0.14** p=0.601	**-0.13** p=0.628	**0.00** p=0.990	0.11 p=0.664	-0.00 p=0.993	0.73 p=0.0009	0.10 p=0.699
	(x=9, y=-3)			**-0.02** p=0.937	**-0.03** p=0.925	-0.21 p=0.418	-0.07 p=0.950	0.07 p=0.776	-0.10 p=0.704
	(x=3, y=-15)				**0.35** p=0.173	-0.34 p=0.182	0.12 p=0.653	-0.06 P=0.821	0.01 p=0.962
	(x=-21, y=3)					**-0.47** p=0.058	**0.33** p=0.194	**0.03** p=0.921	**0.06** p=0.815
SWAP	(x=3, y=9)						**0.10** p=0.703	**0.14** p=0.588	**0.15** p=0.565
	(x=9, y=-3							**0.13** p=0.621	**-0.05** p=0.835
	(x=3, y=-15)								**0.18** p=0.494
	(x=-21, y=3)								

Table 5.1b The correlation matrix for k at each eccentricity for W-W perimetry and for SWAP.

		W-W perimetry				SWAP			
		(x=3, y=9)	(x=9, y=-3)	(x=3, y=-15)	(x=-21, y=3)	(x=3, y=9)	(x=9, y=-3)	(x=3, y=-15)	(x=-21, y=3)
W-W	(x=3, y=9)		**0.13** p=0.611	**0.30** p=0.241	**0.10** p=0.707	0.17 p=0.520	0.24 p=0.353	0.14 p=0.593	-0.31 p=0.223
	(x=9, y=-3)			**0.26** p=0.314	**0.10** p=0.707	0.08 p=0.759	-0.30 p=0.236	-0.29 p=0.255	-0.00 p=0.997
	(x=3, y=-15)				**0.37** p=0.139	0.10 p=0.715	-0.25 p=0.331	-0.22 p=0.400	-0.17 p=0.505
	(x=-21, y=3)					**0.17** p=0.523	**-0.46** p=0.064	**-0.33** p=0.186	**-0.20** p=0.431
SWAP	(x=3, y=9)						**-0.23** p=0.380	**-0.56** p=0.021	**0.08** p=0.769
	(x=9, y=-3							**0.25** p=0.342	**-0.20** p=0.432
	(x=3, y=-15)								**-0.05** p=0.859
	(x=-21, y=3)								

Table 5.1c The correlation matrix for the root mean square error at each eccentricity for W-W perimetry and for SWAP.

The FOS curves based upon the Group Mean z_0 for W-W perimetry and for SWAP at each of the four eccentricities, are given in Figure 5.4a. The corresponding FOS curves based upon the Group Median z_0 are given in Figure 5.4b. The Group Mean of the z_0, slope and error for the third approximation at each eccentricity are given for W-W perimetry and for SWAP in Figure 5.4a. The Group Median of the z_0, slope and error for the third approximation at each eccentricity for W-W perimetry and for SWAP are given in Figure 5.4b.

The ANOVA summary tables for z_0, slope and error at the third approximation are given in Tables 5.2a, 5.2b, and 5.2c respectively. The magnitude of z_0 decreased with increase in eccentricity for both W-W perimetry and SWAP ($p<0.001$). Sensitivity was lower for SWAP than for W-W perimetry ($p=0.0009$) (Table 5.2a). The slope of the FOS curve flattened with increase in eccentricity for both W-W perimetry and SWAP ($p=0.0003$). The slope was flatter for SWAP than for W-W perimetry ($p=0.010$) (Table 5.2b). The magnitude of the root mean square error was independent of eccentricity ($p=0.598$) and of the type of perimetry ($p=0.628$) (Table 5.2c).
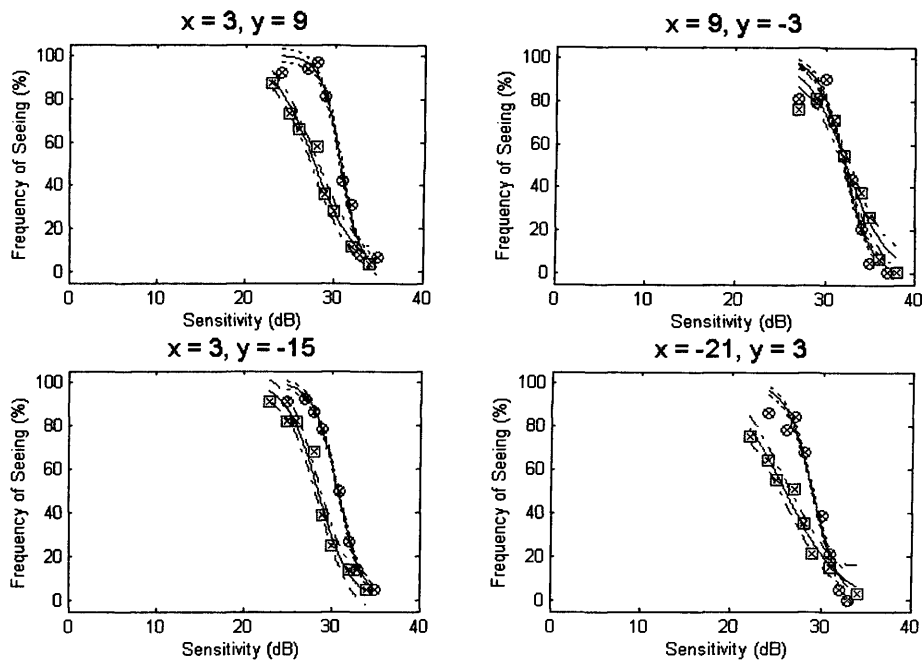
	x = 3, y = 9	x = 9, y =-3	x = 3, y =-15	x = -21, y = 3
Slope W-W	0.86	0.68	0.71	0.66
Z_0 W-W	30.77	32.20	30.80	28.99
Error W-W	13.22	24.00	9.67	18.87
Slope SWAP	0.42	0.44	0.56	0.33
Z_0 SWAP	27.83	32.40	28.53	26.00
Error SWAP	11.71	21.27	14.96	12.88

Figure 5.4a The FOS Curve, based upon the Group Mean sensitivity for each of the eight different stimulus luminances, as a function of eccentricity, for W-W perimetry (circles) and for SWAP (squares) and the corresponding Table of Values giving the magnitude of the z_0, slope, and root mean square error. The dotted lines either side of each FOS curve represent the standard deviation.
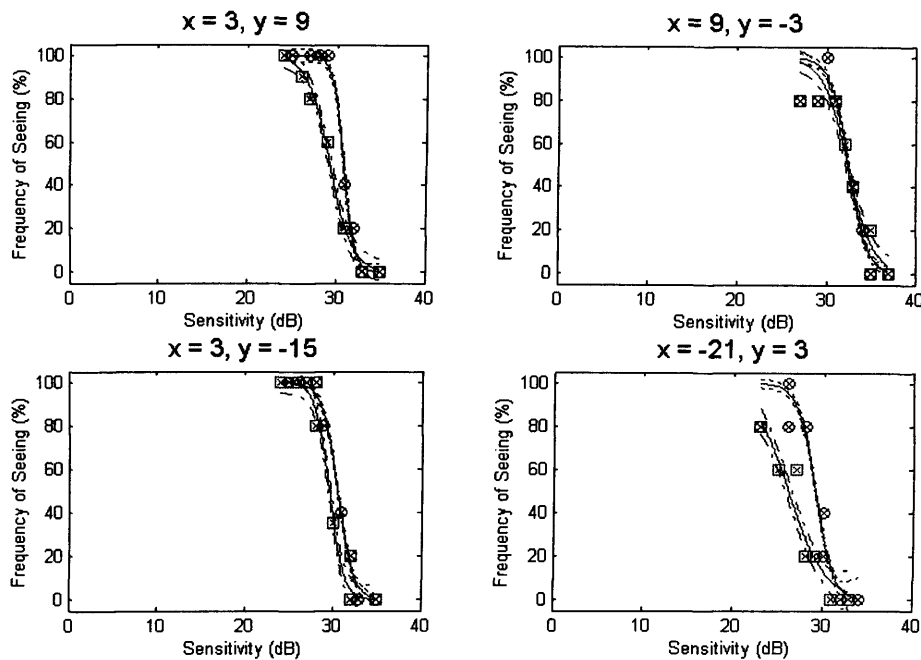
	x = 3, y = 9	x = 9, y = -3	x = 3, y =-15	x = -21, y = 3
Slope W-W	1.58	0.97	0.71	0.99
Zo W-W	30.84	32.48	32.40	29.14
Error W-W	9.52	28.30	27.51	30.13
Slope SWAP	0.77	0.71	1.22	0.49
Zo SWAP	29.3	32.4	29.63	26.17
Error SWAP	9.62	27.51	21.67	24.59

Figure 5.4b The FOS Curve, based upon the Group Median sensitivity for each of the eight different stimulus luminances, as a function of eccentricity, for W-W perimetry (circles) and for SWAP (squares) and the corresponding Table of Values giving the magnitude of the z_0, slope, and root mean square error. The dotted lines either side of each FOS curve represent the standard deviation.

Source	Df	Sums of Squares	Mean Square	F value	P
Location	3	546.23	182.08	14.00	<0.001
Test	1	151.12	151.12	11.62	0.0009
Location x Test	3	54.80	18.27	1.40	0.2453

Table 5.2a The ANOVA summary table for z_0 at the third approximation.

Source	Df	Sums of Squares	Mean Square	F value	P
Location	3	12.99	4.33	6.84	0.0003
Test	1	4.33	4.33	6.76	0.010
Location x Test	3	2.78	0.93	1.47	0.228

Table 5.2b The ANOVA summary table for the slope at the third approximation.

Source	Df	Sums of Squares	Mean Square	F value	P
Location	3	465.15	155.05	0.63	0.5975
Test	1	58.30	58.30	0.24	0.6276
Location x Test	3	147.20	49.07	0.20	0.8967

Table 5.2c The ANOVA summary table for the root mean square error at the third approximation.

5.4.1 Discussion

In the current study, OMA increased by 0.66dB for each decade of increase in age. This value is compatible with that of Johnson et al (1988a) who calculated that for each decade of increase in age, the increase in OMA for short-wavelength stimuli was 0.03-0.06 log units.

The ANOVA confirmed the hypothesis for the study that the slope and, therefore z_0, of the FOS curves for W-W perimetry and for SWAP would flatten with increase in eccentricity and that the magnitude of the slope would be flatter at any given eccentricity for SWAP than for W-W perimetry.

The findings for the FOS curves for W-W perimetry in the current study are substantiated by the limited literature (Chauhan et al 1993; Henson et al 2000; Weber and Rau 2002; Wall et al 2002). The analysis in the current study described the format of the FOS curve in terms of the slope, z_0, (50th percentile of the curve) and the root mean square error for each individual. Other authors have described the FOS curve in terms of the interquartile range (the dB width on the x axis which corresponds to y=25% and y=75% frequency-of-seeing) (Wall et al 1993; Chauhan et al 1993). The corresponding interquartile range for the Group Mean and for the Group Median curves at each eccentricity for W-W perimetry and for SWAP are given Tables 5.3a and Table 5.3b. For W-W perimetry, Chauhan et al (1993) reported a median interquartile range of 2.9dB (range1.0 to 16.1dB), based upon a cohort of 22 normal individuals (mean age 54.27 years, range 34 to 76 yerars), and a median threshold of 30.2dB (range, 13.3dB to 35.9dB) at 21.2° from the fovea. In the current study, the interquartile range and z_0 value for the Group Mean and for the Group Median FOS curves at the same eccentricity for W-W perimetry were 3.40dB and 28.99dB, and 2.20dB and 29.14dB, respectively. Wall et al (2002) measured FOS curves in 10 normal individuals and also found that the gradient of the FOS curves reduced with increase in eccentricity although this relationship was not quantified. Henson et al (1996) also found that the FOS curve was shallower with reduction in sensitivity.

The interquartile range was substantially greater for SWAP than for W-W perimetry for the Mean FOS curve at all eccentricities, and for the Median FOS curve at three out of the four eccentricities.

Eccentricity	x = 3, y = 9 (9.49° SUP)	x = 9, y =-3 (9.49° INF)	x = 3, y =-15 (15.30° INF)	x = -21, y = 3 (21.21° SUP)
Interquartile Range W-W (dB)	2.50	3.90	3.10	3.40
Interquartile Range SWAP (dB)	5.30	4.30	3.90	6.60

Table 5.3a Table of Results for the Interquartile Range for the Group Mean FOS Curve at each eccentricity.

Eccentricity	x = 3, y = 9 (9.49° SUP)	x = 9, y =-3 (9.49° INF)	x = 3, y =-15 (15.30° INF)	x = -21, y = 3 (21.21° SUP)
Interquartile Range W-W (dB)	0.40	2.31	2.00	2.20
Interquartile Range SWAP (dB)	2.82	3.00	1.80	4.50

Table 5.3b Summary Table of the Interquartile Range for the Group Median FOS Curve at each eccentricity.

In the normal eye, the sensitivity gradient for SWAP is flatter than for W-W perimetry (de Jong et al 1990) and this rate of decline increases with increased eccentricity (Johnson et al 1988b; Sample et al 1997; Wild et al 1997, 1995). Olsson et al (1998) proposed that the increased variability for SWAP at more eccentric locations in the visual field resulted from the flattening of the FOS curve with SWAP. The FOS results obtained from the study described in this Chapter confirm this opinion. The flattening of the FOS curve for both W-W perimetry and SWAP with increase in eccentricity is

consistent with the increase in the between-subject normal variability of the threshold response with increase in eccentricity for W-W perimetry (Katz and Sommer 1986; Brenton and Phelps 1986; Heijl et al 1987a) and for SWAP (Johnson et al 1988b; Sample et al 1997; Wild et al 1995, 1997). The flatter FOS curve for SWAP compared to W-W perimetry is also consistent with the greater between-subject normal variability for SWAP compared to W-W perimetry (Wild et al 1995, 1997). The between-subject normal variability in the threshold estimate at each stimulus location, for the commercially available SWAP with the HFA, is, on average, 2.7 times greater for SWAP than for W-W perimetry. After correction for OMA, the magnitude is reduced to 1.9 times greater (Wild et al 1998). The SF derived in normal individuals by SWAP is larger than for W-W perimetry (Wild et al 1998; Kwon et al 1998). This flatter slope of the FOS curve, and therefore the increased variability, with SWAP could occur due to a number of factors, for example: the increased within- and between- individual intraocular light scatter of the blue stimulus (Moss and Wild 1994), the within- and between-subject variations in OMA (Moss et al 1995) and, for the immediate central regions, the between-individual variations in the density of macular pigment (Wild and Hudson 1995). Various techniques can be used to correct for the absorption by the macular pigment and to correct for OMA (Wild 2001) but they are either not commercially available or not clinically viable.

The increased between-subject normal variability for SWAP results in wider confidence limits for normality compared to W-W perimetry for the HFA Full Threshold and FASTPAC algorithms. The reduction in sensitivity required to indicate abnormality for SWAP is therefore proportionately greater than for W-W perimetry. The inherent variability with SWAP renders it difficult to interpret and implement in a clinical setting.

The SITA algorithms for W-W perimetry utilize information derived from FOS curves in the determination of the threshold estimate. Recently, the SITA technology has been applied to SWAP and has become commercially available for the HFA perimeters. The results from the current study suggest that the new SITA SWAP algorithm will still be

associated with increased variability compared to that derived by SITA Standard and SITA Fast for W-W perimetry and is therefore unlikely to be a success.

The FOS curves derived for each individual demonstrated considerable within- and between-individual variation for both W-W perimetry and for SWAP. In some cases, the FOS data could not be modeled by the psychometric function, indicating the difficulty associated with the measurement of such a function. Such findings are compatible with those of Olsson et al (1992) who concluded that FOS curves in normal individuals, in patients with glaucoma and in patients with cataract, exhibited large variation, both within- and between-individuals.

Surprisingly, the correlation matrices (Tables 5.1a, 5.1b and 5.1c) show that, overall, the magnitude of the correlation coefficients for slope, z_0, and the root mean square error, is higher for SWAP than for W-W perimetry. The reason for this finding is unknown. The correlation matrix for z_0 between stimulus locations for W-W perimetry decrease with increasing eccentricity. This finding would be expected given the increasing variability of the threshold estimate with increase in eccentricity (Lachenmayr et al 1995). It would also be expected from the decreasing correlation with increasing eccentricity reported for the estimate of sensitivity between stimulus locations using the conventional staircase algorithm. Surprisingly, the magnitude of the correlation coefficients for SWAP increased for combinations of locations exhibiting increasing eccentricity. The reason for this is unknown.

The correlation matrix for the slope indicates an increase in magnitude with increasing eccentricity for both W-W perimetry and SWAP although, not all comparisons conform to this trend. The correlation coefficient values for root mean square appear to increase for W-W perimetry with eccentricity, but do not show any relationship between error and eccentricity for SWAP.

The software for the determination of the FOS curve commenced by obtaining the threshold estimate at the designated locations using the standard 4-2dB staircase of the

HFA Full Threshold algorithm. The software then presented stimuli with luminances above and below the threshold estimate as determined by the 4 levels within each custom program. The exact luminances, relative to the threshold estimate, and the number of stimulus presentations at each luminance level are at the discretion of the operator. The FOS software only thresholds the FOS location once and does not take into account the variability in the threshold estimate; consequently, all subsequent stimulus luminance levels are derived relative to this single estimate of threshold. If the initial estimate of threshold is either an overestimate or an underestimate of the 'true' threshold, then all the stimulus presentations used to derive the FOS curve will not be referenced to the 'true' threshold. The influence of the variability in the threshold estimate could be reduced by increasing the number of threshold estimates at the FOS location and by calculating the mean threshold from which all subsequent luminance levels are determined. The magnitude of the variability reduces by the square root of the number of additional threshold estimates (Wild et al 1993).

Another factor that may influence the appearance of some individual FOS curves is the number of luminance levels that the software is able to use in any particular custom program. In the current study, each custom program was repeated twice to provide 8 luminance levels for the derivation of the FOS curve. Due to the variability in the threshold estimate at the FOS location, the subsequent luminance levels intended for the derivation of the FOS curve were not achieved in some instances, as the threshold estimate was different for the first and second repetitions of the custom program. Any given FOS custom program permits 4 luminance levels relative to the initial threshold estimate. If the initial threshold estimate is the same for both custom programs, then eight data points will be used in the derivation of the FOS curve. However, at some levels of sensitivity, more than one data entry occurred and the average of the two values was used as the data point; as a consequence, the resulting FOS curve would only have been derived from 7 data points.

In the current study, five stimulus presentations were undertaken at each luminance level The accuracy of the derived FOS curve could have been improved by a greater number of

stimulus presentations at each luminance level. Indeed, the optimum study design would be that incorporating a greater number of luminance levels and a greater number of stimulus presentations. However, it is necessary to balance the validity of the study design with the practical implications of the duration of each visit. Longer more extensive custom programs might enable the derivation of more accurate FOS curves; however, if the increased duration of the visit induces patient fatigue, with the associated increased variability, there may be little benefit from the longer examination. Lengthy perimetric visits can also be tedious for the given volunteer and can even deter individuals from agreeing to participate in the given study.

5.4.2 Conclusion

In summary, considerable within- and between-subject variation was present in the format of the slope of the FOS curve for both W-W perimetry and SWAP. The slope of the Group Mean FOS curve and of the Group Median FOS curve for both W-W perimetry and SWAP flattened with increase in eccentricity. The slope was flatter for SWAP than for W-W perimetry. These findings largely explain the increased within- and between-subject normal variability which increases with increase in eccentricity and which is greater for SWAP than for W-W perimetry.

5.5 METHODS
5.5.1 Cohort of Patients with Glaucoma
The cohort comprised 9 patients with OAG (6 males and 3 females) recruited from the Glaucoma Clinic at the Cardiff Eye Unit, University Hospital of Wales, Cardiff. The cohort was chosen such that the stratification of individuals to each decade of age was approximately proportionately equivalent to the normal Group. The mean age was 67.1 years (SD 5.8), and the range 58-78 years.

The inclusion criteria for the patients with glaucoma were the same as for the patients described in Chapter 4 and comprised in either eye, a visual acuity of 6/9 or better; distance refractive error of less than or equal to 5 dioptres mean sphere and less than 2.5 dioptres cylinder; lenticular changes not greater than NCIII, NOIII, CI or PI by LOCS III (Chylack et al. 1993); treated IOP's of less than 22mmHg; an optic nerve head appearance characteristic of glaucoma, open anterior chamber angles, no medication known to affect the visual field, no previous ocular surgery or trauma, and no history of diabetes mellitus. An optic nerve head characteristic of glaucoma was defined as one or more of the following: increase in cup size, increase in cup/disc ratio, disc asymmetry, changes in the lamina cribrosa, loss of neuroretinal rim, pallor, evidence of peripapillary atrophy, vessel changes or disc margin haemorrhage.

One eye of each individual was selected for inclusion in the study. Five of the 9 individuals manifested mild visual field loss and 4 moderate loss defined relative to the SITA Standard algorithm Litwak (2001).

5.5.2 Examination Protocol
The individuals attended for four perimetric visits at the Cardiff School of Optometry and Vision Sciences, Cardiff University. The examination protocol was identical to that used for the normal individuals in that each visit consisted of two sessions and each session lasted approximately 30 minutes and was separated by a rest period of 30 minutes.

FOS curves were generated at 4 stimulus locations which varied for each individual depending upon the spatial extent, and depth, of the field loss. The given location either

exhibited apparently normal values of sensitivity within a generally abnormal field, represented varying degrees of eccentricity, or lay on the border of, or was within, a relative focal defect. Three individuals completed the identical stimulus locations as those in the normal Group.

5.5.3 Analysis

The FOS curves were fitted to the W-W perimetry and SWAP data for each patient with OAG. The procedure was identical to that undertaken for each normal individual.

5.6 RESULTS

The FOS curves for W-W perimetry and for SWAP, together with corresponding values for the slope, z_0 and the root means square error, for each of the 9 patients are illustrated in Figures 5.5 to 5.13.

The relationship between z_0 and the slope for W-W perimetry and for SWAP for each of the 9 patients is given in Figures 5.14a, 5.14b and 5.15a and 5.15b.

Patient 1
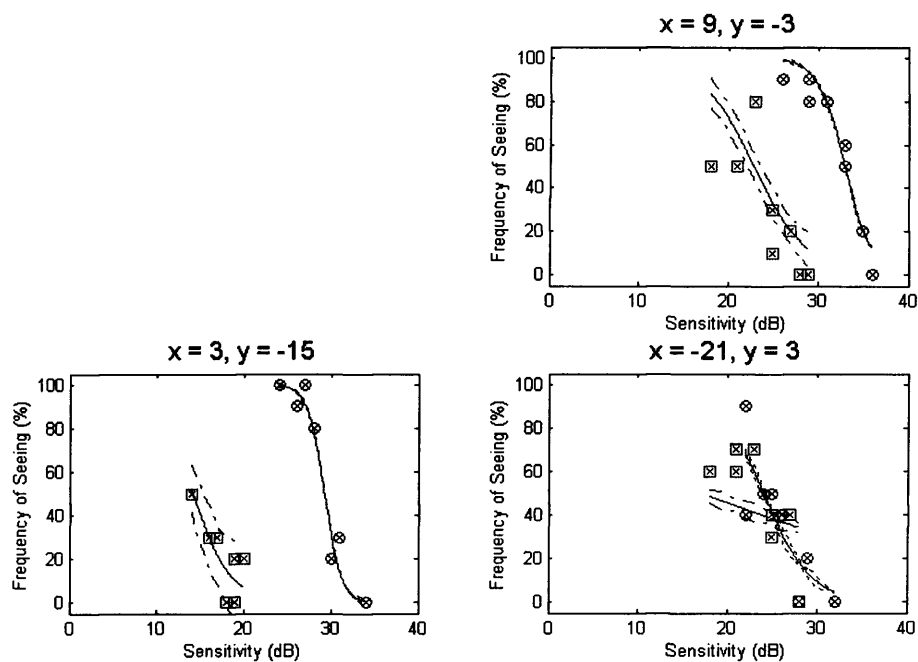
	x = 9, y =-3	x = 3, y =-15	x = -21, y = 3
Slope W-W	0.66	1.02	0.38
Z₀ W-W	33.00	29.27	24.10
Error W-W	22.81	22.64	42.61
Slope SWAP	0.33	0.45	0.06
Z₀ SWAP	22.81	14.2	17.10
Error SWAP	56.91	26.00	56.00

Figure 5.5 Top: The FOS curves for W-W perimetry (circles) and for SWAP (squares) at each of three eccentricities for Patient 1. Bottom: the corresponding Table of Values giving the magnitude of the slope, z_0 and root mean square error for each type of perimetry. The dotted lines either side of each FOS curve represent the standard deviation.

219

Patient 2

Figure 5.6 Top: The FOS curves for W-W perimetry (circles) and for SWAP (squares) at each of four eccentricities for Patient 2. Bottom: the corresponding Table of Values giving the magnitude of the slope, z_0 and root mean square error for each type of perimetry. The dotted lines either side of each FOS curve represent the standard deviation.

	x = 3, y = 9	x = 9, y =-3	x = 3, y =-15	x = -21, y = 3
Slope W-W	1.00	1.18	1.49	0.30
Zo W-W	24.33	26.51	25.91	2.30
Error W-W	12.27	27.92	10.40	55.73
Slope SWAP	0.52	0.65	1.05	0.46
Zo SWAP	24.54	28.90	27.10	16.90
Error SWAP	60.59	62.12	18.95	22.02

Patient 3

	x = 3, y = 9	x = 9, y =-3	x = 3, y =-15	x = -15, y = 9
Slope W-W	0.65	0.59	0.68	0.62
Zo W-W	29.00	31.10	31.20	22.57
Error W-W	34.47	44.07	33.56	44.81
Slope SWAP	0.44	0.38	0.80	0.43
Zo SWAP	29.78	29.81	30.10	20.42
Error SWAP	40.28	54.63	20.00	31.71

Figure 5.7 Top: The FOS curves for W-W perimetry (circles) and for SWAP (squares) at each of four eccentricities for Patient 3. Bottom: the corresponding Table of Values giving the magnitude of the slope, z_0 and root mean square error for each type of perimetry. The dotted lines either side of each FOS curve represent the standard deviation.

Patient 4

Figure 5.8 Top: The FOS curves for W-W perimetry (circles) and for SWAP (squares) at each of four eccentricities for Patient 4. Bottom: the corresponding Table of Values giving the magnitude of the slope, z_0 and root mean square error for each type of perimetry. The dotted lines either side of each FOS curve represent the standard deviation.
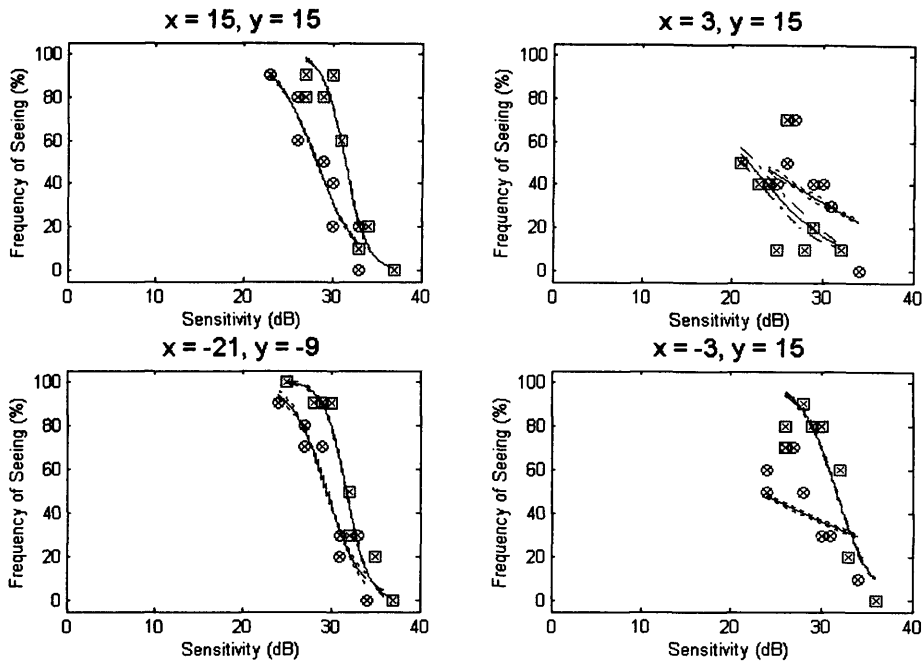
	x = 15, y = 15	x = 3, y = 15	x = -21, y = -9	x = -3, y = 15
Slope W-W	0.80	0.11	0.50	0.08
Zo W-W	31.45	23.10	29.52	23.10
Error W-W	28.81	41.37	27.25	45.98
Slope SWAP	0.11	0.20	0.80	0.52
Zo SWAP	23.10	21.90	31.72	31.69
Error SWAP	41.37	48.84	23.38	37.74

Patient 5

Figure 5.9 Top: The FOS curves for W-W perimetry (circles) and for SWAP (squares) at each of four eccentricities for Patient 5. Bottom: the corresponding Table of Values giving the magnitude of the slope, z_0 and root mean square error for each type of perimetry. The dotted lines either side of each FOS curve represent the standard deviation.

	x = 9, y = 9	x = 15, y = -15	x = -15, y = 9	x = -9, y = 9
Slope W-W	1.64	0.44	0.28	0.81
Zo W-W	31.36	28.12	28.20	29.21
Error W-W	20.08	36.20	54.24	23.35
Slope SWAP	0.64	0.40	3.26	0.09
Zo SWAP	27.42	25.48	7.90	23.10
Error SWAP	20.83	34.33	27.80	67.18

223

Patient 6

	x = -21, y = -9	x = 3, y = 9	x = -9, y =-15	x = 9, y = 3
Slope W-W	0.52	0.53	1.54	0.16
Zo W-W	32.55	28.12	31.46	9.60
Error W-W	33.85	45.57	10.47	36.73
Slope SWAP	0.69	0.08	7.70	1.10
Zo SWAP	31.97	17.10	28.82	5.60
Error SWAP	25.89	49.81	14.14	10.72

Figure 5.10 Top: The FOS curves for W-W perimetry (circles) and for SWAP (squares) at each of four eccentricities for Patient 6. Bottom: the corresponding Table of Values giving the magnitude of the slope, z_0 and root mean square error for each type of perimetry. The dotted lines either side of each FOS curve represent the standard deviation.

224

Patient 7

Figure 5.11 Top: The FOS curves for W-W perimetry (circles) and for SWAP (squares) at each of four eccentricities for Patient 7. Bottom: the corresponding Table of Values giving the magnitude of the slope, z_0 and root mean square error for each type of perimetry. The dotted lines either side of each FOS curve represent the standard deviation.

	x = 3, y = 9	x = -27, y =-3	x = -15, y =-15	x = -3, y = 9
Slope W-W	0.35	0.66	0.89	0.36
Zo W-W	18.30	30.84	27.60	28.10
Error W-W	27.79	22.24	28.82	31.95
Slope SWAP	1.11	0.48	0.75	0.81
Zo SWAP	8.02	35.85	29.67	33.36
Error SWAP	18.90	25.20	25.57	34.51

225

Patient 8

Figure 5.12 Top: The FOS curves for W-W perimetry (circles) and for SWAP (squares) at each of four eccentricities for Patient 8. Bottom: the corresponding Table of Values giving the magnitude of the slope, z_0 and root mean square error for each type of perimetry. The dotted lines either side of each FOS curve represent the standard deviation.
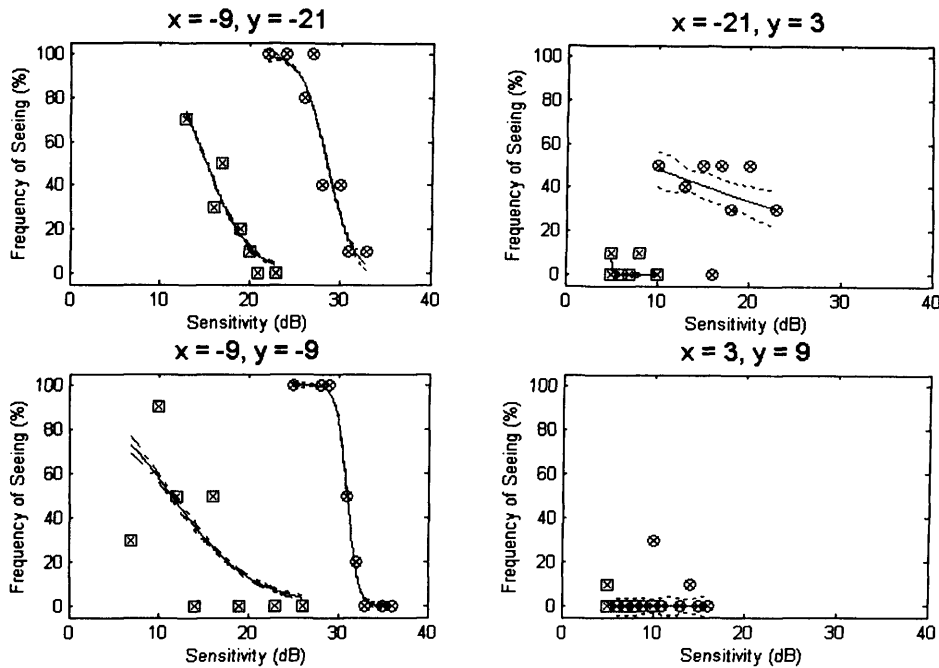
	x = -9, y = -21	x = -21, y = 3	x = -9, y =-9	x = 3, y = 9
Slope W-W	0.71	0.06	1.67	7.99
Zo W-W	28.60	8.90	31.04	4.90
Error W-W	36.01	45.88	6.11	31.62
Slope SWAP	0.42	6.28	0.22	6.66
Zo SWAP	15.30	4.60	11.50	4.45
Error SWAP	23.88	13.23	71.10	8.66

Patient 9
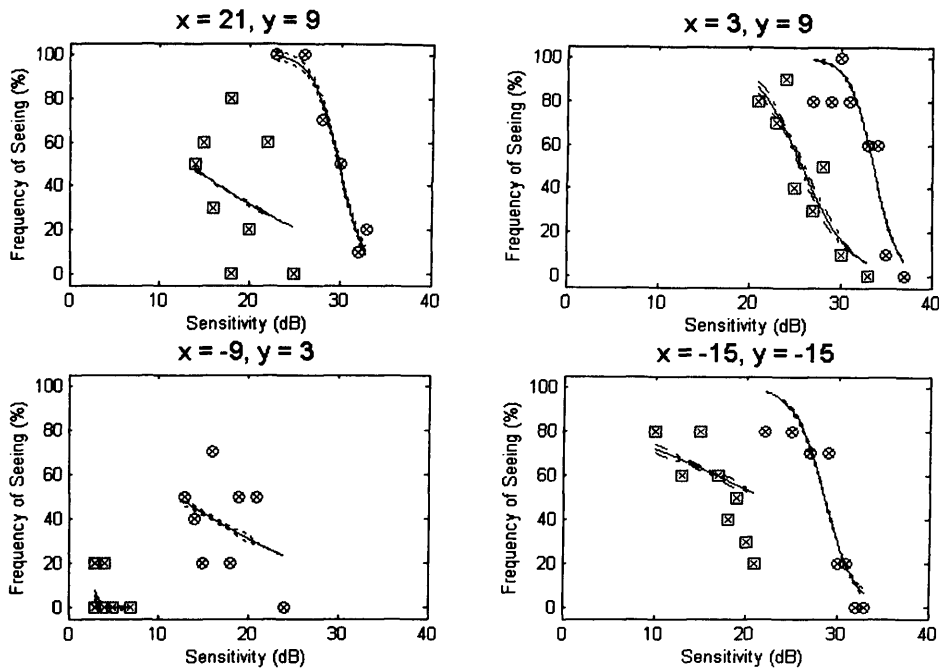
	x = 21, y = 9	x = 3, y = 9	x = -9, y =-3	x =-15, y =-15
Slope W-W	0.70	0.75	0.10	0.60
Zo W-W	29.87	33.60	12.10	28.60
Error W-W	18.28	36.97	54.14	37.18
Slope SWAP	0.11	0.38	2.53	0.08
Zo SWAP	13.10	25.82	1.90	21.90
Error SWAP	72.57	38.33	26.15	48.07

Figure 5.13 Top: The FOS curves for W-W perimetry (circles) and for SWAP (squares) at each of four eccentricities for Patient 9. Bottom: the corresponding Table of Values giving the magnitude of the slope, z_0 and root mean square error for each type of perimetry. The dotted lines either side of each FOS curve represent the standard deviation.
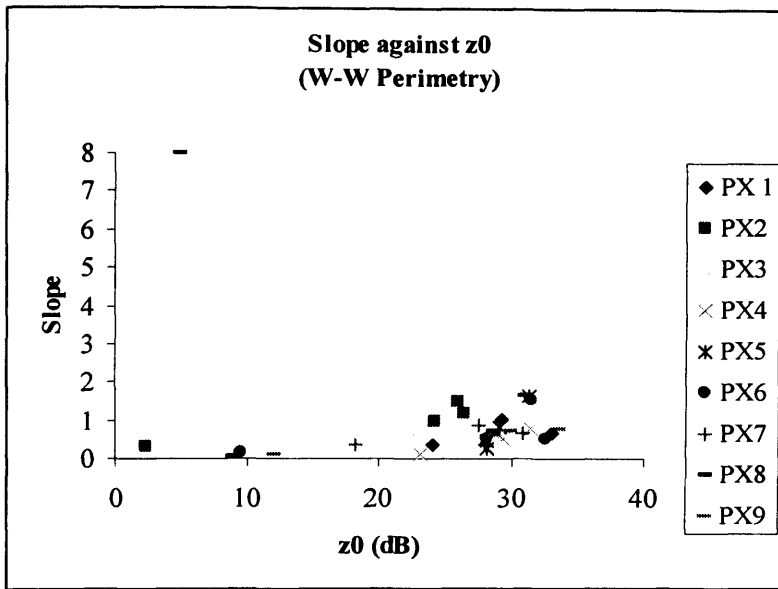
Figure 5.14a The slope of the FOS curve for W-W perimetry against z_0 for each location measured for each of the 9 patients with OAG.
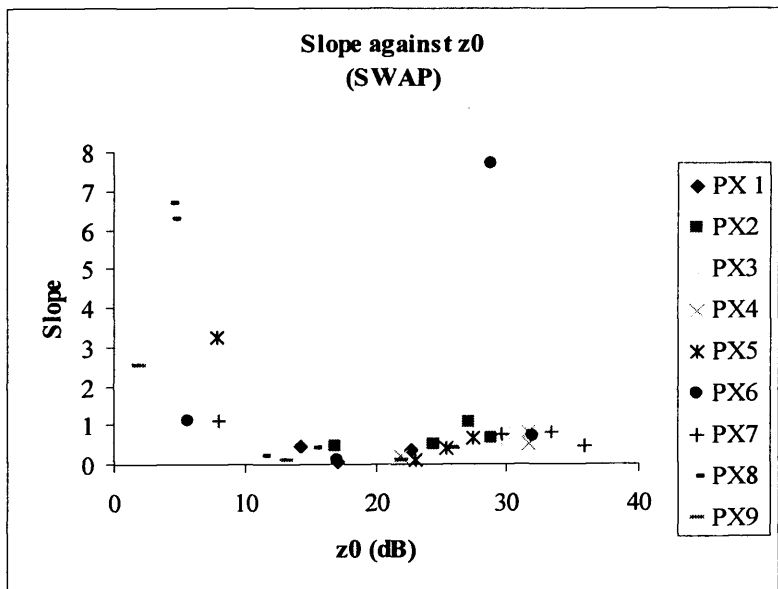
Figure 5.14b The slope of the FOS curve for SWAP against z_0 for each location measured for each of the 9 patients with OAG.

228
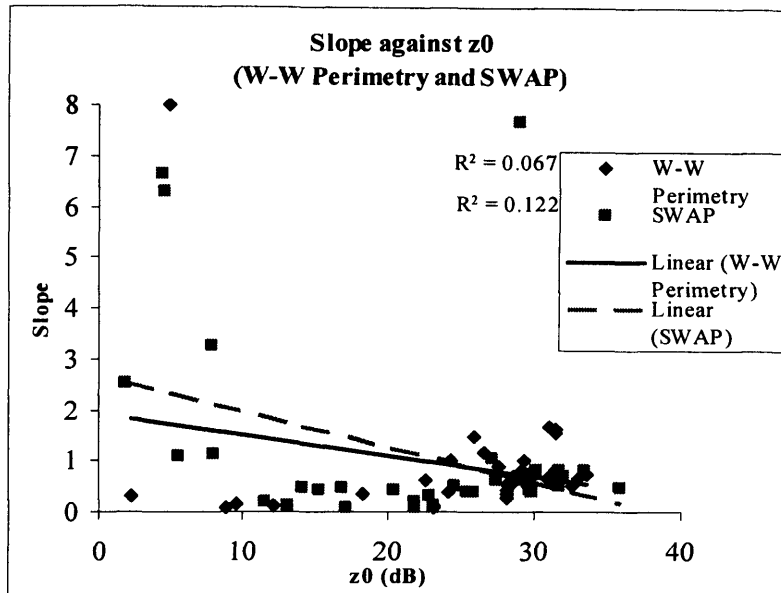
Figure 5.15 The slope of the FOS curve against z_0 for W-W perimetry and for SWAP for each location measured for each of the 9 patients with OAG.
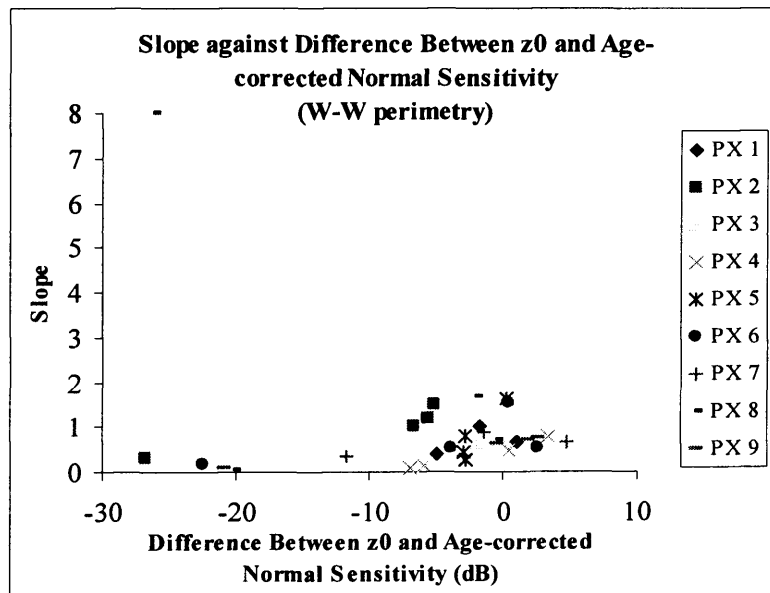
Figure 5.16a The slope of the FOS curve for W-W perimetry against z_0 minus the age-corrected normal sensitivity for each location measured for each of the 9 patients with OAG.
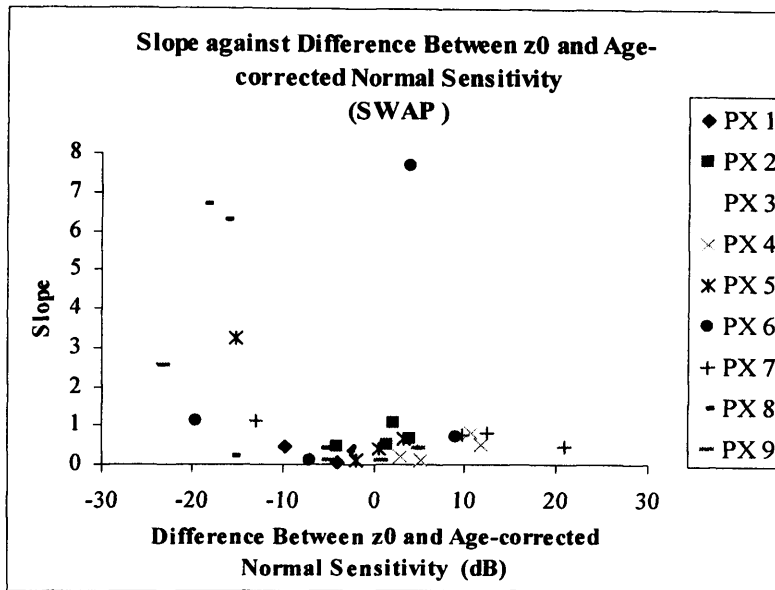
Figure 5.16b The slope of the FOS curve for SWAP against z_0 minus the age-corrected normal sensitivity for each location measured for each of the 9 patients with OAG.

5.6.1 Discussion

The comparison of the FOS curves for W-W perimetry and for SWAP at each of the four eccentricities for each of the nine patients makes compelling reading. At locations exhibiting normal, or near normal, levels of sensitivity, the FOS curves were, in general, flatter for SWAP than for W-W perimetry. The lack of dynamic range for SWAP was also evident in that the FOS curves for SWAP are to the left of those for W-W perimetry. Of particular interest was the apparent loss of shape of the characteristic FOS curve at locations exhibiting mild reductions of sensitivity for SWAP (e.g. Patient 1, x=-21, y=3; Patient 5, x=-9, y=9 and x=-15, y=9; Patient 6, x=3, y=9 etc) or for both types of perimetry at locations exhibiting more profound defect depths (Patient 4, x=3, y=15; Patient 8, x=-21, y=3; Patient 9, x=-9, y=3). Some normal individuals also lacked the consistency in response necessary to derive the FOS curve either for W-W perimetry or for SWAP, or for both, at one or more given locations. In such cases, the FOS curves also failed to conform to the well-accepted shape of the psychometric function. Such difficulty highlights the problem associated with the subjective nature of perimetry.

230

The correlation coefficient between the slope of the FOS curve and the magnitude of z_0 for W-W perimetry (r=-0.26) is in accord with the correlation between the interquartile range and the magnitude of z_0 for W-W perimetry reported by Chauhan et al (1993). They found values of r=-0.71 for normal individuals, r=-0.32 for patients with suspected glaucoma and r=-0.37 for patients with glaucoma. The correlation coefficient of r=-0.35 for SWAP in the current study is also compatible with these values. The magnitude of a correlation coefficient is dependent upon the range of values used for each of the two variables, can be heavily influenced by the presence of outliers and also decreases as a function of the number of data points. The graph illustrated in Figure 5.15 contains at least three outlying values for SWAP and one for W-W perimetry. Two of the three outlying values for SWAP were from one patient (Patient 8) and were associated with z_0 values of 4.6dB and 4.5dB respectively. One of the values corresponded with the outlying value for W-W perimetry. Numerous such outlying values are present in the plot of Chauhan and colleagues for the interquartile range against the threshold in patients with glaucoma. Olsson and colleagues reported a negative correlation between the slope of the FOS curve for W-W and the deviation of the magnitude of z_0 from the age corrected normal value at the given location. The magnitude of the coefficient was not stated although it was highly significantly different from zero. The corresponding correlations in the current study were r=-0.28 for W-W perimetry and r=-0.36 for SWAP (Figures 5.16a and 5.16b). The latter correlations are almost identical to those reported for the slope against z_0 and would be expected given the narrow range of ages within the current study.

The FOS curves based upon the Group Mean and Median responses, as adopted for the normal individuals, were not appropriate for the patients with OAG due to the varying extents and depths of field loss across the patients.

The choice of stimulus locations for the derivation of the relationship between the magnitude of the slope and the level of sensitivity for both W-W perimetry and SWAP was based upon a representative range of varying eccentricities and defect depths. An alternative approach could have compared, between-patients or between the patients and

the normal individuals, the characteristics of the FOS curves at locations exhibiting identical levels of sensitivity. However, such a task would have been difficult due to the inherent variability associated with the threshold estimate.

5.6.2 Conclusion

The FOS curves for SWAP are flatter than those for W-W perimetry both in normal individuals and in patients with OAG. The flatter FOS curve for SWAP explains the increased short and long-term fluctuation and the increased between-subject normal variability for SWAP compared to W-W perimetry. Such increased variability limits the clinical utility of SWAP.

CHAPTER 6

The Influence of Fatigue on the Prevalence of False-negative Responses in Perimetry

6.1 INTRODUCTION
6.1.1 The Fatigue Effect in Perimetry

The fatigue effect describes the reduction in sensitivity, and the increased variability of the threshold estimate, for W-W perimetry which occurs with increasing examination duration (Heijl and Drance 1983; Hudson et al 1994). The fatigue effect has been noted in normal individuals (Heijl 1977b; Johnson et al 1988b; Searle et al 1991; Fujimoto and Adachi-Usami 1993; Hudson et al 1994); in patients with ocular hypertension (Langerhost et al 1987; Wild et al 1991; Hudson et al 1994); in patients with open angle glaucoma (Heijl 1977b; Heijl and Drance 1983, Johnson et al 1988b); and in neuro-ophthalmological disorders (Fujimoto and Adachi-Usami 1993; Keltner and Johnson 1995).

The fatigue effect opposes the learning effect. The learning effect is the term given to the apparent increase in sensitivity with increased experience and familiarity of the perimetric examination (Wood et al 1987; Heijl et al 1989; Searle et al 1991). The learning effect can be dominant over the first five visual field examinations. As the learning effect declines, the influence of the fatigue effect becomes more apparent (Wild et al 1991; Searle et al 1991; Hudson et al 1994).

The fatigue effect occurs within the examination of a given eye (Heijl and Drance 1983; Hudson et al 1994) and is present between eyes of the same subject at a single examination (Searle et al 1991; Wild et al 1991; Hudson et al 1994). As a consequence, the order in which the eyes are tested during any visual field examination needs to be taken into account when interpreting the resultant data collected (Searle et al. 1991).

The reduction in sensitivity resulting from the fatigue effect, increases as a function of the examination duration (Heijl 1977b; Heijl and Drance 1983; Johnson et al 1988b;

Searle et al 1991; Hudson et al 1994; Marra and Flammer 1991); increases with the age of the individual (Langerhorst et al 1987; Hudson et al 1994); is greater for the second eye examined (Searle et al 1991; Olsson and Asman 1997; Hudson et al 1994); is more pronounced in more eccentric locations (Johnson et al 1988a; Hudson et al 1994), particularly for glaucoma patients (Johnson et al 1988a); and is greater in areas adjacent to, and within, focal loss (Holmin 1979; Suzamura 1988; Heijl and Drance 1983).

An extreme manifestation of the fatigue effect is the 'clover-leaf' field. The central stimulus locations show normal sensitivity; however, the more peripheral locations, which are thresholded later in the examination, exhibit an apparent depressed sensitivity. The resultant grayscale printout exhibits a distinctive cloverleaf pattern (Anderson and Patella 1999).

In the normal eye, the fatigue effect within an examination may cause a general reduction in sensitivity of between 1dB (Johnson et al 1988a) and 2.5 dB (Hudson et al 1994). In patients with ocular hypertension, the reduction in sensitivity is, on average, 2.2dB (Hudson et al 1994) whilst in patients with OAG, it is approximately 3dB (Johnson et al 1988a). As the examination duration increases, the Loss Variance increases and this increase is greater for normal individuals than for patients with ocular-hypertension (Hudson et al 1994). The superior visual field exhibits a greater decline in sensitivity (Searle et al 1991) and a greater increase in the Loss Variance (Hudson et al 1994), compared to the inferior visual field. A decline in sensitivity at the more peripheral eccentricities but the absence of an overall fatigue effect was found by Marra and Flammer (1991).

The magnitude of the fatigue effect is unaffected by changes in background luminance between 0.1cdm^{-2} and 101cdm^{-2} (Heijl and Drance 1983). However, the magnitude is less for a stimulus duration of 100ms compared to a duration of 200ms (Searle et al 1991).

Some authors (Heijl 1977b; Heijl and Drance 1983) have suggested that perimetric fatigue could, in itself, be used as a provocative test for glaucomatous field loss due to the

fact that the fatigue effect is greater at stimulus locations adjacent to and within, areas of focal loss. However, normal individuals, patients with ocular-hypertension and patients with glaucoma demonstrate a considerable overlap in the magnitude of the fatigue effect (Langerhorst et al 1987).

The fatigue effect can be reduced by rest periods within an examination at a single visit (Johnson et al 1988a) and/or by utilising shorter thresholding algorithms such as the SITA algorithms (Bengtsson et al 1997b; Wild et al 1999). Hudson et al (1994) found that a three-minute rest period between the eyes was insufficient to overcome the fatigue effect in the second eye.

6.1.2 The Mechanism for the Fatigue Effect

The precise mechanism of the perimetric fatigue effect is unknown. It has been proposed that the Troxler phenomenon leading to Ganzfeld Blankout and psychological influences may be contributing factors.

6.1.2.1 The Troxler Phenomenon and Ganzfeld Effects

The Troxler Phenomenon is the term given to the fading of a stabilized retinal image which is reversed immediately following an eye movement (Riggs et al 1953; Davson 1990; Steinman and Levinson 1990). The reduction or cessation of eye movements during a perimetric examination results in a stabilized retinal image. Patients have described this effect as a 'smudging' of the contours of the stimulus, followed by an apparent reduction in brightness and chromatic saturation and, finally, a fading of the image. This fading and accompanied reduction in subjective brightness continues to become more apparent for several minutes (Gerrits et al 1966).

The Troxler effect in conjunction with the uniform illumination of the perimeter bowl are thought to be major contributers to Ganzfeld Blankout (Bolanowski and Doty 1987; Gur 1989, 1991) and this, in turn, is thought to be a principle cause of perimetric fatigue (Searle et al 1991; Hudson et al 1994). There are two Ganzfeld Effects. Ganzfeld

Blankout describes the instance where the whole visual field briefly appears black and has been shown to arise only with monocular viewing when there is a differential retinal luminance between the eyes of a at least 0.75 log units (Bolanowski and Doty; Gur 1991) Ganzfeld Fade Out is when the evenly illuminated background gradually changes in brightness, hue and saturation (Gur 1991). It is more prevalent for backgrounds of greater wavelengths (Gur 1989) and can occur in the binocularly observed visual field (Gur 1991). Ganzfeld Blankout can be delayed by the use of a translucent occluder to enable the occluded eye to obtain a degree of low level luminance stimulation which in turn can aid a reduction in the fatigue effect (Fuhr et al 1990).

Some explanations of the probable causative factors of these visual effects have been proposed. The increase in size of the receptive fields of cortical cells when the eye is presented with a continuous image may account for the fading images reported during the fatigue effect (Campbell and Andrews 1992). The activation of dendrites that are usually dormant may result in this physiological change.

6.1.2.2 Psychological Factors that can Influence the Fatigue Effect

It is probable that psychological, as well as the physical factors already discussed, may influence perimetric fatigue. Perimetry requires maintained attention from the subject. Such tasks are termed vigilance tasks. There are several factors that can influence performance during a vigilance task (Stroh 1971; Warm 1984); however, much on this matter is not fully understood (Mackworth 1969). The 'vigilance decrement' is the term given to the decline in performance that can occur during tasks requiring a high degree of concentration and is correlated with the duration of the task in question (Stroh 1971; Warm 1984). Other factors that can increase the vigilance decrement are: the position of the stimuli relative to threshold; the temporal frequency of the stimulus presentation; spatial uncertainty; and the addition of non-signal stimuli.

At least 50% of the decline in the vigilance decrement occurs in the first 15 minutes of the examination (Teichner 1974). The magnitude of the vigilance decrement increases

with the approach of the stimulus to threshold (Warm 1984). Introducing short rest breaks, or interacting with the subject, will increase the temporal frequency of stimulus presentations and can reduce the vigilance decrement (Stroh 1971). Spatial uncertainty is the phenomenon whereby observers bias their responses towards the spatial location which has a greater proportion of signals (Niceley and Miller 1957; Milosevic 1974; Cohn and Wardlaw 1985; Lindblom and Westheimer 1992). This phenomenon can be minimised by the use of cues prior to stimulus presentation to indicate the position of the next stimulus (Hubner 1996), a method not plausible in perimetry. Non-signal stimuli (stimuli not requiring the subject to respond) are best avoided in vigilance tasks as they result in an increase in the vigilance decrement which is in proportion to the rate of presentation of the non-signal stimuli (Jerrison and Pickett 1964).

6.1.3 False-negative (FN) Catch Trials

As was discussed in Chapter 1, FN catch trials are presented throughout the visual field examination as a means of determining the level of compliance. With the HFA, FN catch trial stimuli are presented at 9dB brighter than the measured sensitivity at the given location. The false-negative catch trial stimuli account for approximately 3% of the total number of stimulus presentations during the examination with the HFA Full Threshold and Fastpac algorithms (Anderson and Patella 1999). The examination of the visual field is deemed to be unreliable in the presence of 33% or more incorrect responses to the FN catch trials.

6.1.3.1 FN Catch Trials and the Variability in the Estimate of the Threshold Response.

As was discussed in Chapter 1, patients with OAG, exhibit increased variability in the threshold estimate within- and between-examinations compared to normal individuals (Flammer et al 1984, Heijl 1989; Werner 1989; Boeglin 1992; Bengtsson and Heijl 2000). The variability at a given stimulus location is a minimum at normal, and near normal, levels of sensitivity, increases to a maximum for defect depths in the region of

-8dB to -18dB after which the variability decreases as the sensitivity approaches absolute loss (Heijl et al 1989).

The magnitude of incorrect responses to the FN catch trials is loosely correlated with severity of the field loss (Bengtsson and Heijl 2000). The FN catch trials are performed randomly within each block of 33 stimulus presentations but may be omitted in the earlier blocks of 33 stimulus presentations if a threshold value has not been determined (Anderson and Patella 1999). If the variability in response at any given location at which the FN catch trial is presented lies, at any given moment, outside the 9dB increment used for the catch trial, then the patient will register a 'seen' response to the catch trial. Thus, an incorrect response to the FN catch trial can arise not only from a lack of attention and vigilance but also from increased variability.

6.2 AIMS

The fatigue effect leads to a reduction in sensitivity at a given location and an associated increase in variability. It can therefore be hypothesized that a reduction in the fatigue effect might reduce the number of those incorrect responses to the FN catch trials which arise from a large variability in the threshold response. The aim of the study, therefore, was to determine whether the introduction of rest periods during the visual field examination of patients with OAG would reduce the rate of incorrect responses to the FN catch trials.

6.3 METHODS

6.3.1 Cohort

The cohort comprised 18 (11 males and 7 females) patients with open angle glaucoma recruited from the Glaucoma Clinic at the Cardiff Eye Unit, University Hospital of Wales, Cardiff. The mean age for the Group was 69.17 years (SD 8.14) and the range 56 to 77 years (Table 6.1 below).

238

Age (years)	Number of Patients
50-59	4
60-69	4
70-79	9
80+	1

Table 6.1 The age distribution within the Group

The diagnosis of OAG was provided by Mr James Morgan, Reader and Honorary Consultant Ophthalmologist, University Hospital of Wales, Cardiff. The inclusion criteria was as that described in Chapter 4 and Chapter 5 and comprised a distance visual acuity of 6/9 or better in either eye; distance refractive error of less than or equal to 5 dioptres mean sphere and less than 2.5 dioptres cylinder; lenticular changes not greater than NCIII, NOIII, CI or PI by LOCS III (Chylack et al 1993); no medication known to affect the visual field; no history of diabetes mellitus; a pre-therapy IOP consistently above 21mmHg; and an optic nerve head characteristic of OAG including increase in cup size, increase in cup/disc ratio, disc asymmetry, changes in the lamina cribrosa, loss of neuroretinal rim, pallor, evidence of peripapillary atrophy, vessel changes or disc margin haemorrhage.

Twelve of the eighteen patients with OAG were undergoing therapy for IOP reduction during their participation in the study. Three of the 12 patients received a single topical agent Latanoprost (prostaglandin analogue); one patient received the single agent Dorzolamide hydrochloride (Trusopt) and Timolol maleate combined (Cosopt); one patient received Carteolol hydrochloride (Teoptic); three patients received Latanoprost and Dorzolamide hydrochloride; two patients received the combined therapy of Latanoprost and Cosopt; and one patient received Latanoprost and Alphagan. No patients were on systemic carbonic anhydrase inhibitors. There was no change in the patients' therapy six weeks prior to, or during, the course of the study. Two of the patients had undergone previous bilateral trabeculectomies and six of the patients had

undergone a unilateral trabeculectomy. Four of the patients had undergone a previous trabeculectomy in the eye selected for the study.

6.3.2 Examination Protocol

The study comprised a two period cross-over design with order randomization between sessions. The patients attended for one visual field visit consisting of two sessions. Perimetry was undertaken on one randomly selected eye of each individual, using the HFA 740 perimeter. One session lasted approximately 18 minutes and the other session lasted approximately 22 minutes. The two sessions were separated by a rest period of 20 minutes. At one session, the visual field examination was undertaken using Program 30-2 and the Full Threshold algorithm without any rest periods for the patient (designated as the 'No-rest Session'). At the other session, the patient underwent the same visual field examination but was given regular rest breaks of 30 seconds duration at intervals of 2 minutes throughout the examination (designated as the 'Rest Session').

The appropriate refractive correction for the viewing distance of the bowl of each perimeter was used for the designated eye of each patient and the non-tested eye was occluded with an opaque patch. Fixation was monitored continuously using the video monitor of each perimeter, the gaze tracker and the standard Heijl-Krakau technique of the HFA.

The time to each incorrect response to the FN catch trial presentations was manually recorded by the perimetrist throughout the examination of each patient using a stopwatch.

The examination duration was converted from the minutes and seconds format of the HFA printout into decimal format.

6.3.3 Analysis

A graphical approach was adopted towards the analysis. The data were considered in four separate ways. Firstly, for each session, the number of incorrect responses to the FN catch trials was plotted against the number of FN catch trials for each session. Secondly, for each session, the percentage of incorrect responses to the FN catch trials was plotted against the ranked order of the severity of the visual field loss (in terms of the classification of Hodapp et al) and also against the MD. The final analysis determined any relationship between the difference in the number of incorrect responses to the false-negative catch trials between the sessions against the mean MD for the two sessions.

6.4 RESULTS
6.4.1 Severity of Field Loss

The severity of visual field loss was classified after Hodapp et al (1993) (described in Chapter 1) in terms of the visual field derived at the No-rest session. The cohort consisted of 5 patients with early visual field loss; 8 patients with moderate visual field loss and 5 patients with severe visual field loss.

6.4.2 Group Mean Examination Duration

The Group Mean examination duration for each Session and for the two Sessions, combined, is shown in Table 6.2. The Group Mean examination duration was not significantly different between the two sessions (p=0.728).

	No-rest Session	Rest Session	Mean for No-rest and Rest Sessions Combined
Group Mean Examination Duration (Mins) (SD)	17.28 (2.03)	17.17 (1.22)	17.22 (1.52)

Table 6.2 The Group Mean examination duration for each Session and the Group Mean examination duration for both Sessions combined.

6.4.3 Group Mean MD and Group Mean number of Incorrect responses to the FN Catch Trials

The Group Mean MD for each session and for the two sessions, combined, is shown in Table 6.3. The Group Mean MD was more negative (i.e. for the No-rest session by 1.08dB ($p<0.012$). The Group Mean SF was similar between the two sessions ($p=0.631$). The Group Mean number of incorrect responses to the FN catch trials (Table 6.3) was similar between the two sessions ($p=0.819$). The Group Mean number of incorrect responses to the False-positive (FP) catch trials (Table 6.3) and to the fixation loss (FL) catch-trials were each similar between the two sessions ($p=0.850$), and $p=0.573$) respectively). No patient exhibited more than 0.11% incorrect responses to the False-positive catch trials and 0.13% to the Fixation Loss catch trials.

	No-rest Session	Rest Session	Mean for No-rest and Rest Sessions Combined
Group Mean MD (SD; range) (dB)	-7.21 (3.76; -0.53 to -14.87)	-6.13 (3.17; -1.57 to -14.24)	-6.67 (3.38; -1.05 to -14.55)
Group Mean SF (SD; range) (dB)	2.57 (1.20; 0.88 to 4.97)	2.43 (0.74; 1.42 to 4.09)	2.50 (0.77; 1.37 to 3.61)
Group Mean Incorrect Responses to the FN catch trials (%) (SD; range) (dB)	11.54 (10.99; 0 to 27.78)	12.24 (9.38; 0 to 23.53)	11.89 (8.01; 0 to 23.38)
Group Mean Incorrect Responses to the FP catch trials (%) (SD; range) (dB)	0.01 (0.03; 0 to 0.09)	0.01 (0.03; 0 to 0.11)	0.01 (0.03; 0 to 0.07)
Group Mean Fixation Losses (%) (SD; range) (dB)	0.03 (0.03; 0 to 0.08)	0.03 (0.04; 0 to 0.15)	0.03 (0.03; 0 to 0.06)

Table 6.3 The Group Mean, SD and range of the MD, the SF, the percentage of incorrect responses to the FN catch trials, the percentage of incorrect responses to the FP catch trials, and the percentage of incorrect responses to the FL catch trials at each session and the corresponding statistics for both sessions combined.

6.4.4 The Number of Incorrect Responses to the FN Catch Trials Relative to the Number of FN Catch Trials

The number of incorrect responses to the FN catch trials against the number of FN catch trials for each session is shown in Figure 6.1.
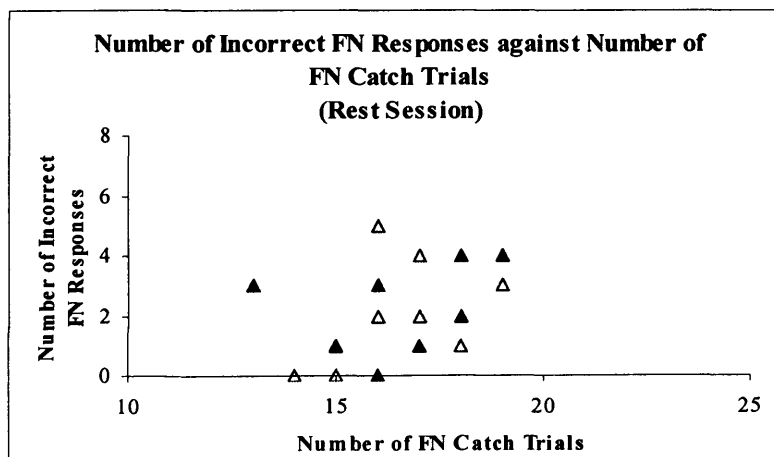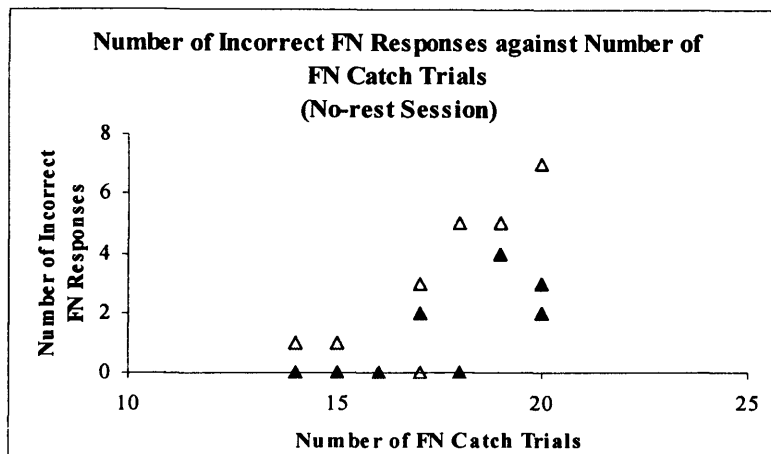
Figure 6.1 The number of incorrect responses to the FN catch trials against the number of FN catch trials for each session. Top: No-rest Session. Bottom: Rest Session followed by No-rest Session. Open symbols: Rest Session followed by No-Rest Session. Closed symbols: No-rest Session followed by Rest Session.

6.4.5 Percentage of Incorrect Responses to the FN Catch Trials as a Function of the Severity of Field Loss

The percentage of incorrect responses to the FN catch trials against the severity of the field loss, ranked in order of increasing severity, for each session is shown in Figure 6.2.
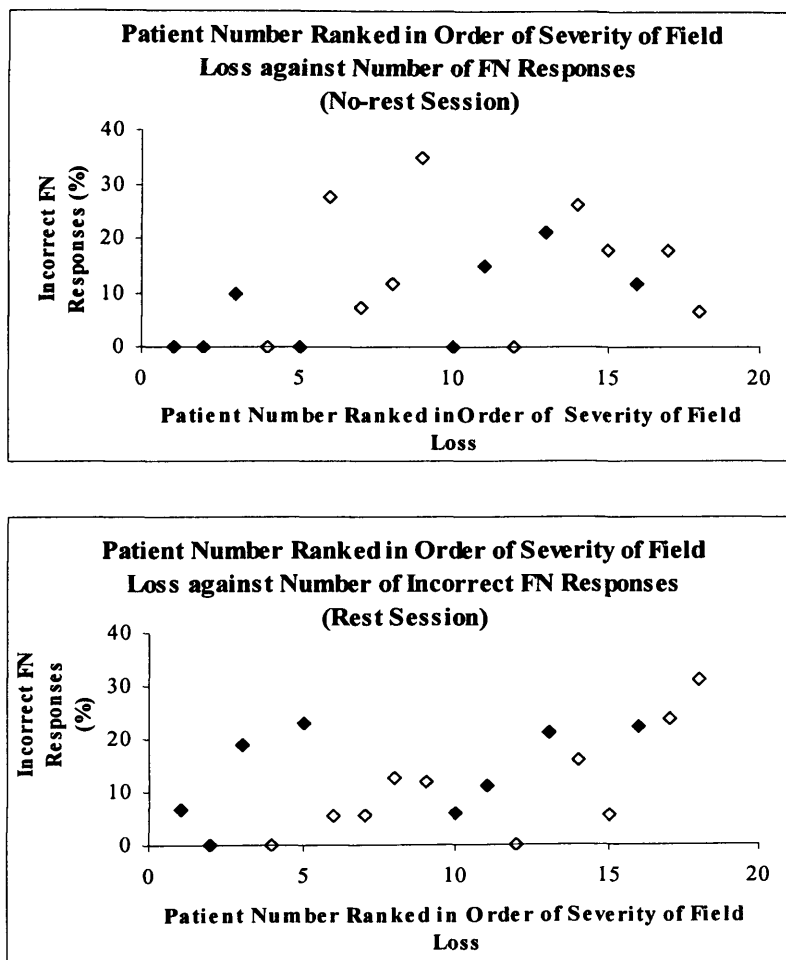
Figure 6.2 The percentage of incorrect responses to the FN catch trials against the patient number (after Hoddapp et al 1993), ranked in order of increasing severity of field loss. Top: No-rest Session. Bottom: Rest Session. Open symbols: Rest Session followed by No-rest Session. Closed symbols: No-rest Session followed by Rest Session.

6.4.6 The Relationship Between the MD and the Number of Incorrect Responses to the FN Catch Trials

The MD for each of the 18 patients against the number of incorrect responses to the FN catch trials for the No-rest Session, the Rest Session and the two sessions, combined, is shown in Figure 6.3.

The correlation coefficient was 0.44 for the No-rest Session, 0.24 for the Rest Session and 0.48 for both Sessions combined.
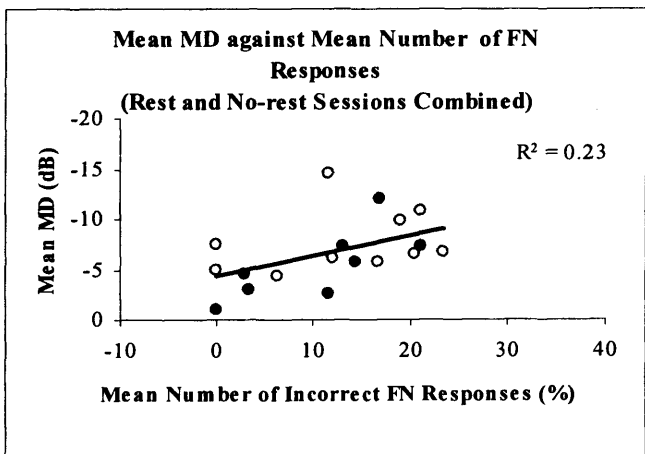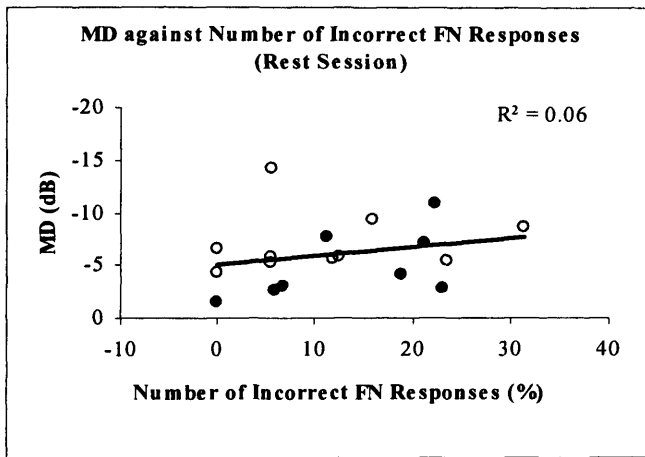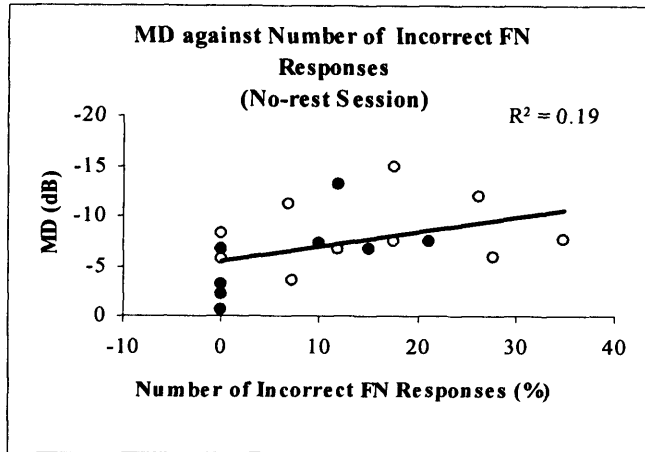
Figure 6.3 The MD for each of the 18 patients against the number of incorrect responses to the FN Catch Trials. Top: No-rest Session, Middle: Rest Session. Bottom: The two Sessions combined. Open symbols: Rest Session followed by No-rest Session. Closed symbols: No-rest Session followed by Rest Session.

6.4.7 The Difference in the Percentage of Incorrect Responses to the FN Catch Trials Between the two Sessions as a Function of the Severity of Field Loss

The difference in the percentage of incorrect responses to the FN catch trials between the

two sessions against the severity of the field loss, ranked in order of increasing severity,

is shown in Figure 6.4.
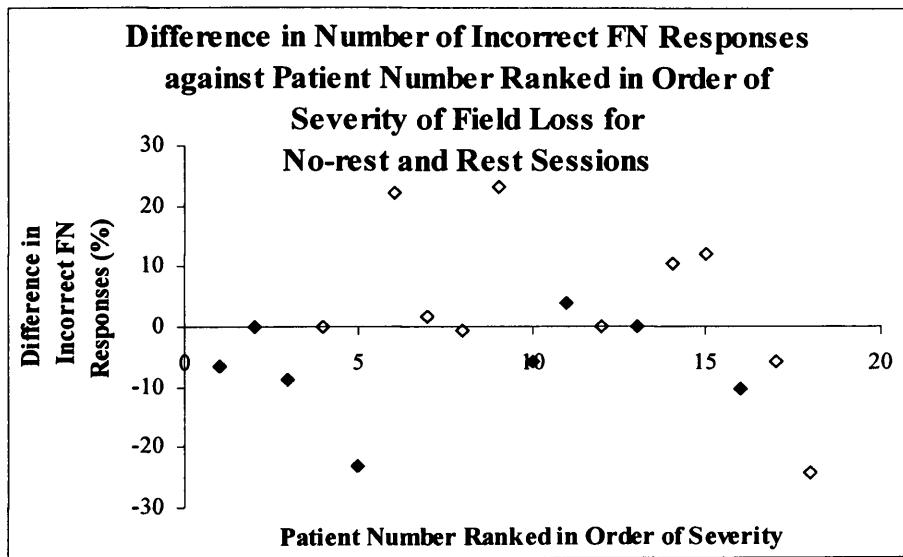
Figure 6.4 The difference between the two sessions (No-rest minus Rest) in the number of incorrect responses to the FN Catch Trials against the patient number ranked in order of severity of field loss. Open symbols: Rest Session followed by No-rest Session. Closed symbols: No-rest Session followed by Rest Session.

6.4.8 The Difference in the Percentage of Incorrect Responses to the FN Catch Trials Between the two Sessions as a Function of the Mean MD

The difference in the number of incorrect responses to the FN catch trials between the two sessions against the Mean MD of the two sessions is shown in Figure 6.5. The correlation coefficient was 0.17.

Difference in Number of Incorrect FN Responses for No-rest and Rest Sessions against Mean MD

$R^2 = 0.03$
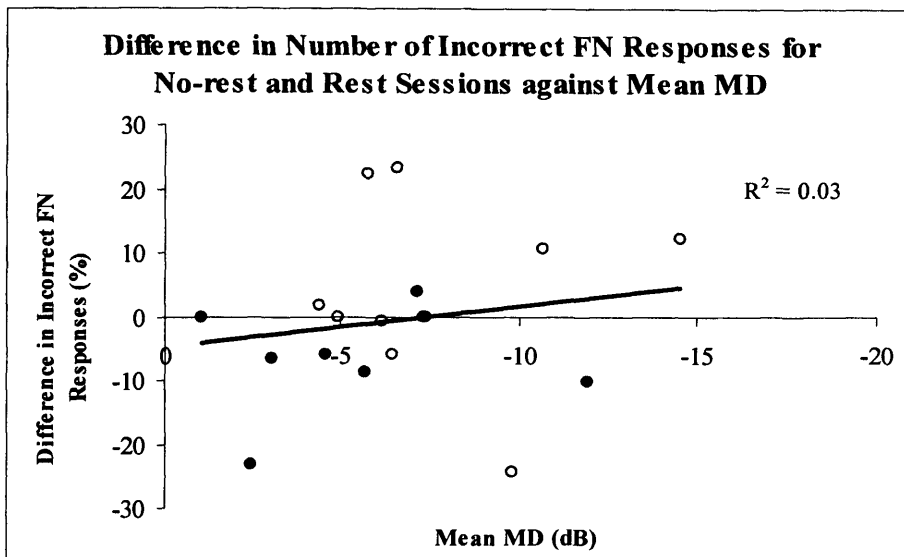
Mean MD (dB)

Figure 6.5 The difference between the two sessions (No-rest minus Rest) in the number of incorrect responses to the FN Catch Trials against the Mean MD of the two sessions as function of order of Session. Open symbols: Rest Session followed by No-rest Session. Closed symbols: No-rest Session followed by Rest Session.

6.5 DISCUSSION

The magnitude of the Group Mean, SD and range of the incorrect responses to the False-positive and to the Fixation loss catch trials indicates that the patients involved in the study were good observers.

The increase in the number of incorrect responses to the FN catch trials with increase in the severity of the MD index is in accordance with those of Bengtsson and Heijl (2000). They found that the between-eye difference in the number of incorrect responses to the

248

FN catch trials in patients with unilateral glaucoma increased as a function of the increasing severity of the MD in the glaucomatous eye.

There was little difference in the number of incorrect responses to the FN catch trials between the No-Rest and Rest Sessions regardless of the order in which the two sessions were undertaken.

The fatigue effect has a greater effect upon those locations exhibiting relative loss compared to those locations exhibiting (near) normal or absolute loss (Holmin 1979; Suzamura 1988; Heijl and Drance 1983). With the Full Threshold and FASTPAC algorithms, the false-negative catch trials are only presented at the stimulus locations at which the threshold estimate has been completed regardless of the magnitude of the threshold. The position of the stimulus locations selected for FN catch-trial assessment therefore varies, in a quasi random manner, between-examinations within a patient and between patients. Consequently, there is no control over the magnitude of sensitivity, and therefore the extent of the variability, at each of the given locations selected for the FN catch-trial assessment. Furthermore, there is no control over the time at which the FN catch-trial is presented at the given location which, as was just stated, manifests an unknown magnitude of sensitivity. Thus, the outcome variable of the study, the difference in the prevalence of incorrect responses to the FN catch-trials, was dependent upon the vagaries of the spatial and temporal positioning of the FN catch-trial within and between any given Program 30-2. It is perhaps for these reasons that the SITA algorithms present the FN catch-trials into those locations exhibiting normal sensitivity.

In view of the above factors, it is perhaps surprising that a modest correlation was obtained between increasing severity of the MD and the number of incorrect FN responses, regardless of the presence of rest periods, and that the higher correlation was obtained for 'No-rest Session'.

The lack of any substantial difference in the prevalence of incorrect responses to the FN catch trials between the 'No-rest' and 'Rest Sessions' rendered analysis of the time-specific onset of each incorrect response to the FN catch trials unnecessary.

6.6 CONCLUSION

The hypothesis that increasing fatigue leads to an increasing number of incorrect responses to the FN catch trials, particularly, with increasing severity of field loss, cannot be rejected from the results obtained in this pilot study. A better outcome should be obtainable with custom software which enables control over the spatial and temporal positioning of the FN catch trials during the examination.

CHAPTER 7

General Summary of Results and Conclusions and Proposals for Future Work

7.1 SUMMARY OF RESULTS AND CONCLUSIONS
7.1.1 Perimetric Sensitivity in the Normal Eye as a Function of the HFA Full Threshold, SITA Standard, SITA Fast, Octopus Threshold and TOP Algorithms

The studies described in Chapters 3 and 4 were designed to investigate the performance of the newer and faster algorithms, SITA Standard, SITA Fast and TOP relative to each other and to the 'gold standard' 4-2dB staircase algorithms.

In normal individuals, the Octopus Threshold and TOP algorithms exhibited the lowest Group Mean MS and the most severe Group Mean MD. As would be expected for a cohort of normal individuals, the $PSD/LV^{0.5}$ did not yield any significant differences between-algorithms. The TOP algorithm, analysed in terms of both the between-individual difference in MD against the mean of the MD and the between-individual pointwise analysis of sensitivity, was the least repeatable from the first examination to the second of the five algorithms investigated. The greatest disparity, between-algorithm within-visit, analysed in terms of the MD and of the pointwise analysis, occurred with the TOP algorithm in relation to both the SITA Standard algorithm and SITA Fast algorithm.

The PD/CC analysis showed that TOP overestimated abnormality compared to the SITA Fast and Octopus Threshold algorithms. This suggests that TOP would have a higher sensitivity and reduced specificity for normal individuals compared to the other algorithms. The findings concerning the comparisons for the Full Threshold algorithm with the SITA Fast algorithms were consistent with the findings of previous studies.

7.1.2 Perimetric Sensitivity in the Glaucomatous Eye as a Function of the HFA Full Threshold, SITA Standard, SITA Fast, Octopus Threshold and TOP Algorithms

As for the normal individuals, the Octopus Threshold and TOP algorithms also produced the lowest MSs and most severe MDs for the cohort of patients with glaucoma. The $PSD/LV^{0.5}$ was largest for the Full Threshold algorithm and smallest for the TOP

algorithm. In agreement with the findings for the cohort of normal individuals, the between-individual difference in MD against the mean of the MDs for the TOP algorithm, was the least repeatable on test-retest, of the five algorithms investigated. The between-algorithm within-visit and the within-algorithm between-visit pointwise analyses in sensitivity yielded similar results for all algorithm comparisons.

The PD/CC analysis was conducted for the cohort of patients with glaucoma, as a whole, and for the subgroups: Very Early field loss; Early field loss; and Moderate and Severe Field loss combined. The between-algorithm within-visit PD/CC analysis showed that for the cohort of normal individuals and for each of the four groups of field loss, the SITA algorithms consistently yielded more extensive focal loss than the Full Threshold algorithm. The corresponding comparisons for the TOP algorithm, however, did not reveal any consistent pattern. For the cohort of normal individuals, TOP revealed a more severe defect than the SITA Fast algorithm. However, the Very Early field loss Group yielded broadly similar results between the Octopus Threshold algorithm and the TOP algorithm and between the TOP algorithm and each of the SITA algorithms. Compared to the SITA algorithms, the TOP algorithm produced similar defects for the PD/CC analysis for the Early field loss Group, but produced larger defects for the Moderate and Severe field loss Group.

Despite the TOP algorithm being considerably faster than the other algorithms investigated in the two studies the time-saving benefit appears to be at the cost of inconsistent performance across the various subject Groups, compared to the remaining four algorithms. However, although the confidence limits for normality with the SITA Fast algorithm are narrower, suggesting that it may produce over-sensitive results, its performance across the subject Groups was consistent. If a perimetric algorithm is to be utilised to screen for and/or monitor a particular progressive ocular disease, it is preferable that it exhibits similar relative performance to the gold standard at each stage of the disease process.

In summary, SITA Fast represents a good compromise between examination duration and the associated financial implications; fatigue considerations for the patient; and reasonable repeatability compared to the Full Threshold algorithm. The inherent differences within- and between-algorithm for TOP suggests that an alternative should be utilised in clinical practice.

7.1.3 Frequency-of-seeing Curves for SWAP and W-W Perimetry in Normal Individuals and in Patients with Glaucoma

Limited published research has been conducted into the characteristics of the FOS curve in W-W perimetry despite the fact that these characteristics are used in the widely available SITA perimetric algorithms. The FOS curve in SWAP has never been formally documented, either in normal individuals or in glaucoma, even though there is considerable evidence of increased perimetric variability for SWAP compared to W-W perimetry.

The hypothesis for this study was that the slope and, therefore z_0, of the FOS curve for W-W perimetry and for SWAP would each flatten with increase in eccentricity and that the magnitude of the slope would be flatter at any given eccentricity for SWAP than for W-W perimetry. This hypothesis was confirmed by the ANOVA.

The study revealed considerable within- and between-individual variation for both the W-W perimetry and SWAP FOS curves. It became apparent during the study that measuring and producing a FOS curve with the well-documented sigmoidal appearance of the psychometric function is a difficult task.

The findings relating to the FOS curve for SWAP were of particular interest. SWAP exhibits increased between-subject normal variability compared to W-W perimetry. The SWAP FOS curve exhibited increased variability in the magnitude of the slope and of the z_0 values compared to that for W-W perimetry. The SITA SWAP algorithm is shortly to become commercially available for the HFA perimeters. The SITA algorithms for W-W perimetry incorporate the characteristics of the FOS curve in their thresholding

procedure. It is therefore very likely that the SITA SWAP algorithm will also incorporate a knowledge of the SWAP FOS curve. The flatter slope of the SWAP FOS curve explains the wider confidence limits for normality of SWAP compared to W-W perimetry for both the HFA Full Threshold and FASTPAC algorithms. The reduction in sensitivity required to indicate abnormality for SWAP is proportionately greater than for W-W perimetry.

Another limitation of SWAP is the absorption of the blue stimulus by the ocular media. OMA can be calculated using various techniques and the resultant field corrected accordingly, but the procedure is either time-consuming or expensive and clinically impractical. A final consideration, is that most subjects find SWAP a difficult and sometimes anxiety-inducing task: if the patient is not comfortable and relaxed during a perimetric examination, erroneous responses may occur.

In summary, it is most likely that the flatter FOS curve associated with SWAP will render the SITA SWAP algorithm difficult both to implement and to interpret in a clinical setting. The outlook for SITA SWAP does not appear to be good.

7.1.4 The Influence of Fatigue on the Prevalence of False-negative Responses in Perimetry

The aim of the pilot study described in Chapter 6 was to determine if the prevalence of incorrect responses to the false-negative catch trials increased with increase in the fatigue effect during a perimetric examination. Comparison of results from the visual field examinations undertaken with and without rest periods neither confirmed nor refuted the hypothesis. The equivocal nature of the findings could be explained by the random positioning of the FN catch trials at the given location and the random timing of the presentation during the visual field examination and, perhaps, by the overall level of field loss for the cohort.

7.2 PROPOSALS FOR FUTURE WORK
7.2.1 Investigation into the Influence of the, HFA, HFA SITA and Octopus Perimeter Normative Data Bases

The findings in Chapters 3 and 4 revealed differences in performance between the five algorithms for normal individuals and for patients with OAG. Potential between-algorithm differences in the Total Deviation/Comparison values and/or in the Pattern Deviation/Corrected Comparison values may arise from the differences in the given algorithms or from the differences in the given normative databases. Ideally, a normative database common to all algorithms should be utilised in any between algorithm evaluation. The creation of such databases would be an enormous undertaking. In addition, the establishment of a normative database poses the question as to what is a normative database. The HFA normative database for the Full Threshold algorithm, for example, is compiled from the visual field recorded from one eye of each individual at the third perimetric examination. The selection of the third examination is an arbitrary choice which, presumably, was selected to represent 'normality' once the majority of the learning effect had been overcome (Wood et al 1987; Werner et al 1988,1990; Heijl et al 1989; Searle et al 1991). The database is used for the evaluation of each eye of the given patient and does not account for the fact that the fatigue effect is known to have a greater influence on the second eye examined (Wilensky and Joondeph 1984). It could be argued that separate databases should exist for each visit and for each eye within a visit. In practical terms, the development of normative databases in this manner would not be feasible due to the large number of normal individuals required.

7.2.2 Investigation of the FOS Curve in Normal Individuals for W-W perimetry and SWAP as a Function of: Age, the presence of Type II Diabetes Mellitis, and the presence of Cataract

Currently, there is sparse literature documenting the FOS curve. Indeed, the study described in Chapter 5 was the first to investigate the FOS curve in SWAP. Consequently, there is much scope for further research into the characteristics of the FOS curve. As more information is obtained on the characteristics of the FOS curve, this knowledge can be applied to the design of improved perimetric algorithms. It would be interesting to undertake a study which investigates the FOS curve in normal individuals

with age. Equal numbers of individuals could be recruited for each decade of age and FOS curves calculated for each age Group.

The FOS software used in the current study could be improved to enable the initial thresholding of the FOS location to be measured more than once (so that an average could be obtained as a starting point for the FOS data) and to enable sufficient stimulus luminances relative to threshold to be examined so that one FOS curve could be derived from a single (rather than two) perimetric examinations.

Perimetry is used extensively to screen for, and monitor the progression, of glaucoma. The prevalence of glaucoma in the population, increases with age, as does the prevalence of cataract and Type II Diabetes. The assumption for the Total and Pattern Deviation analysis is that cataract uniformly reduces the height of the visual field. However, magnitude of the attenuation of the height of the visual field varies as a function of the type and location of the cataract. In addition, it is assumed that the reduction in the height of the field occurs solely due to non-retinal factors. The attenuation in the height of the hill of vision in Type II diabetes, for example, is unknown. Such factors confound the interpretation of the glaucomatous visual field. Consequently, it would be useful to determine the magnitude of the slope of the FOS curve in W-W perimetry and in SWAP as a function of cataract type and position and as a function Type II diabetes.

7.2.3 The Performance of SITA SWAP in Normal Individuals and in Patients with Open Angle Glaucoma

The results obtained in Chapter 5 for the FOS curve in SWAP suggest that the new SITA SWAP algorithm will have wide confidence limits relative to SITA Standard and SITA Fast and will be clinically difficult to interpret. The performance of SITA SWAP needs to be thoroughly investigated both in normal individuals and in patients with OAG.

7.2.4 Investigation of the Prevalence of Incorrect Responses to the FN Catch Trials in Locations of the Visual Field Exhibiting Varying Defect Depths, with Respect to Patient Fatigue

The pilot study (Chapter 6) concerning the prevalence of incorrect responses to the False-negative catch trials as a function of fatigue was inconclusive. The main difficulty arose from the random nature in which the temporal presentation and spatial location of a FN catch trial was selected by the Full Threshold algorithm. Modified software is required to overcome these difficulties. Custom software would enable FN catch trials to be presented at predetermined positions within the field; the prevalence of incorrect responses to the FN catch trials could then be calculated in relation to defect depth and to the time point within the examination.

REFERENCES

Adams AJ, Heron G and Husted R (1987). Clinical measures of central visual function in glaucoma and ocular hypertension. *Archives of Ophthalmology*, 105, 782-787.

Adams AJ, Johnson CA and Lewis RA (1991). S-cone pathway sensitivity loss in ocular hypertension and early glaucoma has nerve fibre bundle pattern. In Drum B, Moreland JD and Serra A (eds.) *Colour Vision Deficiencies*, Kluwer Academic Publishers, Dordrecht. 535-542.

Adams CW, Bullimore MA, Wall M, Fingeret M and Johnson CA (1999). Normal aging effects for Frequency Doubling Technology. *Optometry and Vision Science*, 76, 582-587.

AGIS (1994). The Advanced Glaucoma Intervention Study 2: Visual field test scoring and reliability. *Ophthalmology*, 101, 1445-1455.

AGIS(1998). The Advanced Glaucoma Intervention Study 3. Baseline characteristics of black and white patients. *Ophthalmology*, 105, 1137-1145.

Alward WLM (2000). Frequency Doubling Technology perimetry for the detection of glaucomatous visual field loss. *American Journal of Ophthalmology*, 129, 376-378.

Anctil JL and Anderson DR (1984). Early foveal involvement and generalized depression of the visual field in glaucoma. *Archives of Ophthalmology*, 102, 363-370.

Anderson AJ (2003). Spatial resolution of the Tendency Oriented Perimetry algorithm. *Investigative Ophthalmology & Visual Science*, 44, 1962-1968.

Anderson DR and Patella VM (1999). *Automated Static Perimetry 2nd Edition*. Mosby Inc., St.Louis.

Armaly MF (1971) Visual field defects in early open angle glaucoma. *Transactions of the American Ophthalmological Society*, 69, 147-162.

Artes P, Iwase A, Yoshiuki K and Chauhan B (2002). Properties of perimetric threshold estimates from Full Threshold, SITA Standard and SITA Fast strategies. *Investigative Ophthalmology & Visual Science*, 43, 2654-2659.

Artes PH and Chauhan BC (2003). Visual field progression with total and pattern deviation glaucoma change probability analyses. *Investigative Ophthalmology & Visual Science*, 44, 1044.

Asman P and Heijl A (1994b). The perimetric 'learners index'. A pilot study. *Investigative Ophthalmology & Visual Science*, s35, 2183.

Asman P, Fingeret M, Robin A, Wild JM, Pacey IE, Greenfield Dl, Liebmann J, Ritch R (1999). Kinetic and static fixation methods in automated threshold perimetry. *Journal of Glaucoma*, 8, 290-296.

Asman P, Olsson J and Heijl A (1993) Learner's Index (LI) to detect low perimetric experience. *Investigative Ophthalmology & Visual Science*, s34, 1262.

Asman P, Britt JM, Mills RP and Heijl A (1988) Evaluation of adaptive spatial enhancement in suprathreshold visual field screening. *Ophthalmology*, 95, 1656-1662.

Asman P and Heijl A (1992) Glaucoma Hemifield Test - automated visual field evaluation. *Archives of Ophthalmology*, 110, 812-819.

Asman P and Heijl A (1994a). Diffuse visual field loss and glaucoma. *Acta Ophthalmologica*, 72, 303-308.

Asman P, Heijl A, Olsson J and Rootzen H (1992). Spatial analyses of glaucomatous visual fields; a comparison with traditional visual field indices. *Acta Ophthalmologica*, 70, 679-686.

Asman P and Olsson J (1995). Physiology of cumulative defect curves; consequences in glaucoma perimetry. *Acta Ophthalmologica*, 73, 197-201.

Asman P, Wild JM and Heijl A (2004). Appearance of the Pattern Deviation Map as a function of change in area of localized field loss. *Investigative Ophthalmology & Visual Science*, 45, 3099-3106.

Atchison DA (1987). Effect of defocus on visual field measurement. *Ophthalmic and Physiological Optics*, 7, 259-265.

Aulhorn E and Harms H (1972). Visual perimetry. In Jameson D. and LM H (eds.), *Visual psychophysics, handbook of sensory physiology* VII. Springer-Verlag, Berlin. 102-145.

Aulhorn E, Harms M (1967). Early visual field defects in glaucoma. In: Leydhecker W, (ed.). Glaucoma Symposium Tutzing Castle, Karger, Basel/ New York. 151-186.

Autzen T and Work K (1990) The effect of learning and age on short-term fluctuation and mean sensitivity of automated static perimetry. *Acta Ophthalmologica*, 68, 327-330.

Balaszi A, Rootman J, Drance S, Schulzer M and Douglas G (1984). The effect of age on the optic nerve fibre population in the human optic nerve. *American Journal of Ophthalmology*, 97, 760-766.

Ballon BJ, Echelmoan DA, Shields MB and Ollie AR (1992). Peripheral visual field testing in glaucoma by automated kinetic perimetry with the Humphrey Field Analyzer. *Archives of Ophthalmology*, 110, 1730-1732.

Baraldi P, Enoch JM and Raphael S (1987). A comparison of visual impairment caused by nuclear (nc) and posterior subcapsular (psc) cataracts. *Documenta Ophthalmologica Proceedings Series*, 49, 43-50.

259

Barlow HB (1958). Temporal and spatial summation in human vision at different background intensities. *Journal of Physiology*, 141, 337-350.

Bebie H (1985). Computerised techniques of threshold determination. In Whalen WR and Spaeth GL (eds.), *Computerized visual fields. What are they and how to use them?* Slack Inc, New Jersey, pp. 31-44.

Bebie H, Fankhauser F and Spahr J (1976). Static perimetry: Strategies. *Acta Ophthalmoloca*, 54, 325-338.

Bebie H and Fankhauser F (1981). Statistical program for the analysis of perimetric data. *Documenta Ophthalmologica Proceedings Series*, 26, 9-10.

Bebie H, Flammer J and Bebie T (1989). The cumulative defect curve: Separation of local and diffuse components of visual field damage. *Graefe's Archive for Clinical and Experimental Ophthalmology*, 227, 9-12.

Benedetto MD and Cyrlin MN (1985). The effect of blur upon static perimetric thresholds. *Documenta Ophthalmologica Proceedings Series*, 42, 563-567.

Bengtsson B (2000). Reliability of computerized perimetric threshold tests as assessed by reliability indices and threshold reproducibility in patients with suspect and manifest glaucoma. *Acta Ophthalmologica*, 78, 519-522.

Bengtsson B (2003). A new rapid threshold algorithm for short-wavelength automated perimetry. *Investigative Ophthalmology & Visual Science*, 44, 1388-1394.

Bengtsson B and Heijl A (1999). Inter-subject variability and normal limits of the SITA Standard, SITA Fast, and the Humphrey Full Threshold computerized perimetry strategies, SITA STATPAC. *Acta Ophthalmologica*, 77, 125-129.

Bengtsson B, Heijl A and Olsson J (1998). Evaluation of a new threshold visual field strategy, Swedish Interactive Thresholding algorithm, SITA, in normal subjects. *Acta Ophthalmologica Scandinavica*, 76, 165-169.

Bengtsson B, Lindgren A, Heijl A, Lindgren G, Asman P and Patella M (1997a). Perimetric probability maps to separate change caused by glaucoma from that caused by cataract. *Acta Ophthalmologica*, 75, 184-188.

Bengtsson B and Heijl A (1998a). Evaluation of a new perimetric threshold strategy, SITA, in patients with manifest and suspect glaucoma. *Acta Ophthalmolgica*, 76, 268-272.

Bengtsson B and Heijl A (1998b). SITA Fast, a new rapid perimetric threshold test. Description of methods and evaluation in patients with manifest and suspect glaucoma. *Acta Ophthalmologica*, 76, 431-437.

Bengtsson B and Heijl A (2000). False-negative responses in glaucoma perimetry: Indicators of patient performance or test reliability? *Investigative Ophthalmology & Visual Science*, 41, 2201-2204.

260

Bengtsson B and Heijl A (2003). Normal inter-subject threshold variability and normal limits of the SITA SWAP and Full Threshold SWAP perimetric programs. *Investigative Ophthalmology & Visual Science*, 44, 5029-5034.

Bengtsson B, Olsson J, Heijl A and Rootzen H (1997). A new generation of algorithms for computerized threshold perimetry, SITA. *Acta Ophthalmologica*, 75, 66.

Bettelheim FA and Ali S (1985). Light scattering of normal human lens. III Relationship between forward and back scatter of whole excised lenses. *Experimental Eye Research*, 41, 1-9.

Bettelheim FA and Chylack LT (1985). Light scattering of whole excised human cataractous lenses. Relationships between different light scattering parameters. *Experimental Eye Research*, 41, 19-30.

Bickler-Bluth M (1989). Assessing the utility of reliability indices for automated visual fields, testing ocular hypertensives. *Ophthalmology*, 96, 616-619.

Birch MK, Wishart PK and O'Donnell NP (1995). Determining progressive visual field loss in serial Humphrey visual fields. *Ophthalmology*, 102, 1227-1235.

Birt CM, Shin DH, Samudrala V, Hughes BA, Kim C and Lee D (1997). Analysis of reliability indices from Humphrey visual field tests in an urban glaucoma population. *Ophthalmology*, 104, 1126-1130.

Blum FG, Gates LK and James BR (1959). How important are peripheral fields? *Archives of Ophthalmology*, 61, 1-8.

Blumenthal EZ, Sample PA, Berry CC, Lee AC, Girkin CA, Zangwill L and Weinreb RN (2000). Evaluating sources of variability for standard and SWAP visual fields in glaucoma patients, suspects and normals. *Investigative Ophthalmology & Visual Science*, 41, 442.

Boeglin RJ, Caprioli J and Zulauf M (1992). Long-term fluctuation of the visual field in glaucoma. *American Journal of Ophthalmology*, 113, 396-400.

Bolanowski SJ and Doty RW (1987). Perceptual 'blankout' of monocular homogenous fields (ganzfelder) is prevented with binocular viewing. *Vision Research*, 27, 967-982.

Brechner RJ and Whalen (1984). Creation of the transformed Q static probability distribution to aid in the detection of abnormal computerized visual field examinations. *Ophthalmic Surgery*, 15, 833-836.

Brenton RS and Argus WA (1987). Fluctuations on the Humphrey and Octopus perimeters. *Investigative Ophthalmology & Visual Science* 28, 767-771.

Brenton RS and Phelps CD (1986). The normal visual field on the Humphrey Field Analyzer. *Ophthalmologica*, 193, 56-74.

Britt JM and Mills RP (1988) The black hole effect in perimetry. *Investigative Ophthalmology & Visual Science*, 29, 795-801.

Brusini P, Nicosia S and Weber J (1991). Automated visual field management in glaucoma with the Peridata program. In Mills RP and Heijl A (eds.), *Perimetry Update, 1991/1992*. Kugler Publications, Amsterdam/ New York. 273-277.

Budenz DL, Feuer WJ and Anderson DR (1993). The effect of simulated cataract on the glaucomatous visual field. *Ophthalmology*, 100, 511-517.

Budenz DL, Rhee P, Feuer WJ, McSoley J, Johnson CA and Anderson DR (2002). Sensitivity and specificity of the Swedish Interactive Threshold Algorithm for glaucomatous visual field defects. *Ophthalmology*, 109, 1052-1058.

Burk ROW and Rendon R (2001). Clinical detection of optic nerve damage: Measuring changes in cup steepness with use of a new image alignment algorithm. *Survey of Ophthalmology*, 45, s297-s303.

Burnstein Y, Ellish NJ, Magbalon M and Higginbotham EJ (2000). Comparison of Frequency Doubling Perimetry with Humphrey Visual Field Analyzer in a glaucoma practice. *American Journal of Ophthalmology*, 129, 328-333.

Calkins DJ (2001) Seeing with s-cones. *Progress in Retinal and Eye Research*, 20, 255-287.

Callaway EM (1998). Local circuits in primary visual cortex of the macaque monkey. *Annual Review of Neuroscience*, 21, 47-74.

Campbell FW and Andrews PR (1992). Motion reveals spatial visual defects. *Ophthalmic and Physiological Optics*, 12, 131-132.

Campbell FW and Green DG (1965). Optical and retinal factors affecting visual resolution. *Journal of Physiology*, 181, 576-593.

Caprioli J (2001). Should we use short-wavelength automated perimetry to test glaucoma patients. *American Journal of Ophthalmology*, 131, 792-794.

Caprioli J and Spaeth GL (1985). Static threshold examination of the peripheral nasal visual field in glaucoma. *Archives of Ophthalmology*, 103, 1150-1154.

Casagrande VA (1994) A third parallel visual pathway to primate area V1. *Trends in Neuroscience*, 17, 305-310.

Cascairo MA, Stewart WC and Sutherland SE (1991). Influence of missed catch-trials on the visual field in normal subjects. *Graefe's Archive for Clinical and Experimental Ophthalmology*, 229, 437-441.

Casson EJ, Johnson CA and Shapiro LR (1993). Longitudinal comparison of temporal-modulation perimetry with white-on-white and blue-on-yellow perimetry in ocular hypertension and early glaucoma. *Journal of the Optical Society of America*, 10, 1792-1806.

Chauhan BC and House PH (1991). Intra-test variability in conventional and high-pass resolution perimetry. *Ophthalmology*, 98, 79-83.

Chauhan BC, Drance SM and Douglas GR (1990). The use of visual field indices in detecting changes in the visual field in glaucoma. *Investigative Ophthalmology & Visual Science*, 31, 512-520.

Chauhan BC, Drance SM and Lai C (1989). A cluster analysis for threshold perimetry. *Graefe's Archive for Clinical and Experimental Ophthlamology*, 227, 216-220.

Chauhan BC, Henson DB and Hobley AJ (1988). Cluster analysis in visual field quantification. *Documenta Ophthalmologica*, 69, 25-39.

Chauhan BC, House PH, McCormick TA and LeBlanc RP (1999). Comparison of conventional and high-pass resolution perimetry in a prospective study of patients with glaucoma and healthy controls. *Archives of Ophthalmology*, 117, 24-33.

Chauhan BC, LeBlanc RP, Shaw AM, Chan AB and McCormick TA (1997). Repeatable diffuse visual field loss in open-angle glaucoma. *Ophthalmology*, 104, 532-538.

Chauhan BC and MacDonald CA (1995). Influence of time separation on variability estimates of topographic measurements with confocal scanning laser tomography. *Journal of Glaucoma*, 4, 189-193.

Chauhan BC, Tompkins JD, Le Blanc RD and McCormick TA (1993). Characteristics of frequency-of-seeing curves in normal subjects, patients with suspected glaucoma and patients with glaucoma. *Investigative Ophthalmology & Visual Science*, 34, 3534-3540.

Cho N, Poulsen GL, Ver Hoeve JN and Nork M (2000). Selective loss of s-cones in diabetic retinopathy. *Archives of Ophthalmology*, 118, 1393-1400.

Choplin NT, Sherwood MB and Spaeth GL (1990). The effect of stimulus size on the measured threshold values in automated perimetry. *Ophthalmology*, 97, 371-374.

Cohn TE and Wardlow JC (1985). Effect of large spatial uncertainty on foveal luminance detectability. *Journal of the Optical Society of America*, 2, 820-825.

Cornsweet TN (1962). The staircase-method in psychophysics. *American Journal of Psychology*, 78, 485-491.

Crook JM (1988). Visual resolution of macaque retinal ganglion cells. *Journal of Physiology*, 396, 205-224.

Crosswell HH, Stewart WC, Cascairo MA and Hunt HH (1991). The effect of background intensity on the components of fluctuation as determined by threshold-related automated perimetry. *Graefe's Archive for Clinical and Experimental Ophthalmology*, 229, 119-122.

Curcio CA, Allen KA, Sloan KR, Lerea CL, Hurley IB, Klock IB and Milam AH (1991) Distribution and morphology of human cone photoreceptors stained with anti-blue opsin. *Journal of Comparative Neurology*, 312, 610-624.

Dacey D (1993). Morphology of a small bi-stratified ganglion cell type in the macaque and human retina. *Visual Neuroscience*, 10, 1081-1098.

Dacey D and Lee B (1994). The 'blue-on' opponent pathway in primate retina originates from a distinct ganglion cell type. *Nature*, 367, 731-735.

Dacey DM (2000). Parallel pathways for spectral coding in primate retina. *Annual Review of Neuroscience*, 23, 743-775.

Dannheim F and Drance SM (1987). First experiences with the new Octopus G1 program in chronic simple glaucoma. *Documenta Ophthalmologica Proceedings Series 49*, 321-328.

Dannheim F and Drance SM (1971). Studies of temporal summation of central retinal areas in normal people of all ages. *Ophthalmic Research*, 2, 295-303.

Davson H (1990) *Physiology of the Eye*. The Macmillan Press Ltd., Basingstoke and London.

de Boer RW, van den Berg TJTP, Greve EL and Bos HJ (1982). The Fieldmaster 101 automatic visual field screener - Technical evaluation and clinical results. *Documenta Ophthalmologica*, 53, 311-320.

de Jong LAMS, Snepvangers CEJ, Van Den Berg TJTP and Langerhorst CT (1990). Blue-yellow perimetry in the detection of early glaucomatous damage. *Documenta Ophthalmologica*, 75, 303-314.

de Monasterio FM (1978). Properties of concentrically organised x and y ganglion cells in the macaque retina. *Journal of Neurophysiology*, 41, 1394-1417.

de Monasterio FM, Schein SJ and McCrane EP (1981). Staining of blue-sensitive cones of the macaque retina by fluorescent dye. *Science*, 213, 1278-1281.

de Monasterio FM, McCrane EP, Newlander JK and Schein SJ (1985). Density profile of blue sensitive cones along the horizontal meridian of macaque retina. *Investigative Ophthalmology & Visual Science*, 26, 289-302.

de Monasterio FM and Hubel A (1978). Spectral interactions in horizontal and gamglion cells of the isolated and arterially-perfused rabbit retina. *Brain Research*, 150, 239-258.

de Natale R, Glaab-Schrems E and Kriegelstein GK (1984). The prognosis of glaucoma investigated with computerized perimetry. *Documenta Ophthalmologica*, 58, 385-392.

Delgado MF, Nguyen NT, Cox TA, Singh K, Lee DA, Dueker DK, Fechtner RD, Juzych MS, Lin SC, Netland PA, Pastor SA, Schuman JS, Samples JR and Panel. (2002). Automated perimetry: A report by the American Academy of Ophthalmology. *Ophthalmology*, 109, 2362-2374.

Demirel S and Johnson CA (2000). Isolation of short-wavelength sensitive mechanisms in normal and glaucomatous visual field regions. *Journal of Glaucoma*, 9, 63-73.

Demirel S and Vingrys AJ (1994) Acceptable false-response rates for reliable perimetric outcomes. In Mills RP and Wall M (eds.), *Perimetry Update 1994/1995*, Kugler Publications, Amsterdam/New York. 433-450.

Dengler-Harles M, Wild JM, Cole MD, O'Neill E. and Crews SJ (1990). The influence of forward light scatter on the visual field indices in glaucoma. *Graefe's Archive for Clinical and Experimental Ophthalmology*, 228, 326-331.

Desjardins D and Anderson DR (1988). Threshold variability with an automated LED perimeter. *Investigative Ophthalmology & Visual Science*, 29, 915-921.

DeValois RL and Wasserman GS (1978). *Colour Vision*. Wiley Interscience, New York.

Devaney K and Johnson H (1980). Neuron loss in the aging visual cortex of man. *Journal of Gerontology*, 35, 836-841.

Dolman C, McCormick A and Drance S (1980). Aging of the optic nerve. *Archives of Ophthalmology*, 98, 2053-2058.

Drance SM (1991). Diffuse visual field loss in open angle glaucoma. *Ophthalmology*, 98, 1533-1538.

Drance SM, Fairclough M, Thomas B, Douglas GR and Susanna R (1979) The early visual field defect in glaucoma and the significance of nasal steps. *Documenta Ophthalmologica*, 19, 119-126.

Drance SM, Schulzer M, Thomas B and Douglas GR (1981). Multivariate analysis in glaucoma. Use of discriminant analysis in predicting glaucomatous visual field damage. *Archives of Ophthalmology*, 99, 1019-1022.

Drance SM, Wheeler C and Pattullo M (1967). The use of static perimetry in the early detection of glaucoma. *Canadian Journal of Ophthalmology*, 2, 249-258.

Drasdo N, Aldebasi YH, Chiti Z, Mortlock KE, Morgan JE and North RV (2001). The S-cone and Pattern ERG in primary open angle glaucoma. *Investigative Ophthalmology and Visual Science*, 42, 1266-1272.

Drummond PD and Anderson M (1992). Visual loss after attacks of migraine with aura. *Cephalalgia*, 12, 349-352.

Duggan C, Sommer A, Auer C and Burkhardt K (1985). Automated differential threshold perimetry for detecting glaucomatous visual field loss. *American Journal of Ophthalmology*, 100, 420-468.

Eisner A and MacLeod DIA (1980). Blue-sensitive cones do not contribute to luminance. *Journal of the Optical Society of America*, 70, 121-123.

Eke T, Talbot JF and Lawden MC (1997). Severe persistent visual field constriction associated with vigabatrin. *British Medical Journal*, 314, 180-181.

Fankhauser F (1979). Problems related to the design of automatic perimeters. *Documenta Ophthalmologica*, 47, 89-138.

Fankhauser F (1993). Influence of missed catch-trials on the visual field in normal subjects. *Graefe's Archive for Clinical and Experimental Ophthalmology*, 231, 58-59.

Fankhauser F and Schmidt TH (1960). Die optomalen bedingungen fur die untersuchung der raumlichen summation mit stehender reizmarke nach der methode der quantitativen lichtsinnperimetrie. *Ophthalmologica*, 139, 409-423.

Fankhauser F, Bebie H and Flammer J (1988). Threshold fluctuations in the Humphrey Field Analyzer and in the Octopus automated perimeter. *Investigative Ophthalmology and Visual Science*, 29, 1466.

Fankhauser F and Haeberlin H (1980). Dynamic range and stray light. An estimate of the falsifying effects of stray light in perimetry. *Documenta Ophthalmologica*, 50, 143-167.

Fankhauser F, Koch P and Roulier A (1972). On automation of perimetry. *Graefe's Archive for Clinical and Experimental Ophthalmology*, 184, 126-150.

Farber D, Flannery J, Lolley R and Bok D (1985). Distribution patterns of photoreceptors, protein and cyclic nucleotides in the human retina. *Investigative Ophthalmology & Visual Science*, 26, 1558-1568.

Felius J, de Jong L, van den Berg T and Greve E (1995). Functional characteristics of blue-on-yellow perimetric thresholds in glaucoma. *Investigative Ophthalmology & Visual Science*, 36, 558-570.

Fitzke FW, Crabb DP, McNaught AI, Edgar DF and Hitchings RA (1995). Image processing of computerized visual field data. *British Journal of Ophthalmology*, 79, 207-212.

Flammer J (1986). The concept of visual field indices. *Graefe's Archive for Clinical and Experimental Ophthalmology*, 224, 389-392.

Flammer J, Drance SM, Fankhauser F and Augustiny L (1984a). Differential light threshold in automated static perimetry. Factors influencing short-term fluctuation. *Archives of Ophthalmology*, 102, 876-879.

Flammer J, Drance SM and Zulauf M (1984b). Differential light threshold. Short- and long-term fluctuation in patients with glaucoma, normal controls, and patients with suspected glaucoma. *Archives of Ophthalmology*, 102, 704-706.

Flammer J and Bebie H (1987). Influence of age on quantitative perimetry. *Archives of Ophthlamology*, 105, 24.

Flammer J, Drance SM, Augustiny L and Funkhouser A (1984b). Quantification of glaucomatous visual field defects with automated perimetry. *Archives of Ophthalmology*, 102, 880-882.

Flammer J, Drance SM, Fankhauser F and Augustiny L (1984a). Differential light threshold in automated static perimetry: Factors influencing short-term fluctuation. *Archives of Ophthalmology*, 102, 876-879.

Flammer J, Drance SM and Schulzer M (1983). The estimation and testing of the components of long-term fluctuation of the differential light threshold. *Documenta Ophthalmologica Proceedings Series 35*, 383-389.

Flanagan JG, Moss ID, Wild JM, Hudson C, Prokopich L, Whitaker D and O'Neill EC (1993a). Evaluation of FASTPAC: A new strategy for threshold estimation with the Humphrey Field Analyser. *Graefe's Archive for Clinical and Experimental Ophthalmology*, 231, 465-469.

Flanagan JG, Wild JM and Trope GE (1993a). The visual-field indices in primary open angle glaucoma. 34, 2266-2274.

Flanagan JG, Wild JM and Trope GE (1993b). Evaluation of FASTPAC, a new strategy for threshold estimation with the Humphrey Field Analyzer, in a glaucomatous population. *Ophthalmology*, 100, 949-954.

Flanagan JG, Wild JM and Hovis JK. The differential light threshold as a function of retinal adaptation - the Weber-Fechner/Rose-de-Vries controversy revisited. In Mills RP and Heijl A (eds.) *Perimetry Update 1990/91*, Kugler Publications, Amsterdam/New York, 551-554.

Fraser S, Bunce C and Wormald R (1999). Risk factors for late presentation in chronic glaucoma. *Investigative Ophthalmology & Visual Science*, 40, 2251-2257.

Frisen L (1987). High-pass resolution targets in peripheral vision. *Ophthalmology*, 94, 1104-1108.

Frisen L (1988). Acuity perimetry: Estimation of neural channels. *International Ophthalmology*, 12, 169-174.

Fuhr PS, Hershner TA and Daum KM (1990). Ganzfeld blackout occurs in bowl perimetry and is eliminated by translucent occlusion. *Archives of Ophthalmology*, 108, 983-988.

Fujimoto N and Adachi-Usami E (1993). Fatigue effect within 10 degrees visual field in automated perimetry. *Annals of Ophthalmology*, 25, 142-144.

Funkhouser A, Flammer J, Fankhauser F and Hirsprunner H (1992b). A comparison of five methods for estimating general glaucomatous visual field depression. *Graefe's Archive for Clinical and Experimental Ophthalmology*, 230, 101-106.

Funkhouser A and Fankhauser F (1991). The effects of weighting the mean defect visual field index according to threshold variability in the central and midperipheral visual field. *Graefe's Archive for Clinical and Experimental Ophthalmology*, 229, 228-231.

Funkhouser AT (1991). A new diffuse loss index for estimating general glaucomatous visual field depression. *Documenta Ophthalmologica*, 77, 57-72.

Funkhouser AT, Fankhauser F and Weale RA (1992). Problems related to diffuse versus localized loss in the perimetry of glaucomatous visual fields. *Graefe's Archive for Clinical and Experimental Ophthalmology*, 230, 243-247.

Gandolfo E (1996). Stato-kinetic dissociation in subjects with normal and abnormal visual fields. *European Journal of Ophthalmology*, 6, 408-414.

Garcia-Perez MA (1998). Forced-choice staircases with fixed step sizes: Asymptotic and small-sample properties. *Vision Research*, 38, 1861-1881.

Gartner S and Henkind P (1981). Aging and degeneration of the human macula: 1. Outer nuclear layer and photoreceptors. *British Journal of Ophthalmology*, 65, 23-28.

Garway-Heath DF, Poinoosawmy D, Fitzke FW and Hitchings RA (2000). Mapping the visual field to the optic disc in normal tension glaucoma eyes. *Ophthalmology*, 107, 1809-1815.

Gasch AT, Wang P and Pasquale LR (2000). Determinants of glaucoma awareness in a general eye clinic. *Ophthalmology*, 107, 303-308.

Gerrits HJM, de Haan B and Vendrick AJH (1966). Experiments with retinal stabilised images. Relations between the observations and neural data. *Vision Research*, 6, 427-440.

Gilpin LB, Stewart WC, Hunt HH and Broom CD (1990). Threshold variability using different Goldmann stimulus sizes. *Acta Ophthalmologica*, 68, 674-676.

Glass E, Schaumberger M and Lachenmayr BJ (1995). Simulations for FASTPAC and the standard 4-2dB Full Threshold strategy of the Humphrey Field Analyzer. *Investigative Ophthalmology & Visual Science*, 36, 1847-1854.

Glowazki A and Flammer J (1987). Is there a difference between patients with predominantly localized and those with diffuse visual-field damage. *Klinische Monatsblatter Fur Augenheilkunde*, 190, 301-302.

Gollamudi SR, Liao P and Hirsch J (1988). Evaluation of corrected loss variance as a visual field index. *Ophthalmologica*, 197, 144-150.

Gonzalez de la Rosa M, Jose Losada M, Serrano M and Morales J Gl- Tendency Oriented Perimetry. In Wall M and Wild JM (eds) *Perimetry* Update 1998/1999, Kugler Publications, Amsterdam/New York, 43-49.

Gonzalez de la Rosa M, Martinez A, Sanchez M, Mesa C, Cordoves L and MJ L (1996) Accuracy of Tendency Oriented Perimetry with the Octopus 1-2-3 perimeter. In Wall M and Heijl A (eds) *Perimetry Update 1996/1997.* Kugler Publications, Amsterdam/New York, 119-123.

Gonzalez de la Rosa M, Reyes JAA and Sierra MAG (1990). Rapid assessment of the visual field in glaucoma using an analysis based on multiple correlations. *Graefe's Archive for Clinical and Experimental Ophthalmology*, 228, 387-391.

Gordon MO, Beiser JA, Brandt JD, Heuer DK, Higginbotham EJ, Johnson CA, Keltner JL, Miller J, Parrish II RK, Wilson MR and Kass MA (2002). The Ocular Hypertension Treatment Study: Baseline factors predict the onset of primary open angle glaucoma. *Archives of Ophthalmology*, 122, 714-720.

Gordon MO and Kass MA (1999). The Ocular Hypertension Treatment Study: Design and baseline description of the participants. *Archives of Ophthalmology*, 117, 573-583.

Graham SL (1996). Comparison of psychophysical and electrophysiological testing in early glaucoma. *Investigative Ophthalmology & Visual Science*, 37, 2651-2662.

Graham SL and Drance SM (1995). Interpretation of high-pass resolution perimetry with a probability plot. *Graefe's Archive for Clinical and Experimental Ophthalmology*, 233, 140-149.

Gramer E, Steinhauser B and Kriegelstein GK (1982). The specificity of the automated suprathreshold perimeter Fieldmaster 200. *Graefe's Archive for Clinical and Experimental Ophthalmology*, 218, 253-255.

Greenstein VC, Halevy D, Zaidi Q, Koenig KL and Ritch RH (1996). Chromatic and luminance systems deficits in glaucoma. *Vision Research*, 36, 621-629.

Greenstein VC, Hood DC, Ritch R, Steinberger D and Carr RE (1989). S (blue) cone pathway vulnerability in retinitis pigmentosa, diabetes and glaucoma. *Investigative Ophthalmology & Visual Science*, 30, 1732-1737.

Greve EL (1973). Single and multiple stimulus static perimetry in glaucoma; the two phases of perimetry. *Documenta Ophthalmologica*, 36, 1-347.

Greve EL (1975). Static perimetry. *Ophthalmologica*, 171, 26-38.

Greve EL and Verduin WM (1977). Detection of early glaucomatous damage. Part 1. Visual field examination. Documenta *Ophthalmologica Proceedings Series* 14, 103-114.

Gur M (1989). Color and brightness fade-out in the ganzfeld is wavelength dependent. *Vision Research*, 29, 1335-1341.

Gur M (1991). Perceptual fade out occurs in the binocularly viewed ganzfeld. *Perception*, 20, 645-654.

Guthauser U and Flammer J (1988). Quantifying visual field damage caused by cataract. *American Journal of Ophthalmology*, 106, 480-484.

Gutteridge IF (1984). A review of strategies for screening of the visual fields. *Australian Journal of Optometry*, 67, 9-18.

Haas AL and Le Blanc RP (1995) The significance of the peripheral visual field in detecting early visual field changes in glaucoma. In Mills RP and Wall M (eds.), *Perimetry Update 1994/1995*. Kugler Publications, Amsterdam/New York. 623-630.

Haas AL and Flammer J (1985). Influence of diazepam on the outcome of automated perimetry. *Documenta Ophthalmologica* 42, 527-532.

Haeberlin H and Fankhauser F (1980). Adaptive programs for analysis of the visual field by automatic perimetry - basic problems and solutions. *Documenta Ophthalmologica*, 50, 123-141.

Haefliger IO and Flammer J (1991). Fluctuation of the differential light threshold at the border of absolute scotomas - comparison between glaucomatous visual field defects and blind spots. *Ophthalmology*, 98, 1529-1532.

Haley MJ (1987). The Humphrey Field Analyzer Primer. Allergan Humphrey, San Leandro., CA.

Harding GFA, Wild JM, Robertson KA, Lawden MC, Betts TA, Barber C and Barnes PMF (2000). Electro-oculography, electroretinography, visual evoked potentials and multifocal electroretinography in patients with vigabatrin-attributed visual field constriction. *Epilepsia*, 41, 1420-1431.

Hart WM and Hartz RK (1982). Computer-generated display for three-dimensional static perimetry. *Archives of Ophthalmology*, 100, 312-318.

Hart WM Jr and Gordon MO (1983). Calibration of the Dicon Auto Perimeter 2000 compared with that of the Goldmann Perimeter. *American Journal of Ophthalmology*, 96, 744-750.

Hart WM, Silverman SE, Trick GL, Nesher R and Gordon MO (1990). Glaucomatous visual field damage. Luminance and color-contrast sensitivities. *Investigative Ophthalmology & Visual Science*, 31, 359-367.

Harwerth RS, Carterdawson L, Shen F, Smith EL and Crawford MLJ (1999). Ganglion cell losses underlying visual field defects from experimental glaucoma. *Investigative Ophthalmology & Visual Science*, 40, 2242-2250.

Harwerth RS, Crawford MLJ, Frishman LJ, Viswanathan S, Smith EL and Carter-Dawson L (2002). Visual field defects and neural losses from experimental glaucoma. *Progress in Retinal and Eye Research*, 21, 91-125.

Harwerth RS, Smith EL and Chandler M (1999). Progressive visual field defects from experimental glaucoma: Measurements with white and colored stimuli. *Optometry and Vision Science*, 76, 558-570.

Harwerth RS, Smith ELI and Desantis L (1993). Mechanisms mediating visual detection in static perimetry. *Investigative Ophthalmology & Visual Science*, 34, 3011-3023.

Hayashi K, Hayashi H, Nakao F and Hayashi F (2001). Influence of cataract surgery on automated perimetry in patients with glaucoma. *American Journal of Ophthalmology*, 132, 41-46.

Heijl A (1977). Time changes of contrast thresholds during automatic perimetry. *Acta Ophthalmologica*, 55, 696-708.

Heijl A (1985). Computerized perimetry. *Transactions of the Ophthalmological Societies of the United Kingdom*, 104, 76-87.

Heijl A (1985). The Humphrey Field Analyzer, construction and concepts. *Documenta Ophthalmologica Proceedings Series*. 42, 77-84

Heijl A (1989). Lack of diffuse loss of differential light sensitivity in early glaucoma. *Acta Ophthalmologica*, 67, 353-360.

Heijl A and Drance SM (1983). Changes in differential threshold in patients with glaucoma during prolonged perimetry. *British Journal of Ophthalmology*, 67, 512-516.

Heijl A and Krakau CE (1977). A note of fixation during perimetry. *Acta Ophthalmologica*, 55, 854-861.

Heijl A, Lindgren A and Lindgren G (1989a). Inter-point correlattions of threshold values in normal and glaucomatous visual fields. In Heijl A (ed) *Perimetry Update 1988/89*. Kugler & Ghendini Publications, Amsterdam / New York 177-183

Heijl A, Lindgren A and Lindgren G (1989b). Test-retest variability in glaucomatous visual fields. *American Journal of Ophthalmology*, 108, 130-135.

Heijl A and Lundqvist L (1984). The frequency distribution of earliest glaucomatous visual field defects documented by automatic perimetry. *Acta Ophthalmologica*, 62, 658-664.

Heijl A and Patella VM (2002). *The Humphrey Field Analyzer Primer. Essential perimetry*. Third edition. Dublin, CA.

Heijl A and Asman P (1989). A clinical study of perimetric probability maps. *Archives of Ophthalmology*, 107, 199-203.

Heijl A and Bengtsson (1996). The effect of perimetric experience in patients with glaucoma. *Archives of Ophthalmology*, 114, 19-22.

Heijl A and Krakau CET (1975). An automatic static perimeter, design and pilot study. *Acta Ophthalmologica*, 53, 293-310.

Heijl A, Leske MC, Bengtsson B and Hussein M (2003). Measuring visual field progression in the Early Manifest Glaucoma Trial. *Acta Ophthalmologica*, 81, 286-293.

Heijl A, Lindgren A and Lindgren G (1989b). Test-retest variability in glaucomatous visual fields. *American Journal of Ophthalmology*, 108, 130-135.

Heijl A, Lindgren G and Olsson J (1987a). Normal variability of static perimetric threshold values across the central visual-field. *Archives of Ophthalmology*, 105, 1544-1549.

Heijl A, Lindgren G and Olsson J (1987b). A package for the statistical analysis of visual fields. *Documenta Ophthalmologica Proceedings Series*, 153-168.

Heijl A, Lindgren G and Olsson J (1989c). The effect of perimetric experience in normal subjects. *Archives of Ophthalmology*, 107, 81-86.

Heijl A, Lindgren G, Olsson J and Asman P (1992). On weighted visual field indices. *Graefe's Archive for Clinical and Experimental Ophthalmology*, 230, 397-398.

Hendry SHC and Reid RC. (2000). The koniocellular pathway in primate vision. *Annual Review of Neuroscience*, 23, 127-153.

Henson DB (1994) *Visual Fields*. Oxford University Press.

Henson DB, Chaudry S, Artes PH, Faragher EB and Ansons A (2000) Response variability in the visual field: Comparison of optic neuritis, glaucoma, ocular hypertension and normal eyes. *Investigative Ophthalmology & Visual Science*, 41, 417-421.

Henson DB, Evans J, Chauhan BC and Lane C (1996). Influence of fixation accuracy on threshold variability in patients with open angle glaucoma. *Investigative Ophthalmology & Visual Science*, 37, 444-450.

Henson DB, Artes PH and Chauhan BC (1999). Diffuse loss of sensitivity in early glaucoma. *Investigative Ophthalmology & Visual Science*, 40, 3147-3151.

Henson DB, Chauhan BC and Hobley A (1988). Screening for glaucomatous visual field defects: the relationship between sensitivity and specificity and the number of test locations. *Ophthalmic and Physiological Optics*, 8, 123-127.

Heron G, Adams AJ and Husted R (1988). Central visual fields for short wavelength sensitive pathways in glaucoma and ocular hypertension. *Investigative Ophthalmology & Visual Science*, 29, 64-72.

Hills JF and Johnson CA (1988). Evaluation of the t-test as a method of detecting visual field changes. *Ophthalmology*, 95, 261-266.

Hirsbrunner H, Fankhauser F, Jenni A and Funkhouser A (1990). Evaluating a perimetric expert system: Experience with Octosmart. *Graefe's Archive for Clinical and Experimental Ophthalmology*, 228, 237-241.

Traquair HM (1957). *Traquair's Clinical Perimetry*. VIIth edition 1957. Kimpton, London.

Hodapp E, Parrish II RK and Anderson D (1993). *Clinical Decisions in Glaucoma*. St. Louis, Mosby-Year Book, Inc.

Holmin C and Krakau CE (1979). Variability of glaucomatous visual field defects in computerized perimetry. *Albrecht von Graefe's Archive for Clinical and Experimental Ophthalmology*, 210, 235-250.

Hubner R (1996). Specific effects of spatial frequency uncertainty and different cue types on contrast detection - data and models. *Vision Research*, 36, 3429-3439.

Hudson C and Wild JM (1992). Assessment of physiologic statokinetic dissociation by automated perimetry. *Investigative Ophthalmology & Visual Science*, 33, 3162-3168.

Hudson C, Wild JM and Archer-Hall J (1993). Maximizing the dynamic range of the Humphrey Field Analyzer for blue-on-yellow perimetry. *Ophthalmic and Physiological Optics*, 13, 405-408.

Hudson C, Wild JM and O'Neill EC (1994). Fatigue effects during a single session of automated static threshold perimetry. *Investigative Ophthalmology & Visual Science*, 35, 268-280.

Hutchings N, Hosking SL, Wild JM and Flanagan JG (2001). Long-term fluctuation in short-wavelength automated perimetry in glaucoma suspects and glaucoma patients. *Investigative Ophthalmology & Visual Science*, 42, 2332-2337.

Hutchings N, Wild JM, Hussey MK, Flanagan JG and Trope GE (2000). The long-term fluctuation of the visual field in stable glaucoma. *Investigative Ophthalmology & Visual Science*, 41, 3429-3436.

Hutchings N, Wild JM, Hussey MK and Trope GE (1993). The homogeneous and heterogeneous components of the long-term fluctuation in glaucomatous field loss. *Investigative Ophthalmology & Visual Science*, 34, 1263.

Jaffe GJ, Alvarado JA and Juster RP (1986). Age-related changes of the normal visual field. *Archives of Ophthalmology*, 104, 1021-1025.

Janz NK, Wren PA, Lichter PR, Musch DC, Gillespie BW, Guire KE and Mills RP (2001). The Collaborative Initial glaucoma Treatment Study: Interim quality of life findings after initial medical or surgical treatment of glaucoma. *Ophthalmology*, 108, 1939-1940.

Jerrison HJ and Pickett RM (1964). Vigilance: The importance of the elicited observing rate. *Science*, 143, 970-971.

Johnson C, Adams C and Lewis R (1988). Fatigue effects in automated perimetry. *Applied Optics*, 27, 1030-1037.

Johnson C, Chauhan B and Shapiro L (1992). Properties of staircase procedures for estimating the thresholds in automated perimetry. *Investigative Ophthalmology & Visual Science*, 33, 2966-2974.

Johnson CA (1994). Selective versus non-selective losses in glaucoma. *Journal of Glaucoma*, 3, 532-544.

Johnson CA (1993). Role of automation in new instrumentation. *Optometry and Vision Science*, 70, 288-298.

Johnson CA, Adams AJ and Casson EJ (1993a). Blue-on-yellow perimetry: A five year overview. *Perimetry Update 1992/1993*, Kugler Publications, Amsterdam / New York. 459-465.

Johnson CA, Adams AJ, Twelker JD and Quigg JM (1988). Age-related changes in the central visual field for short-wavelength-sensitive pathways. *Journal of the Optical Society of America A*, 5, 2131-2139.

Johnson CA and Choy D (1987). On the definition of age-related norms for visual function testing. *Applied Optics*, 26, 1449-1454.

Johnson CA, Keltner JL, Cello KE, Edwards M, Kass MA, Gordon MO, Budenz DL, Gaasterland DE and Werner EB (2002). Baseline visual field characteristics in the Ocular Hypertension Treatment Study. *Ophthalmology*, 109, 432-437.

Johnson CA, Adams AJ, Casson EJ and Brandt JD (1993b). Blue-on-yellow perimetry can predict the development of glaucomatous visual field loss. *Archives of Ophthalmology*, 111, 645-650.

Johnson CA, Adams AJ, Casson EJ and Brandt JD (1993c). Progression of early glaucomatous visual field loss as detected by blue-on-yellow and standard white-on-white automated perimetry. *Archives of Ophthalmology*, 111, 651-656.

Johnson CA, Adams AJ and Lewis RA (1989). Evidence for a neural basis of age-related visual-field loss in normal observers. *Investigative Ophthalmology & Visual Science*, 30, 2056-2064.

Johnson CA, Brandt JD, Khong AM and Adams AJ (1995). Short-wavelength automated perimetry in low- medium, and high-risk ocular hypertensive eyes. *Archives of Ophthalmology*, 113, 70-76.

Johnson CA, Casson EJ, Adams AJ, Shapiro LR and Brandt JD (1992b). Progression of glaucomatous visual field loss over five years: A comparison of white-on-white and blue-on-yellow perimetry. *Investigative Ophthalmology & Visual Science*, 33, 1384.

Johnson CA and Keltner JL (1981). Computer analysis of visual field loss and optimization of automated perimetric test strategies. *Ophthalmology*, 88, 1058-1065.

Johnson CA and Keltner JL (1987). Optimal rates of movement for kinetic perimetry. *Archives of Ophthalmology*, 105, 73-75.

Johnson CA, Keltner JL and Balestrery F (1978). Effects of target size and eccentricity on visual detection and resolution. *Vision Research*, 18, 1217-1222.

Johnson CA and Marshall D (1995). Aging effects for opponent mechanisms in the central visual field. *Optometry and Vision Science*, 72, 75-82.

Johnson CA and Nelson-Quigg J (1993c). A prospective three-year study of response properties of normal subjects and patients during automated perimetry. *Ophthalmology*, 100, 269-274.

Johnson CA and Samuels SJ (1997). Screening for glaucomatous visual field loss with Frequency Doubling perimetry. *Investigative Ophthalmology & Visual Science*, 38, 413-425.

Johnson CA and Shapiro LR (1989). A comparison of MOBS (Modified Binary Search) and staircase test procedures in automated perimetry. *Optical Society of America Technical Digest Series*, 7, 84-87.

Johnson CA and Shapiro LR A rapid heuristic test procedure for automated perimetry. In Mills RP and Heijl A (eds.), *Perimetry Update 1990/91*. Kugler Publications, Amsterdam/New York, 251-256.

Jonas JB, Schmidt AM, Müller-Bergh JA (1992). Human optic nerve fiber count and optic disc size. *Investigative Ophthalmology & Visual Science*, 33, 2012-2018.

Kaplan E and Shapley RM (1982). X and Y cells in the lateral geniculate nucleus of macaque monkeys. *Journal of Physiology*, 330, 125-143.

Katz J (1999). Scoring systems for measuring progression of visual field loss in clinical trials of glaucoma treatment. *Ophthalmology*, 106, 391-395.

Katz J, Congdon N and Friedman DS (1999). Methodological variations in estimating apparent progressive visual field loss in clinical trials of glaucoma treatment. *Archives of Ophthalmology*, 117, 1137-1142.

Katz J, Quigley HA and Sommer A (1995). Repeatability of the Glaucoma Hemifield Test in automated perimetry. *Investigative Ophthalmology & Visual Science*, 36, 1658-1664.

Katz J and Sommer A (1986). Asymmetry and variation in the normal hill of vision. *Archives of Ophthalmology*, 104, 65-68.

Katz J and Sommer A (1987). A longitudinal study of the age-adjusted variability of automated visual fields. *Archives of Ophthalmology*, 105, 1083-1086.

Katz J and Sommer A (1988). Reliability indices of automated perimetric tests. *Archives of Ophthalmology*, 106, 1252-1254.

Katz J and Sommer A (1990). Reliability of automated perimetric tests. *Archives of Ophthalmology*, 108, 777-778.

Katz J, Sommer A and Witt K (1991). Reliability of visual field results over repeated testing. *Ophthalmology*, 98, 70-75.

Kaufmann H and Flammer J (1988). Clinical experience with the Bebié curve. In Heijl A (ed.), *Perimetry Update*, Kugler Publications, Amsterdam/New York. 235-238.

Keele SW (1986). Motor Control. In Boff KR, Kaufmann L and Thomas JP (eds.), *Handbook of Perception of Human Performance. Cognitive Processes and Performance*. Wiley, New York, 30-34.

Kelly D (1976). Frequency doubling in visual responses. *Journal of the Optical Society of America*, 56, 1628-1633.

Kelly D (1981). Non-linear visual responses to flickering sinusoidal gratings. *Journal of the Optical Society of America*, 71, 1051-1055.

Kelly DH, Boynton RM and Baron WS (1976). Primate flicker sensitivity: psychophysics and electrophysiology. *Science*, 194, 1077-1079.

Keltner JL and Johnson CA (1995). Short-wavelength automated perimetry in neuro-ophthalmological disorders. *Archives of Ophthalmology*, 113, 475-481.

Keltner JL, Johnson CA and Balestrery FG (1979). Suprathreshold static perimetry. Initial clinical trials with the fieldmaster automated perimeter. *Archives of Ophthalmology*, 97, 260-272.

Kilbride P, Hutman L, Fishman M and Read J (1986). Foveal cone pigment density differences in the aging human eye. *Vision Research*, 26, 321-325.

Kim LS (2002). PhD Thesis. Cardiff School of Optometry and Vision Sciences, Cardiff University.

Kim YY, Kim JS, Shin DH, Kim C and Jung HR (2001). Effect of cataract extraction on the blue-on-yellow visual field. *American Journal of Ophthalmology*, 132, 217-220.

King AJW, Taguri A, Wadood AC and Azuara-Blanco A (2002). Comparison of two fast strategies, SITA Fast and TOP, for the assessment of visual fields in glaucoma patients. *Graefe's Archive for Clinical and Experimental Ophthalmology*, 240, 481-487.

King D, Drance SM, Douglas GR and Wijsman K (1986). The detection of paracentral scotomas with varying grids in computed perimetry. *Archives of Ophthalmology*, 104, 524-525.

King-Smith PE and Carden D (1976). Luminance and opponent-color contributions to visual detection and adaptation and to temporal and spatial integration. *Journal of the Optical Society of America*, 66, 709-717.

King-Smith PE, Grigsby SS, Vingrys AJ, Benes SC and Supowit A (1994). Efficient and unbiased modification of the Quest threshold method: Theory, simulations, experimental evaluation and practical implementation. *Vision Research*, 34, 885-912.

Klein BEK, Klein R, Sponsel WE, Franke T, Cantor LB, Martone J and Menage MJ (1992). Prevalence of glaucoma. The Beaver Dam Eye Study. *Ophthalmology*, 99, 1499-1504.

Koch P, Roulier A and Fankhauser F (1972). Perimetry - the information theoretical basis for its automation. *Vision Research*, 12, 1619-1630.

Kono Y, Chi QM, Tomita G, Yamamoto T and Kitazawa Y (1997). High-pass resolution perimetry and the Humphrey Field Analyzer as indicators of glaucomatous optic disc abnormalities. A comparative study. *Ophthalmology*, 104, 1496-1502.

Kono Y, Yamamoto T and Kitazawa Y (1997). A new scoring system for comparing the results of high-pass resolution perimetry and differential light sensitivity perimetry in glaucoma patients. *Acta Ophthalmologica*, 75, 537-540.

Koskela PU, Airaksinen PJ and Tuulonen A (1990). The effect of jogging on visual field indices. *Acta Ophthalmologica*, 68, 91-93.

Kulze J, Stewart W and Sutherland S (1990). Factors associated with a learning effect in glaucoma patients using automated perimetry. *Acta Ophthalmologica*, 68, 681-686.

Kunimatsu S, Suzuki Y, Shirato S and Araie M (2000). Usefulness of gaze tracking during perimetry in glaucomatous eyes. *Japanese Journal of Ophthalmology*, 44, 187-191.

Kutzko KM, Brito CF and Wall M (2000). Effect of instructions on conventional automated perimetry. *Investigative Ophthalmology & Visual Science*, 41, 2006-2013.

Kwon Y, Park H, Jap A, Ugurlu S and Caprioli J (1998). Test-retest variability of blue-on-yellow perimetry is greater than white-on-white perimetry in normal subjects. *American Journal of Ophthalmology*, 129, 29-36.

Lachenmayr BJ, Kiermeir U and Kojetinsky S (1995). Points of a normal visual field are not statistically independent. *German Journal of Ophthalmology*, 4, 175-181.

Lachkar Y, Barrault O, Lefrancois A and Demailly P (1998). Rapid Tendency Oriented Perimetry (TOP) with the Octopus visual field analyzer. *Journal Francais d' Ophtalmologie*, 21, 180-184.

Lam BL, Alward WL and Kolder HE (1991). Effect of cataract on automated perimetry. *Ophthalmology*, 98, 1066-1070.

Langerhorst CT, van den Berg T, Veldman E and Greve E (1987). Population study of global and local fatigue within prolonged threshold testing in automated perimetry. *Documenta Ophthalmologica Proceedings Series*, 49, 657-662.

Langerhorst CT, Van Den Berg TJTP, Van Spronsen R and Greve EL (1984). Results of a fluctuation analysis and defect volume program for automated static threshold perimetry with the scoperimeter. *Documenta Ophthalmologica Proceedings Series*, 42, 1-6.

Langerhorst CT, Vandenberg T and Greve EL (1989). Is there a general reduction of sensitivity in glaucoma? *International Ophthalmology*, 13, 31-35.

Lennie P (1980). Parallel visual pathways: A review. *Vision Research*, 20, 561-594.

Lewis RA, Johnson CA and Keltner JL (1986). Variability of quantitative automated perimetry in normal observers. *Ophthalmology*, 93, 878-881.

Lindblom B and Westheimer G (1992). Uncertainty effects in orientation discrimination of foveally seen lines in human observers. *Journal of Physiology*, 454, 1-8.

Lidenmuth KA, Skuta GL, Rabbani R (1990). Effects of pupillary dilation on automated perimetry in normal patients. *Ophthalmology*, 97, 367-370.

Lindenmuth KA, Skuta GL, Rabbani R and Musch DC (1989). Effects of pupillary constriction on automated perimetry in normal eyes. *Ophthalmology*, 96, 1298-1301.

Litwak AB (2001) *Glaucoma Handbook*. Butterworth-Heinemann, Boston.

Livingstone MS and Hubel DH (1987). Psychophysical evidence for separate channels for the perception of form, color, movement, and depth. *Journal of Neuroscience*, 7, 3416-3468.

Livingstone MS and Hubel DH (1988). Do the relative mapping densities of the magno- and parvocellular systems vary with eccentricity. *Journal of Neuroscience*, 8, 4334-4339.

Lutze M and Bresnick GH (1991). Lenses of diabetic patients 'yellow' at an accelerated rate similar to older normals. *Investigative Ophthalmology & Visual Science*, 32, 194-199.

Lynch S, Johnson CA and Demirel S. Is early damage in glaucoma selective for a particular cell type or pathway? In Wall M and Heijl A (eds.), *Perimetry Update, 1996/1997*, Kugler Publications, Amsterdam/New York. 253-261.

Lynn JR (1969). Examination of the visual field in glaucoma. *Investigative Ophthalmology & Visual Science*, 8, 76-86.

Lynn JR and Tate GW (1975). Computer controlled apparatus for automatic visual field examination. *United States Patent No. 3*, 883, 234.

Maddess T, James AC, Goldberg I, Wine S and Dobinson J (2000). Comparing a parallel PERG, automated perimetry, and Frequency Doubling thresholds. *Investigative Ophthalmology & Visual Science*, 41, 3827-3832.

Maeda H, Nakaura M and Negi A (2000). New perimetric threshold test algorithm with dynamic strategy and Tendency Oriented Perimetry (TOP) in glaucomatous eyes. *Eye*, 14, 747-751.

Mandava S, Zulauf M, Zeyen T and Caprioli J (1993). An evaluation of clusters in the glaucomatous visual field. *American Journal of Ophthalmology*, 116, 684-691.

Mann CG, Orr AC, Rubillowicz M and Le Blanc RD (1988). Automated static perimetry in chloroquine and hydroxychloroquine therapy. In Heijl A (ed.), *Perimetry Update 1988/1989*. Kugler & Ghedini Publications, Amsterdam/ New York. 523-560.

Marchini G, Pisano F, Bertagnin F, Maraffa M and Bonomi L (1991). Perimetric learning effect in glaucoma patients. *Glaucoma*, 13, 102-106.

Marra G and Flammer J (1991). The learning and fatigue effect in automated perimetry. *Graefe's Archive for Clinical and Experimental Ophthalmology*, 229, 501-504.

Marraffa M, Marchini G, Albertini R and Bonomi L (1989). Comparison of different screening methods for the detection of visual field defects in early glaucoma. *International Ophthalmology*, 13, 43-45.

Marrocco RT, McClurkin JW and Young RA (1982). Modulation of lateral geniculate nucleus cell responsiveness by visual activation of the corticogeniculate pathway. *Journal of Neuroscience*, 2, 256-263.

McNaught AI (1996). Visual field progression: Comparison of Humphrey Statpac 2 and pointwise linear regression analysis. *Graefe's Archive for Clinical and Experimental Ophthalmology*, 234, 411-418.

Merigan WH and Maunsell JHR (1993). How parallel are the primate visual pathways. *Annual Review of Neuroscience*, 16, 369-402.

Meyer DR, Stern JH, Jarvis JM and Lininger LL (1993). Evaluating the visual field effects of blepharoptosis using automated static perimetry. *Ophthalmology*, 100, 651-659.

Midelfart A, Midelfart E and Brodtkrop E (2000). Visual field defects in patients taking vigabatrin. *Acta Ophthalmologica*, 78, 580-584.

Mikelberg FS and Drance SM (1984). The mode of progression of visual field defects in glaucoma. *American Journal of Ophthalmology*, 98, 443-445.

Mikelberg FS, Drance SM, Schulzer M (1989). The normal human optic nerve. *Ophthalmology*, 96, 1325-1328.

Miller KN, Shields MB and Ollie AR (1989). Automated kinetic perimetry with two peripheral isopters in glaucoma. *Archives of Ophthalmology*, 107, 1316-1320.

Miller RJ, Pigion RG, Wesner MF and Patterson JG (1983). Accommodation fatigue and dark focus - the effects of accommodation-free visual work as assessed by two psychophysical methods. *Perception & Psychophysics*, 34, 532-540.

Mills RP (1984). A comparison of Goldmann, Fieldmaster 200, and Dicon AP2000 perimeters used in a screening mode. *Ophthalmology*, 91, 347-354.

Mills RP, Barnebey HS, Migliazzo CV and Li Y (1994). Does saving time using FASTPAC or suprathreshold testing reduce the quality of visual fields? *Ophthlamology*, 101, 1596-1603.

Milosevic S (1974). Effect of time and space uncertainty on a vigilance task. *Perception & Psychophysics*, 15, 331-334.

Morales J, Weitzman ML and Gonzalez de la Rosa M (2000). Comparison between Tendency Oriented Perimetry (TOP) and Octopus Threshold perimetry. *Ophthalmology*, 107, 134-142.

Moss ID and Wild JM (1994). The influence of induced forward light scatter on the normal blue-on-yellow perimetric profile. *Graefe's Archive for Clinical Experimental Ophthalmology*, 232.

Moss ID, Wild JM and Whitaker DJ (1995). The influence of age-related cataract on blue-on-yellow perimetry. *Investigative Ophthalmology & Visual Science*, 36, 764-773.

Musch DC, Lichter PR, Guire KE, Standardi CL and Group CS (1999). The Collaborative Initial Glaucoma Treatment Study. *Ophthalmology*, 106, 653-662.

Niceley PE and Miller GA (1957). Some effects of unequal spatial distribution on the detectability of radar targets. *Journal of Experimental Psychology*, 53, 195-198.

Nordmann JP, Brion F, Hamard P and Mouton-Chopin D (1998). Evaluation of the Humphrey perimetry programs SITA Standard and SITA Fast in normal probands and patients with glaucoma. *Journal of the French Ophthalmology Society*, 21, 549-554.

Nork TM, Poulsen GL, Nickells RW, Ver Hoeve JN, Cho N, Levin LA and Lucarelli MJ (2000). Protection of ganglion cells in experimental glaucoma by retinal laser photocoagulation. *Archives of Ophthalmology*, 118, 1242-1250.

Noureddin BN, Poinoosawmy D, Fitzke FW and Hitchings RA (1991). Regression-analysis of visual field progression in low tension glaucoma. *British Journal of Ophthalmology*, 75, 493-495.

Nouri-Mahdavi K, Hoffman D, Gaasterland D and Caprioli J (2004). Prediction of visual field progression in glaucoma. *Investigative Ophthalmology & Visual Science*, 45, 4346-4351.

O'Brien C, Poinoosawmy D, Wu J and Hitchings R (1994). Evaluation of the Humphrey FASTPAC threshold program in glaucoma. *British Journal of Ophthalmology*, 78, 516-519.

O'Connor DJ, Zeyen T and Caprioli J (1993). Comparisons of methods to detect glaucomaous optic nerve damage. *Ophthalmology*, 100, 1498-1503.

Octopus (1997). *Octopus Tendency Oriented Perimetry*. Interzeag AG, Schlieren, Switzerland.

Octopus (2002). *Octopus 301/311 User's Manual. Revision 1.* Interzeag AG, Schlieren, Switzerland.

Ogawa T and Suzuki R (1979). Relation between central and peripheral visual field changes with kinetic perimetry. *Documenta Ophthalmologica Proceedings Series*, 19, 469-474.

Olsson J, Asman P and Heijl A (1997b). A perimetric learner's index. *Acta Ophthalmologica*, 75, 665-668.

Olsson J, Bengtsson B, Heijl A and Rootzen H (1997). An improved method to estimate frequency of false positive answers in computerized perimetry. *Acta Ophthalmologica*, 75, 181-183.

Olsson J, Heijl A, Bengtsson B and Rootzen H (1992) Frequency-of-seeing in computerised perimetry. In Mills RP (ed.) *Perimetry Update1992/1993*, Kugler Publications, Amsterdam/ New York. 551-556.

Olsson J and Rootzen H (1994). An image model for quantal response analysis in perimetry. *Scandinavian Journal of Statistics*, 21, 375-387.

Olsson J, Rootzen H and Heijl A. Maximum likelihood estimation of the frequency of false-positive and false-negative answers from the up-and-down staircases of computerized threshold perimetry. In Heijl A (ed.), *Perimetry Update 1988/1989* Kugler & Ghedini, Amsterdam/ New York. 245-251.

Orzalesi N, Miglior S, Lonati C and Rosetti L (1999). Microperimetry of localised retinal nerve fibre layer defects. *Vision Research*, 38, 763-771.

Pacey IE (1998) PhD Thesis. Department of Vision Sciences, Aston University, Birmingham.

Panda-Jonas S, Jonas JB and Jakobczyk-Zmija M (1994). Retinal photoreceptor density decreases with age. *Ophthalmology*, 102, 1853-1859.

Parrish RK, Schiffman J and Anderson DR (1984). Static and kinetic visual field testing; reproducibility in normal volunteers. *Archives of Ophthalmology*, 102, 1497-1502.

Patel SC, Freidman DS, Varadkar P and Robin AL (2000). Algorithm for interpreting the result of Frequency Doubling Perimetry. *American Journal of Ophthalmology*, 129, 323-327.

Pearson PA, Baldwin LB and Smith TJ. The q-statistic in glaucoma and ocular hypertension. In Heijl A (ed.), *Perimetry Update 1988/89*, Kugler Publications, Amsterdam/ New York. 229-233.

Pearson PA, Baldwin LB and Smith TJ (1990). The relationship of Mean Defect to Corrected Loss Variance in glaucoma and ocular hypertension. *Ophthalmologica*, 200, 16-21.

Pennebaker GE, Stewart WC, Stewart JA and Hunt HH (1992). The effect of stimulus duration upon the components of fluctuation in static automated perimetry. *Eye*, 6, 353-355.

Peridata: *Peridata Manual (v 6.3a)*. Interzeag AG, Schlieren, Switzerland.

Philipson B (1969). Light scattering in lenses with experimental cataract. *Acta Ophthalmologica*, 47, 1089-1101.

Pollack I (1968). Computer simulation of threshold observations by Method of Limits. *Perceptual and Motor Skills*, 26, 583-586.

Polo V, Abecia E, Pablo LE, Pinilla I, Larrosa JM and Honrubia FM (1998). Short-wavelength automated perimetry and retinal nerve fiber layer evaluation in suspected cases of glaucoma. *Archives of Ophthalmology*, 116, 1295-1298.

Portney GL and Krohn MA (1978). Automated perimetry: Background, instruments and methods. *Survey of Ophthalmology*, 22, 271-278.

Pupura K, Tranchina D, Kaplan E and Shapley RM (1990). Light adaptation in the primate retina: Analysis of the changes in gain and dynamics of monkey retinal ganglion cells. *Visual Neuroscience*, 4, 75-93.

Quach TD, Nguyen BV, Eilliott III WR, Redmond RM and Sponsel WE, Evaluating the Delphi system for rapid assessment of visual function using the Humphrey perimeter. In Wall M and Heijl A (eds.), *Perimetry Update 1996/1997*, Kugler Publications, Amsterdam/ New York. 113-118.

Quigley HA (1987). Are some ganglion cells killed by glaucoma before others? In Kriegelstein GK (ed.) *Glaucoma Update III*, Springer-Verlag, Berlin/Heidelberg. 23-26.

Quigley HA (1994). Selective cell-death in glaucoma - does it really occur? *British Journal of Ophthalmology*, 78, 879-880.

Quigley HA (1996). Number of people with glaucoma worldwide. *British Journal of Ophthalmology*, 80, 389-393.

Quigley HA (1998). Neuronal death in glaucoma. *Progress in Retinal and Eye Research*, 18, 39-57.

Quigley HA, Addicks EM and Green WR (1982). Optic-nerve damage in human glaucoma. 3. Quantitative correlation of nerve-fiber loss and visual field defect in glaucoma, ischemic neuropathy, papilloedema, and toxic neuropathy. *Archives of Ophthalmology*, 100, 135-146.

Quigley HA, Dunkelberger GR and Green R (1988). Chronic human glaucoma causing selectively greater loss of large optic nerve fibers. *Ophthalmology*, 95, 357-363.

Quigley HA, Dunkelberger GR and Green WR (1989). Retinal ganglion cell atrophy correlated with automated perimetry in human eyes with glaucoma. *American Journal of Ophthalmology*, 107, 453-464.

Radius RL (1987). Anatomy of the optic nerve head and glaucomatous optic neuropathy. *Survey of Ophthalmology*, 32, 35-44.

Reed H and Drance SM (1972). *The Essentials of Perimetry. Static and Kinetic.* 2nd Edition. Oxford University Press, London, New York and Toronto.

Reitner A, Tittl M, Ergun E and Baradaran Dilmaghani R (1996). The efficient use of perimetry for neuro-ophthalmic diagnosis. *British Journal of Ophthalmology*, 80, 903-905.

Repka MX and Quigley HA (1989). The effect of age on normal human optic nerve fiber number and diameter. *Ophthalmology*, 96, 26-32.

Reynolds M, Stewart WC and Sutherland S (1990). Factors that influence the prevalence of positive catch-trials in glaucoma patients. *Graefe's Archive for Clinical and Experimental Ophthalmology*, 228, 338-341.

Riggs LA, Ratliff F, Cornsweet TN and Cornsweet E (1953). The disappearance of steadily fixated visual test objects. *Journal of the Optical Society of America*, 43, 495-501.

Rose RM (1970). Statistical properties of staircase estimates. *Perception & Psychophysics*, 8, 199-204.

Rutishauser C and Flammer J (1988). Retests in static perimetry. *Graefe's Archive for Clinical and Experimental Ophthalmology*, 226, 76-77.

Rynes RI (1983). Ophthalmic safety of long-term hydroxychloroquine sulfate treatment. *American Journal of Medicine*, 75, 35-39.

Safran AB, Bader C, Brazitikos PD, Deweisse C and Desangles D (1992). Increasing short-term fluctuation by increasing the intensity of the fixation aid during perimetry. *American Journal of Ophthalmology*, 113, 193-197.

Sample PA and RN W (1993). Variability and sensitivity of short-wavelength color visual fields in normal and glaucoma eyes. In: *Non-invasive Assessment of the Visual System*. Optical Society of America, Washington DC, 293-295.

Sample PA, Bosworth CF, Blumenthal EZ, Girkin C and Weinreb RN (2000). Visual function-specific perimetry for indirect comparison of different ganglion cell populations in glaucoma. *Investigative Ophthalmology & Visual Science*, 41, 1783-1790.

Sample PA, Boynton RM and Weinreb RN (1988). Isolating the color vision loss in primary open angle glaucoma. *American Journal of Ophthalmology*, 106, 686-691.

Sample PA, Esterson FD and Weinreb RN (1989). A practical method for obtaining an index of lens density with an automated perimeter. *Investigative Ophthalmology & Visual Science*, 30, 786-787.

Sample PA, Irak I, Martinez GA and Yamagishi N (1997). Asymmetries in the normal short-wavelength visual field: Implications for short-wavelength automated perimetry. *American Journal of Ophthalmology*, 124, 46-52.

Sample PA, Johnson CA, Haegerstrom-Portnoy G and Adams AJ (1996). Optimum parameters for short-wavelength automated perimetry. *Journal of Glaucoma*, 5, 375-383.

Sample PA, Taylor JDN, Martinez GA, Lusky M and Weinreb RN (1993). Short-wavelength color visual fields in glaucoma suspects at risk. *American Journal of Ophthalmology*, 115, 225-233.

Sample PA and Weinreb RN (1990). Color perimetry for assessment of primary open angle glaucoma. *Investigative Ophthalmology & Visual Science*, 31, 1869-1875.

Sample PA and Weinreb RN (1992). Progressive color visual field loss in glaucoma. *Investigative Ophthalmology & Visual Science*, 33, 2068-2071.

Sanabria O, Feuer WJ and Anderson AJ (1991). Pseudo-loss of fixation in automated perimetry. *Ophthalmology*, 98, 843.

Saunders RM (1975). The critical duration of temporal summation in the human central fovea. *Vision Research*, 15, 699-703.

Savage GL, Haegerstrom-Portnoy G, Adams AJ and Hewlett SE (1993). Age-changes in the optical density of human ocular media. *Clinical Vision Sciences*, 8, 97-108.

Schaumberger M, Schafer B and Lachenmayr BJ (1995). Glaucomatous visual fields FASTPAC versus Full Threshold strategy of the Humphrey Field Analyzer. *Investigative Ophthalmology & Visual Science*, 36, 1390-1397.

Scheibel ME, Lindsay RD, Tomiyasu U and Scheibel AB (1975). Progressive dendritic changes in aging human cortex. *Experimental Neurology*, 47, 392-403.

Scheifer U, Nowomiejska K and Paetzold J (2004). Semi-automated kinetic perimetry for assessment of advanced glaucomatous visual field loss. In Grehn F and Stamper R (eds.), *Glaucoma*. Springer, New York, 1, 51-61.

Schenone M, Traverso CE, Molfino F, Capris P, Corallo G and Semino E (1997). Comparison between computerized static perimetry and high-pass resolution perimetry in the follow-up of glaucomatous patients. *Acta Ophthalmologica*, 75, 48-49.

Schiefer U, Malsam A, Flad M, Stumpp F, Dietrich TJ, Paetzold J, Vonthein R, Knorr M and Denk PO (2001). Evaluation of glaucomatous visual field loss with locally condensed grids using Fundus-Oriented Perimetry (FOP). *European Journal of Ophthalmology*, 11, S57-62.

Schiefer U, Schiller J, Paetzold J, Benda N, Vonthein R and TJ D (2000). Evaluation and follow-up of advanced visual field defects with semi-automated kinetic perimetry (s-akp). *Investigative Ophthalmology & Visual Science*, 41, 1556B 1931 Suppl. S.

Schiefer U, Stercken-Sorrenti G, Dietrich TJ, Friedrich M and N B (1996). Fundus-Oriented Perimetry. Evaluation of a new visual field examination method for detecting angioscotoma. *Klinische Monatsblatter Fur Augenheilkunde*, 209, 62-71.

Schimiti RB, Avelino RR, Kara-Jose N and Costa VP (2002). Full Threshold versus Swedish Interactive Threshold Algorithm (SITA) in normal individuals undergoing automated perimetry for the first time. *Ophthalmology*, 109, 2084-2092.

Schmeid U (1980). Automatic (Octopus) and manual (Goldmann) perimetry in glaucoma. *Graefe's Archive for Clinical and Experimental Ophthalmology*, 213, 239-244.

Schwartz B and Nagin P (1985). Probability maps for evaluating automated visual fields. In Heijl A (ed.) *Perimetry Update 1985/1986,* Kugler Publications, Amsterdam /New York. 39-48.

Searle AET, Wild JM, Shaw DE and Oneill EC (1991). Time-related variation in normal automated static perimetry. *Ophthalmology*, 98, 701-707.

Sekhar GC, Naduvilath TJ, Lakkai M, Jayakumar AJ, Pandi GT, Mandal AK and Honavar SG (2000). Sensitivity of Swedish Interactive Threshold Algorithm compared with standard Full Threshold algorithm in Humphrey visual field testing. *Ophthalmology*, 107, 1303-1308.

Sharma AK, Goldberg I, Graham SL and Moshin M (2000). Comparison of the Humphrey Swedish Interactive Thresholding Algorithm (SITA) and Full Threshold strategies. *Journal of Glaucoma*, 9, 20-27.

Sherafat H, Spry PG, Waldock A, Sparrow JM and Diamond JP (2003). Effect of a patient training video on visual field test reliability. *British Journal of Ophthalmology*, 87, 153-156.

Siik S, Chylack LT, Friend J, Wolfe J, Teikari J, Nieminen H and Airaksinen PJ (1999). Lens autofluorescence and light scatter in relation to the lens opacities classification system, LOCS III. *Acta Ophthalmologica*, 77, 509-514.

Smith SD, Katz J and Quigley HA (1996). Analysis of progressive change in automated visual fields in glaucoma. *Investigative Ophthalmology & Visual Science*, 37, 1419-1428.

Sommer A, Enger C and witt K (1987). Screening for glaucomatous field loss with automated threshold perimetry. *American Journal of Ophthalmology*, 103, 681-684.

Sommer A, Katz J, Quigley HA, Miller NR, Robin AL, Richter RC and Witt KA (1991). Clinically detectable nerve fiber atrophy precedes the outset of glaucomatous field loss. *Archives of Ophthalmology*, 109, 77-83.

Spahr J (1975). Optimization of the presentation pattern in automated static perimetry. *Vision Research*, 15, 1275-1281.

Spenceley SE and Henson DB (1996). Visual field test simulation and error in threshold estimation. *British Journal of Ophthalmology*, 80, 304-308.

Sponsel WE, Arango S, Cot T, Y. and Mansah J (1998). Clinical classification of glaucomatous visual field loss by frequency doubling perimetry. *American Journal of Ophthalmology*, 125, 830-836.

Spry PGD, Henson DB, Sparrow JM and North RV (2000). Quantitative comparison of static perimetric strategies in early glaucoma: Test-retest variability. *Journal of Glaucoma*, 9, 247-253.

Spry PGD and Johnson CA (2002). Identification of progressive glaucomatous visual field loss. *Survey of Ophthalmology*, 47, 158-173.

Steinman RM and Levinson JZ (1990). The role of eye movements in the detection of contrast and spatial detail. In Kowler E (ed.), *Eye movements and their Role in Visual and Cognitive Processes. 4th edition.* Elsevier, Amsterdam, New York, Oxford. 115-208.

Stewart WC and Chauhan BC (1995). Newer visual function tests in the evaluation of glaucoma. *Survey of Ophthalmology*, 40, 119-135.

Stewart WC, Shields MB and Ollie AR (1989). Full Threshold versus Quantification of Defects for visual field testing in glaucoma. *Graefe's Archive for Clinical and Experimental Ophthalmology*, 227, 51-54.

Stiles W (1939). The directional sensitivity of the retina and the spectral sensitivity of the rods and cones. *Proceedings of the Royal Society, London (Series B)*, 127, 64-105.

Stroh CM (1971) *Vigilance: The Problem of Sustained Attention.* Pergamon Press, Oxford, New York, Toronto.

Suzumura H (1988). Visual fatigue-like effect in glaucomas with repeated threshold measurement. *Nippon Ganka Gakkai zasshi*, 92, 220-224.

Szatmary G, Biousse V and Newman NJ (2002). Can Swedish Interactive Thresholding Algorithm Fast perimetry be used as an alternative to Goldmann perimetry in neuro-ophthalmic practice? *Archives of Ophthalmology*, 120, 1162-1173.

Takada S, Matsumoto C, Okuyama S, Iwagi A and Otori T . Comparative evaluation of four strategies (Standard, Dynamic, TOP, 2-level) using the automated perimeter Octopus 1-2-3. In Heijl A (ed) *Perimetry Update 1998/1999*, Kugler Publications, Amsterdam/ New York. 35-41.

Taylor MM (1971). On the efficiency of psychophysical measurement. *Journal of the Accoustical Society of America*, 49, 505-508.

Taylor MM and Creelman CD (1967). PEST, efficient estimates on probability functions. *Journal of the Accoustical Society of America*, 41, 782-787.

Teeslau P, Airaksinen PJ, Tuulonen A, Nieminen H and Alank H (1996). Flourometry of the crystalline lens for correcting blue-on-yellow perimetry results. *Investigative Ophthalmology & Visual Science*, 37, 697-703.

Teichner WH (1974). The detection of a simple visual signal as a function of time of watch. *Human Factors*, 16, 339-353.

Tielsch JM, Katz J, Singh K, Quigley HA, Gottsch JD, Javitt J and Sommer A (1991). A population-based evaluation of glaucoma screening: The Baltimore eye survey. *American Journal of Epidemiology*, 134, 1102-1111.

Treutwein B (1995). Adaptive psychophysical procedures. *Vision Research*, 35, 2503-2522.

Trible JR, Schultz RO, Robinson JC and Rothe TL (2000). Accuracy of glaucoma detection with frequency doubling perimetry. *American Journal of Ophthalmology*, 129, 740-745.

Trope GE and Britton R (1987). A comparison of Goldmann and Humphrey automated perimetry in patients with glaucoma. *British Journal of Ophthalmology*, 71, 489-493.

Turpin A, McKendrick AM, Johnson CA and Vingrys AJ (2002a). Development of efficient threshold strategies for frequency doubling technology perimetry using computer simulation. *Investigative Ophthalmology & Visual Science*, 43, 322-331.

Turpin A, McKendrick AM, Johnson CA and Vingrys AJ (2002b) Performance of efficient test procedures for Frequency Doubling Technology perimetry in normal and glaucomatous eyes. *Investigative Ophthalmology & Visual Science*, 43, 709-715.

Turpin A, McKendrick AM, Johnson CA and Vingrys AJ (2003). Properties of perimetric threshold estimates from Full Threshold, ZEST, and SITA-like strategies, as determined by computer simulation. *Investigative Ophthalmology & Visual Science*, 44, 4787-4795.

Tyrrell RA and Owens DA (1988). A rapid technique to assess the resting states of the eyes and other threshold phenomena: The modified binary search (MOBS). *Behaviour Research Methods, Instruments & Computers*, 20, 137-141.

Van Coevorden RE, Mills RP, Chen YY and Barnebey HS (1999). Continuous visual field test supervision may not always be necessary. *Ophthalmology*, 106, 178-181.

Van Den Berg TJTP (1987). Relationship between media disturbances and the visual field. *Documenta Ophthalmologica Proceedings Series*, 49, 33-38.

Van Den Berg TJTP, Van Spronsen R, Van Veenendaal WG and Bakker D (1985). Psychophysics of intensity discrimination in relation to defect volume examination on the scoperimeter. *Documenta Ophthalmologica Proceedings Series*, 42, 147-151.

van Norren D and van Meel G (1985). Density of human cone photopigments as a function of age. *Investigative Ophthalmology & Visual Science*, 26, 1014-1016.

Vesti E, Johnson CA and Chauhan BC (2003). Comparison of different methods for detecting glaucomatous visual field progression. *Investigative Ophthalmology & Visual Science*, 44, 3873-3879.

Vingrys AJ and Demirel S (1998). False-response monitoring during automated perimetry. *Optometry & Vision Science*, 75, 513-517.

Vingrys AJ and Pianta M (1999). A new look at threshold estimation algorithms for automated static perimetry. *Optometry and Vision Science*, 76, 588-95.

Viswanathan AC, Fitzke FW and Hitchings RA (1997). Early detection of visual field progression in glaucoma: A comparison of Progressor and Statpac 2. *British Journal of Ophthalmology*, 81, 1037-1042.

Volbrecht VJ, Nerger JL, Imhoff SM and Ayde CJ (2000). Effect of the short-wavelength-sensitive cone mosaic and rods on the locus of unique green. *Journal of the Optical Society of America*, 17, 628-634.

Wadood AC, Azuara-Blanco A, Apsinall P, Taguri A and King AJW (2002). Sensitivity and specificity of Frequency Doubling Technology, Tendency Oriented Perimetry, and Humphrey Swedish Interactive Threshold Algorithm Fast perimetry in a glaucoma practice. *American Journal of Ophthalmology*, 133, 327-332.

Wall M (2004). What's new in perimetry. *Journal of Neuroophthalmology*, 24, 46-55.

Wall M, Kutzko KE and Chauhan BC (1997). Variability in patients with glaucomatous visual field damage is reduced using size V stimuli. *Investigative Ophthalmology & Visual Science*, 38, 426-435.

Wall.M, Kutzko KE and Chauhan BC (2002). The relationship of visual thresholds and reaction time to visual field eccentricity with conventional automated perimetry. *Vision Research*, 42, 781-787.

Wall M, Kardon R and Moore P (1992) Effects of stimulus size on test-retest variability. In Heijl A and Mills RP (eds.) *Perimetry Update 1992/93*, Kugler Publications, Amsterdam/ New York. 553-560.

Warm JS (1984). *Sustained Attention in Human Performance.* John Wiley & Sons., Chichester, New York, Brisbane, Toronto, Singapore.

Watson AB and Pelli DG (1983). QUEST - a Bayesian adaptive psychometric method. *Perception & Psychophysics*, 33, 113-120.

Weber J (1990). A new strategy for automated static perimetry. *Fortschritte der Ophthalmologie : Zeitschrift der Deutschen Ophthalmologischen Gesellschaft*, 87, 37-40.

Weber J, Dannheim F and Dannheim D (1990). The topographical relationship between optic disc and visual field in glaucoma. *Acta Ophthalmologica*, 68, 568-574.

Weber J and Klimaschka T (1995). Test time and efficiency of the Dynamic Strategy in glaucoma perimetry. *German Journal of Ophthalmology*, 4, 25-31.

Weber J and Baltes J (1994). Spatial summation in glaucomatous visual fields. In Mills RP and Wall M (eds.), *Perimetry Update 1994/1995*, Kugler Publications, Amsterdam/ NewYork. 63-72.

Weber J and Dobek K (1986). What is the most suitable grid for computer perimetry in glaucoma patients. *Ophthalmologica*, 192, 88-96.

Weber J and Geiger R (1988) Gray scale display of perimetric results. The influence of different interpolation procedures. In Heijl A (ed.), *Perimetry Update 1988/1989*, Kugler & Ghedini Publications, Amsterdam/ New York. 447-454.

Weber J and Klimaschka T (1995). Test time and efficiency of the dynamic strategy in glaucoma perimetry. *German Journal of Ophthalmology*, 4, 25-31.

Weber J and Krieglstein GK (1989). Graphical analysis of topographical trends in automated perimetry. *International Ophthalmology*, 13, 351-356.

Weber J and Rau S (1992). The properties of perimetric thresholds in normal and glaucomatous eyes. *German Journal of Ophthalmology*, 1, 79-85.

Webster AR, Luff AJ, Canning CR and Elkington AR (1993). The effect of pilocarpine on the glaucomatous visual field. *British Journal of Ophthalmology*, 77, 721-725.

Weijland A, Fankhauser F, Bebie H and Flammer J (2004). *Octopus Visual Field Digest. Automated perimetry.* Fifth edition. Interzeag AG, Schlieren, Switzerland.

Werner EB, Adelson A and Krupin T (1988). Effect of patient experience on the results of automated perimetry of clinically stable glaucoma patients. *Ophthalmology*, 95, 764-767.

Werner EB and Drance SM (1977). Early visual field disturbances in glaucoma. *Archives of Ophthalmology*, 95, 1173-1175.

Werner EB, Krupin T and Adelson A (1990). Effect of patient experience on the results of automated perimetry in glaucoma suspect patients. *Ophthalmology*, 97, 44-48.

Werner EB, Petrig B, Krupin T and Bishop KI (1989). Variability of automated visual fields in clinically stable glaucoma patients. *Investigative Ophthalmology & Visual Science*, 30, 1083-1089.

Werner EB, Saheb N and Thomas D (1982). Variability of static visual threshold responses in patients with elevated IOPs. *Archives of Ophthalmology*, 100, 1627-1631.

Westcott MC, McNaught AI, Crabb DP, Fitzke FW and Hitchings RA (1997). High spatial resolution automated perimetry in glaucoma. *British Journal of Ophthalmology*, 81, 452-459.

Whitaker D, Steen R and Elliott DB (1993). Light scatter in the normal young, elderly, and cataractous eye demonstrates little wavelength dependency. *Optometry and Vision Science*, 70, 963-968.

Wild JM (1997). SITA-a new outlook for visual field examination in primary and shared care. *Optician*, 213, 35-39.

Wild JM (2001). Short Wavelength Automated Perimetry. *Acta Ophthalmologica*, 79, 546-559.

Wild JM, Pacey IE, Hancock SA and Cunliffe IA (1999a). Between-algorithm, between-individual differences in normal perimetric sensitivity: Full Threshold, FASTPAC, and SITA. *Investigative Ophthalmology & Visual Science*, 40, 1152-1161.

Wild JM, Pacey IE, O'Neill EC and Cunliffe IA (1999b) The SITA perimetric threshold algorithms in glaucoma. *Investigative Ophthalmology & Visual Science*, 40, 1998-2009.

Wild JM, Betts TA, Ross K and Kenwood C (1998) Influence of antihistamines on central visual field assessment. In A. Heijl (ed.) *Perimetry Update 1988/1989*, Kugler Publications, Amsterdam/ New York. 439-445.

Wild JM, Betts TA and Shaw DE (1990). The influence of a social dose of alcohol on the central visual field. *Japanese Journal of Ophthalmology*, 34.

Wild JM, Cubbidge RP, Pacey IE and Robinson R (1998). Statistical aspects of the normal visual field in Short-wavelength Automated Perimetry. *Investigative Ophthalmology & Visual Science*, 39, 54-63.

Wild JM, Dengler-Harles M, Searle AET and O'Neill EC (1989). The influence of the learning effect on automated perimetry in patients with suspected glaucoma. *Acta Ophthalmologica*, 67, 537-545.

Wild JM, Hosking SL, Hutchings N, Flanagan JG and O'Donoghue EP (1997). Long-term fluctuation in Short-wavelength Automated Perimetry. *Investigative Ophthalmology & Visual Science*, 38, 2660.

Wild JM and Hudson C (1995). The attenuation of blue-on-yellow perimetry by the macular pigment. *Ophthalmology*, 102, 911-917.

Wild JM, Hutchings N, Hussey MK, Flanagan JG and Trope GE (1997). Pointwise univariate linear regression of perimetric sensitivity against follow-up time in glaucoma. *Ophthalmology*, 104, 808-815.

Wild JM, Kim LS, North RV and Morgan JE (2001). Stimulus size and the variability of the threshold response in short wavelength automated perimetry (SWAP). *Investigative Ophthalmology & Visual Science*, 42, 818.

Wild JM, Moss ID and O'Neill EC (1996). Baseline alterations in blue-on-yellow normal perimetric sensitivity. *Graefe's Archive for Clinical and Experimental Ophthalmology*, 234, 141-149.

Wild JM, Moss ID, Whitaker DJ and O'Neill EC (1995). The statistical interpretation of blue on yellow visual field loss. *Investigative Ophthalmology & Visual Science*, 36, 1398-1410.

Wild JM, Searle AET, Dengler-Harles M and O'Neill EC (1991). Long-term follow-up of baseline learning and fatigue effects in automated perimetry of glaucoma and ocular hypertensive patients. *Acta Ophthalmologica*, 69, 210-216.

Wild JM, Wood JM, Flanagan JG, Good PA and Crews SJ (1986). The interpretation of the differential threshold in the central visual field. *Documenta Ophthalmologica*, 62, 191-202.

Wild JM, Wood JM, Worthington FM and Crews SJ (1987). Some concepts on the use of three-dimensional isometric plots for the representation of differential sensitivity. *Documenta Ophthalmologica*, 65, 423-432.

Wildberger H and Robert Y (1988). How good are the correlations between contrast sensitivity and differential light sensitivity in the visual field center in optic neuropathies? *Klinische Monatsblatter Fur Augenheilkunde*, 192, 113-116.

Wilensky JT, Mermelstein JR and Siegel HG (1986). The use of different-sized stimuli in automated perimetry. *American Journal of Ophthalmology*, 101, 710-713.

Wilson MR, Kosoko O, Cowan CL, Sample PA, Johnson CA, Haynatzki G, Enger C and Crandall D (2002). Progression of visual field loss in untreated glaucoma patients and glaucoma suspects in St. Lucia, West Indies. *American Journal of Ophthalmology*, 134, 399-405.

Wishart P, Wardrop PK and Kosmin S (1998). Is visual field evaluation using multiple correlations and linear regressions useful? An evaluation of Delphi perimetry. *Graefe's Archive for Clinical and Experimental Ophthalmology*, 236, 493-500.

Wood JM, Wild JM, Bullimore MA and Gilmartin B (1988). Factors affecting the normal perimetric profile derived by automated static threshold led perimetry. 1. Pupil size. *Ophthalmic and Physiological Optics*, 8, 26-31.

Wood JM, Wild JM, Hussey MK and Crews SJ (1987b). Serial examination of the normal visual field using Octopus automated projection perimetry evidence for a learning effect. *Acta Ophthalmologica*, 65, 326-333.

Wood JM, Wild JM and Crews SJ (1987a). Induced intraocular light scatter and the sensitivity gradient of the normal visual field. *Graefe's Archive for Clinical and Experimental Ophthalmology*, 225, 369-373.

Wood JM, Wild JM, Smerdon DL and Crews SJ (1989). Alterations in the shape of the automated perimetric profile arising from cataract. *Graefe's Archive for Clinical and Ophthalmology*, 227, 157-161.

Yamamoto S, Kamiyama M, Nitta K, Yamada T and Hayasaka S (1996). Selective reduction of the s-cone electroretinogram in diabetes. *British Journal of Ophthalmology*, 80, 973-975.

Yucel Y, Zhang Q, Weinreb RN, Kaufman PL and Gupta N (2001). Atrophy of relay neurons in magno- and parvocellular layers in the lateral geniculate nucleus in experimental glaucoma. *Investigative Ophthalmology & Visual Science*, 42, 3216-3222.

Yucel YH, Zhang Q, Gupta N, Kaufman PL and Weinreb RN (2000). Loss of neurons in the magnocellular and parvocellular layers of the lateral geniculate nucleus in glaucoma. *Archives of Ophthalmology*, 118, 378-384.

Zalta A (1991). Use of a central 10 degree field and size V stimulus to evaluate and monitor small central islands of vision in end-stage glaucoma. *British Journal of Ophthalmology*, 75, 151-154.

Zalta AH (1989). Lens rim artifact in automated threshold perimetry. *Ophthalmology*, 96, 1302-1311.

Zalta AH (2000). Limitations of the Glaucoma Hemifield Test in identifying early glaucomatous field loss. *Annals of Ophthalmology*, 32, 33-45.

Zalta AH and Burchfield JC (1990). Detecting early glaucomatous field defects with the size I stimulus and statpac. *British Journal Ophthalmology*, 74, 289-293.

Zulauf M (1994) Efficiency of the standard Octopus bracketing procedure compared to the 'Dynamic Strategy' of Weber. In Mills RP and Wall M. (eds.), *Perimetry Update 1994/1995*. Kugler Publications, Amsterdam/ New York. 422-437

Zulauf M, Caprioli J, Hoffman DC and Tressler CS (1991). Fluctuation of the differential light sensitivity in clinically stable glaucoma. In Heijl A (ed.), *Perimetry Update*. Kugler Publications, Amsterdam/New York.183-188.

Zulauf M, Flammer J and Signer C (1986). The influence of alcohol on the outcome of automated static perimetry. *Graefe's Archive for Clinical and Experimental Ophthalmology*, 224, 525-528.

Zulauf M, LeBlanc RP and Flammer J (1994). Normal visual fields measured with Octopus Program G1. Global visual field indices. *Graefe's Archive for Clinical and Experimental Ophthalmology*, 232, 516-522.

APPENDIX: KEY TO THE ABBREVIATIONS USED IN THE TEXT

ANOVA	Analysis of Variance
CC	Corrected Comparison
CPSD	Corrected Pattern Standard Deviation
dB	Decibels
FDT	Frequency Doubling Technology
FDP	Frequency Doubling Perimetry
FL	Fixation Losses
FN	False-negative
FOS	Frequency-of-seeing
FOP	Fundus Oriented Perimetry
FP	False-positive
GCP	Glaucoma Change Probability
GHT	Glaucoma Hemifield Test
HFA	Humphrey Field Analyzer
HRP	High Pass Resolution Perimetry
HSRP	High Spatial Resolution Perimetry
IOP	Intraocular Pressure
LF	Long-term Fluctuation
LI	Learner's Index
LOCS	Lens Opacities Classification System
LWS	Long-wavelength-sensitive
M	Magnocellular
MD	Mean Defect/Mean Deviation
MOBS	Modified Binary Search
MS	Mean Sensitivity
MWS	Medium-wavelength-sensitive
NC(II)	Nuclear Colour Grade 2
NO(III)	Nuclear Opalescence Grade 3
NRR	Neuroretinal rim
NTG	Normal Tension Glaucoma
OAG	Open Angle Glaucoma
OHT	Ocular Hypertension
OMA	Ocular Media Absorption
ONH	Optic Nerve Head
P	Parvocellular
P(I)	Posterior Subcapsular Cataract Grade 1
PD	Pattern Deviation
PEST	Parameter Estimation by Sequential Testing
PSD	Pattern Standard Deviation
QUEST	Quick Estimation by Sequential Testing
RNFL	Retinal Nerve Fibre Layer
ROI	Region of Interest
SD	Standard Deviation
SF	Short-term Fluctuation
SITA	Swedish Interactive Threshold Algorithm
SWAP	Short-wavelength Automated Perimetry
SWS	Short-wavelength-sensitive

TD	**Total Deviation**
TOP	**Tendency Oriented Perimetry**
W-W	**White-on-White**
ZEST	**Zippy Estimation of Sequential Testing**